THE STRUCTURAL RESPONSE OF STEEL I-SECTION MEMBERS SUBJECTED TO ELEVATED TEMPERATURE GRADIENTS ACROSS THE SECTION

by

Gordon Michael Eyre Cooke, BSc, CEng, MIMechE, MICE, FIFireE.

A thesis submitted in partial fulfilment of the requirement for the Award of Degree of Doctor of Philosophy in Civil Engineering (structures)

Department of Civil Engineering
The City University
London

September 1987

TABLE OF CONTENTS

LIST OF TABLES

LIST OF TABLES

LIST OF TABLES

LIST OF TABLES

LIST OF TABLES

LIST OF TABLES

LIST OF TABLES

LIST OF ILLUSTRATIONS

LIST OF ILLUSTRATIONS

LIST OF ILLUSTRATIONS

ACKNOWLEDGEMENTS

The author wishes to express his thanks to Dr K S Virdi, Head of Department of Civil Engineering, The City University, London for support and encouragement throughout this thesis.

I would also like to thank Mr K Palmer, Head, Fire Research Station (FRS) and Mr P Thorne who provided encouragement and recognised that the work could usefully complement other research at FRS. The experiments were undertaken at FRS. Thanks go also to Mr D Annable, Mr D Armitage and colleagues in the FRS Workshops who have assisted in the design and manufacture of test specimens and experimental apparatus.

I wish also to thank the staff of the Computing Department of The City University for help in early work. The majority of the computing has been done at FRS and I would particularly like to thank Mrs Olive Osborne for her help in running PAFEC jobs. Thanks also go to Miss Mary Foley for typing this thesis.

ABSTRACT

This work is primarily concerned with the structural response of steel I-section beams and columns heated along one flange to the elevated temperatures likely to be reached in real fires in buildings or ISO 834 fire resistance tests. Experiments have employed nominally ¼ full size models, heated using high powered, ceramic insulated, electrical heating elements at temperatures up to 1000°C. The experiments have been conducted on: a non-loaded, simply supported beam; a design-loaded, simply supported beam; a non-loaded 2-span beam on simple supports; and design-loaded, pin-ended columns free to bow about both axes.

Load, displacement and temperature data have been recorded and analysed for a number of heating, imposed loading and restraint conditions likely to be met in practice. One of the experiments simulates the loading and restraint conditions used in the BS 476 : Part 8 : 1972 standard fire resistance test on beams. The data may be used as benchmarks for the validation of analytical studies.

Simple theories for the bowing displacements of non-loaded members having temperature gradients across the section have been derived and validated not only with the model experiments but also with data from full scale compartment fires in a collaborative programme of research undertaken by the British Steel Corporation Swinden Laboratories and Fire Research Station. The practical application of the theory has been demonstrated in other ways. A finite element method, using the PAFEC program, has also been used which takes account of phase transformation - the sudden temporary shrinkage in steel as it is raised above a temperature of 720°C - but it has not proved possible to use PAFEC for plasticity analyses of beams or columns at elevated temperatures.

The phenomenon of reverse direction bowing has been observed in the model column tests and this confirms observations made by other workers.

Keywords:

Steel, beams, columns, models, fire resistance, fire engineering, non-uniform heating, critical temperature, limiting temperature, electrical heating elements, finite elements, elastic analysis, thermal bowing, phase transformation.

NOTATION

A	area of steel cross section
d	depth of member cross section
ε,e	strain
E	modulus of elasticity
h	distance from neutral axis to extreme fibre; height of column
I	second moment of area of section
L	length of member
M	bending moment
P	heated perimeter of steel cross section; load
R	radius of curvature
r	radius of gyration
T	temperature difference across section; temperature
t	time
W	total load
w	uniformly distributed load
x,y	rectangular co-ordinates
α	coefficient of linear thermal expansion
Δ	linear displacement of member
σ	stress
ℓ	effective length of column
Θ	angular rotation
ν	Poisson's ratio

BSC	British Steel Corporation
FRS	Fire Research Station
Constrado	Constructional Steel Research and Development Organisation, now (1987) known as the Steel Construction Institute.

CHAPTER 1. INTRODUCTION

In this chapter it is briefly shown that the requirements for stability of structural steel members exposed to a fire in a building are governed by building regulations and codes of practice which prescribe appropriate periods of fire resistance. The term 'fire resistance' is explained with reference to the present and proposed future British Standard 476, and several developments are described in which fire resistance is optimised, some of which rely on the existence of large temperature gradients across the section.

Some current fire engineering analyses are also reviewed. The concept of limiting temperature is introduced and it is pointed out that while this concept is useful for steel members uniformly heated it may not apply to members with large temperature gradients across their section, which is the subject of the research reported herein. Some full scale fire tests on internal and external steel members heated predominantly from one side are summarised. The chapter concludes with a description of the objectives and scope of the research covered in this thesis.

1.1 Building regulations and codes of practice

In the United Kingdom the design and construction of new buildings, and of alterations of existing buildings, are controlled by the following statutory provisions which are collectively referred to as building regulations.

England and Wales (excluding Inner London) - The Building Regulations

Scotland - The Building Standards (Scotland) Regulations

Northern Ireland - Building Regulations (Northern Ireland)

Inner London - London Building Acts 1930 to 1978.

London Building (Constructional) By-laws

The Greater London Council has also issued Codes of Practice for guidance on fire protection in high buildings and in large trade, manufacture and warehouse buildings.

The main objectives of fire precautions in building regulations are the safety of the occupants and limiting the size of the fire to reduce damage to the building and its contents. The regulatory needs are concerned with ensuring that the occupants have proper facilities to escape from a fire, that the fire does not grow rapidly or spread without restriction, and that it does not involve other buildings. Many requirements are specified for this purpose, and among these are requirements for the fire resistance of the building construction.

In the main, the passive fire precautionary requirements are intended to secure the stability of the building and limit fire spread even if the entire contents of the building or part of the building are consumed by fire. The beneficial action afforded by active fire precautions, such as automatic fire suppression systems, eg. sprinklers, and manual fire fighting, eg. by the brigade, are thus ignored except in special cases where reliable active fire precautions and other features compensate for an increase in compartment size (which the regulations also control) or a reduction in the amount of fire resistance needed. In these special cases a variation of the regulations or their provisions may be sought with the aid of a fire engineering analysis to prove that the proposed design is structurally safe in fire.

Provisions in the regulations give requirements for fire resistance (½, 1, 1½ hours etc) depending upon the purpose of the building, floor area, cubic capacity of fire compartment and height of the building. These statutory fire requirements represent targets which must be met for all structural mediums such as steel, concrete and timber unless a fire engineering method is followed. The minimum period of fire resistance, for structural elements, other than nil, is ½ hour and this presents an obstacle to the use of bare steel structural members of common size and shape which inherently have less than ½ hour fire resistance (but see 1.3).

The regulations or their provisions provide schedules of thicknesses of generic fire protection materials that will give stated periods of fire resistance when applied to steel elements of construction. Such schedules do not always reflect the fact that steel sections with different perimeter to cross section area ratios require different thicknesses of protecting material to achieve a given fire resistance. This is now included in a new draft code, BS 5950: Part 8. The regulations may refer to other documents which give more comprehensive details. Such documents include British Standards and other Approved Documents[1.1] introduced in England and Wales to accompany functional regulations in the recent Building Regulations 1985. One such Approved Document is a BRE report[1.2] by Read et al.

The relevant British Standard dealing with the design of hot rolled steel sections is BS 5950: Part 1:1985.[1.3] A new part of this standard (BS 5950: Part 8) dealing with fire protection of steelwork, is at present in draft.[1.4] It is expected that this standard, when

published, will encourage designers increasingly to adopt fire engineering analyses.

1.2 Meaning of fire resistance

All structural materials are affected by fire: timber chars; concrete weakens and may spall away from the reinforcing steel; steel gradually loses strength. Fire resistance is a measure of the ability of full-scale elements of construction of whatever materials to withstand, for stated periods of time, the effects of a standard time temperature exposure (typical of a fully developed fire) so that collapse of the structure does not occur under the imposed loading. In addition, separating elements, ie. walls and floors, should not transmit fire to other areas either by the passage of flames and hot gases through cracks, or through the development of temperatures on the unexposed face which could lead to ignition of combustibles nearby. It is clearly very important that the stability of beams and, moreso, columns can be assured in fire conditions in order to guard against local or widespread collapse of the building, especially if the building is high or large so as to put many people at risk both within and outside the building.

The fire resistance test is specified in BS 476: Part 8:1972[1.5]. This adopts the time/temperature curve of ISO 834. In the BS, a column is deemed to have failed when it can no longer support the load (which is maintained constant during the test). The column must also be able to support the test load 24 hours after the end of the heating period. However, should collapse occur during heating or during the reload test the notional maximum period for stability is construed as 80% of the

time to collapse or the duration of heating if failure occurs in the reload test. In practice, steel columns uniformly heated on all faces usually fail in the test by buckling.

In the case of beams, the standard gives a displacement criterion which must be satisfied. Details of this important criterion are as follows. BS 476: Part 8: 1972 allows the central displacement of a flexural element to reach span/30 before it is deemed to have failed. It is recognised that this failure criterion is restrictive for some elements, such as profiled steel and concrete composite floors, because such elements are able to carry their load without collapse well after the span/30 criterion is exceeded.

As a result, the draft revision of the British Standard, BS 476: Part 20[1,6] states the following:

"12.1.4 Loadbearing horizontal elements. The test specimen shall be deemed to have failed if it is no longer able to support the test load. For the purposes of this standard, this shall be taken as either of the following, whichever is exceeded first:

(a) a deflection of L/20; or

(b) where the rate of deflection, calculated over 1 min intervals on each minute from the commencement of the heating period, exceeds the limit set by the following expression:

$$\text{rate} = \frac{L^2}{9000d}$$

except that this rate of deflection limit shall not apply before a deflection of L/30 is exceeded.

Where L is the clear span of specimen (mm);

d is the distance from the top of the structural section to the bottom of the design tension zone."

The unit for d is not given but mm is known to be the correct unit.

It is clear that irrespective of which displacement criterion is used, it is important to be able to establish from a test or analysis the displacement time curve.

The current trend, which is likely to accelerate due to the high cost and time involved in full-scale fire resistance tests, is toward acceptance of analytical techniques which permit, for instance, absolute displacement and rate of displacement to be calculated with reasonable accuracy, as well as the ultimate load capacity.

1.3 Optimising the fire resistance of structural steelwork

Structural steel has a melting point of approximately 1550°C which is well above the maximum temperature experienced in real fires or the BS 476: Part 8 fire resistance test in which temperatures do not normally exceed 1200°C. Steel does, however, progressively weaken with increasing temperature, and eventually failure occurs in a member as a result of its inability to sustain the applied load; eg. buckling in the case of a column or excessive rate of displacement in the case of flexural members. This limiting temperature at which failure occurs varies and is dependent on the loading which the member is carrying, its structural support conditions, the change in its mechanical properties

as the temperature rises, and the temperature distribution across the cross-section.

Steel members, which are the subject of the present work, can have their survival times in a fire optimised in several ways:

i) in the case of bare members, by increasing the area of cross-section (A) so as to increase the heat capacity, and by reducing the heat-exposed perimeter of the section (P) to reduce the amount of heat entering the section. The ratio of P/A is termed the thermal response factor in the draft BS 5950: Part 8. The lower the P/A ratio the longer the survival time.

ii) by placing the steel member where the fire exposure is less severe; the use of the unprotected external steelwork is an example of this approach.

iii) in the case of a beam, by providing rotational restraint at the ends

iv) by reducing the working stress well below the maximum permissible

v) in the case of a hollow steel section column, by cooling with a filling of water

vi) by encasing the member in fire protecting material

vii) by protecting part of the member's cross-section, exemplified by the column-in-wall concept in which one flange is exposed to fire while the other is protected by masonry (this recent concept is further described in 1.6).

The above techniques have been discussed elsewhere as follows. The benefits, in terms of different thicknesses of fire protection, of using P/A ratios are detailed in a publication[1.7] jointly sponsored by Constrado and the Association of Structural Fire Protection Contractors and Manufacturers Ltd (ASFPCM). An analytical approach to the design of bare external steelwork has been made by Law[1.8] and a state of the art given by Cooke.[1.9] Similarly, the analytical thermal design of water filled columns has been made by Bond[1.10]. The effect of beam end restraint and partial protection has been explored by The British Steel Corporation (BSC)[1.11,1.12], and Fire Research Station (FRS) has examined the effect of beam end restraint using model steel bar beams[1.13].

1.4 Fire engineering analyses

The procedure of calculating the thermal response and then the structural response of a structural element is known as a fire engineering analysis. The full extent of the fire engineering analysis for the design of structural steel elements is epitomised by Pettersson et al who show[1.14] how, from knowledge of the fire load density, ventilation factor and thermal properties of the linings of the fire compartment, it is possible to calculate the combustion gas temperature time curve and, from this, the temperatures attained by a structural element in the fire compartment and hence its structural stability.

There are practical difficulties in the approach by Pettersson and others used to establish the thermal response and some of these have been reviewed by Cooke.[1.15] Nonetheless, several projects based on structural steel framing have gone ahead in the United Kingdom and a review of these has been included in a recent report by Kirby.[1.16]

There is little doubt, according to Cooke[1.17] that fire engineering of steel structures is gaining importance and recognition throughout the world, and some more practical applications of fire engineering in the United Kingdom have recently been reported by Latham[1.18] and Newman[1.19]. The writer believes that the use of steel models in fire research has the potential for making a significant contribution to scientific and engineering knowledge.[1.20]

1.5 The concept of limiting temperature

In early research and testing into the behaviour of steel members when subjected to the BS 476 fire resistance test, it was found that beams and columns carrying their maximum permissible loads became unstable, eg. collapsed, when the average temperature of the steel reached approximately 550°C. This temperature was called the 'critical temperature', and corresponded to the temperature at which the yield stress or 0.2% proof stress (see Figure 2.6) had fallen to the value of the applied stress. The concept of critical temperature was found to be particularly useful in making assessments of fire resistance for non-tested fire protected steel constructions: if a thermal calculation showed that the thickness of fire protection prevented the critical temperature of 550°C from being exceeded and if it could be shown that the protective material stayed in place during the required period of

fire resistance, then the element was said to have adequate fire resistance. This was a crude approach by present standards but nonetheless extremely useful to the fire protection industry which wished to minimise the high cost and time involved in testing.

As a result of almost a decade of research and testing work by BSC and Constrado (now the Steel Construction Institute), partly funded by the Department of Environment on behalf of FRS, the term 'critical temperature' has been superceded by 'limiting temperature'. The concept of limiting temperature discourages industry from thinking of a fixed temperature, namely the critical temperature of 550°C, and encourages, in its place, the simple idea that the temperature at which a structure will fail (ie reach its limit state) - the limiting temperature - depends on the stress level. An example of the benefit derived from this approach is illustrated as follows. A column of uniform section throughout its 5 storey height is clearly operating under a very low stress in its top storey. This means that the limiting temperature can be higher than that for the ground floor column, so that less thickness of fire protection is needed, resulting in cost economies.

There is now sufficient UK fire resistance data for unprotected steel members of different section size and shape ie. different P/A ratio, to produce curves of fire resistance versus P/A for different limiting temperatures. This information has been included in the draft BS 5950: Part 8 code and it is interesting to observe from Table 1.1, which reproduces a few rows of data from Tables 8 and 9 of the draft code, that the limiting temperatures for universal beams and columns having the same P/A ratio and heating times are marginally different.

The above discussion has implicitly assumed that any steel beam or column is heated uniformly across its section and along its length. It is implicit because standard fire resistance testing practice normally involves a) a column being exposed to heat on all faces over the entire length where uniformity in temperature is clearly assured and b) a beam being exposed to heat on 3 faces (the upper flange being in contact with, and, thereby 'protected' by, a concrete slab resting on the top face) such that the majority of the section ie. web and lower flange, are again assumed to be at a roughly uniform temperature (but see Figure 1.3), with the top flange being at a lower temperature.

The question can be asked "Is the limiting temperature concept still useful and valid for a member which has a large temperature gradient across its section?"

Large temperature gradients across the section can exist in I section members heated predominantly along one flange only, as in bare steel columns partly built into a wall, or in the case of a bare steel shelf angle floor beam. In 1.8 it is shown that temperature differences across a column section can reach 800°C.

In answering the above question there are two aspects to consider. One is the instability effect, if any, caused by the thermal bowing that arises from temperature gradients. This is clearly of importance in the case of a column. The other aspect is to what extent the high temperature portion of the section will dominate the structural stability of the whole member, and this may be of greater relevance to steel beams where the hot flange, once it reaches its limiting

temperature, begins to yield rapidly under tension but may be partly constrained from doing so due to the cooler adjacent web material. Both these aspects are explored in the present work.

1.6 Temperature gradients and thermal bowing

In a fire, separating elements such as walls and floors are exposed to heat from one side. This gives rise to temperature differences across the thickness of the element which induces thermal bowing. In metallic or concrete material the direction of bowing is toward the fire due to expansion of the hot material on the fire side; with timber, however, thermal bowing is usually away from the fire due to loss of moisture which causes shrinkage in the hot face material.

Structural steel members may be used externally and internally in buildings. In both situations a member, when exposed to fire, may attain a temperature gradient across the section which induces thermal bowing along the length if the member is unrestrained, or induces thermal bending moments if the member is restrained from bowing.

External steelwork may be chosen by the designer because i) it is outside the fire compartment and when spaced sufficiently away from a window may be used in its uninsulated form to economic advantage, ii) it provides an opportunity to visually express the structural medium which, using steel, allows optimum slenderness ratios to be achieved in columns to aesthetic benefit, iii) it results in column-free floor space and greater flexibility in internal planning, iv) it enables nil-maintenance weathering steel to be used. In a fire, external steelwork can become partly attacked by flame or be exposed to high levels of radiation mainly

from one side due to flames from openings in the facade. Temperature differences across the section can reach 300°C, as shown in 1.8.

Building regulations in some countries, notably in Italy and France, recognise the fact that the farther away the external column is from an opening in the facade through which fire can jet, the lesser the required resistance to fire. In the Italian regulations, for instance, the column needs to be 100 mm and 1000 mm away from the facade to qualify for use in buildings requiring ½ and 3 hour fire resistance respectively. However these regulations are not scientifically based and have not been found acceptable by other European countries.

It is more usual to use structural steelwork inside the building. Here members can also experience large temperature gradients especially when placed next to a heat sink because of the heat flow processes shown in Figure 1.1. This illustrates that the temperature gradient may be caused by:

a) unequal heat flow from the fire into the member because the whole perimeter of the section is not receiving heat, and
b) unequal heat loss from the member which is exacerbated if a heat sink material is in contact with the web and one of the flanges.

Hence by positioning a steel member next to, or partially within, a heat sink such as a masonry wall or concrete floor, it is possible, as shown in Figure 1.2, to reduce the rate of heating and thus increase the time before the member reaches its limiting temperature and loses stability. On the other hand the effect of the heat sink material is to increase the

temperature difference across the section and thus the magnitude of thermal bowing, and this may have several detrimental effects. First, in the case of a horizontal flexural member exposed to fire from below, greater clearance would be needed at mid-span to avoid crushing of non-loadbearing partitions below. Secondly, the criterion for absolute displacement (eg span/30) specified in the BS 476: Part 8 standard fire resistance test method for floors or beams may be exceeded relatively early in the test. Thirdly, and perhaps most importantly, thermal bowing in columns could become a dangerous feature where the eccentricity so caused leads to early buckling: this feature could be pronounced in columns of large slenderness ratio.*

1.7 Research on steel beams having temperature gradients across the section.

It is normally assumed that an unprotected steel beam exposed to heat on three sides, eg supporting a concrete floor slab on its upper flange, is at a uniform temperature throughout its depth. That this assumption is not valid can be seen from Figure 1.3 which shows temperature profiles for three steel beams which were tested according to Section 6 of the BS 476: Part 8: 1972 standard test for beams. The tests, which were sponsored by BSC and reported by Thomson et al [1.21], were for beams with different P/A ratios. The maximum temperature differences approached 300°C. The profiles also show, incidentally, that sections which are heavier and more compact (ie sections having lower P/A ratios) heat up more slowly, especially in the early stages of a test.

---

*Slenderness ratio in this thesis means the effective length divided by the radius of gyration, as in BS 449. In BS 5950 : Part 1 : 1985 this is termed slenderness.

If the P/A ratio can be reduced, the fire resistance can be increased. One practical way of reducing P/A is to reduce the perimeter exposed to heat. This can be achieved by partly embedding the section in the adjoining construction. This can be done with I-section beams and columns forming a part of a floor or wall respectively.

The shelf angle floor beam is an example of this approach. A practical design is shown in Figure 1.4. BSC has undertaken several fire resistance tests on shelf angle floor beam constructions. A feature of these tests has been the large amount of thermal bowing in relation to the elastic displacement, and this means that the flexural behaviour is governed by the BS 476 : Part 8 : 1972 mid-span displacement criterion of span/30. Hence they fail the test well before they suffer runaway displacement, and this is in contrast to an I-section beam exposed to fire on 3-sides which collapses by runaway displacement shortly after attaining the governing displacement of span/30.

The central displacement curve[1.22] for a 305 mm deep shelf angle floor beam with 25% of its depth exposed to fire is given in Figure 1.5 for the construction shown in Figure 1.6. Another displacement time curve obtained from a BSC test[1.23] is shown in Figure 1.7 for the 406 mm deep shelf angle floor beam having 40% of its depth exposed to fire shown in Figure 1.8. It can be seen from the displacement curves that there is no hint of runaway displacement at the end of each test even when roughly 40% of the beam depth is exposed to fire.

Also shown in Figures 1.5 and 1.7 are the average heated and unheated flange temperatures plotted by the writer from data given in the

references. The heated flange temperatures are over 900°C at the end of the two tests, well above the so-called critical temperature of 550°C.

The shape of the temperature distribution [1.23] across the depth of the 305 mm deep shelf angle floor is shown in Figure 1.9. The S-shaped profile is typical of shelf angle floor beams.

1.8 Research on steel columns having temperature gradients across the section

Before reviewing what research has been accomplished on non-uniformly heated columns it will be of interest to state briefly the research on, and conditions of testing for, uniformly heated columns.

In Europe a considerable amount of fire research on columns has been conducted[1.24,1.25] and the Fire Committee of the European Convention for Constructional Steelwork (ECCS-T3 Committee) has recently published[1.26] a set of non-dimensional buckling curves for steel columns uniformly heated along the length and across the section.

In the United Kingdom fire resistance tests on columns are currently undertaken at the Fire Insurers's Research & Testing Organisation (FIRTO), now part of the Loss Prevention Council, Borehamwood. The furnace, the only furnace available for testing columns in the UK, is basically a vertical cylinder with natural gas burners in both vertically-split halves. It has a maximum concentric load capacity of 5000 kN (but is only calibrated for 3000 kN) and permits the testing of columns with a fire-exposed height of 3 metres. It cannot, without modification, be used for eccentric loading or non-uniform heating. Tests using this furnace have shown that protected and unprotected steel columns

(using a 203 mm x 203 mm x 52 kg/m Universal Column section), subjected to the maximum permissible design load maintained constant throughout the test, have a limiting temperature of approximately 550°C when buckling failure occurs. Up until 1986 the foot of the steel column specimen was cast into a refractory concrete base which was position- and direction-fixed. The top of the column was position- and partly direction-fixed and the effective length was usually assumed to be 0.70 x fire-exposed height of 3 metres.

There has been a considerable amount of international research, of an experimental and analytical nature, into the thermal response of external steel columns. A large programme of experiments made by the Fire Research Station is reviewed below. There has, however, been only a small amount of research into the structural response of steel columns. Two recent programmes - one on internal steel columns, the other on external steel columns - are also reviewed below.

i) FRS/BISF thermal response tests

Work in the mid-1960's by the Fire Research Station in cooperation with the British Iron and Steel Federation involved a large programme of tests using various fuels (mainly timber cribs for repeatability) in a brick compartment roughly 7.6 m long by 3.7 m wide by 2.9 m high. A view of the fire compartment showing the uninsulated external steel beams and columns and the insulated internal columns with the timber crib fire load is given in Figure 1.10. A fully developed fire is shown in Figure 1.11. The effect on combustion gas and steel temperatures of varying fire load density and ventilation was examined and the results and their potential application were briefly reviewed by Butcher and Cooke[1.27].

Comprehensive data for the tests and their analysis have been reported elsewhere[1.28,1.29]. It is of interest to reproduce the time-temperature curves for the unshielded external column resulting from two fire tests using a common fire load density of 30 kg/m^2 but different ventilation openings of ½ and ¼, the latter producing higher temperatures particularly near the bottom of the window openings. (½ and ¼ mean that one half and one quarter of the area of the front wall respectively was open as ventilation). It can be seen from Figure 1.13 that temperature differences between front and rear flanges reached 200°C. A conclusion of the Fire Research Station work was that "large differences in temperature were recorded in the external steel members (as between the front and back flanges, for instance) and this gave rise to temporary distortion of the members owing to differential thermal expansion".

The above mentioned tests and many others conducted internationally have been reviewed in a technical report[1.30] forming part of a design guide for fire safety of bare exterior structural steel jointly sponsored by the American Iron & Steel Institute (AISI) and Constrado. The report concluded that "There can be large temperature differences across the section, of order 300°C, particularly when there is shielding. This can give distortion which should be allowed for in the structural design". A comprehensive design guide on the method to be used to calculate average steel temperature has now been published by the AISI[1.8].

ii) CTICM structural response tests

Recent work[1.31] in France for the Commission of the European Communities (ECSC-EEC-EAEC) examined beam/column interaction where the beam was loaded at two points and the pin-ended steel column was axially loaded. The

column was placed outside the fire compartment and was subjected to non-uniform heating. The structural configuration is shown in Figure 1.14. Typical steel temperature profiles are given in Figure 1.15 and it is interesting to note the large temperature difference of nominally 200°C between front and rear flanges which agrees with the Fire Research Station findings.

In Kruppa's comprehensive report[1,32] of the work it appears that some tests were conducted with pin-ended columns (analagous to the FRS model tests described later), but in the majority of tests with a beam framing in at mid-height to the column since this was considered to be more representative of practice in multi-storey buildings.

The CTICM work showed that column failure could take place in several different ways. One way, of particular relevance to the present work, involved failure "by plastification of the hottest zone of the column after the column had returned (from bowing towards the fire) to its initial position, and then has continued to deform away from the fire". It was also found that, for sections with flanges parallel to the facade (ie parallel to the plane of heating), a lightly loaded column would ultimately fail in its plane of high inertia, away from the fire.

Figures 1.16 and 1.17 reproduce figures in the reference. Figure 1.16 shows the deformation half-way up the columns away from the fire. It can be seen that in two tests (Tests 5 and 6) the columns initially bowed towards the fire, then straightened out and failed by bowing away from the fire. The writer has called this unexpected behaviour "reverse direction bowing". Figure 1.17 shows the axial displacements of the columns and

illustrates the consistent shape of the curves and the rapid failure judged to have occurred when the column had attained its original length after expansion and "contraction". Kruppa's work was not known to the writer at the time of planning the model column tests reported later herein.

iii) BSC structural response tests

The British Steel Corporation Swinden Laboratories has, also recently, undertaken 4 column-in-wall fire resistance tests[1.33,1.34,1.35], which are summarised in Table 1.2. These were undertaken in the expectation that the unexposed portion of the column would be at a lower temperature and thus able to contribute to support the design load for a longer period than if the column was exposed to fire on all faces. In each test a pair of identical I-section members, spaced approximately 1.3 metres apart, formed columns in part of a 3 metre x 3 metre double leaf cavity masonry wall specimen. Figure 1.18 shows a horizontal section through a column used in Test 1, and the S-shaped temperature profiles at 30, 60 and 90 minutes.

The masonry did not carry any vertical load but was able to give lateral restraint to the web of the I-section, so that the columns could not buckle about the minor (yy) axis. However, in calculating the design load it was assumed for all 4 tests, that failure would occur about the minor (yy) axis. The height of each I-section column between welded end plates was 3 m. The amount of rotational restraint at the ends in each test was uncertain and for the purpose of calculating the design load according to BS 449 : Part 2 : 1969, effective lengths between 0.75 L and 1.0 L were used by BSC assuming bending about the yy axis.

Data used in the design load calculations are given in Table 1.2. The test loads varied from 40 to 115 per cent of the maximum permissible loads. Table 1.2 also includes heated and unheated flange temperatures when maximum mid-span bowing occurred, first towards and then away from the furnace. In all 4 tests the phenomenon of reverse direction bowing occurred, as in the CTICM tests.

To see if the observed initial mid-span bowing toward the furnace was dominated by thermal bowing, the unrestrained thermal bow Δ was calculated using Equation (3.6) given in 3.2. The data, given in Table 1.3, show that the calculated mid-height displacements are of the right order and are generally greater than the measured displacements. There is however a little uncertainty about the accuracy of the mid-height displacement measurements made in the experiment - they were measured only at mid-height relative to a fixed point in space and not relative to the upper and lower ends of the colum which, in the writer's view, would have been preferable since this would avoid the dubious assumption that the top and bottom of the columns did not move perpendicular to the plane of the specimen wall as the test progressed.

What, then, are the practical implications of the column-in-wall concept? There is no doubt that survival times can be usefully extended. Assuming a limiting temperature of 550°C, the 203 x 203 x 52 kg/m section would only achieve a fire resistance of approximately 15 minutes when fully loaded and exposed to heat on all sides in the BS 476 : Part 8 : 1972 fire resistance test[1.36]. The results summarised in Table 1.2 show that a fire resistance of slightly more than 30 minutes is feasible when such a section is fully loaded. Using a Universal Beam section as a column it is

possible to achieve a 3 hour fire resistance when the load is 40% of the maximum allowable (see results for Test 3 in Table 1.2). It also appears that the fire-exposed flange can be allowed to reach temperatures in excess of 900°C when the column is fully loaded - compare this with nominally 550°C when uniformly heated on all faces and similarly fully loaded. Some other considerations are described in Chapter 8.

This small selection of fire test data shows that temperature differences across partly protected steel I-section members can be appreciable, and in excess of 700°C. Such members can achieve fire resistances in excess of 1 hour and this should be compared with a fire resistance of 15 minutes for a free standing unprotected 203 x 203 mm x 52 kg/m column carrying its maximum design load corresponding to a stress of 138 N/mm^2.

1.9 Objectives and scope of research

It has been shown that the main thrust of international experimental and analytical work has been to elucidate factors affecting the structural response of steel members heated uniformly across the section, and the most recent authoritative work to emerge in Europe which demonstrates this point is the ECCS Recommendations[1.26] But these findings cannot be applied to members whose sections have non-uniform temperature distributions across them.

It has also been shown that there has been surprisingly little theoretical work aimed at predicting the structural response of building elements such as beams, columns, walls and floors when subjected to non-uniform heating. In the case of external steelwork the research effort has tried to overcome the difficulties of defining the thermal response, and the

criterion suggested by Law and O'Brian[1,30] is that the structure is considered safe if the average steel temperature does not exceed 550°C; the theoretical work does not extend to cover the structural effects of non-uniform heating and it is not clear if a member such as a steel column which has 'hot' and 'cold' face temperatures of, for instance, 750 and 350°C respectively (having an average temperature of 550°C) will be as structurally safe as a column which has a uniform temperature throughout the section of 550°C and is thus free of thermal bowing.

The immediate need for practical guidance in the UK arises from two activities. First is the work of the British Standards Institution Committee CSB 27/8 preparing a Code of Practice on fire protection of steelwork as Part 8 of BS 5950. Second is the current interest of the British Steel Corporation in finding ways of using unprotected steel to achieve commercially useful periods of fire resistance (eg ½ and 1 hour) and this includes inter alia steel sections partially embedded in walls and floors to exploit the thermal advantage of the heat sink material.

1.9.1 Objectives of research

The principal objective of this elevated temperature research was to determine, experimentally and analytically, the structural response of I-section steel beams and columns heated along one flange. The experiments would simulate practical constructions, such as an unprotected steel column partly built into a masonry fire separating wall or an unprotected steel shelf angle beam supporting a concrete floor where the adjoining construction - masonry or concrete in these examples - acts fortuitously as fire protection and a heat sink to one flange and a portion of the web of the steel member, so producing a temperature differential across the section and, unfortunately, a tendency to bow.

Hence the research would be concerned with the effect of heating such that, at any particular time in the heating process, temperatures were higher in one flange of the member than in the other. Temperatures would vary curvi-linearly across the section of the member and, in some experiments, along the length of the member. Maximum steel temperatures of 1000°C would be sought which is well above the limiting temperature (roughly 550°C) for members heated uniformly across the section when failure under the maximum permissible stress would normally be expected.

From the theoretical viewpoint, the objective was to develop, wherever possible, simple rules, for use by the fire engineer or structural engineer, for predicting the structural response of full scale metal structures in fire conditions. Where simple rules could not be formulated, the analytical techniques were, like the simple rules, to be validated against the experimental results so that confidence in their use could be assured. An important objective of the research would be to demonstrate and communicate the need for, and practical application of, the research findings: Chapter 8 has been included for this purpose.

The finite element method, using the PAFEC proprietary computer program, would be used for elastic analyses of the beam members, but would not be used for the columns because the PAFEC program does not cater for change in geometry when the material properties are changing with temperature. An attempt would be made to use a modified PAFEC program for plastic analyses of beams. Creep would be ignored as creep analyses have been made by others, with difficulty, at least for statically determinate steel beams.

The experimental objective would be to provide structural response data, such as displacements and forces, in a comprehensive and highly accurate form so that they could be confidently used as benchmarks for validating the analytical studies. In meeting the experimental objective it was anticipated that it would be necessary to explore the efficacy of proprietary electrical heating elements for heating parts of the models.

One test rig, shown conceptually in Figure 1.19(a), would be designed to undertake all the model beam tests. The use of two heating elements, each covering half the length of the flange of the I-section, would mean that one test could be made in which the whole of the flange length was heated, and another in which half the flange length was heated.

1.9.2 Scope of research

Four series of model experiments were chosen - Experiments Series 1 to 4. With increasing complexity they progress from a non-loaded beam, a restrained beam, to a loaded beam and hence to a loaded column. Experiments would also be conducted on a full scale unrestrained, non-loaded, partly built-in column in a large fire compartment rig. The series are described in i) to iv) below.

i) Experiment Series 1 would determine the thermal bowing displacements of a non-loaded, simply supported, I-section model steel beam electrically heated along one flange, Figure 1.19(b). A secondary objective would be to find out if high powered ceramic insulated electrical heating elements could heat models at the required rate and to the required elevated temperatures. Supplementary tests would be conducted on an unrestrained full-size partly built-in-column exposed to heating along one flange in two compartment fire tests of different severity.

ii) Experiment Series 2 would determine the restraint force at the central support needed to prevent bowing at the central support of a simply supported, 2-span, I-section steel model beam electrically heated along one flange, Figure 1.19(c).

iii) Experiment Series 3 would determine the mid-span displacements and limiting temperatures of a simply supported I-section steel model beam carrying its maximum permissible uniformly distributed design load when electrically heated along one flange, Figure 1.19(d). A secondary objective would be to see if there were any problems using model I-sections fabricated by welding 3 strips together.

iv) Experiment Series 4 would determine the mid-length lateral displacement and axial displacement, as well as the limiting temperatures, for three pin-ended I-section model steel columns of different slenderness ratio when carrying their maximum permissible design loads when electrically heated along one flange.

Supplementary tests would also be undertaken to determine the following properties of the steel used in the test specimens: coefficient of thermal expansion and the effect of different heating rates on thermal strain in the phase transformation range; chemical composition; yield stress and modulus of elasticity at room temperature.

In addition control tests would be made where appropriate to enable elastic theory to be correlated with experiments at room temperature before proceeding to the elevated temperature tests. The two test rigs used in

the experiments would be proof tested at room temperature using dummy specimens.

A new specimen would be used in each of Experiment Series 1 and 2, but to reduce the amount of specimen preparation the same specimen would be used in the half flange and whole flange heating experiments. Two assumptions were made. First that any change in strength properties after the first heating would be immaterial, and this seemed reasonable for the second test in Experiment Series 1 in which the specimen was free of external loads and restraints, and strength properties were therefore unimportant. The second assumption was that any change in strength properties would not be significant in the temperature range of interest. This assumption was satisfied in Experiment Series 2 in which the behaviour before hot flange temperatures of 600°C were reached was of interest. Figure 1.20 shows the room temperature strength reductions reported by Smith et al[1.37] which results from the heating of specimens of BS 4360: Grade 43A steel at various temperatures up to 1000°C. It can be seen that strength reductions commence at about 600°C which is above the temperature of interest in Experiment Series 2.

Comprehensive experimental measurements would be made of: temperatures, using K type thermocouples; displacements, using dial gauges or linear displacement transducers; and forces using load transducers. No attempt would be made to measure strain at elevated temperatures since weldable electrical strain gauges are difficult to use, are of dubious reliability, and very expensive.

The experiments would be performed on small scale models, approximately one quarter to one third full scale.

CHAPTER 2. STEEL PROPERTIES AT ELEVATED TEMPERATURES

2.1 Introduction

The temperature-dependent material properties required for a structural analysis of the behaviour of a steel structure include Poisson's ratio, coefficient of linear thermal expansion and phase transformation, elastic modulus, yield stress or proof stress, and stress strain relationships. These are reviewed in this chapter.

2.2 Poisson's ratio

2.2.1 General

When a body is pulled, it becomes longer and thinner; when compressed it becomes shorter and thicker. Poisson's ratio quantifies this phenomenon.

Poisson's ratio, ν, is defined as $\frac{\text{lateral strain}}{\text{longitudinal strain}}$

Most values given in the literature for Poisson's ratio for mild steel have been derived from separate determinations of Elastic Modulus (E) and Shear Modulus (G) using the relationship $\nu = \frac{E}{2G} - 1$.

Woolman and Mottram point out[2.1] that values so determined are subject to considerable errors, since slight errors in either E or G are magnified in the subsequent estimation of ν. For example, if E were measured 2% high and G 2% low, the calculated value of ν would be in error by 17%. The authors reinforce the generally held view that the values of the elastic constants, E and G, are not sensitive to the structure or composition of he steel, and they say that the best estimates of ν for the family of low alloy steels (of which structural steel is a member) are all between 0.27 and 0.30. The recent British Standard, BS 5950 : Part 1 : 1985[1.3]

recommends that a value of $\nu = 0.30$ should be used.

If a rectangular block is subjected to tensile stresses σ_x and σ_y, then the strains will be as follows:

$$e_x = \frac{\sigma_x}{E} - \frac{\nu\sigma_y}{E}$$

$$e_y = \frac{\sigma_y}{E} - \frac{\nu\sigma_x}{E}$$

$$e_z = -\frac{\nu\sigma_x}{E} - \frac{\nu\sigma_y}{E}$$

Equations of this kind are used in the constitutive relations in 2-dimensional finite element elastic theories[2.2].

2.2.2 Variation of Poisson's ratio with temperature

There appears to be a paucity of data on the variation of Poisson's ratio with temperature. Clarke[2.3] has reported values up to a temperature of 650°C for a mild steel (En 2) containing 0.15%C, 0.46%Mn and 0.28% Si, and the variation is not great, as shown in Table 2.1.

BSC has reported[2.4] a value of $\nu = 0.34$ at 1000°C (which is in line with the trend exhibited in Table 2.1) and has recommended that a value of 0.30 should be used for calculation purposes for all steel grades.

A constant value of 0.3 has been adopted for the finite element analyses in the present work.

2.3 Thermal expansion and phase transformation

2.3.1 General

To predict the performance of building structures in fire it is necessary to know the thermal expansion properties of structural materials and composites. There are precise data for metals, but for complex materials, such as concretes employing different aggregates, the data tends to be scarce and subject to much variation.

The amount of thermal expansion in a structure will depend not only on the coefficient of linear expansion, which is determined in tests under stress-free conditions, but also on the restraint imposed by adjoining construction. With metals this does not present a problem in the elastic range because metals are Hookean materials; that is, stress is proportional to strain. With inorganic composite materials, such as concrete, Hookean behaviour cannot be assumed due to cracking and phenomena associated with loss of water and phase changes in the cement matrix and aggregate upon heating.

2.3.2 Coefficient of linear expansion

When a solid material is heated it increases in length according to the equation:

$$L_t = L_o (1 + \alpha T + \alpha_1 T^2 + \alpha_2 T^3)$$

where L_o = length at the initial temperature

and L_t = length after a temperature rise of T.

For pure metals the constants α, α_1 and α_2 have values of the order of 10^{-5}, 10^{-11} and 10^{-14} respectively. Because α_1 and $\alpha_2$are small compared with α, the following relation is adequate for most purposes.

$$L_t = L_o (1 + \alpha T)$$

The constant α is called the coefficient of linear expansion and is defined as the increase in length per unit length for a temperature rise of 1 degree. Its numerical value is independent of length but it does depend on the temperature.

The coefficients of linear expansion of some materials at room temperature are given[2.5] in Table 2.2.

2.3.3 Variation of thermal expansion with temperature, and phase transformation

It has, for many years, been assumed for structural calculations that the coefficient of linear thermal expansion for mild steel is nominally 10 x 10^{-6} per °C for ambient conditions, ie at 20°C.

Precise determinations at elevated temperatures were reported for 22 different steels in 1952 as a result of work undertaken by the National Physical Laboratory for the British Iron and Steel Research Association. The relevant data for 3 carbon steels annealed at 930°C are reproduced in Table 2.3 which is taken from columns 1, 3 and 4 of Table IVA of the report[2.6]. The chemical compositions corresponding to these three steels is given in Table 2.4. Structural steels fall in the mild and

micro-alloyed steel category, and because the maximum carbon content of weldable structural steels (BS 4360 steels) is nominally 0.3% (it varies depending upon grade) it follows that the 2nd row of data in Table 2.3 is of main interest here. It can be seen that α varies from a mean value of 11.92×10^{-6} per °C in the temperature range 0-50°C to 14.81×10^{-6} per °C in the range 0-1200°C. Over the range 0-550°C the mean value is 14.17×10^{-6} per °C. Since this is the temperature range of main interest in the behaviour of structural steel in fire, it can be seen that a nominal value of 14×10^{-6} per °C might be a sensible choice. The data in Table 2.3 apply only to mild steel: for a high alloy steel - stainless steel (18% chromium/8% nickel) for instance - the coefficient of linear expansion is higher and varies from 13.88×10^{-6} to 19.59×10^{-6}/°C over temperature ranges of 0-50 and 0-1,200°C respectively.

Table 2.3 also shows that the mean coefficient of expansion of mild steel gradually increases as the temperature increases up to approximately 700°C and then temporarily reduces with further increase in temperature. This is caused by a phenomenon called phase transformation. The temporary sudden shrinkage is caused by a transformation of pearlite to austenite. This is accompanied by a rearrangement in the atomic structure from the body-centred cubic structure to the face-centred cubic structure. This phenomenon is explained by Gregory and Simons[2.7], Walker[2.8] and Kennedy et al[2.9]. The temporary shrinkage is roughly 15% of the expansion for a temperature range of 20 to 700°C. The reverse occurs upon cooling but not at the same temperature as will be shown later, but this is of no importance in fire engineering analyses.

Some typical thermal expansion-temperature curves in the phase transformation range are shown in Figure 2.1. These are taken from Reference 2.6 and apply to steels of low and medium carbon content. It can be seen that the shapes of the curves are strongly dependent on carbon content: the magnitude of the dip varies, and while the 0.43%C and 0.23%C steels commence phase transformation at around 720°C, the 0.06%C steel does not until around 800°C. These data and others in the reference suggest that the temperatures at which phase transformation begin and end vary with chemical composition.

To determine if variation of heating rate would affect the magnitude of shrinkage and temperature of onset of phase transformation, discussion was held with researchers in the British Steel Corporation Laboratories at Teesside. As a result the Corporation, which had conducted many such tests but under different conditions, conducted dilatometer tests[2.10] using a MMC High Speed Vacuum Dilatometer on two identical mild steel specimens (0.28%C, 0.67% Mn) for two heating/cooling rates of 10°C/min and 50°C/min which the writer considered to represent the extremes of heating rate likely to be experienced with protected steel exposed to the heating conditions of the BS 476 : Part 8 : 1972 standard fire resistance test.

Figure 2.2 presents this data from which it can be seen that marked contraction during heating commences at approximately 730°C and ceases at approximately 830°C irrespective of heating rate. The magnitude of contraction is, referring to Figure 2.2, distance EB and distance FD, for the two heating rates: this is 0.15% strain and 0.2% strain for heating rates of 50°C/min and 10°C/min respectively and this represents contractions of 15 and 20% respectively. It is also clear from Figure 2.2

that ignorance of the transformation effect would lead to an overestimate of strain at temperatures above 830°C of 0.30 and 0.38% for heating rates of 50 and 10°C/min respectively (derived from lengths AB and CD).

The 2 heating curves in Figure 2.2 have been idealised as a single tri-linear curve for finite element analyses reported later. The idealisation is shown in Figure 2.3.

The coefficient of linear expansion corresponding to the slope of the curve up to phase transformation in Figure 2.3 is 14.48 x 10^{-6}/°C. The recommended value of the coefficient of linear expansion for structural steel is 14 x 10^{-6}/°C in the draft BS 5950 Part 8[1.4]. Both values have been used in the finite element analyses reported herein (see 4.4).

2.4 Elastic-plastic behaviour

2.4.1 Stress-strain at room temperature

If a bar of homogeneous material, such as steel, of cross sectional area A and gauge length L is mounted in a tensile testing machine and a load P is applied, the bar will elongate by an amount δ. If, on removal of the load, the elongation disappears, the material is said to be elastic. If, on the other hand, there is residual elongation, the material is said to have passed the elastic limit and has become plastic.

Figure 2.4 shows the typical behaviour of mild steel when tensile tested at room temperature[2.11]. The elastic limit is reached at a strain (elongation/original length) which is small, roughly 0.15%. Up to the elastic limit it is found that stress (direct tensile load/cross section area) is proportional to strain, and this is shown by the constant slope of

the stress strain curve up to point A in Figure 2.4. At point A - the yield point - the material is said to have yielded and the corresponding stress is the yield stress.

The elastic modulus E, also called Young's Modulus, is the ratio of stress to the strain it produces, ie $E = \frac{\sigma}{\varepsilon}$ and for the bar of material $E = \frac{PL}{A\delta}$. It represents the stress required to produce unit strain. This linear relation between stress and strain up to the elastic limit has a profoundly simplifying effect upon structural analyses, and analyses are often classified as elastic or plastic.

It is clear from Figure 2.4 that the strain at the elastic limit, typically 0.15%, is a very small portion of the total strain to failure, which can be 30% at room temperature.

2.4.2 Stress-strain at elevated temperatures

As steel is heated above a temperature of about 150°C its strength reduces. Because the strength of steel reduces with increasing temperature, the strain increases for a given stress and the slope of the initial part of the stress strain graph reduces. Therefore the E value (the slope) reduces with increasing temperature. Figure 2.5 shows a family of stress strain curves for mild steel at different temperatures from which it is clear that the "yield stress" reduces with temperature.

At high temperatures the clearly defined yield point vanishes and the concept of yield stress is invalid. An alternative is to adopt the proof stress concept. Figure 2.6 shows a slightly curved stress strain diagram. If a tangent to the curve at the origin is drawn (OA) and a line BC is

drawn parallel to OA such that OB is 0.2%, then the stress at C is called the 0.2% proof stress. In other words the 0.2% proof stress is the stress required to produce a permanent strain of 0.2%.

2.4.3 Anomalies in elastic modulus data at elevated temperatures

A comparison of elevated temperature E value data quoted in international literature reveals that there is little agreement for steel grades within the family of structural steels. There may be several reasons for this and some, relevant to the tensile test method (static test), are listed below.

i) Different tensile test machines have different accuracies for measuring very small strains and for achieving a uniform and accurately known temperature over the entire gauge length.

ii) Inaccuracy in strain measurements will mean that the shape of the stress strain curve is affected and, of major importance, the shape of the curve near the origin. This makes it very difficult to plot a tangent to the curve and since the slope of the tangent at the origin is the E value, inaccuracies in tangent plotting produce inaccuracies in E.

iii) Most static testing has adopted the isothermal test method in which the specimen is taken up to, and maintained thereafter, at a constant temperature (ie isothermally). When the specimen has achieved the prescribed temperature over the entire gauge length, which usually requires a soaking period, the machine is programmed to apply a constant rate of strain (as defined in BS 3688) and the corresponding stress is measured. However, there is an alternative test method -

the anisothermal test - in which the stress is maintained constant while the temperature is increased at a prescribed rate and the corresponding strains are measured.

In practice the isothermal test is relevant to a structure in which the temperature is constant and the stress fluctuates, as in a steel boiler for instance. In building structures subjected to fire it is argued that the applied load is constant (as on a floor beam for instance) while the temperature varies, so that anisothermal data should be used. There are situations, however, where the load and temperature varies with time (for instance in a lightly loaded continuous beam with temperature gradients across the section such as to cause thermal bowing and varying restraint forces at the supports) and it is then not clear whether isothermal or anisothermal data should be used.

Graphs of strain versus temperature are obtained from anisothermal tests, and plots of stress against strain from isothermal tests, and it is therefore clear by which method the data has been obtained. However isothermal and anisothermal data can be used to produce elastic modulus data and the problem is that the test method used may not be mentioned.

iv) The researcher may not have subtracted the thermal strain from the measured strain before plotting the stress strain curve. Deducting the thermal strain results in higher derived E values; this can only affect the results of anisothermal tests. However, it is unlikely that such a fundamental factor would be overlooked.

v) Differences in chemical composition of test specimens can affect the strain. For instance, small amounts of aluminium added to give improved notch toughness can result in larger plastic strains.

vi) At high temperatures, the soaking period prior to application of stress in an isothermal test can relieve residual stresses and regularise the grain structure, causing grains elongated in the hot rolling process to return to their original shape which could result in shrinkage such that the measured strain in a tensile test is reduced.

vii) Different researchers may have adopted different rates of strain. A fast rate of strain in the isothermal test would be expected to produce less measured strain than a slow rate. It should be noted that BS 3688 : Part 1 : 1963[2.12], which deals with tensile testing of metals at elevated temperatures, prescribes a rate of strain within a range of 0.001 to 0.003 per minute up to the elastic limit, but other countries may adopt different rates.

viii) It is possible that some reported E values are secant modulus values and not tangent modulus values.

There is, however, yet another, perhaps the most important, reason for the differences in reported E values. There is, in addition to the static test described above, a dynamic test. In the static test the measured strain in the specimen includes thermal strain and elastic strain and also, depending upon the stress level and temperature, plastic and creep strains. In the dynamic test, the specimen is usually a wire which is caused to vibrate and

E is determined from the measured frequency of vibration at each temperature. In this test the stress reversals are sufficiently rapid to prevent plastic and creep strains from occurring and this is the principal reason why, for a given steel at a given temperature, the dynamically-derived E value is greater than the E value obtained from a static test.

It is also possible that researchers concerned with structural analyses will adopt an E versus temperature relationship which, though falling within the scatterband of experimentally determined E values, is chosen so that it best correlates with the benchmark data, such as flexural displacement, for the experiment. In other words the E values used are those which provide the best correlation of theory and experiment for the beam or column under consideration.

From the foregoing discussion it is clear that E values can be determined from dynamic tests and from isothermal or anisothermal static tests. It should not be forgotten that if E is defined as the initial slope of the stress strain curve and the only relevant strain is the elastic strain, then in principle there should be no difference between the E values obtained by each of the test methods for a given temperature.

2.4.4 Review of elevated temperature stress-strain data

The first major British work on the elevated tensile properties of steels up to 800°C was reported by Woolman and Mottram in 1964[2.1]. A very comprehensive study[2.13] was made by Skinner et al in 1972 at the Australian Broken Hill Proprietary (BHP) Company Ltd. Other studies have been reported by Witteveen[2.14,2.15], Anderberg[2.16] and Harmathy and Stanzak[2.17].

In 1980 Crook examined, among other British steels, the tensile strength properties of hot rolled mild steel reinforcing bars, of grade similar to the BS 4360 Grade 43 structural steels, up to 700°C under isothermal test conditions. Lengths of full size sections were tested by heating the specimen up to the test temperature, leaving it to soak for 30 minutes, then loading at a rate of 0.1% to 0.3% strain per minute according to BS 3688. Figure 2.7 (consolidating Figures 7.8, 7.9 and 7.10 of the reference[2.18]) shows the variation of E with temperature. It can be seen that the E value at 550°C has reduced to about 65% of the room temperature value, and that there is some scatter in the results. A summary of the tests have been reported by Holmes et al[2.19].

Committee T3 of the European Convention for Constructional Steelwork (ECCS) has produced a recommendation[1.26] for the variation of E with temperature for use in analytical studies of structural steel. The curve (Figure r-3 in the recommendations) is shown in Figure 2.8. The ECCS recommendations state that E is the tangent modulus for $\sigma \to 0$ and is not defined for temperatures above 600°C because the effect of creep has to be analysed explicitly for such temperatures.

The British Steel Corporation disagreed with the proposed ECCS recommendation as a result of an international survey in 1980 of E value data[2.20]. Included in this survey were many dynamically and some statically derived data for different grades (FE310, 360, 430 and 510) of Euronorm 25-1972 structural steel, which the writer has extrapolated from and averaged to obtain the curve shown in Figure 2.9. This relationship has been used in this thesis, where it is called 'BSC/Euronorm E'data.

Jerath et al of the British Steel Corporation Teesside Laboratories reported[2.21] in 1980 a study of the isothermal tensile properties for about 15 different low carbon steels which fell between Grades 43A and 50D of BS 4360. The principal object was to establish a relationship between 1% proof stress and temperature since the authors claimed it had been found that full scale members, beams for example, were at the point of collapsing in fires when the strain reached 1%. Some stress strain curves were also presented and Figure 2.10 (Figure 20 in the reference) illustrates typical data for a Grade 43A steel. Particular features in these curves, such as the serrated flow at 125°C, are discussed in a later report[2.22]. In these tests the specimens were maintained at constant temperature (at the appropriate elevated temperature) for 30 minutes before straining at a rate of 1 mm/minute over the 60 mm gauge length.

The BSC test programme was extended to provide anisothermal test data for structural steels. The test variables were composition and strength for the different grades of steel, heating rate, and level of applied stress. Preliminary results were reported[2.23] in 1982 by Kirby and Thomas. Analysis of the data showed moderate agreement with the data derived by BHP for the 1% total strain temperature as shown by Table 2.5.

BSC's anisothermal test work was taken further and completed in 1983. Kirby has reported[2.22] the results. Two grades of steel were tested. These conformed to Grades 43A and 50B of BS 4360 : 1979, which are said to represent 98% of the structural steel sections manufactured by BSC, and have room temperature properties approximately corresponding to Euronorm 25-72 : Fe 430 and Fe 510 respectively. The heating rates were 20, 10, 5 and, sometimes, 2.5°C/min corresponding to failure times in the range of

0.5 to 4 hours in the BS 476 : Part 8 : 1972 fire resistance test for steel beams, assuming a limiting temperature of approximately 600°C. The applied stress, which was maintained constant in each test, varied from 15 to 250 N/mm² for Grade 43A and from 15 to 400 N/mm² for Grade 50B, and wherever possible each test was continued to 5% strain. Note, however, that the maximum strain of normal interest is 2-3% (see 2.4.7).

A typical family of strain temperature curves are shown in Figure 2.11 (Figure 10 of the reference). These data are for a Grade 43A steel having a measured room temperature yield stress of 267 N/mm² (compared with a BS 5950 : Part 1 : 1985 design stress of 275 N/mm²) heated at 10°C/min. The strains are the sum of the elastic and plastic components, the thermal strains having been previously deducted. The curves show several important features:

i) the occurrence of large initial strains at relatively low temperature when the stress level is high and yielding occurs. For instance a strain of 0.5% at a temperature of roughly 200°C for a stress of 250 N/mm²

ii) the onset of large rates of strain for little increase in temperature, sometimes called 'runaway displacement' in beam tests.

iii) the effect of phase transformation shows itself at temperatures around 720°C for low stresses. It can be seen that a sudden increase in strain from 0.2 to 0.4% occurs with little increase in temperature for a stress of 25 N/mm².

From the strain temperature curves, such as those shown in Figure 2.11, it is possible to produce stress strain relationships and from these to obtain the elastic moduli at different temperatures. Each stress strain relationship is produced for the relevant temperature in the following way. Assume the stress strain curve for 500°C is required. Using Figure 2.11 a vertical line is drawn at 500° and the strain at A is read off. This corresponds to a stress of 25 N/mm^2. Similarly the strain at B is read off corresponding to 50 N/mm^2, and so on for points C to F. If instead of stress, the ratio of applied stress divided by room temperature yield stress is required, then a family of strength reduction factor versus strain curves can be derived.

This BSC work has been used to produce the strength reduction factor versus strain relationships for BS 4360 Grades 43 and 50 presented in the draft BS 5950 : Part 8 code. The data are shown in Figure 2.12. The anisothermal E value data, derived by calculating slopes from tabular data in the draft code, is given in Table 2.6.

Also quite recently, the Luxembourg steel company, Arbed, has produced E value data[2·24] for steel used in a finite element computer program for composite I-section steel and concrete columns. The data, taken from Figure 12 of the reference, are shown in Figure 2.13.

In summary it can be seen that many different E versus temperature relationships exist. In the course of the analytical work reported herein, the writer has used the ECCS recommendation (Figure 2.8), and the averaged BSC/Euronorm data (Figure 2.9) - the former representing 'low' values, the latter, 'high' values, for use in sensitivity analyses. The Arbed data

(Figure 2.13) has also been used. The most recent BSC data (Table 2.6) has not been used since it was not available when the analyses were made.

2.4.5 Significance of differences in elastic modulus at elevated temperatures

The importance of the amount of reduction in E at elevated temperature depends upon the full scale fire test conditions. On the one hand it is shown in Figure 6.12 that the increase in displacement (due to the reduction of E) of a loaded steel I beam having a large temperature difference between the flanges is a small part of the total displacement up to the point of runaway displacement and this is due to the dominance of thermal bowing. In other words the total displacement is not sensitive to the precise amount of reduction in E at elevated temperatures. On the other hand if thermal bowing is absent, as in a steel suspension bar for instance, the effect of the reduction in E is a maximum but is nonetheless small as the following example shows.

Assume a BS 4360 : Grade 43A steel member 1000 mm long is heated from 0°C to 500°C when subjected to the maximum permissible stress (165 N/mm^2) in uni-axial tension. Ignore plastic strain.

Thermal expansion $= \Delta_{ex} = \alpha LT = 0.000014 \times 1000 \times 500 = 7$ mm

Elastic displacement $= \Delta_{el} = \frac{\sigma L}{E} = \frac{1.65 \times 10^5}{E}$

$\therefore \Delta_{el} = 1.46$ mm for ECCS $E = 1.125 \times 10^5$

$\therefore \Delta_{el} = 0.948$ mm for Euronorm $E = 1.74 \times 10^5$

Total displacement $= \Delta_{ex} + \Delta_{el}$

$= 7.948$ mm (ECCS)

$= 8.46$ mm (Euronorm)

Thus the percentage difference in total displacement when using these two different E values is $\frac{0.5}{8} \times 100 = 6$

However, the choice of E versus temperature relation has a trivial effect once plasticity has set in because the plastic displacements are relatively large.

2.4.6 Idealised stress-strain data at elevated temperatures

Most finite element programs require input of the stress-strain curves as bi-linear or multi-linear idealisations for each temperature. The program may then linearly interpolate values of stress and strain for intermediate temperatures.

Making the idealisations is not an easy matter especially if the elastic and plastic domains are to be idealised bi-linearly, that is using one straight line to represent the elastic modulus and another to represent the plastic modulus. The difficulty can be appreciated from Figure 2.14 which shows for clarity a single stress strain curve corresponding to a particular temperature - in this example an isothermal curve for 500°C. Two extreme but plausible alternative bi-linear idealisations are shown by OAA' and OBB'. It will be apparent that OAA' may be appropriate for strains up to 0.3% but will overestimate the stress at higher strains. OBB', on the other hand, is a good fit for large strains but greatly overstates the stress at the knee, B. Another problem is that small increases in stress above the knee causes large increases in strain and this could result in many computer iterations if the load steps are not small.

The problem of choosing a best fit bi-linear curve is clearly made easier if the strain range can be minimised. Alternatively, the problem can be minimised using multi-linear idealisations.

2.4.7 Limiting plastic strain

Full scale fire resistance tests on simply supported I-section steel beams spanning 4.5 m have shown that plastic strains attained by the lower (hottest) flange, when measured at room temperature after tests, can exceed 3% in the centre of the span where the bending stress is greatest (and equal to the maximum permissible elastic stress). In one test[2.25] on a 356 x 171 x 67 kg/m I-section beam, exposed to heat on 3 sides and loaded to produce the maximum permissible elastic stress of 165 N/mm^2, the strain over the central 500 mm gauge length of the lower flange was 3.78% while the strain in the adjacent 500 mm gauge lengths was an average of 2.2%. In another test[1.23], on a 305 x 165x 40 kg/m I-section shelf angle floor beam exposed to heat on the bottom flange and the lower part of the web and loaded to produce the maximum permissible stress of 165 N/mm^2, the maximum strain over the central 500 mm gauge length was 1.4%. Both of the above tests were stopped when the central displacement was approximately 150 mm corresponding to the BS 476 : Part 8 displacement criterion of span/30.

Observations such as these raise the thought that perhaps all steel beams fail the displacement criterion when a plastic strain of 2 to 3% is reached. The notion of a limiting strain is important since if it were shown to be generally valid it would mean that tensile tests could be confined to 3% strain and it would make easier the job of idealising stress strain data for analytical work (see 2.4.6).

The general validity can be checked by considering 2 beams with greatly different depths but identical span. At failure the radius of curvature of both beams must be the same. To achieve a given radius of curvature the deeper beam will have to experience a larger strain in the extreme fibres because of the greater distance to the neutral axis, and vice versa for the shallow beam. It follows that there is no such thing as a common limiting strain for beams of all depths.

What can be said, however, is that in anisothermal tensile tests, runaway displacement is well established at 1% strain (Figure 2.11) such that large increases in displacement occur for small increases in temperature.

CHAPTER 3. THEORY OF UNRESTRAINED THERMAL BOWING OF A MEMBER

In this chapter a simple theory of thermal bowing is developed based solely on geometry. It covers the case of an unrestrained simply supported beam and an unrestrained fixed-base cantilever which has a linear temperature profile across the section. The theory provides linear displacements in the direction of heat flow, and rotational displacements at the ends and intermediate positions along the member. The theory provides these data for a member in which the linear temperature profile across the section varies, and does not vary, along the length of the member. Some example calculations are given. The chapter concludes with a qualitative discussion of the effect of internal stresses developed across the section when the temperature profile across the section is curvi-linear and when the elastic modulus varies across the section due to temperature effects.

3.1 Assumptions

In the following theory the assumptions are that:

i) The coefficient of linear thermal expansion α does not vary throughout the member ie the material is homogenous and is independent of temperature, and is assumed to be nominally $14 \times 10^{-6}/°C$.

ii) The variation of temperature across the section in the direction of heat flow is linear.

iii) There is no variation of temperature in the section normal to the direction of heat flow.

iv) Plane sections remain plane so that strain is proportional to the distance from the neutral axis.

v) The section is free of internal stresses. It would not be if the temperature distribution was non-linear or if the member was subjected to external loads.

3.2 Displacements of a non-loaded, simply supported member having a linear temperature profile across its depth which does not vary with length

Consider a simply supported member of length L and depth d, Figure 3.1. It is subjected to heating on the upper face such that the upper face is at a constant temperature throughout its length and the lower face is also at a constant but lower temperature throughout its length, with the temperature varying linearly between the faces by an amount T_1. No external loads are applied. The beam bows upwards in a circular arc and each end rotates through angle θ. It remains free of internal stresses. For an element length dx, the expansion of the uppermost fibre is:-

$$de = \alpha \frac{T_1}{2} dx$$

The angular change in element dx is:

$$d\theta = \frac{de}{h} = \alpha \frac{T_1}{2h} dx \qquad (3.1)$$

Integrating Equation (3.1) gives:

$$\theta = \int_0^{L/2} d\theta = \frac{\alpha T_1}{2h} \int_0^{L/2} dx = \frac{\alpha T_1}{2h} \cdot \frac{L}{2} = \frac{\alpha T_1 L}{2d} \qquad (3.2)$$

It is now necessary to express θ in terms of central displacement Δ. Using the properties of similar triangles it follows from Figure 3.2 that CB/AC = ED/EB. For small θ, CB = L/4 so that:

$$\frac{L/4}{R} = \frac{\Delta}{L/2} \quad \text{from which}$$

$$R = \frac{L^2}{8\Delta} \tag{3.3}$$

Ignoring Δ which is small compared with R,

$$\theta = \tan^{-1} \frac{L/2}{R} \quad \text{from which, for small angles}$$

$$\theta = \frac{L}{2R} \tag{3.4}$$

Substituting R from Equation (3.3) in Equation (3.4) gives:

$$\theta = \frac{4\Delta}{L} \quad \text{and substituting this in Equation (3.2) gives:}$$

$$\theta = \frac{\alpha T_1 L}{2d} = \frac{4\Delta}{L} \quad \text{so that} \tag{3.5}$$

$$\Delta = \frac{\alpha T_1 L^2}{8d} \tag{3.6}$$

Hence knowing the length L and depth d of member, the coefficient of linear expansion α and the temperature difference T_1 between heated and unheated faces, it is possible to calculate the bowing displacement at mid span. Equation (3.6) can also be used to calculate θ and Δ for finite lengths of member each of which is subjected to a different temperature difference. The theory is developed in 3.4.

3.3 Displacements of a non-loaded, cantilevered member having a linear temperature profile across its section which does not vary with length

A cantilever, such as a column or wall, of height H and the thickness d has a linear temperature profile arising from a temperature difference across the two faces of T_1. The member, if fixed at its base and free of external forces, will bow into a circular arc, Figure 3.3

Consider the displacements of a small element of length dx. The thermal expansion of one face relative to the other is de and this causes an elemental rotation of $d\theta$. From Figure 3.3

$$d\theta = \frac{de}{d} = \frac{\alpha T_1 \, dx}{d} \tag{3.7}$$

$$\Delta_H = \int_0^H x \, d\theta \tag{3.8}$$

Substituting Equation (3.7), in (3.8) gives:

$$\Delta_H = \int_0^H x \, \frac{\alpha T_1 \, dx}{d} = \frac{\alpha T_1}{d} \int_0^H x dx = \frac{\alpha T_1}{d} \left[\frac{x^2}{2}\right]_0^H$$

$$\Delta_H = \frac{\alpha T_1 H^2}{2d} \tag{3.9}$$

Alternatively, from geometry:

$$(2R - \Delta_H) \, \Delta_H = (H + \Delta_V)^2$$

$$2R \, \Delta_H - \Delta_H^2 = \left\{H + \frac{\alpha T_1 H}{2}\right\}^2$$

Ignoring Δ^2_H, Δ_V and Δ^2_V as small quantities gives:

$2R \, \Delta_H = H^2$ from which

$$\Delta_H = \frac{H^2}{2R} \qquad (3.10)$$

Curvature $= \frac{1}{R} = \frac{d\theta}{dx}$ and from Equation (3.7)

$$\frac{1}{R} = \frac{d\theta}{dx} = \frac{\alpha T_1}{d} \qquad (3.11)$$

Substituting Equation (3.11) in (3.10) gives:

$$\Delta_H = \frac{\alpha T_1 H^2}{2d} \qquad (3.12)$$

Note that Equations (3.12) and (3.9) are the same.

3.4 Displacements of a non-loaded, simply supported member comprising 4 finite lengths, each having a different linear temperature profile across the section

Consider a member of total length L in which the linear temperature profile differs in each of four finite lengths, Figure 3.4.

Expressions will be developed for (i) rotations at the ends and at intermediate points and (ii) vertical displacement at any point along the member.

$\frac{d^2y}{dx^2} = \frac{1}{R}$ and as $L = R\theta$ when θ is small

$\frac{d^2y}{dx^2} = \frac{\theta}{L}$ and from Equation (3.1), $\theta = \frac{\alpha T_i L}{d}$ so that:

$$\frac{d^2 y}{dx^2} = \frac{\alpha T_i}{d}$$ and integrating gives:

$$\frac{dy}{dx} = A + \frac{\alpha}{d}\int T_i \, dx$$, where A is the constant of integration which equals θ_o since $dy/dx = \theta_o$ when $x = 0$. So that:

$$\frac{dy}{dx} = \theta_o + \frac{\alpha}{d}\int T_i \, dx \qquad (3.13)$$

$$\frac{dy}{dx} = \theta_o + \frac{\alpha}{d} T_1 x \quad \text{for } x < L_1$$

$$\frac{dy}{dx} = \theta_o + \frac{\alpha}{d}\left[T_1 L + T_2 (x - L_1)\right]$$

$$\frac{dy}{dx} = \theta_o + \frac{\alpha}{d}\left[T_1 x + (T_2 - T_1)(x - L_1)\right] \text{ for } L_1 < x < (L_1 + L_2)$$

$$\frac{dy}{dx} = \theta_o + \frac{\alpha}{d}\left[T_1 x + (T_2 - T_1)(x - L_1) + (T_3 - T_2)(x - L_1 - L_2)\right]$$

for $L_1 + L_2 < x < L_1 + L_2 + L_3$

Hence, by further integration:

$$y = \theta_o x + \frac{\alpha}{2d} T_1 x^2 \quad \text{for } x < L_1$$

$$y = \theta_o x + \frac{\alpha}{2d}\left[T_1 x^2 + (T_2 - T_1)(x - L_1)^2\right] \qquad (3.14)$$

for $L_1 < x < L_1 + L_2$

etc.

$y = 0$ when $x = L$ or $L_1 + L_2 + L_3 + L_4$ hence:

$$y = \theta_o (L_1 + L_2 + L_3 + L_4) + \frac{\alpha}{2d} [T_1 (L_1 + L_2 + L_3 + L_4)^2$$

$$+ (T_2 - T_1)(L_2 + L_3 + L_4)^2 + (T_3 - T_2)(L_3 + L_4)^2$$

$$+ (T_4 - T_3) L^2_4 = 0$$

Transposing gives:

$$\theta_o = - \frac{\alpha}{2d (L_1 + L_2 + L_3 + L_4)} [T_1 (L_1 + L_2 + L_3 + L_4)^2 +$$

$$(T_2 - T_1)(L_2 + L_3 + L_4)^2 + (T_3 - T_2)(L_3 + L_4)^2 +$$

$$(T_4 - T_3) L^2_4] \qquad (3.15)$$

When $x = L_1$, $\theta_1 = \frac{dy}{dx} = \theta_o + \frac{\alpha}{d} T_1 L_1$

Similarly:

$$\theta_2 = \theta_o + \frac{\alpha}{d} (T_1 L_1 + T_2 L_2)$$

$$\theta_3 = \theta_o + \frac{\alpha}{d} (T_1 L_1 + T_2 L_2 + T_3 L_3)$$

$$\theta_4 = \theta_o + \frac{\alpha}{d} (T_1 L_1 + T_2 L_2 + T_3 L_3 + T_4 L_4) \qquad (3.16)$$

Worked example to validate theory.

To check that the theory for end rotation is valid, a worked example is given based on the following data:

$L_1 = 1000$ mm; $L_2 = 1500$ mm; $L_3 = 1000$ mm; $L_4 = 500$ mm; $T_1 = 200°C$;

$T_2 = 250°C$; $T_3 = 160°C$; $T_4 = 100°C$; $d = 50$ mm; $\alpha = 0.000014/°C$ for steel

The sum of θ_0 and θ_4 using Equations (3.15) and (3.16) should equal the total rotation of the beam obtained by using an average temperature difference applied to the total length L from Equation (3.15):

$$\theta_o = - \frac{0.000014}{2 \times 50 \times 4000} [200\ (4000)^2 + 50\ (3000)^2 - 90\ (1500)^2 - 60\ (500)^2]$$

$$\theta_0 = -3.5 \times 10^{-4} \times 343.25 = - 0.12013 \text{ radians}$$

From Equation (3.16)

$$\theta_4 = \theta_0 + \frac{0.000014}{50} (785000) = - 0.12013 + 0.2198$$

$$= 0.09967 \text{ radians}$$

Total rotation $= \theta_0 + \theta_4 = 0.1201 + 0.09967$

$= 0.21977$ radians

Now, using average temperature difference method:

Average temperature difference/unit length =

$$\frac{L_1 T_1 + L_2 T_2 + L_3 T_3 + L_4 T_4}{L_1 + L_2 + L_3 + L_4}$$

$$= \frac{1000.200 + 1500.250 + 1000.160 + 500.100}{4000}$$

$= 196.25°C$

As the total rotation is $2\theta_0$, using Equation (3.5) the total rotation is:

$$\frac{2\alpha\, TL}{2d} = \frac{0.000014 \times 196.25 \times 4000}{50} = 0.2198 \text{ radians}$$

It can be seen that the two approaches give the same answer ie 0.21977 radians compared with 0.2198 radians.

3.5 Displacements of a non-loaded, simply supported member comprising many finite lengths, each having a different linear temperature profile across the section

From the theory presented in 3.4 it can be seen that to calculate the lateral displacement at any point it is first necessary to calculate the rotation at one end, say θ_o, using a generalised form of Equation (3.15) and then substitute this in a generalised form of Equation (3.14) to obtain the displacement. The generalised equations used for this purpose are derived below.

From Equation (3.15) we can write:

$$\theta_o = -\frac{\alpha}{2dL}\left[T_1 (L)^2 + (T_2 - T_1)(L - L_1)^2 + (T_3 - T_2)\{L - (L_1 + L_2)\}^2 + (T_4 - T_3)\{L - (L_1 + L_2 + L_3)\}^2 + (T_5 - T_4)\{L - (L_1 + L_2 + L_3 + L_4)\}^2 + \ldots\right]$$

From inspection it is clear that any term in the square brackets may be written in the general form:

$$(T_i - T_{i-1})\left\{L - \sum_{i}^{i-1} L_i\right\}^2 \text{ so that:}$$

$$\theta_o = -\frac{\alpha}{2dL} \sum (T_i - T_{i-1})\left\{L - \sum_{i}^{i-1} L_i\right\}^2 \qquad (3.17)$$

Similarly, from Equation (3.14) we can write:

$$y = \theta_0 x + \frac{\alpha}{2d}\left[T_1 x^2 + (T_2 - T_1)(x - L_1)^2 + (T_3 - T_2)\{x - (L_1 + L_2)\}^2 + (T_4 - T_3)\{x - (L_1 + L_2 + L_3)\}^2 + (T_5 - T_4)\{x - (L_1 + L_2 + L_3 + L_4)\}^2 + \ldots\right]$$

$$\text{for } L_1 + L_2 + L_3 + L_4 < x < L_1 + L_2 + L_3 + L_4 + L_5$$

Similarly from inspection it is clear that any term in the square brackets may be written in the general form:

$$(T_i - T_{i-1})\left\{x - \sum_1^{i-1} L_i\right\}^2 \text{ for } \sum_1^{i-1} L_i < x < \sum_1^{i} L_i \text{ hence:}$$

$$y = \theta_0 x + \frac{\alpha}{2d} \sum (T_i - T_{i-1})\left\{x - \sum_1^{i-1} L_i\right\}^2$$

$$\text{for } \sum_1^{i-1} L_i < x < \sum_1^{i} L_i \qquad (3.18)$$

From Equations (3.17) and (3.18) we have:

$$y = -\frac{x\alpha}{2dL} \sum (T_i - T_{i-1})\left\{L - \sum_1^{i-1} L_i\right\}^2 + \frac{\alpha}{2d} \sum (T_i - T_{i-1})\left\{x - \sum_1^{i-1} L_i\right\}^2 \text{ for } \sum_1^{i-1} L_i < x < \sum_1^{i} L_i \qquad (3.19)$$

These equations are used in an analysis of experimental data for an unrestrained beam heated along half the flange, see 4.2.2 and 4.3.2.

3.6 Effect of variable elastic modulus on unrestrained thermal bowing.

In the theory given above it was assumed that the temperature varied linearly across the depth of a member. For a homogeneous material such as structural steel which has a coefficient of linear thermal expansion mainly independent of temperature, a member free of external forces would bow in a stress-free condition, Figure 3.5(a).

In practice however, and as demonstrated in the experiments described herein, temperature variation is non-linear across the member section. This means that different longitudinal fibres would, if free of any restricting shear stresses from its neighbours, expand by different amounts. If sections are to remain plane the result is that some fibres will be placed in compression and others in tension. The stress distribution for a member subjected to a non-linear temperature variation are shown qualitatively in Figure 3.5(b) and (c). The effect of variable modulus of elasticity is to reduce the compression stress block on the heated side: compare stress block ABC for reduced modulus of elasticity with stress block ABD in Figure 3.5(b) and (c). The reduced size of the compressive stress block on the heated side of the member could have the result of reducing the magnitude of bowing. This effect has been examined in PAFEC finite element analyses in 4.4.5; see particularly Table 4.5.

CHAPTER 4. EXPERIMENTS ON UNRESTRAINED BEAMS AND COLUMNS HEATED ALONG ONE FLANGE

This chapter begins with the results of experiments on an unrestrained model beam heated over the whole flange and half the flange, and compares the experimentally observed mid-span displacements with those predicted from the simple theory given in 3.2 and 3.5. Predicted displacements are then presented for finite element analyses based on elastic theory using the PAFEC suite of programs, and a number of sensitivity analyses are reported. The chapter concludes with a comparison of the experimental and theoretical mid-height bowing displacements of an unrestrained full size column partly built into the external wall of a large fire test compartment at Cardington, showing that the simple theory is valid for model scale and full scale members.

4.1 Experiments on an unrestrained model beam

The object of the experiments described in this chapter was to heat a steel member non-uniformly across its section so as to cause unrestrained thermal bowing and to measure accurately the temperature distribution throughout the member and the central displacement. The experiments were preceded by thermal bowing experiments on unrestrained small steel plate beams and I-section beams heated along one face with quartz fabric insulated flexible electrical heating tapes of relatively low heat output. Although the mid-span displacements obtained in these tests correlated well[4.1] with the displacements predicted from the theory given in 3.2, the heat output of the tapes was not sufficient to produce steel temperatures in the phase transformation range (ie temperatures above 720°C) which were known to occur in full size building elements.

4.1.1 Test apparatus

An elevation and section of the apparatus is shown schematically in Figures 4.1 and 4.2. An overall view is given in Figure 4.3.

(i) Strong beam

The I-section strong beam was a 305 mm by 165 mm by 54 kg/m universal beam of 2 m length rolled from ordinary mild steel (BS 4360 Grade 43).

(ii) Restraint frames

Three identical rectangular restraint frames were fabricated by welding 50 mm square hollow steel section having a wall thickness of 5 mm.

To enable the restraint frames to be held up in position before positioning of the test specimen, a small length of steel angle section was welded onto the inner face of each side member leaving sufficient clearance to enable the frames to be slid along the bottom flange of the strong beam. Once spaced the correct distance apart, the restraint frames were prevented from further longitudinal movement using bolts in tapped holes in the centre of the angle which bore onto the strong beam flange. The frames were, however, free to rotate about the strong beam so that axial thermal movement of the specimen would be unrestrained.

The three restraint frames incorporated a) horizontal 9 mm dia long bolts used to adjust and retain the web of the specimen centrally and, in the case of the central restraint frame, to provide lateral stability to the test specimen, b) vertical projections from the lower member to locate the restraint frame centrally with respect to the strong beam section, c) pairs of plates welded to the top member to act as vertical guides for the straight edge and, d) bolt heads projecting below the

knife edge on the upper member for supporting the ends of the specimen. Details a), c) and d) are shown in Figure 4.4.

(iii) Electrical heating equipment and thermal insulation

From earlier tests on shorter lengths of steel and aluminium section it was evident that the power output of quartz insulated electrical heating tapes would be inadequate for larger specimens bearing in mind that higher temperatures were required. It was therefore decided to use coiled heating elements enclosed in high temperature ceramic insulators. A survey of proprietary heaters suggested that channel heaters (having a surface loading of 7.5 W/cm^2 and capable of operating up to 1050°C) manufactured by Electrothermal Engineering Ltd, Southend-on-Sea, Essex,. might be suitable. For the tests two heaters (Type NC 8711) each 67 mm wide by 30 mm thick by 680 mm long, rated at 3.5 kW and operating at 60 V were purchased, Figure 4.5.

To provide a 60 V supply it was necessary to procure two transformers with a primary and secondary voltage of 240 and 60 V respectively capable of producing a secondary current of approx 50 A. To vary the secondary power two variacs already available at Fire Research Station were used.

The heaters were held against the lower face of the bottom flange of the specimen using galvanised wire ties threaded through 2 mm dia holes at roughly 130 mm pitches in the web of the specimen. To reduce heat loss from the heaters, 25 mm thick strips of Triton Kaowool ceramic (alumino silicate) fibre insulation board manufactured by Morganite Ceramic Fibres Ltd, Wirral, Merseyside, were cut and arranged to encapsulate the

lower flange of the specimen and heating elements. These strips were held in place with a row of galvanised steel wire ties threaded through holes in the web of the specimen.

(iv) Straight edge and displacement transducer

The straight edge was made of ordinary mild steel flat bar 1340 mm long by 70 mm deep by 6.35 mm thick, Figure 4.6. End legs 80 mm long by 12 mm wide were welded on. The straight edge was a close sliding fit between the guide plates on the restraint frames so as to ensure that the straight edge always rested on the specimen in the same place and could not tilt so as to give inacurrate displacement readings. Thus the straight edge could be placed in position, the displacement reading taken, and the straight edge removed in a time of roughly 10 seconds. In addition a trough of cold water was provided into which the straight edge assembly could be stored between readings without immersing the body of the transducer, and this was used in the later stages of a test to be certain that thermal bowing of the straight edge and expansion of the displacement transducer shaft did not occur as a result of conducted, convected and radiated heat from the specimen below.

Vertical displacement at the mid-span of the specimen was measured using a precision linear displacement transducer, having a limiting excitation of 130 V and an operational temperature range of -50 to +80°C, manufactured by Penny and Giles Potentiometers Ltd, Christchurch, Dorset. The transducer, model HLP 190-FS1-75-3K, had a lightly sprung-loaded shaft with a travel of 75 mm. It was attached to the centre of the straightedge with rapid setting epoxy adhesive. The displacement transducer was connected to a constant voltage device. This was a Thurlby PL Series power supply, Type PL 310.

(v) Data logging

The 60 pairs of thermocouple wires were connected to 5 terminal boxes each having 12 channels which in turn were connected, using 5 Plessey connectors, to a Fluke 2240B data logger manufactured by John Fluke Manufacturing Co Inc, Washington, USA. This was programmed to print out the 60 rows of data on 60 mm wide paper every 2 minutes.

The displacement transducer when excited by a constant 20 V supply had its output connected to a single channel of a 30 channel Solartron 3430 data logger programmed to print out every 2 minutes.

4.1.2 Test specimen and thermocouples

The smallest rolled I-section steel 'joist' commercially available in the United Kingdom was used. It was 104 mm deep by 44 mm wide by 7.35 kg/m and nominally 1500 mm long. It had tapered flanges and a second moment of area about the major axis of 152.3 cm^4. The steel was BS 4360, Grade 43 (ie ordinary mild steel).

To obtain a comprehensive profile of temperatures across the depth and along the length of the specimen, 12 stations of thermocouples were adopted, the station spacing being 128 mm. At each station 5 thermocouples were used; these were equi-spaced over the depth of the section except for the thermocouple nearest the flange to be heated which was fixed to the inner flange face - fixing to the outer flange face would have meant that the wires a) would prevent the heating element making direct contact with the flange face and b) might give false readings if the insulating sheath failed where the wires had to bend to follow the contour of the specimen section. The details of the

60 thermocouple positions are given in Figure 4.7. Blind holes for the thermocouple wires were drilled 0.5 mm diameter by 3 mm deep spaced 6 mm apart and the thermocouple wires carefully peened in and additionally secured using Autostic high-temperature resisting adhesive and left to dry for 24 hours. Autostic is a high performance ceramic and industrial cement capable of operating up to 1500°C while providing electricial insulation. It is manufactured by Carlton Brown and Partners Ltd, Elford, Tamworth, Staffs. The thermocouples were asbestos sheathed 0.47 mm dia wires of Ni/Ch and Ni/Al, manufactured by BICC General Cables Ltd, Liverpool. In addition two rows of holes were drilled in the web near the flange to be heated; these were to enable wires to be passed through so as to keep the heating elements and insulation in place.

4.1.3 Test procedure

The constant voltage supply and data loggers were switched on roughly 30 min before commencement of test so that they could stabilise, with some of the laboratory windows open to provide ventilation for dilution of the noxious and irritant fumes given off by the binder incorporated in the Kaowool insulation board. The data loggers were run so as to obtain ambient temperature readings. The displacement transducer was calibrated for a 20 V excitation and it was found that 1 volt output equalled 3.8 mm shaft movement.

The power to the two electrical heating elements was switched on and input to each element equalised using the two variacs. The straightedge was placed on the specimen roughly 10 seconds before the data logger printed out and removed immediately after print out and placed in the

water trough; this was repeated every 2 minutes. Frequent checks were made to ensure that the temperatures in one half of the specimen were roughly the same as in the other half, and it was found unnecessary to have different settings on the two variacs to accomplish this.

The same procedure was followed for the half heated specimen except that only one heater was switched on.

4.1.4 Test results

The temperature data at intervals of 2 minutes are given in Tables 1 and 2, Appendix 2 for the whole length heated test and half length heated test respectively.

The central displacements, computed using the calibration factor of 3.8 mm/volt, for the whole length heated test and the half length heated tests are given in Figures 4.8 and 4.9 respectively.

4.1.5 Comments on test results

(i) Temperature distribution, whole length heated

From the tabular form of the thermocouple data it is not easy to visualise the temperature profiles and it was therefore considered desirable to plot the data at three stages in the test duration, ie at 16 min, 32 min and 48 min. These profiles are shown in Figure 4.10. The cuvilinear form of the profiles across the member depth is to be expected for heating along one flange. The slight depression in temperature at mid-span is caused by the discontinuity of heating where the heating elements abut and less effective thermal insulation in that zone.

It is clear from Figure 4.10 that the temperature distribution is symmetrical on either side of the centreline and this is to be expected as the two variacs were adjusted to supply the same electrical power to each heating element.

(ii) Temperature distribution, half length heated

Temperature profiles at 16, 32 and 48 min are given in Figure 4.11. The figure shows that conduction of heat into the unheated central portion results in appreciably lower temperatures at the two stations bounded by thermocouples 26 to 30 and 31 to 35. Comparison of Figures 4.10 and 4.11 shows that the temperatures attained in the heated portions bounded by thermocouples 36 to 60 are approximately the same for the member when heated over the whole length and half the length.

(iii) Displacement, whole length heated

In the curve of central displacement, Figure 4.8, there is an unexpected depression between 26 and 36 minutes of heating, with no increase in displacement over a period of 4 minutes. This phenomenon could not be explained by malfunction of the heating elements or performance of the displacement transducer and it was therefore assumed that it was due to phase transformation and/or reduction in modulus of elasticity (see 2.3.3 and 2.4.4).

(iv) Displacement, half length heated

The curve of central displacement, Figure 4.9, also shows a slight depression between 26 and 34 minutes. The magnitude of the depression

is approximately half that for the member heated over the whole length and this further supports the conclusion that this is a phase transformation effect as the contraction is present over only half the member length. It can also be seen that the central displacement is, as might be expected, roughly half that of the member when heated over the whole length.

4.2 Theory of unrestrained thermal bowing applied to unrestrained model beam experiments

As explained in 3.1 the theory assumes that the temperature variation across the section is linear. The experimental results, however, show a marked curvilinear variation. To obtain a best-fit straight line from the experimental data a commercial computer program (GLIM) was used. Using temperature and thermocouple location as x and y co-ordinate inputs the program produced the slope of the best-fit line (temperature/depth of section) which could be used directly in the theory.

4.2.1 Central displacement, whole flange heated

Table 4.1 provides temperature data averaged over the twelve stations (average of data given in Table 1 of Appendix 2). Also included in the table are the slopes of the best-fit line using GLIM and the corresponding computed central displacement. The computed displacement was obtained using Equation (3.6) from 3.2:

$$\Delta = \frac{\alpha\, TL^2}{8d} = \frac{14 \times 10^{-6} \times 1320^2}{8} \frac{T}{d} = 3.0492\ T/d \qquad (4.1)$$

4.2.2 Central displacement, half flange heated

In this analysis it is assumed that the temperatures at each station given in Table 2 of Appendix 2 apply throughout a distance equal to half the station spacing either side of the station in question. This gives rise to finite lengths L_1, L_2 .... L_{11} to be used in the theory as shown in Figure 4.12.

It will be recalled that it is necessary to calculate θ_0 and use this to calculate the central displacement y (or Δ). From Equation (3.15) or (3.17) in 3.4 and 3.5 respectively:

$$\theta_0 = -\frac{\alpha}{2dL}\left[T_1 L^2 + (T_2-T_1)(L-L_1)^2 + (T_3-T_2)(L-L_1-L_2)^2 + (T_4-T_3)(L-L_1-L_2-L_3)^2 + (T_5-T_4)(L-L_1-L_2-L_3-L_4)^2 + (T_6-T_5)(L-L_1-L_2-L_3-L_4-L_5)^2 + (T_7-T_6)(L-L_1-L_2-L_3-L_4-L_5-L_6)^2 + (T_8-T_7)(L-L_1-L_2-L_3-L_4-L_5-L_6-L_7)^2 + (T_9-T_8)(L-L_1-L_2-L_3-L_4-L_5-L_6-L_7-L_8)^2 + (T_{10}-T_9)(L-L_1-L_2-L_3-L_4-L_5-L_6-L_7-L_8-L_9)^2 + (T_{11}-T_{10})(L-L_1-L_2-L_3-L_4-L_5-L_6-L_7-L_8-L_9-L_{10})^2\right]$$

To use best fit T/d data the equation must be rewritten so:

$$\theta_0 = -\frac{\alpha}{2L}\left[\frac{T_1}{d}L^2 + \left\{\frac{T_2}{d}-\frac{T_1}{d}\right\}(L-L_1)^2 + ...\right]$$

Using the temperature data in Table 2 of Appendix 2, GLIM was used to obtain the slopes (T/d) of the best-fit straight lines at heating increments of 8 minutes. The data for each of the 12 stations are given in Table 4.2.

Substituting data for L, L_1, L_2 ..... L_{10} and α in the equation for θ_0 gives:

$$\theta_0 = -\frac{.000014}{2 \times 1310}\left[\frac{T_1}{d} \times 1310^2 + \left\{\frac{T_2}{d} - \frac{T_1}{d}\right\} 1276^2 + \left\{\frac{T_3}{d} - \frac{T_2}{d}\right\} 1148^2\right.$$

$$+ \left\{\frac{T_4}{d} - \frac{T_3}{d}\right\} 1020^2 + \left\{\frac{T_5}{d} - \frac{T_4}{d}\right\} 892^2 + \left\{\frac{T_6}{d} - \frac{T_5}{d}\right\} 764^2$$

$$+ \left\{\frac{T_7}{d} - \frac{T_6}{d}\right\} 636^2 + \left\{\frac{T_8}{d} - \frac{T_7}{d}\right\} 508^2 + \left\{\frac{T_9}{d} - \frac{T_8}{d}\right\} 380^2$$

$$\left. + \left\{\frac{T_{10}}{d} - \frac{T_9}{d}\right\} 252^2 + \left\{\frac{T_{11}}{d} - \frac{T_{10}}{d}\right\} 124^2\right] \qquad (4.2)$$

where suffix to T denotes the thermocouple station number, Figure 4.12.

In a similar way the equation for central displacement may be written from Equation (3.18) or an extension of Equation (3.14), as:

$$y = \theta_0 x + \frac{\alpha}{2}\left[\frac{T_1}{d} x^2 + \left\{\frac{T_2}{d} - \frac{T_1}{d}\right\} (x - L_1)^2 + \left\{\frac{T_3}{d} - \frac{T_2}{d}\right\} (x - L_1 - L_2)^2\right.$$

$$+ \left\{\frac{T_4}{d} - \frac{T_3}{d}\right\} (x - L_1 - L_2 - L_3)^2 + \left\{\frac{T_5}{d} - \frac{T_4}{d}\right\} (x - L_1 - L_2 - L_3 - L_4)^2$$

$$\left. + \left\{\frac{T_6}{d} - \frac{T_5}{d}\right\} (x - L_1 - L_2 - L_3 - L_4 - L_5)^2\right]$$

Substituting values for x, L, L_1 ..... L_5 gives:

$$y = 655\,\theta_0 + \frac{0.000014}{2}\left[\frac{T_1}{d} 655^2 + \left\{\frac{T_2}{d} - \frac{T_1}{d}\right\} 621^2 + \left\{\frac{T_3}{d} - \frac{T_2}{d}\right\} 493^2\right.$$

$$\left. + \left\{\frac{T_4}{d} - \frac{T_3}{d}\right\} 365^2 + \left\{\frac{T_5}{d} - \frac{T_4}{d}\right\} 237^2 + \left\{\frac{T_6}{d} - \frac{T_5}{d}\right\} 109^2\right] \qquad (4.3)$$

A simple computer program using BASIC language was written to solve Equations (4.2) and (4.3) substituting the T/d data from Table 4.2, to obtain central displacement at each time interval, and the values so obtained are included in the right hand column of Table 4.2.

4.3 Comparison of theory and experiment for unrestrained model beam

4.3.1 Central displacement, whole flange heated

A comparison of experimental and theoretical displacement is given in Figure 4.13. In this figure the experimental displacement is reproduced from Figure 4.8 and the theoretical displacement is taken from the last row of data in Table 4.1.

As can be seen the correlation is very good up to 26 minutes of heating which corresponds to an average heated flange temperature of approximately 650°C. Thereafter the experimental displacement is less than the theoretical displacement, and as mentioned in 4.1.5, this is thought to be due to phase transformation. To determine if this was so, temperature profiles were plotted, Figure 4.14, for those heating times which corresponded to temperatures in the heated flange within the phase transformation range of 730-830°C (this was the range established from Figure 2.2). The supposition was that sudden contraction of the heated flange would induce tensile stresses in that flange causing the member to exhibit temporary reduced bowing. From Figure 4.14 it can be seen that the heating times of interest are in the range 26 to 34 minutes if the average thickness of the tapered flange is taken as 7 mm. These times correspond very closely to the times when, as shown in Figure 4.13, the discontinuity in displacement occurred, suggesting very

strongly that phase transformation was the principal cause for the departure of experimental and theoretical displacement curves.

From Figure 4.14 the heated flange would be above the upper limit phase transformation temperature of 830°C at 34 minutes at which time the bowing of the member should increase at the same rate as before (before 730°C). The fact that the experimental displacement increasingly lags behind the theoretical displacement when the heated flange increases in temperature above 830°C, may be due to the effect of reduced modulus of elasticity - an effect discussed in 3.6.

4.3.2 Central displacement, half flange heated

A comparison of experimental and theoretical displacement is shown in Figure 4.15. In this figure the experimental displacement is reproduced from Figure 4.9 and the theoretical displacement from the last column of data in Table 4.2. In general the correlation is good, but when examined in detail there are some discrepancies which warrant further discussion.

The experimental displacement lags behind the theoretical displacement markedly in the early stages of heating, eg up to 15 minutes, but this cannot be explained. However the correlation is very good after 20 minutes of heating when the heated flange temperature exceeds 500°C and the average steel temperature exceeds nominally 300°C. Since in practice the interest is in temperatures above these, it follows that the discrepancy observed at lower temperatures is of little practical importance.

Again there is evidence of temporary reduced bowing between 24 and 34 minutes of heating. Since the temperatures in the heated half were approximately the same as the temperatures in the specimen when heated over the whole length, it is reasonable to assume that the reduction in the experimental displacement is also due to phase transformation.

4.4 Finite element analyses for unrestrained model beam

4.4.1 Introduction

A number of finite element analyses are presented here and the results compared with displacements derived from experiments reported fully in 4.1. The analyses have been made for two experimental conditions: for the unrestrained beam heated over its whole length and for the unrestrained beam heated over half its length.

It will be recalled (3.2) that a simple, albeit limited, theory for predicting the thermal bowing displacement of a member, was derived and validated against the experiments. The simple theory was based purely on geometry and assumed a linear temperature gradient across the section and a stress-free condition. The simple theory did not take account of i) phase transformation or ii) change of elastic modulus with temperature. Nevertheless the simple theory correlated well with the experimental results as Figures 4.13 and 4.15 showed. It was, however, considered important to be able to predict displacements of structural members more accurately and this led to the use of PAFEC. Some notes on the PAFEC finite element program are given in Appendix 1.

The analyses are confined to elastic analyses for two reasons. First, the beams in the experiments were free of externally applied forces.

In-elastic behaviour was therefore confined to yielding due to the curvilinear temperature distribution within the section (which causes compression along the outer fibres and tension within the inner zone); and such effects were assumed to have negligible effect upon the overall bowing displacements. The second reason was that it had not been possible to get the PAFEC plasticity software to work satisfactorily.

The elastic analyses were made with and without the PRELOAD module designed to model phase transformation. Details about the PRELOAD module and its validation are given in Appendix 1 (1.7 and 1.8).

4.4.2 Summary of experimental data used in analyses

The steel I beam used in the experiments was a hot rolled section 104 mm deep by 44 mm wide by 7.35 kg/m nominally 1500 mm long. The section had tapered flanges and a second moment of area about the major axis of 152.3 cm^4. The steel was BS 4360: Grade 43, ie ordinary mild steel. The arrangement of the thermocouples is shown in Figure 4.7. Mid-span displacements were recorded every 2 minutes relative to the ends of a straight edge, spaced 1310 mm apart. Two tests were conducted; the temperature data are given in Tables 1 and 2 of Appendix 2.

4.4.3 Derivation of equivalent parallel flange thickness

The flanges in the test specimen were tapered. To model the specimen in finite elements an equivalent parallel flange thickness was needed. This was derived by weighing a length of section and calculating the total cross section area, deducting the web area and hence obtaining the flange area as follows:

A 1.216 m length was weighed and found to be 8.947 kg. Assuming a density for steel of 7850 kg/m^3, the cross section area is given by area $= \frac{\text{mass}}{\text{density x length}} = \frac{8.947 \times 10^6}{7850 \times 1.216} = 937.3$ mm^2. The area of the web is 89 mm x 4.2 mm. Therefore area of flange $= \frac{937.3 - 411.6}{2} = 262.7$ mm from which the flange thickness = 262.7/44 = 5.97 mm. It should be noted that this method depends on where the web is assumed to end and the flange to start, and the 89 mm dimension was taken to the flange web intersection ignoring the root radius.

As a check, the flange thickness of 5.97 mm was used to calculate the second moment of area of the section which should equate with the published value of $I_{xx} = 152.3$ cm^4.

$I_{xx} = 2$ (A.h^2 + I of flange about own axis + I of half web about xx)

where A = area of flange, h = distance from neutral axis to centre line of flange

$$I_{xx} = 2 \left[(44 \times 5.97 \times 49.015^2) + \frac{1}{12} (44 \times 5.97^3) + \frac{1}{3} (4.2 \times 46.03^3)\right]$$

$I_{xx} = 1536794$ mm^4 = 153.6794 cm^2 which agrees well with the published value. A flange thickness of 5.97 mm was therefore used in the analyses.

4.4.4 Element mesh models used in PAFEC analyses

In the case of the beam heated along the whole flange, it is possible, and cheaper in terms of computing time, to model only half the beam length since the temperature distribution and thus the bowing is symmetrical about the centreline. This can be achieved, Figure 4.16, by restraining nodes 1, 3, 5, 7, 9 in the x direction and restraining

only node 1 in the y direction to prevent whole body movement. This permits unrestrained movement of nodes 3, 5, 7 and 9 (as well as 2, 4, 6, 8 and 10) in the y direction which corresponds to the experimental condition. Displacement Uy_2 is the displacement of primary interest, as this corresponds to the central displacement of the whole beam length.

For the beam heated over half the length it is necessary to model the whole beam length. To reduce the amount of nodal temperature data it is convenient to consider the beam length to be divided into 3 portions: a heated portion where at any particular time the temperature profile does not vary along the portion length but does vary across the section depth; an unheated portion which remains for all times at room temperature, throughout its whole extent; and a portion at the centre where the temperature profile changes within its length and across its depth. This is shown in Figure 4.17. In this case node 1 can be restrained in the x and y direction while node 2 is restrained in the y direction only. All other nodes are free to move in the x and y directions. The displacement at the centre of the beam, say Uy_{11}, is of interest.

4.4.5 Analyses, whole flange heated

To model the temperature distribution in the test specimen when heated over its entire length, the average temperature of the test specimen at each horizontal line of nodes is needed. Since the positions of the element nodes do not necessarily correspond with the positions of the thermocouples in the y direction, it is necessary to i) average the thermocouple temperatures over the 12 stations for each horizontal line of thermocouples, ii) plot the temperature profile across the section

depth to provide a curve, and iii) read from the curve the temperatures at each horizontal line of nodes. This procedure is followed for each interval of heating.

To obtain the average temperature data is a tedious activity as it requires listing the relevant thermocouple temperatures for each time of heating and then computing the average. Table 4.3 is an example of the data needed for a particular depth - in this case 25 mm from the unheated flange.

Table 4.4 gives the average temperature for each horizontal line of thermocouples, when the whole beam is heated, at 6 minute intervals. Figure 4.18 shows these data plotted with horizontal node lines superimposed.

7 analyses have been made, as shown in Table 4.5. The reasons for the choice of parameters given in the table are as follows.

(i) An α value of $14 \times 10^{-6}/°C$ is a nominal value which engineers might use in such analyses. The value of $14.8648 \times 10^{-6}/°C$ has also been adopted since it was derived from a dilatometer test on a mild steel thought to be of similar chemical composition and hence dilatation characteristics as the mild steel used in the beam experiments. Comparison of the displacements from Analyses 130 and 131 would quantify the importance of choice of α value.

(ii) The importance of element size and shape would be quantified by comparing Analysis 131 (which is based on 4 elements across the

depth and 10 along the half length resulting in an element aspect ratio of 11) with Analysis 132 (which adopts 7 elements across the depth and 40 along the half length resulting in a recommended small element aspect ratio of nominally 5.5). It should be noted (Appendix 1) that the preferred aspect ratio should not be greater than 5 for PAFEC element type 36210.

(iii) The effect of phase transformation, using the PAFEC PRELOAD module, would show from a comparison of Analyses 130 and 130a.

(iv) The effect of varying the modulus of elasticity with temperature would show from a comparison of Analyses 132 and 133, and of Analyses 132 and 233.

(v) The effect of choosing different E versus temperature relationships would show from comparison of Analyses 133 (Euronorm E) and 233 (Arbed E).

Data files for Analyses 130, 132 and 133 (for one of 8 temperature load cases) are given in Appendix 3. They are typical datafiles for the analyses made. The bowing displacements at the free end of the half beam model for each of the analyses are given in Table 4.6. Also included, as the bottom row of data, are the corresponding displacements observed during the experiment.

4.4.6 Comparison of analyses and experiment, whole flange heated. Examination of Figure 4.19 shows that the central displacement is greater when using a value of $\alpha = 14.8648 \times 10^{-6}/°C$ compared with

α = 14.0 x 10^{-6}/°C, and, as expected, the difference in displacements for the two values of α is a linearly varying difference.

Figure 4.19 also shows that the displacement curve obtained when using the PRELOAD module is closer to the experimental curve, and the computed curve reflects the phase transformation effect but at a different time: in the experiment the maximum depression in the displacement curve occurs at 30 minutes but in the computed curve at 36 minutes. Possible reasons for this time difference have not been explored, nor the reason for the larger magnitude of dip in the computed displacement curve compared with the experimental curve.

It is clear from Figure 4.19 that after phase transformation has been passed (at 36 minutes in this experiment) the computed displacement curve incorporating phase transformation is, as mentioned above, reasonably close to the experimental curve, but the slope of the curve appears greater in the computed curve, and this could be due to the effects of plasticity as explained in 3.6.

It appears from Figure 4.20 that the choice of element size and shape has little effect upon the computed displacement curve. However it must be recognised that this negligible difference might not be reflected in a flexural member which was externally loaded and where stress levels and consequent distortions of the elements would be greater possibly leading to greater differences in computed displacements.

It is particularly interesting that the computed displacement curves for constant E and variable E are virtually identical, Figure 4.21. With an exception at 36 minutes of heating, the curve for variable E lies

slightly below that for constant E, and the reason for the cross over at 36 minutes is not known., This comparison does however show that an elastic analysis based on a constant E value provides a reasonable general approach, and this is a useful observation because it avoids the need, when using PAFEC, to run a separate analysis for each temperature load case which is necessary when E varies with temperature.

Figure 4.22 shows the displaced form of the half beam model for a typical analysis (Analysis 130), using the PAFEC OUT.DRAW module for graphics plotting.

4.4.7 Analyses, half flange heated

As mentioned in 4.4.4, the temperature distribution in the beam was modelled in 3 portions. An examination of the temperature profiles in Figure 4.11 shows that at any particular instant in time the temperature profile only varies over two thermocouple stations at the centre of the beam. Figure 4.17 shows the lengthwise zoning adopted for the analyses, in which the two outer zones (of length = 0.655 m - 0.128 m, where 0.128 m is the thermocouple station spacing) have temperatures which do not vary in the x-direction thus allowing the use of the PAFBLOCK module for mesh generation.

To produce the data for the TEMPERATURE modules in these analyses, the average temperatures were calculated for the uniformly heated portion of the beam, and the data are given in Table 4.7. The average temperature profiles were then plotted and are shown in Figure 4.23 from which the nodal temperatures were read off. For the central portion of the beam the temperature for the relevant thermocouples (thermocouples 26 to 30,

and 31 to 39 at the two stations) were plotted in Figure 4.24 and the nodal temperatures read off. The nodal temperatures so obtained were then listed in the appropriate TEMPERATURE module.

Since the effective flange thickness is 0.00597 m and the thermocouple station spacing is 0.128 m it follows that the number of elements/station spacing must be at least 2 if the element aspect ratio is not to be too large - the element aspect ratio for this configuration is 0.064/.00597 = 11 which is considered acceptable in view of the negligible effect demonstrated in Figure 4.20.

In view of the small effect of number of elements in the mesh, which was demonstrated by a comparison of displacement curves for Analyses 131 and 132 for the beam heated over its whole length (Figure 4.20), it was decided to model the overall depth of beam with 4 elements - one for each flange and 2 for the web. The maximum element aspect ratio was approximately 12, and the number of user-defined nodes was 35, Figure 4.25.

In order to find node numbers in each of the 8 PAFBLOCKS an IN.DRAW graphic was first produced at A1 size. Eight temperature load cases were chosen so that displacements would be computed at 6 minute intervals up to 48 minutes.

4 analyses were made as shown in Table 4.8. The effects of phase transformation and variable E value were to be examined. All 4 analyses use the same mesh so as to eliminate the need to interpolate and extrapolate the experimental temperatures for the nodal points more

than once, since this requires considerable effort. Thus the TEMPERATURE module is the same in all 4 analyses. The datafile for Analysis 133x is shown in Appendix 3 which shows the amount of data which had to be compiled. The datafile for Analysis 133z is not included as it is identical to that for Analysis 133x but with the addition of the PRELOAD module. Eight separate datafiles were required for Analysis 134.

The bowing displacements at the centre of the beam, taken from Phase 7 of the 4 analyses, are given in Table 4.9 along with the experimental displacements, and the data are plotted in Figure 4.26.

Figure 4.27 shows the displaced form for a typical analysis using the PAFEC OUT.DRAW module.

4.4.8 Comparison of analyses and experiment, half flange heated

Figure 4.26 shows that all the computed displacements are greater than the experimentally observed values, markedly so between 6 and 12 minutes when the computed values were at least double the experimental values. No explanation for this difference is offered.

From about 18 minutes onwards, which is of most interest, the computed displacement curves for analyses which take account of phase transformation agree reasonably well with the experimental curve. Again the computed magnitude of phase transformation dip was greater than the experimental dip, but the dips occurred at roughly the same time, 27 min. It also appears that the lower the elastic modulus the better the agreement between the computed and experimental result

(compare curve for Analysis 135 with the experimental curve), and this is as expected.

4.5 Full scale experiments for unrestrained thermal bowing of a column

4.5.1 Introduction

The British Steel Corporation and FRS have conducted tests in a compartment fire test rig at Cardington, Figures 4.28 and 4.29, to assess the heating rates of non-loaded I section steel beams and columns having different thermal response factors ie different perimeter to cross-section area ratios[4.2]. As part of the test rig, two columns were partly built into the double leaf external wall such that one flange was exposed to fire while the other flange was located in the cavity and was thus protected from fire by a single leaf of brickwork, in the manner shown in Figure 1.18.

One of the two columns was a 203 x 203 x 52 kg/m universal column and the writer decided to use this to examine the extent of thermal bowing because (i) it was less deep (203 mm deep) than the other column and would therefore experience most bowing (since bowing is inversely proportional to the depth of section for a given temperature difference), ii) there was an identical column exposed to heat on all sides in the compartment, and this would enable the temperature rise in the 2 identical columns to be compared, and iii) the test would yield full scale test data with which the simple theory could be compared.

The comparison mentioned in ii) above might prove of practical help in the following way. If it was shown experimentally that the temperature of the heated flange of the column-in-wall was roughly the same as the

temperature of the flange in the fully exposed column, (ie column exposed to fire on all faces), and if, from a fire engineering analysis, the steel temperature time relationship for a fully exposed column could be computed (from a knowledge of the fire load density, area and height of ventilation openings, and insulation properties for the compartment walls and ceiling), it would thus prove possible to compute the heated flange temperature of the column-in-wall. Knowing the temperature of the unheated flange of the column-in-wall, which is not sensitive to the severity of the compartment fire (see later), the temperature difference across the section and hence the unrestrained thermal bow could be calculated.

The following experiments and analyses are for 2 compartment fires of markedly different fire severity (for fire load densities of 10 kg/m^2 and 20 kg/m^2 but for the same ventilation).

4.5.2 Experimental Arrangement

The partly built-in-column had 24 Pyrotenax 3 mm diameter thermocouples attached in the positions shown in Figure 4.30, before the adjoining walls were built. A plan view of the fire compartment showing the positions of the 2 columns (CIW1 and CIW2) in relation to the construction is shown in Figure 4.31. Figure 4.32 shows these features. The columns were position- and direction-fixed at their bases. Column CIW1 was instrumented for measurements.

A Solartron 3430 datalogger was used by the writer to record steel temperatures for the column-in-wall. Temperatures for the fully exposed column were recorded by BSC personnel.

As shown in Figure 4.30, mid-height bowing displacements were measured over a 2400 mm length of column CIW1 using a dial gauge at mid-height fixed to a steel straight edge which had two rods welded to it 2400 mm apart which penetrated the outer leaf of brickwork and contacted the unheated flange to act as reference points. Similarly, the dial gauge had an extension shaft which penetrated the wall to touch the column flange. The lower end of the straight edge was extended down to a floor level so as to support the dead weight of straight edge and make it easier to use. The straight edge was held in place by hand and readings taken at appropriate time intervals, Figure 4.33.

4.5.3 Analysis of results

The temperatures measured by the 24 thermocouples are given in Tables 3 and 4 in Appendix 2 for Tests 1 and 2 respectively. The temperatures measured along the heated and unheated flanges were averaged over the length and are given in Table 4.10. Note that the bowing displacement = $\frac{.000014 \times 2400^2 T}{8 \times 203}$ = 0.0469 T where T = temperature difference.

Measured bowing displacements are given in Table 4.11 for Tests 1 and 2.

The variation of temperature across the section and along the length for the more severe fire, Test 2, is shown in Figure 4.34.

Calculated values of mid-height bowing displacement for Tests 1 and 2 are given in Table 4.10. The calculations were made using the equation:

$$\Delta = \alpha \frac{TL^2}{8d}$$ where L = 2400 mm, d = 203 mm, α = 0.000014/°C, and

T = average heated flange temp - average unheated flange temp, °C

The experimental and calculated bowing displacements of column CIW1 for Tests 1 and 2 are shown in Figure 4.35. In both tests it can be seen that the calculated displacements are marginally lower than the experimental displacements, but the agreement is generally good.

Figure 4.36 shows, for Test 1, the temperature attained by the heated flange of the column-in-wall (CIW1) and the free standing column (FSC1). There is very close agreement between the two, from which it appears that heat flow toward the unheated flange, such as to lower the temperature of the heated flange of CIW1, has negligible effect. The same conclusions can be reached from Figure 4.37.

For a maximum temperature difference in Test 2 of 409.73°C (Table 4.10), the calculated mid-height bowing over the 2.4 m height is 19.22 mm. Over a 4 m height it would be 19.22 x $(4/2.4)^2$ = 53.38 mm, and the corresponding horizontal displacement at the column head, assuming the column was fixed at the base, would be 53.38 x 4 = 213.5 mm.

4.6 Conclusions

4.6.1 Conclusions from unrestrained model beam experiments

i) The successful conduct of these experiments proved that the use of high powered electrical heating elements to heat steel I-section model members is a viable alternative to the use of

gas-fired furnaces conventionally used in fire resistance testing. A proprietary heating element with a surface heat flux of 7.5 W/cm^2 produced maximum steel temperatures of 1000°C within 45 minutes in the 104 mm x 44 mm wide by 7.35 kg/m I-section steel specimen. This was representative of the rate of heating attained in full size structural elements in fires in buildings. Due to the confined form of heating possible with electrical heating elements, it was also possible to achieve temperature gradients across the specimen section of up to 700°C (Figure 4.18) and to facilitate accurate measurements of displacements using a linear displacement transducer.

ii) Phase transformation and reduced elastic modulus at elevated temperatures both have the effect of reducing the observed central displacement of a non-loaded beam heated along one flange when compared with the mid-span displacement determined from the simple theory ($\Delta = \alpha TL^2/8d$). The correlation of experimental displacement and displacement derived from the simple theory was good however up to heated flange temperatures of 650°C and 900°C for the test beam heated along the whole flange and half flange respectively (Figures 4.13 and 4.15).

iii) In practice the temperature distribution across an I-section heated along one flange is curvi-linear. The simple theory assumes a linear temperature distribution. It was found in these experiments that a best-fit linear equivalent of the curvi-linear temperature distribution gave the good agreement between theoretical and experimental displacements mentioned in ii) above.

iv) The PAFEC finite element program, modified to take account of phase transformation, has predicted central displacements which agree well with measured values, both for the condition when the whole flange and half flange were heated. These analyses were confined to elastic analyses since it was not possible to get the PAFEC plasticity program to work properly.

4.6.2 Conclusions from unrestrained full scale column experiments

i) Two full scale fire tests have been carried out successfully in a large fire compartment test rig at the FRS Cardington Large Laboratory. Measurements of unrestrained thermal bowing of the fixed base, partly built-in column at mid-height agree well with the simple theory given in 3.2. The temperature difference T was taken as the heated flange temperature minus the unheated flange temperature and the fact that the agreement with the experimental data was good in both tests, Figure 4.35, is justification for using the average flange temperature data instead of best fit data used in the previous model beam analysis.

(ii) On the basis of two compartment fire tests of markedly different fire severity it seems that the heated flange temperature for the column-in-wall is approximately equal to the temperature that it would achieve if the column was fully exposed to fire. On the other hand the temperature of the unheated flange did not rise markedly above ambient - in the most severe fire (Test 2) the temperature rise was only 10 and 60°C at 16 and 24 minutes respectively. These two facts mean that the bowing can be calculated having first found the heated flange temperature from a

fire engineering analysis assuming the column is fully exposed to fire.

(iii) The horizontal displacement at the top of a fixed-base column due to thermal bowing can be large. For a temperature difference of 409°C experienced in Test 2, the horizontal movement at the top of a fixed-base column 4 m high would be 213 mm, using the theory given in 3.3. These movements have to be catered for in design, unless they are prevented, otherwise adjoining construction such as masonry can be damaged and made unstable, possibly causing a life hazard, especially to firefighters who may be unaware, from the outside of a building, that a fire wall is about to collapse onto them.

CHAPTER 5. EXPERIMENTS ON A RESTRAINED MODEL 2-SPAN CONTINUOUS BEAM HEATED ALONG ONE FLANGE

5.1 Introduction

It was shown in 1.7 and 1.8 that in a fire, structural members, such as beams and columns, may be exposed to heat mainly from one side, and that this can give rise to large temperature differences across the thickness of the member which induces thermal bowing. If the bowing is restrained, internal stresses are set up in the member, and rigidly fixed adjoining members, and member connections, are also placed under stress.

The primary aim in this chapter is to present experimental data of the magnitude of force needed to prevent a model steel beam from bowing as it is heated along one face to elevated temperatures. The nature of the experimental work is illustrated in Figure 1.19(c). An I-section steel beam, simply supported at its ends, is heated along one flange - over half the length in one experiment, and over the whole length in another. It is prevented from displacing downwards at mid-span by application of a restraint force. Hence it may be described as a 2-span continuous beam on rigid position-fixed supports. The variation in restraint force and the transient temperature field is recorded as the beam is heated. A secondary aim is to develop a simple theory for use by the practising engineer for predicting the restraint force.

Structural engineering intuition suggests that the restraint force will depend upon the following factors:

i) the section stiffness (EI) in relation to the span. In the limit a member with large stiffness and small span will produce a large

restraint force, and this restraint force will be developed early in the heating process because plasticity will be reached early. At the other extreme, a long slender member will be able to undergo much flexure before plasticity is reached, and the maximum restraint force will therefore be exerted later for a given temperature.

ii) the temperature difference between the heated and unheated flanges. The larger the temperature difference the greater the unrestrained thermal bowing and the greater the force needed to suppress the bowing, in the elastic domain.

iii) the maximum temperature attained. The higher the temperature of the heated flange, the weaker it will get and the less the restraint force. For this reason one would expect the maximum restraint force to be generated early in the heating process, Figure 5.1.

The experimental configuration has many practical counterparts. One example is a 2-storey external steel column subjected to fire from within the building. The column would like to bow towards the fire at first floor level but cannot due to its connection to the foundations and first and second floor beams, and the result is that restraining forces are induced.

Another example is a 2-span continuous beam supported and vertically restrained by 3 columns. The lower flange of both beam spans is hotter than the upper flange so that the beam would like to bow downwards but cannot because of the centre column. The result is that restraining forces are induced in the beam.

The experiments described were preceded by restrained thermal bowing experiments on short model beams of steel and structural aluminium alloy heated with quartz fabric insulated flexible electrical heating tapes of relatively low heat output, but these tests are not reported here.

The apparatus would need to allow tests to be conducted on model steel I-section beam specimens of length governed by:

i) a length to depth ratio such that shear deformation could be assumed minimal (an important assumption if simple bending theory was used)

ii) a length to flange width ratio such that lateral instability, ie instability normal to the web, was unlikely to occur,

iii) the availability of standard lengths and widths of proprietary electrical heating elements,

iv) a support system such that heat losses at the contact areas (centre and ends) were minimal so that temperatures at the contact areas were not markedly different from those in the main length of the specimen.

One beam specimen would be used for both tests; the flange would be heated over half its length, the beam allowed to cool, and the second test conducted in which the whole flange length would be heated. Re-use was considered acceptable because the reduction in room temperature strength after heating in the first test was likely to be negligible, Figure 1.20.

5.2 Elastic theory for calculating the restraint force

It has been shown that a steel beam, when subjected to a linear temperature difference T across its depth (which does not vary with length), will, if it is unrestrained, bow into a circular arc such that the mid-span displacement Δ is given by $\Delta = \alpha TL^2/8d$.

If a restraint force P is then applied to the stress-free beam at mid-span so as to produce zero displacement at mid-span, then, using the principle of superposition (valid only in the elastic domain) we can say that the force so applied is equal to the force needed to sustain zero displacement at mid-span. Thus if the unrestrained thermal bowing displacement Δ can be calculated (as it can be in this case), the load applied at mid-span to 'straighten out' the initially curved beam can be obtained from the well known relation $\Delta = PL^3/48EI$ which corresponds to a simply supported beam subjected to a central point load.

Transposing gives $P = 48EI\Delta/L^3$ and substituting for Δ gives

$$P = \frac{48EI}{L^3} \cdot \frac{\alpha TL^2}{8d} = \frac{6EI\alpha T}{Ld} \qquad (5.1)$$

Assuming that the section geometry does not change and that α is constant with temperature, the relationship shows that P is directly proportional to E and T in the elastic domain. In the experiment the temperature difference T would increase (in the transient stage) as time of heating increased, but E would decrease.

5.3 Experiments

5.3.1 Details of model test beam specimen and thermocouples

The specimen and the arrangement of thermocouples was identical to that used in the unrestrained bowing experiment. See 4.1.2 and Figure 4.7.

5.3.2 Chemical composition and mechanical properties

i) Chemical composition

A sample of the unheated steel I-beam flange was sent to Harry Stanger Ltd, Materials and Testing Consultants, Elstree, Herts, for tests to determine the chemical composition. Harry Stanger Ltd is an approved test house under the National Testing Laboratory Accreditation Scheme (NATLAS). Determinations for the principal elements such as C, S_i, M_n, S and P were made in house. Determinations for trace elements such as N_b were sub-contracted to Keighley Laboratories in Yorkshire since this required the use of spark emission techniques. The composition is given in Table 5.1.

The relevant table (Table 18) in BS 4360 : 1979[5.1], which deals with weldable structural steels, shows that the composition of the test specimen corresponds most closely to an ordinary mild steel, Grade 43B of BS 4360. This grade permits C = 0.22% max, S_i = 0.50% max, M_n = 1.5% max, P = 0.050% max and S = 0.050%.

ii) Mechanical properties

A sample of flange from the steel I-section was sent to Harry Stanger Ltd to conduct a standard tensile test principally to determine yield stress or 0.2% proof stress, and ultimate tensile strength (UTS) at room temperature. An Avery 600 kN tensile test machine was used. The steel had an abnormally

high 0.2% proof stress of 421 N/mm² associated with an upper limit UTS of 517 N/mm² when compared with BS 4360 Grade 43 values of 255 N/mm² for yield strength and 430 to 510 N/mm² for UTS.

Because of the high ratio of proof stress to UTS (the normal ratio is 0.50 to 0.6 but from the tests it was approximately 0.80) it was decided to repeat the tensile tests at a different laboratory.

The repeat tests were undertaken at the British Steel Corporation Swinden Laboratories. Since these tensile tests were conducted after the heating experiment on the beam, the opportunity was taken to test the material before and after heating to 800°C. The flange thickness was not sufficient to enable a threaded cylindrical test specimen conforming to BS 18 : Part 2[5.2] to be obtained and so a Hounsfield No.12 specimen of 4.54 mm diameter and gauge length of 22.7 mm was used. The strain rate was 3.67 x 10^{-4}/sec for both tests. The results are given in Table 5.2.

It can be seen that for the unheated specimen the ratio of yield stress to UTS is 0.68 and the yield stress of 315 N/mm² is appropriate for a BS 4360 Grade 43 steel. The drop in yield stress after heating to 800°C, from 315 to 223 N/mm² agrees well with other data shown in Figure 1.20.

5.3.3 Apparatus

The apparatus was the same as that used in the experiments described in Chapter 4 (see 4.1.1 and Figures 4.1 and 4.2). As before the I-section specimen was heated on the underside such that it would tend to bow downwards, but the centre of the specimen was restrained from bowing by a screw jack and compression load transducer reacting against the strong

beam. The screw jack, which had a ball-bearing race, was incorporated to allow height adjustments so as to maintain zero mid-span displacement of the specimen if the test apparatus displaced due to the increasing restraint force. Zero mid-span displacement would be constantly checked using a purpose made straight edge bearing near the ends of the specimen and a simple optical device.

The straight edge used in the unrestrained bowing tests was used, Figure 4.6. However the steel contact point of the centre leg was electrically insulated from the main body of the straight edge. The steel contact was connected electrically via an insulated wire, battery and 4.5 V light bulb to the specimen. Displacement of the specimen away from the central contact would break the circuit and extinguish the light. The screw jack would then be adjusted to make contact and light the bulb thus confirming zero displacement.

Two electrical heating elements were used, one either side of the screw jack. It was important to ensure that the heated flange of the specimen would be at uniform temperature along its length when both heating elements were switched on. The only non-uniformity in temperature would result from i) the slight heat sink presented by the Syndanio insulation spacer at mid-span where the screw jack would bear against the specimen via the spacer and ii) discontinuity in the electrical heating element at the screw jack position which would mean that a 100 mm length of the flange would not be directly heated - this latter effect would probably be small for a steel specimen owing to its high thermal conductivity and the large indirect longitudinal heat flow that could be expected.

A compressive pillar load transducer having an overall height of 100 mm and a load rating of 8 tonne was used. The load cell was purchased from Strainstall Ltd, Cowes, Isle of Wight, and was a standard Load Cell Type 1590 CNR3M having a calibrated output sensitivity of 1.493 mV/V at its full load rating of 8 tonnes. The maximum supply voltage was 25 with a preferred (normal) supply of 10 V. The temperature rating allowed its use over an ambient range of 0 to 60°C compensated to 0.05% per °C. It was supplied with a Test and Calibration Certificate. The load transducer was excited with a Thurlby PL Series constant voltage device, Type PL310. For the experiments the excitation voltage was 15 V.

Because it was inconvenient to transport and connect the load cell, constant voltage device and datalogger off site to calibrate against an accurate dead load machine, it was decided to calibrate the load cell with an Enerpac 10 ton hydraulic jack, a Budenberg 10,000 lb/in^2 Standard Test Gauge, and hand pump which had previously been calibrated with a Denison 50 ton dead weight machine in the Structural Engineering Laboratory at Building Research Station, Garston. The jack and load cell were placed end to end between the platens of a disused compression test machine at Fire Research Station and using a 15 V constant excitation the datalogger mV output was noted for hydraulic jack pressure gauge increments of 500 lb/in^2 up to 3,500 lb/in^2.

5.3.4 Experimental procedure

i) Heating test, half flange heated

The constant voltage supply and data loggers were switched on roughly 30 min before commencement of test so that they could stabilise. The dataloggers were run so as to obtain ambient temperature readings. The

power to one of the electrical heating elements was switched on. The straight-edge was placed on the specimen roughly 10 seconds before the datalogger printed out, the screw jack adjusted, and the straightedge removed immediately after print out and placed in the water trough; this was repeated every 2 minutes. Measurements of temperature and transducer readings were continued for 38 minutes at which time steel temperatures at some positions had exceeded 1100°C and the power to the heaters and dataloggers was switched off because the restraint force had passed its peak and had reduced to a small value.

ii) Heating test, whole flange heated

The above procedure was followed except that both heaters were switched on. Frequent checks were made to ensure that the temperatures in one half of the specimen were the same as in the other half. The test was terminated after 32 minutes of heating.

5.3.5 Results of experiments

i) Calibration of load transducer

By plotting the data it was found that 1 mV output corresponded to 357 lb/in^2, and that 1 lb/in^2 corresponded to 2.159 lbf so that 1 mV corresponded to 357 x 2.159 x 0.4536 x 9.81 N = 3.429 kN. As a double check the Calibration Certificate supplied by the load cell manufacturer was used as follows. The stated sensitivity is 1.493 mV/V at 8 tonnes. Therefore for an excitation voltage of 15 V the mV reading when transmitting 8000 kgf is 22.395 mV so that 1 mV = 357.22 kgf = 3.504 kN. This represents an error of 2% compared with the dead weight machine calibration method. A calibration factor of 1 mV = 3.43 kN was therefore used.

ii) Heating tests

The temperature data at intervals of 2 minutes are given in Tables 5 and 6 of Appendix 2 for the half flange length and whole flange length heating tests respectively. The load transducer voltage outputs and corresponding restraint forces for both tests are given in Table 5.3. The mid-span restraint forces are shown in Figure 5.2.

5.3.6 Discussion of experimental results

i) Temperature distribution, half flange heated.

There was no reason to suppose that the general shape of the temperature profiles across the depth and along the length would be much different to those obtained in the test on the unrestrained beam, (Figure 4.11).

ii) Temperature distribution, whole flange heated.

Since, for analytical purposes, it was necessary to know if it could be assumed that the temperatures at a particular depth were constant along the length, it was considered prudent to plot the temperature profiles at 10, 20 and 30 minutes of heating. These are given in Figure 5.3. It is clear that the temperature distributions are symmetrical on either side of the centreline and this is to be expected as the two variacs were adjusted to supply the same electrical power to each heating element. The slight depression in temperatures at mid-span, apparent at 30 minutes, was expected since, over a length of 100 mm, there was i) no heat input and ii) heat loss into the insulation spacer. The magnitude of depression, however, was not considered sufficient to invalidate the assumption that an average of all the station thermocouples could be safely taken for analytical purposes.

Temperatures at common thermocouple depths were averaged over the length of the beam at 8 periods of heating, and are given in Table 5.4. The corresponding temperature profiles are shown in Figure 5.4. The dashed lines are extrapolations. The average temperature of the heated flange, assuming the effective flange thickness is 5.97 mm, has been taken from Figure 5.4 and plotted together with the average temperature of the unheated flange in Figure 5.5. From this it can be seen that the difference between the average heated and unheated flange temperatures continues to increase as heating proceeds reaching a maximum difference of approximately 550°C upon termination of the test at 32 minutes.

iii) Restraint force, half flange heated

The restraint force increases elastically in the initial heating stage due to the increasing difference in temperatures of the heated and unheated flanges. This is followed by yielding of the heated flange so that the maximum restraint force is reached and is followed by spread of yielding up through the section and outwards from the centre where the induced bending moment is greatest, and a consequent reduction in restraint force. The time at which yield first occurs cannot be interpreted from Figure 5.2 since the temperature difference between heated and unheated flange temperatures in the heated half is continuously increasing.

iv) Restraint force, whole flange heated

The comments in iii) apply equally. There is no indication of a kink in the curve, Figure 5.5, which might be expected if phase transformation occurred, and this is because the experiment did not continue long enough for phase transformation temperatures to be reached.

v) Relation of temperature distributions and restraint forces

For the beam heated over the whole flange, the most striking feature is the early stage at which the maximum restraint force is reached. This occurs at 18 minutes, Figure 5.5, when the heated and unheated flange temperatures were quite low, ie nominally 380°C and 100°C respectively.

5.4 Elastic theory applied to experiment

Here, Equation (5.1), derived in 5.2, is applied to the experimental data in which the steel I beam was heated along the whole flange.

The following data apply: $I = 152.3\ cm^4$; $\alpha = 0.000014/°C$; T = difference between average heated flange temperature and average unheated flange temperature, derived from the experiment; L = distance between supports = 1422 mm; d = distance between centres of heated and unheated equivalent flanges = 98 mm (ie 104-6 mm).

Therefore

$$P = \frac{6EI\alpha T}{Ld}$$

$$P(kN) = \frac{6 \times 152.3 \times 10^4 \times .000014}{1422 \times 98} ET = 9.18 \times 10^{-4}\ ET \qquad (5.2)$$

or, from transposing Equation (5.2), the effective E value is

$$E = \frac{P}{9.18 \times 10^{-4}\ T} \qquad (5.3)$$

From an examination of Equation (5.2) it is clear that the only uncertain factor is the E value to use. Two E versus temperature relationships have been used. One is based on the BSC/Euronorm isothermal data, Figure 2.9,

as this represents an E value relationship minimally affected by temperature. The other relationship is based on Arbed data, Figure 2.13, and represents a relationship in which E reduces more rapidly with temperature, especially above 500°C.

The analyses also cover two sets of temperature data. One assumes that the E value should be based on the average temperature of the whole member; the other on the temperature of the heated flange if it is assumed that the behaviour of the heated flange will dominate the overall behaviour moreso than the average temperature of the member. These temperature data are shown in Figure 5.6.

In the analyses, which are presented in Table 5.5, the effective E value has been derived using Equation (5.3) and the experimentally determined restraint force P.

All the analyses assume elastic behaviour which is clearly not valid in the later stages of heating where the temperatures are high and plasticity has clearly set in. Nevertheless the elastic analyses were made in order to facilitate comparisons of the effects of making different assumptions for elastic modulus and temperature values in Equation (5.2).

To check when the yield stress was likely to be exceeded, the simple relation $\frac{M}{I} = \frac{\sigma}{y}$ was transposed so that

$\sigma = \frac{My}{I}$ where $M = \frac{P}{2} \cdot \frac{L}{2}$ so that

$$\sigma = P \times \frac{1422}{4} \times \frac{104}{2} \times \frac{1}{152.3 \times 10^{-4}} = 0.1214\ P \qquad (5.4)$$

This equation was used to derive the maximum flexural stress data given in the bottom row of Table 5.5. Assuming a room temperature yield stress of around 250 N/mm^2, it is clear, Figure 5.7, that the elastic limit is exceeded at 4½ minutes of heating. This, intuitively, is surprisingly early on in the experiment, bearing in mind that the maximum restraint force is not reached until 20 minutes.

5.5 Comparison of theory and experiments.

The data in rows 7, 8, 11 and 12 in Table 5.5 have been plotted in Figure 5.8 to show the way in which the calculated elastic restraint force varies with test time. The experimental curve is included in the figure.

Similarly the data in rows 5, 6, 9 and 10 in Table 5.5 have been plotted in Figure 5.9 to show the variation with time of actual E which depends on the temperature adopted, ie maximum or average temperature. The effective E value, derived from the experiment, is also shown in the figure.

5.6 Conclusions

i) Two experiments have been successfully performed on a model 2-span I-section steel beam restrained from bowing downwards at the centre support, and the variation of restraint force at the centre support has been obtained when the whole of the lower flange was heated and when half of the lower flange was heated.

ii) The experiments have their full scale practical counterparts in buildings. One is a multi-storey external steel column where one storey height is heated predominantly from one face by flames jetting through an opening such as a window. The column would like to bow

towards the fire but is prevented (assuming it is continuous) by the connecting beams above and below the fire. Another example is a 2-span beam which is continuous (or has moment-resisting connections) and is heated from the underside over both spans. It would like to bow downwards but cannot because of the vertical restraint offered by the central column.

iii) In the experiment in which the whole flange was heated, the restraint force reached a maximum value when the heated and unheated flange average temperatures were approximately 380°C and 100°C respectively, although the maximum average temperature of the heated flange subsequently reached around 750°C before the experiment was stopped, Figure 5.5. These limiting temperatures of 380 and 100°C apply only to the geometry of the beam tested. Beams of different stiffness (EI) to length ratios and different ratios of heated flange temperature to unheated flange temperature would be expected to generate their maximum restraint force at different temperatures.

iv) It was found that the maximum restraint force measured when half the flange was heated, was roughly 85% of the restraint force when the whole flange was heated, and both reached their maximum values at the same time, Figure 5.2.

v) Using elastic theory and the principle of superposition an equation has been derived for the restraint force P for a beam heated along the whole flange, such that $P = 6EI\alpha T/Ld$ where T is the difference between the average heated and average unheated flange temperatures. It is found, Figure 5.8, that best agreement between calculated and

experimental restraint force occurs when a) an elastic modulus - temperature relation is chosen which exhibits a large reduction in modulus at temperatures above 500°C, such as the Arbed data, and b) the elastic modulus is based on the assumption that the whole beam is at the heated flange temperature and not the average temperature of the beam, Figure 5.6. However it cannot be claimed that the agreement is good - the calculated maximum elastic restraint force is roughly 100% greater than that measured. Also, it cannot be claimed that the theory is valid, since it is based on elastic behaviour whereas it is shown that the model beam enters the plastic regime at a very early stage (see below): the agreement might be better or worse for other ratios of stiffness to length. In other words the qualitatively-good agreement may be fortuitous for this experiment.

vi) The elastic theory suggested that the heated flange at the central support began to yield at a surprisingly early stage in the experiment in which the whole flange was heated: yielding occurred at 4½ minutes when the heated and unheated flange temperatures were only 32 and 21.7°C respectively, whereas the maximum restraint force occurred at 20 minutes. Structural engineering intuition suggests that the greater the stiffness (EI) and the smaller the length of beam between supports, the smaller the temperature difference between flanges required to cause yielding, and vice versa.

CHAPTER 6. EXPERIMENTS ON A DESIGN-LOADED MODEL BEAM HEATED ALONG ONE FLANGE

6.1 Design of experiment

The objective was to heat a simply supported steel I section beam along one flange so as to produce a temperature gradient across the section while supporting its maximum allowable load based on elastic design, Figure 1.19(d), and to accurately measure temperatures throughout the specimen and the mid-span displacement during the heating process. The rig used in the previous experiment was suitable for testing a nominal 1.5 m long specimen and this led to the adoption of a section size which was roughly one-third the size of a commonly used fire test beam (254 x 146 mm x 43 kg/m). The actual model section size would be rounded off to give an 80 mm deep x 50 mm wide symmetrical section having flange and web thicknesses of 5 and 3 mm respectively. These thicknesses were also dictated by the desire to fabricate the section by welding strips together, and strip material (to BS 4360 : Grade 43 ordinary mild steel) was readily available. To avoid lateral instability of the section, or local buckling of the web at the knife edge supports, a 6 mm thick plate would be welded onto each end of the beam.

In a standard fire resistance test on a beam conducted in the UK, a uniformly distributed load (UDL) of w/unit length applied to a beam is simulated by 6-point loading with the loads applied at span/4, equi-spaced, Figure 6.1. This produces the same maximum bending moment (and roughly the same shape bending moment diagram) as for a UDL (see below) and therefore represents a practical test laboratory loading condition.

$$\text{Maximum bending moment for UDL} = \frac{wL}{2}\left[\frac{L}{2} - \frac{L}{4}\right] = \frac{wL^2}{8} = \frac{WL}{8}$$

where $W = wL$ = total load

Maximum bending moment for 6-point loading $= \frac{W}{2} \cdot \frac{L}{2} - \left[\frac{W}{4} \cdot \frac{3L}{8} - \frac{W}{4} \cdot \frac{L}{8} \right]$

$= \frac{WL}{4} - \frac{WL}{8} = \frac{WL}{8}$

The loads would be applied upwards at 4-points using a load spreader system and hydraulic jack with the ends of the beam held down. Displacements would be recorded continuously using linear displacement transducers fixed to the strong beam. Since the design load was to be maintained constant during the test, displacements of the strong beam or restraint frames would be of no consequence. The top flange of the steel beam would be heated with 2 high powered electrical heating elements abutting at mid span. To achieve a comprehensive record of steel temperatures, thermocouples would be placed at 7 positions across the depth of section and at 8 equi-spaced stations along the length, involving a total of 56 thermocouples.

The magnitude of the test load was determined by calculating the second moment of area for the section and then, adopting the maximum allowable stress from BS449, calculating the total load, in the following way.

$\frac{I_{xx}}{2}$ = I half web + I one flange $= \frac{3 \times 35^3}{3} + [(50 \times 5 \times 37.5^2) + (\frac{50 \times 5^3}{12})]$

where the first term in the square bracket is Ah^2 = I of flange about neutral axis, and second term is I of flange about centreline of flange. Therefore

$\frac{I_{xx}}{2} = 42875 + [351562.5 + 520.8] = 394957$, therefore $I_{xx} = 789914$ mm^4

From the classical equation for elastic bending

$\frac{M}{I} = \frac{\sigma}{y}$ from which $M = \frac{\sigma I}{y}$

From BS 449 : Part 2 : 1969, the allowable elastic bending stress = 165 N/mm^2, so that

$M = \frac{165 \times 789914}{40} = 3258395$ N.mm

Since M = WL/8, W = 8M/L = 8 x 3258395/1500 = 17378 N. Therefore, ignoring weight of load spreader system, the test load to be applied by the hydraulic jack is 17,378 N.

6.2 Fabrication of test specimen

Three methods of fabricating the I-section model steel beam were considered: extrusion, milling, and welding. These methods are now briefly discussed.

i) Extrusion

Although small steel I-sections can be extruded and are available on special order, the dimensional tolerances on cross section size and shape, straightness and twisting were considered unacceptable for model beam work. Apart from poor dimensional accuracy, extrusion was considered unsuitable because it was not possible to obtain I-sections without radiused flange tips and the range of existing die sizes was severely limited.

ii) Milling

Work on milling model steel columns for fire research at the Building Research Station workshops showed that accurate sections could be produced but the milling time was large. Whereas uniform section shape, absence of residual stresses and straightness are of great importance in model column work, these are not so important in beams where the failure mode is in flexure rather than local or overall buckling. It was therefore decided to produce a prototype beam section by welding.

iii) Welding

An I-section can be formed by welding 3 steel strips together given that an appropriate jig is used to locate the strips accurately during the welding process - for both the initial tack welding and final fillet welding. The

camber of the flange which can result from weld metal contraction using an intially flat flange strip can be overcome by using an initially outward cranked flange.

However, welding trials at the Building Research Station workshops showed that the flange tips were drawn in by less than 0.25 mm after welding of the 50 mm wide x 5 mm thick flange to the web. The resulting camber, which was uniform over the whole beam length, was considered acceptable and initial outward cranking was considered unnecessary.

The specimen beam, Figure 6.2, was therefore fabricated in the following way. The flange (50 x 5 mild steel flat to BS 4360 : Grade 43A) was guillotined and milled to size. A 3 mm x 1 mm deep slot was milled centrally along one face so as to locate the web. The web (hot rolled black mild steel HR15, 3 mm thick) was machined to length. A T1G (Tungsten Inert Gas) welding kit was used to minimise oxidation and distortion. Triple dioxidised copper-coated 1 mm diameter mild steel was used as the filler rod. The I-section assembly was tack welded at roughly 150 mm spacing along all 4 joints. This was followed by back step, full penetration welding (short lengths of fillet weld) along 2 joints on one flange/web intersection in the sequence shown in Figure 6.3. This procedure was repeated for the other flange/web intersection. This procedure produced an I-section with minimal distortion. Finally the 6 mm thick end plates were attached by fillet welding.

6.3 Tensile tests at room temperature

Two specimens of the 5 mm thick flange steel were submitted to the Structural Design Division of the Building Research Station, Garston. The specimens were nominally 500 mm long x 40 mm wide with a necked portion 200 mm long x 20 mm

wide. Each specimen was mounted in a 2500 kN Avery Machine with an Amsler extensometer measuring over a 152.4 mm (6 inch) gauge length. The load was applied in 2.5 kN increments up to yield and then taken to failure to determine the maximum load while at ambient temperature (20°C).

The results for the two tests are shown in Figure 6.4. Specimen A yielded at 32.5 kN and carried a maximum load of 47.3 kN. Specimen B yielded at 32.5 kN and carried a maximum load of 47.2 kN.

Although both specimens of flange material yielded at the same load, ie at 32.5 kN, their load extension curves were different, Figure 6.4, possibly due to slippage of the extensometer on Specimen A. The results for Specimen A have therefore been ignored.

Specimen B had a yield stress of $\frac{32.5 \times 1000}{20 \times 5} = 325$ N/mm²

Dividing this by a load factor of 1.6 gives an allowable elastic stress of 203 N/mm² which is 23% higher than the allowable stress of 165 N/mm² given in Table 2 of BS 449 : Part 2 : 1969. However, this is not surprising since code values are lower bound values.

The elastic modulus $E = \frac{\sigma}{\varepsilon} = \frac{P}{A} \times \frac{L}{\Delta}$, and from Figure 6.4.

$$E = \frac{30}{20 \times 5} \times \frac{152.4}{23.5} \times 100$$

$$E = 194.55 \text{ kN/mm}^2.$$

This is close to the normally accepted value of 205-210 kN/mm².

6.4 Attachment of thermocouples

Thermocouples were spot welded rather than inserted into drilled holes and peened because:

i) holes may have caused local weakness in the section, but more importantly,

ii) temperature gradients were expected to be steep in the heated flange and the response of a thermocouple wire inserted in a hole whose temperature varied considerably over the thermocouple contacting length of at least 2 mm, was unknown - on the other hand, the use of thermocouples welded to inner and outer faces of the heated flange would provide unambiguous data of the face temperatures - and

iii) the drilling of holes in the inner faces of the flanges would have required the purchase of a 90° cranked pneumatic dentist drill capable of use near a compressed air supply, with the attendant difficulty of access for peening in the wires.

Slee Semiconductor Equipment Co Ltd, London, E13, specialises in the manufacture of lightweight portable and heavy fixed spot welding equipment. The Company was asked to recommend suitable portable equipment that could be used to spot weld 0.5 mm diameter Ni/Ch or Ni/Al wire to mild steel in the thickness range of interest. Initially they recommended and supplied a CT2/905/1 tweezer welder unit which comprised a 230 V mains supply welding unit with a pair of tweezers. However it was not possible to achieve satisfactory welds to clean steel sheet 1 mm thick when using maximum tweezer pressure, time and welding current, so that it would be unsuitable for thicker steel. The equipment was replaced by the same firm. The new system comprised i) a pair of CT2 tweezer welder pliers with microswitch initiation, ii) an SS905/2 solid state synchronous welding timer, range ½ to 10 cycles, iii) an HC22 heat

controller complete with transformer tapping switch allowing 36 pre-set weld positions, mounted in a box with the timer, and iv) a K2 type welding transformer having a nominal rating of 2 KVA mounted in a similar box with plug and socket interconnections. The new equipment proved to be very satisfactory and easy to use after modification to the tweezer pliers.

Modification to the pliers came about as follows. The standard cranked electrodes were suitable for welding thermocouple wires to the specimen flanges but new U-shaped electrodes had to be made from 3 mm diameter copper rod so that the wires could be welded to the web, and this proved difficult. The problem was solved by disconnecting one of the leads to the tweezer and connecting it via an extension lead direct to the steel specimen with a clamp. The redundant electrode was removed from the pliers leaving one electrode which could be applied with ease. This meant that one hand could be used to position the thermocouple wire while the other held the pliers in place and operated the microswitch to produce the weld. The specimen surface had to be thoroughly clean and polished in order to achieve a satisfactory weld, and this was done by polishing immediately before welding using a carborundum flapwheel mounted in an electric drill.

To accurately position the wires across the depth of the web, a plastic template was made which slotted between the flanges and had grooves to mark the required position of the thermocouples. Use of a template saved a considerable amount of time. To avoid unnecessary flexure of the thermocouple wires after welding, they were temporarily secured to a wooden strip clamped to the specimen. This enabled the specimen to be rotated on the bench which was necessary to get access to all faces. Finally the thermocouples were additionally secured in place using Autostic high-temperature resisting

adhesive, using a plastic syringe to put the material in place without disturbing or bending the thermocouples. This was left to dry for 24 hours - see Section through thermocouples in Figure 6.2.

6.5 Experimental apparatus

General details of the test apparatus are shown in Figures 6.5 and 6.6.

The strong beam, restraint frames, heating equipment and insulation, are as described in 4.1.1. Load spreaders were fabricated by welding together two 50 mm square hollow steel sections having a wall thickness of 5 mm. To achieve point contact between the spreaders, and between the spreaders and the specimen, 19 mm dia bar, milled to a semi-circular section, was used.

To prevent lateral instability of the beam under load, the cap of the hydraulic ram was replaced by a square steel plate welded to a steel spigot which was a close sliding fit in the end of the ram shaft. This meant that the ram effectively provided lateral restraint to the unheated flange of the specimen beam.

Automatic measurement of vertical displacement at mid-span was needed and this dictated the use of linear displacement transducers. Since it was not possible to place a transducer in line with the web (because the heating elements and load spreaders were in the way on the heated and unheated flanges respectively), it was decided to measure the displacement of the unheated flange using two transducers spaced roughly 230 mm apart such that the ends of the transducer shafts located in recesses in a 10 mm square steel bar tack welded across the bottom flange of the specimen, Figure 6.6. The bodies of the transducers were clamped to the upper flange of the strong beam.

Two transducers were used in order to allow for any rotation of the specimen flange. Any rotation would increase the displacement of one transducer and decrease by an equal amount the displacement of the other assuming they were equi-spaced either side of the specimen. The average reading would thus give the true displacement.

Each transducer was a precision linear displacement tranducer, having a limiting excitation of 130 V and an operational temperature range of -50 to +80°C, manufactured by Penny and Giles Potentiometers Ltd, Christchurch, Dorset. Each transducer, model HLP 190-FS1-75-3K, had a lightly sprung loaded shaft with a travel of 75 mm. They were connected to a constant voltage device. This was a Thurlby PL Series power supply, Type PL 310. For the experiment the excitation voltage was 4 V.

Because the test load was to be kept constant throughout the test, any flexure of the strong beam or extension of the restraint frame, which could result in an increase in the observed displacement, would be irrelevant. But even if this were not so, such displacement would be negligible bearing in mind the low magnitude of test load (17,378 N) and the robust design of the apparatus.

The hydraulic jacking system comprised a hand pump and an accurate pressure gauge mounted on a plywood base, a hydraulic lead and jack, all having a maximum operating pressure of 10,000 lb/in^2. An economy, medium size hydraulic hand pump with a maximum pressure of 10,000 lb/in^2 was used. This was an Enerpac P-39 single speed pump supplied by Enerpac Ltd, Newhaven, East Sussex, which was purchased together with a length of hose rubber reinforced with braided steel webbing and appropriate couplers. To measure accurately the hydraulic pressure up to pressures of 10,000 lb/in^2 a Budenberg Standard Test

Gauge was purchased. It was a Type 215, graduated every 50 lb/in^2, with a 10 inch (254 mm) diameter face supplied by Budenberg Gauge Co Ltd, London. The hydraulic jack used was manufactured by Enerpac Ltd. The main details taken from Enerpac's catalogue EE.10.81, Page 4, are given in Table 6.1.

Because it was not possible, because of lack of time, to calibrate the jack before the experiment, it was necessary to calculate the hydraulic pressure from Enerpac's literature in the following way: required load on beam = 17,378 N; effective cylinder area = 6.41 cm^2; therefore pressure = force/area = 17,378/641 = 27.1 N/mm^2; using conversions 1 kgf = 9.81 N = 2.2 lb gives a pressure of 3920.9 lb/in^2.

The 2 displacement transducers and the 56 pairs of thermocouple wires (asbestos-sheathed 0.47 mm diameter wires of Ni/Ch and Ni/Al) were connected directly to a 100 channel Christie CD248 data logger manufactured by Christie Electronics Ltd, Stroud, Glos.

6.6 Conduct of experiments

The displacement transducers were calibrated prior to the experiment using a vernier micrometer depth gauge: 0.01875 mm/mV was obtained for a 4 V excitation.

The constant voltage supply and datalogger were switched on roughly 20 minutes before commencement of test so that they could stabilise.

Two magnetically based dial gauges reading to 0.01 mm accuracy were placed on the strong beam so that the shafts rested on the bottom flange of the specimen at its ends. These were used to quantify any upward movement of the

specimen when applying the load of 17,378 N. The load was applied but negligible deformation occurred in the test rig.

The power to the two electrical heating elements was switched on and input to each element equalised using the two variacs. Frequent checks were made to ensure that the temperatures in one half of the specimen were roughly the same as in the other half, and it was found unnecessary to have different settings on the two variacs to accomplish this. The hydraulic pressure of 3920 lb/in^2 was maintained as the specimen bowed upwards, by frequent pumping of the hand pump. Measurements of temperature, transducer and dial gauge readings continued for 32 minutes at which time steel temperatures at some positions had reached 700°C, and the power to heaters and datalogger was then switched off.

After the main experiment the jack and hand pump assembly was taken to Building Research Station, Garston, to calibrate using the Avery Denison dead weight test machine. The dead load was applied in 0.2 ton increments up to 4.2 ton and the pressure gauge reading (lb/in^2) noted. The load versus pressure relation was linear and it was found that the experimental pressure of 3920 lb/in^2 corresponded to a load of 1.7 imperial tons.

6.7 Results of first heating experiment

Temperature data at intervals of 2 minutes are given in Table 7 of Appendix 2 while Table 8 of Appendix 2 provides initialised displacement transducer data at 2 minute intervals. Data of vertical displacement of ends of specimen measured with the dial gauges are plotted in Figure 6.7.

6.8 Analysis of results for first heating experiment

6.8.1 Temperature distribution

Figure 6.8 shows the averaged temperatures at different distances from the heated flange for different times. The temperatures for the two end stations (thermocouples 1 to 7 and 50 to 56) are not included in the averaged data, Table 6.2, since the heat losses from the ends and consequent lower temperatures would have led to slightly lower averages if they had been included; besides, the ends of the beam were subjected to minimal bending moment.

It can be seen that the temperature profiles are not markedly curvilinear and this is to be expected due to the small depth (80 mm) of section and the small area of beam from which heat may be lost. The maximum temperature difference across the section was 380°C at the end of the test.

Figure 6.8 shows an unaccountable reduction in temperature on the inside face of the unheated flange relative to the outer face: at the end of the test this difference was approximately 15-20°C. There is a similar, though less pronounced, effect on the heated flange but this can be explained by the high thermal conductivity of steel. The profiles were drawn so as to ignore such subtleties. Table 6.3 presents the temperature data taken from the profiles.

6.8.2 Test load and stress level

It was explained earlier, 6.6, that it was not possible to calibrate the jack before the experiment and it was therefore necessary to calculate the required hydraulic pressure from the jack manufacturer's data. This was 3920 lb/in^2 and corresponded to a dead load of 1.7 imperial tons. This corresponds to a load of 16,980 N. This is 397.8 N less than the load applied in the experiment

which represents a difference of 2.28%. In other words the test load was 2.28% greater than it should have been. Bearing in mind the practical difficulty of maintaining the pressure constant during the experiment, it is considered that a 2.28% overload is acceptable.

If stress level is defined as the maximum applied stress (ie at mid-span) divided by the maximum permissible elastic stress, then, since the measured yield stress was 325 N/mm^2, the maximum permissible elastic stress is 325/1.6 = 203 N/mm^2, assuming a load factor of 1.6. Hence the stress level is 165/203 = 0.81 or 81%.

6.8.3 Corrected displacements

The transducer displacements were derived by multiplying the transducer output voltages recorded on the datalogger by the calibration factor of 0.01875 mm/mV, Table 6.4. Because both ends of the beam displaced slightly according to the dial gauge readings, the transducer displacements were modified to give the true displacement relative to the strong beam. Up to a time of 24 minutes the dial gauge readings cancelled each other out (one end of specimen went up, the other end came down by roughly equal amounts). However, from 24 minutes on, the upward bowing of the beam caused the ceramic insulator at one end of the heating element to become wedged between the guide plates of the restraint frame and the specimen such that further bowing caused the beam to pivot about the corner of the guide plates (and not the knife edge) causing the beam end to move down, and this effect is shown in the curve for dial gauge B in Figure 6.7. To allow for this effect and so obtain the true displacement of the centre of the beam relative to its ends, the transducer displacements were corrected as in Table 6.5.

The displacement time curve is shown in Figure 6.9 and the final displaced form in Figure 6.10. (The Kaowool insulation board encasement has been partially removed for clarity in Figure 6.10). The displacement curve is practically linear with time up to 24 minutes. At 24 minutes the temperature of the heated flange has reached 550°C - the old so-called 'critical' temperature - and thereafter a runaway displacement is observed.

6.8.4 Performance under BS476 deflection criteria.

The rate of displacement with time appears to be roughly constant when the displacement criterion of span/30, corresponding to a central displacement of 50 mm, has been reached. It is of interest to calculate the rate of displacement from 24 minutes onwards and to see when the proposed limiting criterion (see 1.2) of $L^2/9000d$, corresponding to 3.125 mm/min (ie $1500^2/9000 \times 80$) is reached. This was done by drawing a tangent to the displacement curve at 2 minute intervals and calculating the rate (slope). The data are given in Table 6.6.

By interpolation, the time when a rate of 3.125 mm/min is reached equals 26.25 min. But L/30 is not exceeded until 30 minutes, so in this case the beam, if heated under BS476 standard test conditions, would be given a 26 minute fire resistance (see 1.2), according to the draft BS 476 : Part 20 : 1984[1.6].

6.8.5 Thermal bowing component of displacement

The total displacement of the beam comprises a displacement due to thermal bowing and an elastic/plastic displacement. It is of interest to know the magnitude of the thermal bowing component. In 3.2 it was shown that the central displacement Δ of a steel member, having a linear temperature gradient across the section which does not change along the length, can be expressed as:

$$\Delta = \alpha T L^2/8d$$

where α is the coefficient of thermal expansion (0.000014/°C for steel), T is the temperature difference between heated and unheated flanges, and L is the length of member of depth d.

Bowing displacement Δ has been calculated at 4 minute intervals, and is given in Table 6.7.

The data for T have been taken from Table 6.3 by assuming that a best-fit straight line for the curvilinear temperature profiles can approximate to a line drawn between the temperatures of the heated and unheated flanges. For the experiment

$$\Delta = \frac{.000014 \times 1500^2}{8 \times 80} \times T = 0.0492\ T$$

The thermal bowing displacements have been plotted in Figure 6.9. It appears that thermal bowing represents roughly 2/3 to 3/4 of the total displacement up to the point of onset of runaway displacement (24 minutes).

6.8.6 Elastic component of displacement

Examination of Figure 6.9 shows an almost linearly increasing difference between the total displacement and the thermal bowing component of displacement up to about 24 minutes. This difference can only be due to the increase in elastic displacement due to the reduction in elastic modulus, since the load was maintained constant throughout the test. However, since the elastic modulus does not significantly reduce until a temperature of 400°C is reached, when, at most, (Figure 2.8), E has reduced to 80% (ie 168 x 100/210) of its

room temperature value, the gradual increase in displacement clearly shown from 8 minutes onwards, but before a heated flange temperature of 400°C is reached, (an increase from 1 mm to 5 mm) cannot be accounted for. To determine the elastic component of displacement, the following calculations were made.

$$\Delta = \frac{5\ wL^4}{384\ EI} = \frac{5\ WL^3}{384\ EI}$$

where W = 17378 N, L = 1500 mm, and I = 789914 mm^4 (see 6.1).

At 20°C (E = 210 kN/mm^2),

$$\Delta = \frac{5 \times 17378 \times 1500^3}{384 \times 210{,}000 \times 789914} = 4.604 \text{ mm}$$

At 400°C (E = 0.80 x 210 = 168 kN/mm^2), Δ = 5.755 mm which represents an increase of 1.151 mm above the room temperature value. The increase observed in the experiment over the same temperature range was, from Figure 6.9, 5 mm. Bearing in mind that the calculated increase in displacement, given above, assumes that the whole section is at 400°C and not just the heated flange (the cold flange was at 150°C), there is clearly a mismatch between the calculated and experimental elastic displacements.

Similarly at 550°C - the temperature of the heated flange when runaway displacement begins - the calculated elastic displacement = 210 x 4.6/90 = 10.733 mm (for E = 90 kN/mm^2 taken from Figure 2.8) which represents an increase of 6.138 mm above the room temperature value. This should be compared with a measured difference of approximately 7.5 mm. However, using an E versus T relationship which does not exhibit such a large drop in E with T, such as the BSC/Euronorm data (Figure 2.9), the increase in elastic displacement for a

heated flange temperature of 550°C is (210 x 4.6/170 - 4.6) = 1.08 mm. Again, this should be compared with an observed value of 7.5 mm. Hence there remains a mismatch of calculated and experimental elastic displacements.

6.9 Supplementary experiments and analysis of results

To explore the above mentioned mismatch a further 2 experiments were conducted using the same specimen.

6.9.1 Elastic displacement at room temperature

First the beam was progressively loaded at 20°C to check that it behaved elastically up to the design load. Two such loadings were applied. The linear load displacement curves, Figure 6.11, confirm elastic behaviour and a displacement under the design load of 4.7 mm which is close to the calculated displacement of 4.604 mm.

6.9.2 Elastic and thermal bowing displacements for reheating experiment.

A reheating test was undertaken with the object of measuring the bowing displacement with zero load applied, and also the elastic displacement under instantaneous application of the design load several times in the heating process. This would a) enable the experimental unrestrained thermal bowing to be determined for comparison with the calculated displacement, and b) enable the increase in elastic displacement to be measured instantaneously at different temperatures so ignoring creep effects.

The two displacement transducers were replaced by 2 dial gauges reading to 0.01 mm accuracy mounted on stands with magnetic bases. The temperatures of the heated and unheated flanges were measured and averaged over the length of the specimen as before. The temperature and displacement data are shown in Figure 6.12.

It can be seen that the calculated and experimental thermal bowing displacements agree reasonably well. More importantly, the experimental elastic displacement is roughly constant (at between 4 to 5 mm) up to 16 minutes when the hot flange temperature had reached 450°C, but increased to 7 mm at 20 min when the hot flange temperature was 550°C. The shape of the elastic displacement time curve agrees well with the shape of the elastic modulus temperature curve. This comparison shows that, within the elastic domain, the total displacement can be accurately predicted by adding the calculated thermal bowing displacement and elastic displacement together, thus using the principle of super-position.

However it remains unclear why, in the first heating experiment, the measured total displacement linearly exceeds, as mentioned in 6.8.6, the calculated total displacement up to the point of runaway displacement. It cannot be due to early yielding of the weld metal due to high residual (tensile) stresses since the weld metal gives little contribution to the 2nd moment of area of the section. Nor was it due to failure of the weld metal which would allow shear slippage (of flange relative to the web) since there was no evidence of this from an examination of the welds and the end plates - the latter remaining normal to the section axis.

6.10 Conclusions

i) Experiments have been successfully conducted on a 6-point loaded model steel I-beam heated along one flange while resting on simple supports. The experiment reproduced the loading, restraint and heating rate conditions appropriate for a full size I-section beam subjected to a BS 476 fire resistance test. It can therefore be claimed that the model test conditions can be made to simulate the full-scale conditions.

No attempt was made to simulate the temperature profiles in a full size I-section beam, and it has to be accepted that a limitation of model scale testing may be the inability exactly to simulate the profiles in a large scale section, and this criticism may be fairly made of attempts to simulate the temperature distributions in shelf angle floor beams where, at full size, the temperature profile has been shown to be S-shaped (Figure 1.9) whereas in the model tests reported herein there has been no point of contraflexure in the temperature profiles.

ii) The model test beam, when loaded to produce the maximum permissible elastic design stress of 165 N/mm^2, attained a central displacement of span/30 at a time of 30 minutes when the average heated and unheated flange temperatures attained 645°C and 280°C respectively, ie an average temperature of 462°C. A displacement of span/20 was reached at 33 minutes when the heated and unheated flange temperatures were 680 and 300°C. Applying the draft BS 476 : Part 20 rate of displacement criterion, showed that failure occurred at 26.25 minutes.

iii) It might be thought that the flexural performance of an I-section steel member in fire is mainly governed by the temperature attained by the hottest flange because the hottest flange is the first part of the section to experience runaway displacement, being both highly stressed and at the highest temperature compared with the rest of the section.

In the model beam test it was shown in 6.8.2 that the stress level was 81%. The beam failed by well-established runaway displacement, Figure 6.9, at approximately 30 minutes (when the mid-span displacement reached span/30) at which point the heated flange temperature was approximately

625°C. If runaway displacement is judged to occur much earlier, say at 24 minutes (when the total displacement curve loses its linearity) the corresponding heated flange temperature is 550°C. However, rough interpolation between the curves for stress levels of 0.727 and 0.909 in Figure 2.11 shows that runaway displacement (assumed to occur atuapproximately 1% strain) in a uniaxial tensile test occurs at a temperature of approximately 470°C for a stress level of approximately 80%. The results of the model beam test therefore suggest that the temperature of the heated flange does not dominate the displacement performance of an I-section member in flexure.

iv) Thermal bowing, Figure 6.9, was shown to represent the major component of displacement (roughly 2/3 to 3/4 of the total displacement) up to the onset of runaway displacement assumed to occur at approximately 24 minutes. At this time, when the heated flange temperature was 550°C, the elastic displacements, due solely to the reduction in elastic modulus, in relation to the total displacement represented 33% experimentally and between 26% (ie 6.138 x 100/23.5) and 4.6% (ie 1.08 x 100/23.5) theoretically.

v) As shown in iv) above, the calculated elastic displacements were considerably less than those obtained experimentally and the results of additional tests were not able fully to explain the anomaly observed in the first heating test.

vi) The fabrication of the specimen, using three strips of steel welded together using the tungsten inert gas (TIG) process, proved satisfactory and could be relied upon to produce small scale I-sections quickly and economically without recourse to time-consuming fabrication by milling from the solid. Guidance is given on welding procedure which results in sections with minimal distortions.

CHAPTER 7. EXPERIMENTS ON DESIGN-LOADED MODEL COLUMNS HEATED ALONG ONE FLANGE

7.1 Design of model column experiments

It is usual to test columns when mounted vertically. A column could however be tested horizontally provided that its behaviour would be unaffected by any forces perpendicular to it (such as its dead weight) which would be absent in the vertical orientation. It was decided to test the model columns horizontally since i) the dead weight of the column and the electrical heating elements was small and so would have negligible effect on the direction of the bowing, ii) the column flanges would be vertical and the induced thermal bowing, due to heating of one flange, would be in the horizontal direction and such bowing displacements were therefore likely to dominate, causing failure in the horizontal direction, and iii) it was more convenient, using the strong beam concept, to test in the horizontal orientation.

Three columns would be tested, having markedly different slenderness ratios assuming that failure would occur by buckling about the weak (y-y) axis. The length of model column would be dictated by the length of proprietary electrical heating element available on the market. Suitable elements were nominally 680 mm long so that two such elements end to end dictated a column length of nominally 1350 mm. Based on this length, the section sizes were deduced to give slenderness ratios (ℓ/r_{yy}) from nominally 90 to 140. Assuming that the columns would be effectively pin-ended, the resulting I-section size would be 60 mm x 60 mm with flange and web thicknesses of 6 mm and 4 mm respectively. The range of slenderness ratios required would be achieved by altering the flange width while keeping all the other column dimensions constant.

Each column would be thermocoupled across the depth of section and along the length so that the temperature distribution would be accurately known throughout. Axial expansion/contraction of the column would be continuously measured. Likewise, the lateral bowing in the plane of the web at mid-length would be measured.

Each column would be loaded with a load which caused the maximum permissible elastic stress allowed in BS 449[7.5], and this load would be maintained constant throughout the test. This would reflect the loading conditions used in the BS 476:Part 8 fire resistance test for columns.

7.2 Fabrication of test specimens

There is, so far as the author is aware, very little reported work of small scale structural steel models employing I-sections used in fire research work. There has, however, been work done using small scale structural models for static and dynamic load testing at ambient temperature. Such work has been sponsored by the American Iron & Steel Institute and was undertaken by the Massachusetts Institute of Technology in the mid-1960's. The work, reported[7.1] by Litle and Foster, explored the use of Heliarc welding - TIG (tungsten inert gas) welding - and proved it suitable for fabricating sections using strips of sheet steel down to 0.025 inch (0.635 mm) thick. An alternative was to mill bar stock which, though satisfactory for single elements, ie a beam or column, still left the problem of forming the element junctions: TIG welding on the other hand could be used to fabricate the sections and join them to make frameworks. The TIG process permits greater control and smoother, cleaner welds without burn-through and spatter. The TIG process employs a non-consumable tungsten electrode and a filler wire which is fed into the arc, melted and propelled toward the joint being formed. Oxidation is prevented by a shield of inert gas (argon or helium) around the weld.

A useful discussion of different fabrication techniques used for fabricating steel models for seismic load simulations is also given by Mills et al in a comprehensive report[7.2] sponsored by the National Science Foundation. The fabrication of the American model I-sections was performed by milling from bar stock because TIG welding gave unacceptably high camber tolerance. Using a scale ratio of 1:6 applied to a W6 x 12 beam with tolerances according to the AISC Steel Construction Manual, resulted in a model beam nominally 0.7 in (18 mm) wide by 1 in (25 mm) deep. Dimensional data are given in Table 7.1, and it can be seen that it was quite feasible to produce very small model sections using the milling method with tolerances within the range of standard hot rolled I-sections.

The dimensions of the model columns in the present work, the need to avoid residual stresses which result from welding, and, most important of all, the need to have specimens free of geometrical imperfections, dictated that milling the models from the solid was the only acceptable method of fabrication. Problems associated with other methods of fabrication are also given in 6.2.

Three specimens were required for the test programme. The required dimensions and tolerances are shown in Figure 7.1. All were the same length and the sections differed only in the width of the flange so as to provide different slenderness ratios. Flange widths were 40, 50 and 60 mm. 78 mm square hot rolled mild steel bar was purchased, and the sections milled from the centre of the bar section so as to remove the surface material (nominally 9 mm from all four faces) which was likely to contain residual stresses from the hot rolling, cooling and, if employed, the roll-straightening process.

It should be noted that large solid sections contain residual stresses which are caused by differences in speed of cooling of the outer and inner material after the hot rolling process. Residual stresses also occur in hot rolled I-sections due to the different rates of cooling of flanges and web, and this has been reported by Kusakabe and Mihara[7.3].

To assess the residual stress pattern likely to be present in a 78 mm solid square steel billet before and after milling, advice was sought from the Product Engineering Department of the British Steel Corporation Sheffield Laboratories. Babb has suggested[7.4] that in an air-cooled billet where roll straightening has not been employed, the shape of the residual stress curve could be expected to be similar to that shown in Figure 7.2. He considers that the maximum stress could be 50 N/mm^2 and that removing 9 mm from all faces could be expected to halve this value. The milling of the I-section would probably further relieve the stresses so that one could expect low stresses in the body of the model I-section.

The columns were milled on a Butler 'Elgamill' heavy milling machine in the workshops of the Building Research Station, Garston. The digitally controlled machine had a moving head and a static table roughly 6 m long. A general view of the machine with a roughed-out column in position is shown in Figure 7.3. The specimen material was gripped in two vices and supported vertically at roughly four equi-spaced points using accurate packing pieces in order to minimise displacement and tool chatter during cutting operations.

Four cutters were used. A 100 mm diameter multi-blade facing cutter was used for roughing out the four outer faces to give a section of 65 mm

square. A 32 mm diameter two-fluted slotting mill was then used to remove the excess web material leaving a web thickness of 9 mm. The 6 mm radii at the ends were formed with a 12 mm dia end mill. The root radii (at the flange web intersection) were then roughed out with an end mill, removing 6 mm of material on each lengthwise run. The outside dimensions were then achieved with the 100 mm multi-blade cutter to a tolerance of 0.5 mm. Finally the inside profile was finished to size using a small feed; it took roughly one hour to complete a 1300 mm long cut along the radius. A portion of a machined column is shown in Figure 7.4.

The machined columns were measured accurately to determine any variation in section size and straightness over the 1300 mm length. The parameters measured, denoted by A to K (10 for each specimen), are shown in Figure 7.5 and the actual measurements obtained for each of the three specimens are given in Table 9 of Appendix 2. It should be noted that the high degree of accuracy attainable with the method of fabrication made it unnecessary to attempt to measure flange-out-of-square. Variations in section dimensions at three points along the length were found to be negligible. Similarly, the straightnesses in the plane of flanges and web were sufficiently accurate, Table 9 of Appendix 2.

60 thermocouples were attached in the positions shown in Figure 7.6 using the method and equipment described in 6.4.

7.3 Physical properties of specimen material

The material was ordered as ordinary mild steel, BS 4360 Grade 43A. It was obtained from a stockholder who believed that the length of 78 mm square hot rolled mild steel bar (billet) supplied came from a British rolling mill.

The British Steel Corporation Swinden Laboratories undertook chemical analysis and dilatometer tests. A tensile test to establish the yield stress and elastic modulus was undertaken by a commercial test laboratory (R.H Harry Stanger of Elstree, Hertfordshire). Samples were taken from the outer part of the bar section.

7.3.1 Chemical composition

The results are as follows: 0.23%C, 0.21%Si, 0.67%Mn, 0.024%P, 0.038%S, 0.12%Cr, 0.03%Mo, 0.10%Ni, 0.013%Al, 0.22%Cu, <0.005%Nb, 0.18%Sn, <0.005%Ti, <0.005%V. The maximum values permitted for a BS 4360 Grade 43A steel are 0.30%C, 0.55%Si, 1.7%Mn, 0.06%P and 0.06%S. The sample was therefore within the limits specified in BS 4360 Grade 43A.

7.3.2 Dilatometer results

The tests were conducted on specimens with their longitudinal axis coincident with the axis of the parent material and thus the longitudinal axis of the model columns. Heating and cooling tests were conducted at a rate of 50%C/min, this being a typical rate of heating of an unprotected steel member exposed to the heating conditions of the BS 476 fire resistance test (ISO 834). The curves are shown in Figure 7.7.

During heating the maximum relative 'shrinkage' was 0.08% which began at 715°C and finished at 824°C. During cooling the maximum relative 'expansion' was 0.16% which began at 730°C and finished at 650°C. Apart from the marked difference (100%) in magnitude of relative shrinkage and relative expansion, the curves are similar to the curves, Figure 2.2,

previously produced by the British Steel Corporation for a structural mild steel.

7.3.3 Mechanical strength

A tensile test was conducted on a specimen milled longitudinally from an outer corner of the 78 mm square bar. The extensometer gauge length was 25 mm with a specimen gauge diameter of 13.82 mm. The yield stress was 346 N/mm^2, the ultimate stress was 517 N/mm^2 and the modulus of elasticity was 192.8 kN/mm^2.

The measured yield stress of 346 N/mm^2 was 1.5 times the minimum yield strength of 230 N/mm^2 for BS 4360: 1979 Grade 43 square bar between 63 and 100 mm square, and 1.4 times the value of 250 N/mm^2 assumed in Table 17a of BS 449: Part 2: 1969. Thus the mechanical properties of the column material were greater than would be expected of ordinary mild steel Grade 43: the properties were nearer those of high strength structural steel, Grade 50, which, according to Table 19 of BS 4360: 1979, has a guaranteed minimum yield strength of 325 N/mm^2 and an ultimate strength of 490/620 N/mm^2.

For the purposes of calculating the column design loads the following values were adopted: yield stress = 346 N/mm^2 and modulus of elasticity = 192.8 kN/mm^2.

7.4 Calculation of column design loads

The design loads for the model columns were calculated in accordance with the code of practice BS 449: Part 2: 1969[7.5]. It was assumed that all three columns would fail about the minor (yy) axis since ℓ/r_{yy} was at least

50% greater than ℓ/r_{yy}. The table (Table 17 in the code) relating slenderness ratio (ℓ/r_{yy}) to permissible average stress (p_c) for BS 4360 Grade 43 steel has not been used, as the measured yield stress for the model column material was 346 N/mm² (see 7.3.3) and this differed from that assumed in Table 17, namely 250 N/mm². The formula for calculating permissible average stress is given in Appendix B of BS 449 and is reproduced as follows:

$$K_2 p_c = \frac{\sigma_s + (\eta + 1)\, C_o}{2} - \left\{ \left(\frac{\sigma_s + (\eta + 1) C_o}{2} \right)^2 - \sigma_s C_o \right\} \qquad (7.1)$$

where p_c = permissible average stress, N/mm²

K_2 = load factor, taken as 1.7

σ_s = minimum yield stress, N/mm²

C_o = Euler critical stress = $\dfrac{\pi^2 E}{(\ell/r)^2}$, N/mm²

η = $0.3\,(\ell/100r)^2$

ℓ/r = slenderness ratio = effective length/radius of gyration.

Equation (7.1) was adopted in the present work assuming the code Appendix value of η was applicable. It should be noted that η is a factor to allow for imperfections in the column such as out-of-straightness and residual stresses. In the model columns the out-of-straightness was imperceptible and residual stresses were minimised by milling the columns from the centre of a steel billet. The model columns could therefore be expected to have an η factor less than the BS 449 value of 0.3 and would lead to a higher load carrying capacity. However, to enable the test results to be directly compared with those for columns tested in the full scale furnace under

BS 476: Part 8: 1972 conditions (which usually assume permissible average stresses are derived from Table 17a for grade 43 steel) it was decided to adopt an η factor of 0.3.

Because the manufacturing tolerances on section size were small, it was considered satisfactory to base the calculation of section properties on the nominal column dimensions rather than the measured dimensions.

Area of section = (2 x 6 x B) + (48 x 4) = 12B + 192 where B = flange width

$I_{xx} = \frac{1}{12} \times B \times 60^3 - (B-4) \times 48^3$

$I_{xx} = 8784B + 36864$

$I_{yy} = (2 \times \frac{1}{12} \times 6 \times A^3) + (\frac{1}{12} \times 48 \times 4^3)$ from which:

$I_{yy} = A^3 + 256$ mm^4

$r_{yy} = (I_{yy}/A)^{\frac{1}{2}}$

ℓ = length of column plus ball joints = 1310 + 2 x 25 = 1360 mm

Table 7.2 gives the section property data for each of the three flange widths.

From the tensile test, see 7.3.3, σ_s = 346 N/mm^2 and E = 192.8 kN/mm^2. Using these data and Equation (7.1) the data in Table 7.3 were prepared. The test loads for Tests 1, 2 and 3 are therefore 32.45 kN, 60.81 kN and 95.69 kN respectively.

7.5 Experimental apparatus

7.5.1 Concept of apparatus

The primary objective was to design an inexpensive and simple rig which would enable compressive loads of up to 100 kN to be applied to model steel pin-ended columns nominally 1350 mm long. A secondary objective was to provide non uniform heating (heating along one flange) but this would not present a problem as a suitable technique had already been developed and proved in tests on model beams.

The horizontal rig would employ a strong beam with robust brackets bolted near the ends between which the compression load would be induced, Figure 7.8. This would place the strong beam in bending and tension, and the 2nd moment of area of the strong beam section would therefore need to be large to minimise deformation. The rig should be capable of being operated by one person and this would mean that displacements and load would need to be recorded automatically leaving the experimenter to operate the hydraulic loading system.

Columns would have separate ball and socket end mountings to which the column ends would be bolted so as to avoid the need to accurately machine spherical ends on each column. The load would be applied and maintained constant with a hand operated hydraulic pump and ram. Load would be measured with a compression load transducer; load would also be measured with an oil pressure gauge calibrated for the particular ram used.

Axial displacement of the column would be measured with a linear displacement transducer attached to the moving end of the column. Dial gauges mounted on the rig or independent of the rig (on the floor of the

laboratory) would also measure axial displacement at both ends of the column in proving tests. To measure lateral displacement in the plane of the web a linear displacement transducer was used, bearing against the middle of the unheated flange at mid-span.

The columns would be placed in the test rig with the web in the horizontal plane, and high-power ceramic insulated electrical heaters would be placed against the vertical face of one flange and insulated to reduce heat losses. If it was desirable to achieve different magnitudes of temperature gradient across the section in later tests, this would be achieved by allowing more or less heat loss to occur from the unheated web and flange by varying the extent of the thermal insulation.

7.5.2 Details of apparatus

A general view of the apparatus is shown in Figure 7.9

i) Strong beam assembly

The strong beam comprised a 2500 mm length of rectangular hollow section 300 mm deep by 200 mm wide with a wall thickness of 12 mm, in ordinary mild steel (BS 4360 Grade 43C).

Holes were drilled and tapped in the upper (200 mm wide) face to accept 10 mm diameter bolts to fix 2 restraint brackets and 6 mm diameter bolts for the jack saddle. In addition 4 holes were drilled and tapped in the side wall of the strong beam to enable the mounting plate (used to support the lateral displacement transducer) to be bolted on using 6 mm diameter bolts.

ii) Restraint brackets

The 2 brackets were made from 12 mm ordinary mild steel plate. One was constructed of three plates welded to form a centre-braced cleat 150 mm long by 110 mm high by 100 mm wide, and the vertical face was drilled with four 7 mm dia holes to allow the load cell to be bolted on. The other bracket was 150 mm long by 100 mm high by 70 mm wide and had four drilled and tapped holes in the vertical face to enable the female spherical bearing to be held in place using 6 mm diameter bolts. Six holes 11 mm dia were provided in each base plate to enable it to be bolted to the strong beam with 10 mm diameter high tensile steel bolts.

iii) Jack guides

It was important to prevent the jack from moving radially whilst allowing it to transfer its load to the load cell without axial restraint. This was achieved using a semi-circular jack guide 115 mm long bolted to the strong beam with two bolts 6 mm dia. The jack was prevented from moving upwards using two jack retention clamps made by bending 5 mm thick mild steel bar 20 mm wide and bolting the ends to the saddle guide with 6 mm diameter bolts.

iv) Spherical bearings and their lubrication

Two pairs of matching male and female bearings were accurately machined from 60 mm square mild steel bar. The spherical radius was 65 mm and in order that friction between the mating faces would be minimised, great attention was given to the machining such that a finish of not less than 0.8 um Ra according to BS 1134: 1972 was achieved. One female bearing was bolted to the fixed end restraint bracket while the other had a cylindrical portion roughly 25 mm diameter which was a close sliding fit in the

recessed end of the ram. The two male bearings were identical and could be bolted to each test column in turn using four bolts 6 mm diameter.

Lubrication of the mating faces was considered essential. In Test 1 an anti-seize grease J166 made by Rocol Ltd., Leeds, was used as this was claimed to be capable of resisting temperatures up to 1000°C but under unspecified compressive stress conditions. Further research into proprietary lubricants revealed that liquid lubricants were not readily available but that a thin carbon tape might be suitable. Pilotgraph 4040 graphite tape 0.5 mm thick in a range of widths from 10 to 25 mm could be obtained from Beldram Packing and Rubber Co Ltd., Brentford. This was capable of operating up to 3000°C which was well in excess of test temperatures, and the fact that it was only 0.5 mm thick would mean that any reduction in thickness under compression at elevated temperatures would be negligible. A 15 m roll 25 mm wide was purchased at a cost of £18.35 (December 1982). The tape was cut into short lengths and applied in single layer strips over the female bearings. This was used in Tests 2 and 3.

v) Column guide

To prevent a column bowing downwards, which would result in the strong beam preventing large displacements of the column, a knife edge plate was fabricated so as to accurately fill the gap between the lower edge of the column flange tips and the top face of the strong beam at mid-span. When each column was placed in the rig and loaded with the design load before heating, the underside of the knife edge plate was packed with steel shim to ensure that any displacement of the specimen in a vertical direction took place only upwards.

vi) Hydraulic loading equipment

The hydraulic system comprised a hand pump and an accurate pressure gauge mounted on a plywood base, a hydraulic lead and jack, all having a maximum operating pressure of 10,000 lb/in^2. It is described in 6.5.

Although the pressure gauge used in the experiment was a 10,000 lb/in^2 Standard Test Gauge manufactured by Budenberg Gauge Co. Ltd., Broadheath, London, it was considered desirable to check its accuracy using a dead weight tester. An Industrial Dead Weight Tester manufactured by Barnet Instruments Ltd., Barnet, Hertfordshire and belonging to the Fire Insurers & Testing Organisation (FIRTO) Borehamwood was used for this purpose. The pressure gauge was screwed to the tester and dead weight applied so that, through a lever mechanism, dead weight increments of 1000 lbf were applied up to 10,000 lbf. The application of each 1000 lbf corresponded to a pressure of 1,000 lbf/in^2. The results are given in Table 7.4. As can be seen the Budenberg gauge read consistently high by approximately 30 lb/in^2. The column tests however never required a pressure less than 3000 lb/in^2 so the inaccuracy of the gauge was never more than 1% which was considered satisfactory.

viii) Hydraulic jacks

The jacks were manufactured by Enerpac Ltd. The main details are given in Table 7.5.

viii) Load transducers

Two compressive pillar load transducers of 8 and 50 tonne rating were used. They were purchased from Strainstall Ltd, Cowes, Isle of Wight and had identical base plates and the same overall height of nominally 100 mm.

The 8 tonne transducer was a standard Load Cell Type 1590 CNR3M. The 50 tonne transducer was an upgraded Load Cell Type 1590 ZNR3M. The maximum supply voltage was 25 with a preferred (normal) supply voltage of 10. The absolute maximum load was 50% over rated full load. The temperature rating allowed their use over an ambient range of 0 to 60°C, compensated to 0.05% per °C. Each transducer was supplied with a Test and Calibration Certificate. The calibration sensitivities were 1.493 mV/V at 8 tonnes and 1.91 mV/V at 50 tonnes. For the 10V excitation used in the experiments, the mV/tonne was therefore 1.8662 and 0.382 for the 8 and 50 tonne load cells respectively.

ix) Displacement transducer assemblies

Precision linear displacement transducers manufactured by Penny and Giles Potentiometers Ltd, Christchurch, Dorset were used. Model HLP 190-FSI-75-3K having a lightly sprung shaft with a travel of 75 mm was used for measuring bowing displacement at mid-span of the column specimen. Model HLP/BC/1/50/2K having an unsprung shaft with a travel of 50 mm was used for measuring axial displacements. Both types of transducer had a maximum allowable excitation of 130V and an operational temperature range of -50 to +80°C.

The axial displacement transducer was initially mounted alongside the jack with its shaft screwed into a small plate welded onto the female spherical bearing. In Test 1 this transducer was subjected to conducted and radiated heat such that it had to be cooled with cold damp rags. The temperature attained by the transducer was within the 80°C maximum allowable and was re-used after recalibration in a position remote from the heat source using a 150 mm long screwed extension rod 6.35 mm diameter made of Tufnol (Tufnol

is a proprietary composite of laminated cloth impregnated with phenolic resin), and was chosen in this situation because it would be unaffected by heat. The arrangement shown in Figure 7.10 was used in Tests 2 and 3. This figure shows the equipment mounted on a plywood box beam which was used for exhibition purposes.

In Test 1 the lateral displacement transducer was mounted horizontally on a plate bolted to the side wall of the strong beam such that the 75 mm long shaft was in direct contact with the unheated flange of the specimen. It was subjected to conducted and radiated heat such that it had to be cooled with cold, damp rags. The transducer was undamaged and was re-used on a new mounting bracket for Tests 2 and 3 (care was taken in the design of the new mounting bracket to ensure that the bracket itself would not deflect due to non uniform heating by radiation, and this accounts for the diagonal bracing). The new mounting bracket, shown in Section B-B of Figure 7.8, enabled an additional transducer to be used so as to measure vertical upward displacement of the specimen web. Both the vertical and horizontal displacement transducers were spaced away from the heated specimen using 10 mm diameter silica rod to lengthen the transducer shafts. The horizontal silica rod was guided by means of a hole in the mounting bracket. The complete assembly is shown in Figure 7.9.

x) Constant voltage supply

A source of constant voltage was required to excite the displacement and load transducers. The preferred voltage for the load transducer was 10V. This was achieved using a Thurlby PL Series power supply, Type PL 310. This supplied a maximum of 3 displacement transducers and one load transducer in parallel.

xi) Electrical heating equipment and thermal insulation

The electrical heating elements, variacs, transformers and thermal insulation boards used to reduce heat loss was as described in 4.1.1. A cross section through the specimen showing the heating element and insulation is given in Figure 7.8.

xii) Data recording

The output from 3 displacement transducers, 1 load transducer, and 60 thermocouples were required to be monitored and recorded at 1 minute intervals. Two 30 channel Solartron 3430 compact dataloggers were available for this purpose and this meant that 4 thermocouple channels had to be allocated to the transducers. The disconnected thermocouples were numbers 56 to 59 inclusive.

7.5.3 Calibration of jacks and transducers

i) Calibration of hydraulic jack loads

Enerpac Jacks were used in the experiments. The 10 and 15 tonne jacks were calibrated using a Denison 50 ton dead weight machine at the Building Research Station. Each jack was placed between the plattens of the Denison machine. The dead weight was slid along the balance arm to correspond to 1 ton (2240 lb) load increments and the corresponding Budenberg gauge pressure noted. The calibration curves are given in Figure 7.11.

The 25 tonne jack was not calibrated. The pressure required to produce the design load in Test 3 was calculated using the following relation: design load = cylinder effective area x pressure, where the cylinder effective area was obtained from Messrs Enerpac's trade literature.

ii) Calibration of central horizontal displacement transducer

Prior to Test 1 the calibration was achieved using a vernier depth gauge set in 10 mm increments. The calibration curve was linear, from which 1 volt positive output corresponded to 7.45 mm displacement away from specimen column. During Test 1 the transducer became heated and it was considered prudent to calibrate it again. This was carried out with the transducer in the new mounting bracket by inserting 20 mm thick spacers between the column flange face and the end of the transducer shaft. 1 volt positive output corresponded to 7.486 mm displacement away from the specimen column for a 10 V excitation. A calibration factor of 1 volt equals 7.486 mm displacement was adopted for all tests.

iii) Calibration of central vertical displacement transducer

This transducer, added for Tests 2 and 3, was calibrated using a vernier depth gauge set in 10 mm increments. 1 volt positive output corresponded to 7.525 mm displacement away from the specimen column for a 10 V excitation.

iv) Calibration of axial displacement transducer

The transducer was calibrated before Test 1 and, because it was heated during the test and repositioned, it was considered prudent to calibrate again before Test 2. In both cases a vernier depth gauge was used for accurately setting the displacement. Before and after Test 1 the calibration factors were 1 volt = 4.955 mm and 1 volt = 4.982 mm respectively for 10 V excitations. A calibration factor of 1 volt equals 4.980 was used in all 3 tests.

v) Calibration of load transducers

The 8 tonne load transducer was calibrated insitu prior to Test 1 using a dummy column by applying pressure in 1000 lb/in^2 increments up to 5000 lb/in^2 measured on the Budenberg gauge and recording the datalogger outputs for an excitation of 10 volts. The calibration curve gave 1mV = 520.8 lb/in^2. The 50 tonne load transducer was calibrated the same way as the 8 tonne transducer. The calibration gave 1mV = 1840 lb/in^2.

7.6 *Conduct of experiments*

The thermocoupled column had the male spherical bearings bolted on at each end. The lubricant was applied (grease for Test 1, carbon tape for Tests 2 and 3) and the column placed between the female spherical bearings and a small load applied with the hand pump so as to get the bearings to engage fully. The knife edge plate was then slid under the column at mid span and packed with steel shim so that the column could not bow downwards but would be free to bow upwards as well as horizontally. The heating elements were then wired in position, leaving a gap of 3 mm where they butted for an electrically insulating packer of Kaowool board. The Kaowool insulation channels were then attached with steel wire in four separate sections so that they would follow the contour of the bowing column without fracture. The electrical installation was earthed, even though the heaters were operating at only 60 V.

The displacement transducers were then mounted with, where appropriate, the transducer shaft extension rods of Tufnol for the axial transducer and 10 mm dia silica for the transducers at mid-span.

The dataloggers and constant voltage supply were switched on 20 minutes before the test so as to stabilize. Both heating elements were switched on as soon as the dataloggers printed out and this was the start of the test. The appropriate hydraulic pressure was maintained constant by allowing oil to bypass the value as the column expanded and pushed oil and the ram into the jack. Later, it was necessary to pump oil into the jack as the column bowed and shortened axially.

A constant check was made to ensure that the displacement transducer shafts were following the specimen, and that the transducers were kept cool, if necessary by the application of cold, damp rags.

When the end of the test was imminent the displacement transducers were removed for safety. In each of the 3 tests, the column initially bowed toward the heat source, then unexpectedly straightened out and began to bow in the opposite direction - this opposite movement would have ruined the horizontal mid-span displacement transducer if left in place.

7.7 Results of experiments

(i) Test 1

Specimen 1 was used, having the specific section dimensions given in Table 9 of Appendix 2. The specimen had a nominal flange width of 40 mm and, like specimens in Tests 2 and 3, was laterally unrestrained so that it could fail by buckling about the weak axis upwards or strong axis horizontally.

The calculated design load, from Table 7.3, was 32.45 kN (3.256 ton f) which assumed that failure could occur by buckling about the weak axis. Using the 10 tonne jack, this load corresponds to a hydraulic pressure of 3440 lb/in^2.

The thermocouple temperatures, displacement and load transducer voltages are given in Table 10 of Appendix 2 at 4 minute increments for the 68 minute test duration.

(ii) Test 2

Specimen 2 was used, having the specific section dimensions given in Table 9 of Appendix 2. The specimen had a nominal flange width of 50 mm. The calculated design load, from Table 7.3, was 60.81 kN (6.103 ton f) which assumed that failure could occur by buckling about the weak axis. Using the 15 tonne jack, this corresponded to a hydraulic pressure of 4450 lb/in^2.

The thermocouple temperatures, displacement and load transducer voltages are given in Table 11 of Appendix 2 at 4 minute increments for the 62 minute test duration.

(iii) Test 3

Specimen 3 was used, having the specific section dimensions given in Table 9 of Appendix 2. It had a nominal flange width of 60 mm. The calculated design load, from Table 7.3, was 95.69 kN (9.6034 ton f) which again assumed that failure could occur by buckling about the weak axis. Using the 25 ton jack, this corresponded to a pressure of 4180 lb/in^2 (ie. 21510 $\times \frac{2.54^2}{33.2}$ where 33.2 = cylinder effective area, cm^2 from Table 7.5).

The thermocouple temperatures, displacement and load transducer voltages are given in Table 12 of Appendix 2 at 4 minute increments for the 44 minute test duration.

7.8 Analysis of results

7.8.1 Load variation

To determine the variations in axial load (which should be minimal if the hydraulic pressure had been maintained constant during the test, as intended), the load transducer readings were initialised then multiplied by the appropriate calibration factor. The data are given in Tables 13, 14 and 15 of Appendix 2.

In all three tests there was an occasional unintended overload applied during the first half of each test. This was because the column was expanding and producing an overpressure in the hydraulic fluid. However, the overload was rarely greater than 10%. Later in each test the overload was small, and, with the exception of Test 1, there came a time when it was not possible to keep the full load on because of rapid bowing and resulting shortening of the column, and this is clear from an examination of the displacement curves, see Figure 7.17 for instance.

7.8.2 Temperature distribution

It is difficult to visualize the temperature profiles from the tabular data. The temperature profiles for Test 1 were drawn for a time, 60 minutes, near the point of failure. The profiles, Figure 7.12, show:

i) that apart from the temperatures at the end of the column, (curve a), the temperatures are very similar within the main length of the column, so that for obtaining average temperatures along the heated and unheated flanges the two end stations of thermocouples should not be included.

ii) that the centre of the column (where the heating elements butt together) is not at an appreciably lower temperature than the rest of the column: compare curves e) and f), which are for the centre two stations, with curves d) and g) for example.

iii) that the temperature profile across the section is almost linear, and this is because the section is small.

A knowledge of the average heated (maximum) and unheated (minimum) flange temperatures has been shown to be important from earlier work. These data have therefore been calculated and are given in Tables 7.6, 7.7 and 7.8 and have been plotted in Figures 7.13, 7.14 and 7.15 for Tests 1, 2 and 3 respectively.

7.8.3 Bowing Displacements

The displacement transducer readings were initialised then multiplied by the appropriate calibration factor. The data are presented in Tables 13, 14 and 15 of Appendix 2 for Tests 1, 2 and 3 respectively.

The mid-span displacements in the plane of the web (the plane in which thermal bowing occurs) are plotted in Figures 7.13, 7.14 and 7.15 for Tests 1, 2 and 3 respectively. In all three tests, reverse direction bowing was observed. In Test 2 the column initially bowed towards the heat source by nominally 15 mm then straightened out and failed by gross displacement away from the heat source. This behaviour was observed to a limited extent in Test 1 in which the initial bow towards the heat source was 11 mm before undergoing reduced bowing. It should be noted that Test 1 was stopped

before runaway displacement occurred - the column was still carrying the full load when the test was stopped at 68 minutes. In Test 3 the initial bow toward the heat source was 18 mm and this later reduced to 16 mm when, at 36 minutes, the horizontal displacement transducer was removed since it was no longer possible to maintain the load and rapid reverse direction bowing was expected following the experience of Test 2. However it was noted by eye that the column had become straight at approximately 40 minutes and subsequently suffered considerable reverse direction bowing, Figure 7.17.

In Tests 2 and 3, measurements from the vertical displacement transducer at mid-span showed that both columns bowed upwards by no more than 2.5 mm. These displacements were considered to be unimportant and did not justify plotting displacement curves.

In the experiments described in Chapter 6 it was found instructive to calculate the unrestrained thermal bowing displacements and compare these with the displacements under load. This has been done also for these column tests, and the data are given in Tables 7.6, 7.7 and 7.8, and the curves included in Figures 7.13, 7.14 and 7.15. The thermal bowing displacements were calculated using Equation (3.6) as follows

$$\Delta = \frac{\alpha T L^2}{8d}$$ where L = distance to ends of spherical bearings = 1360 mm, d = 60 mm, $\alpha = 14 \times 10^{-6}/°C$, T = difference between average temperatures of flanges, °C

$$\text{So that } \Delta = \frac{.000014 \times 1360^2}{8 \times 60} T = 0.0539T$$

Comparison of calculated and experimental horizontal bowing at mid-span shows the following.

i) That there is very close agreement in Test 1 and reasonable agreement in Test 2 up to 42 and 36 minutes respectively

ii) That there is reasonable agreement in Test 3 up to 16 minutes. Thereafter the experimental displacement was greater up to 36 minutes when it was no longer possible to maintain the load.

iii) The bowing displacement is a combination of thermal bowing and bowing due to the P.Δ effect. It follows that the observed displacement should be greater than the calculated displacement due to thermal bowing alone. Examination of Figures 7.13 and 7.15 confirms this. Figure 7.14 also confirms this from point A onwards, but up to point A the experimental displacement is unaccountably less than the thermal bowing displacement.

In Test 1 the experimental displacement departed from the thermal bowing displacement when the heated flange temperature was approximately 640°C (at 42 min). In Test 2 this occurred when the heated flange temperature was 700°C (at 36 min). In Test 3, this point was more difficult to establish since the curves for experimental displacement and thermal bowing displacement were not close together from 12 minutes onwards, but there was a noticeable change in the different slopes of the two curves when the heated flange temperature was 680°C (at 32 min). These observations could be interpreted to mean that the columns became partly plastic at heated flange temperatures of 640, 700 and 680 for Tests 1, 2 and 3 respectively, assuming that the elastic P.Δ displacements were minimal.

It is of interest to know the average temperature of each column when thermal bowing no longer dominated the behaviour. The data are given in Table 7.9 from which it is clear that this occurred in the temperature range of 540 to 580°C.

7.8.4 Axial displacements

As with the mid-span displacement transducers, the axial displacement transducer readings were initialised then multiplied by the calibration factor. The displacements are given in Tables 13, 14 and 15 of Appendix 2. Axial displacements have also been calculated, using the relation $\Delta = \alpha LT = 0.000014 \times 1360 \times T = 0.019T$ where T is the average temperature rise of the column. The calculated value so obtained can be compared with the displacement obtained from the axial displacement transducer. The data are given in Tables 7.6, 7.7 and 7.8 and plotted in Figures 7.16, 7.17 and 7.18.

In all 3 tests the calculated axial displacement is greater than the experimental displacement before the onset of reverse direction bowing, but the shapes of the curves are similar. Possible explanations for these differences in magnitude are as follows.

i) The calculated displacement assumes there is no restraint to the expansion, whereas in all 3 tests the maximum permissible compressive load was present tending to reduce the experimental axial displacements. In Test 1 for example the axial compressive displacement due to the load would be $\Delta_A = PL/AE$ (from $E = \frac{\sigma}{\varepsilon}$). Substituting values gives:

$$\Delta_A = \frac{32.45 \times 1000 \times 1360}{672 \times 210 \times 1000} = 0.322 \text{ mm at } 20°C.$$

Assuming, at worst, an E value at 500°C equal to 0.5 x E value at room temperature, results in an elastic axial compressive displacement of roughly 0.65 mm. From Figure 7.13 an average temperature of 500°C was reached at approximately 36 minutes, and from Figure 7.16 the difference between calculated and experimental displacements at 36 minutes is roughly 2.75 mm. It can be seen that the elastic displacement of 0.65 mm calculated above only accounts for roughly a quarter of the difference.

ii) The calculated axial displacement assumes that the column remains straight whereas the column bowed resulting in less observed outward axial displacement.

The equation $\Delta_L = \Delta_N^2 / 0.375\ L$, derived in Appendix 3, gives the amount of shortening Δ_L between the ends of a member of length L when it bows into a circular arc such that the mid-span displacement is Δ_N. The equation is based on geometry and assumes that compressive strain is absent. Applying this equation to the model columns of L = 1360 mm gives the relationship of Δ_L to Δ_N shown in Table 7.10.

It can be seen that the shortening effect due to bowing is small: for example, a mid-span displacement of 15 mm produces a shortening of 0.44 mm.

iii) The restraint bracket, or its fixings, supporting the 'fixed' end of the column moved, but this could not explain the large difference (4½ mm for Test 2 at 28 minutes for instance) nor the increasing difference as the test proceeded (the test load being maintained constant).

iv) The plate welded to the female bearing (to which the transducer shaft was attached off centre) rotated, but again this could not explain the large difference which increased with time.

v) The strong beam expanded due to a temperature rise caused by heat radiated downwards from the heating element and specimen. To explore this effect it was assumed that the upper face of the rectangular hollow section steel was raised through a temperature of 40°C, and that the lower face in contact with the concrete floor of the laboratory did not increase in temperature. Assuming the length between fixed restraint brackets is 1700 mm, the expansion = αLT = .000014 x 1700 x 20 = 0.475 mm. There is also rotation to consider, due to the temperature gradient across the strong beam section. However it is clear that these effects are small compared with the unaccounted difference which is, at 36 minutes for instance, 2.75 mm for Test 1, 4.3 mm for Test 2, and 5 mm for Test 3.

It is seen that factors i) to v) above are additive and tend to reduce the difference between the calculated and measured axial displacements.

One criterion of failure is when the column has attained its initial length after expansion and 'contraction'. The heated flange temperature and average temperature at which this occurred is given in Table 7.11. It is clear from Table 7.11 that the initial column length is reached when the heated flange temperatures are in excess of 700°C. The average temperatures of 570 and 610°C are greater than the normally accepted limiting ('critical') temperature of 550°C for columns uniformly heated across their section. A possible explanation for the high temperatures associated with these model column tests is given in 7.8.5.

7.8.5 Relationship of bowing and axial displacements

In 7.8.3 and 7.8.4 the bowing and axial displacements were commented on separately. Here their interdependence is discussed.

Figures 7.19, 7.20 and 7.21 provide, for tests 1 to 3 respectively, experimental curves for axial displacement, Δ_A, and mid-span bowing displacement Δ_N. It is a feature of Figs 7.20 and 7.21 that i) Δ_A reached its maximum value after Δ_N reached its maximum value (towards the heat source), and ii) in the case of Test 2, Δ_A reached its maximum value when Δ_N reached zero after bowing towards the heat source. This behaviour appears to be due to the increase in the distance between the ends of the column (the effect measured by the axial displacement transducer) as the column commences its reverse direction bowing from its position of maximum thermal bow, thus straightening out.

If reverse direction bowing did not occur, then continued bowing toward the heat source could lead to earlier failure times at lower flange temperatures and it would then be necessary, for safety purposes, to ensure that lower steel temperatures (especially the heated flange temperature) were adopted in design.

7.8.6 Justification for use of BS 449 Appendix B method of calculating model column test loads

In 7.4 it was pointed out that the test load was calculated assuming failure would take place about the minor axis. The slenderness ratios, ℓ/r_{yy}, of the columns used in Tests 2 and 3 (which most clearly exhibited reverse direction bowing) were 107.4 and 87.7. In the event the model columns failed about the major axis, but this is not relevant to the

present discussion. It was also pointed out that the test loads were calculated using the formula given in Appendix B of BS 449 because the tensile test, 7.3.3, showed that the room temperature yield stress of 346 N/mm^2 was 1.5 times the minimum yield strength for BS 4360 : Grade 43 and 1.4 times the value assumed in BS 449 : Part 2 : 1969, so that the use of Table 17 in BS 449 would be inappropriate.

If the design loads derived from Table 17 of BS 449 had been used the percentage error using the data in Table 7.3 would be as shown in Table 7.12. It is clear that these errors should have been avoided, thus justifying the use of the BS 449 Appendix B formula.

7.8.7 Explanation of reverse direction bowing

Reverse direction bowing - the phenomenon of an I-section column, which is heated predominantly along one flange, bowing toward the heat source and then straightening out and bowing in the reverse direction to failure - has been exhibited in full size columns (see results of CTICM and BSC tests in 1.8). It has also been exhibited in the model column tests reported herein. Figure 7.22 for instance shows the deformed shape of the model column used in Test 3 and shows that ultimate failure was away from the heated flange.

The phenomenon may be explained in the following way. As one flange of the column begins to heat up the column bows towards the heat source due to the combination of thermal bowing and the P.Δ effect. With further heating the rate of increase in temperature difference between the flanges begins to slow down so that the magnitude of bowing (discounting the P.Δ effect) reaches a constant value. During this further heating both unheated and heated flange temperatures are increasing. The heated flange temperature

begins to approach the temperature at which the reduction in elastic modulus becomes significant. In order that the section remains in equilibrium with the externally applied compressive load P and the bending moment P.Δ at mid-span, the neutral axis moves towards the unheated flange. Provided that the movement of the neutral axis is greater than the magnitude of the initial thermal bow, the compressive load P will tend to reverse the direction of bowing, leading to failure by gross bowing away from the heat source.

To a rough approximation we may say that the maximum possible movement of the neutral axis is half the distance between the inner faces of the flanges. Furthermore, assuming that the P.Δ component of displacement is small compared with the thermal bowing component of displacement (as it was in the model column tests), we may say that if the calculated thermal bowing displacement is greater than the maximum movement of the neutral axis, then reverse direction bowing will not occur, and the column will continue to bow toward the heat source. In this condition the P.Δ effect would accelerate the occurrence of ultimate failure.

7.9 Conclusions

i) Elevated temperature experiments have been successfully conducted on three pin-ended I-section model columns each 1360 mm long with common web depths of 60 mm in which different slenderness ratios were obtained by varying the flange width. The columns were heated along one flange and were maintained under a constant load equal to the maximum elastic design load calculated in accordance with BS 449 : Part 2 : 1969 assuming that failure could occur about the weak (yy) axis. All three columns failed by bowing about the major (xx) axis, even for the column which had the largest slenderness ratio ℓ/r_{yy} of

138 (when ℓ/r_{xx} was 56) corresponding to the section having the smallest flange width of 40 mm.

ii) All three model columns failed by reverse direction bowing, Figure 7.20 for instance. That is by initially bowing toward the heat source, then straightening out again due to movement of the neutral axis away from the hottest flange, and then by continued bowing away from the heat source, as described in 7.8.7.

iii) If failure is deemed to occur when the column has regained its room temperature length after initial expansion and then contraction due to buckling, then column 2 failed when its heated flange temperature and average temperature of whole column reached 760° and 610°C respectively, and column 3 failed when these temperatures were 710 and 570°C respectively (Table 7.11).

iv) The average temperatures at failure (610° and 570°C for column tests 2 and 3 respectively) were higher than the traditionally accepted critical temperature of 550°C for fully loaded columns exposed uniformly to heat in the BS 476 : Part 8 : 1972 fire resistance test. This is surprising in view of the fact that the model columns were indeed fully loaded on the basis of the measured yield stress and ultimate strength values rather than the minimum specified values given in BS 4360. To make the point entirely clear, a column whose test load is calculated according to the tables in BS 449 : Part 2 : 1969 is assumed to have minimum values of yield stress and ultimate strength whereas the measured values may be up to 50% greater and such a column would therefore be expected to withstand higher temperatures before failing.

v) It was earlier reported (Table 1.2) that BSC had undertaken a number of full scale fire resistance tests on columns partly built into masonry walls and that the columns had all failed by reverse direction bowing about the major (xx) axis (like the model column tests) since they were prevented from buckling about the minor (yy) axis by the presence of the masonry. For maximum design load, and assuming failure could occur about the minor axis, the maximum slenderness ratio (ℓ/r_{yy}) tested was 58 (and periods of fire resistance ranged from 30 to 63 minutes depending upon the amount of web protected). In the case of the model column tests reported herein, reverse direction bowing still occurred when the maximum slenderness ratio was 138 (see Table 7.3). On the basis of these full scale and model scale tests it may be said that reverse direction bowing could be anticipated for slenderness ratios up to 140 when columns are fully loaded assuming that failure can occur about the minor axis.

vi) The behaviour of steel I-section columns having slenderness ratios and magnitudes of temperature gradient across the section different to those of the model columns cannot be predicted from these three model column test results. Further tests would be needed, or finite element sensitivity analyses undertaken, to show i) when reverse direction bowing did or did not occur, ii) which axis (or axes) buckling occurred about and iii) what the limiting temperatures were for heated and unheated flanges.

vii) The method of fabricating the columns by highly accurate milling to ensure good initial straightness was not entirely justified bearing in mind the eccentricities induced by thermal bowing.

CHAPTER 8 APPLICATION OF RESEARCH FINDINGS

The research has covered both analytical work (simple theory and the PAFEC finite element method) and experimental work, and it is the purpose in this chapter to indicate some ways in which the research findings can be applied.

8.1 Application of simple theory of thermal bowing to metal members.

Figure 8.1 summarises the relationships derived in Chapter 3 for a non-loaded simply supported beam and a cantilever heated such that there is a linear temperature profile across the section which does and does not vary along the length of the member. Equations a), b), c), f) and g) apply to members in which the temperature profile does not vary with length, whereas Equations d) and e) are for a member where the temperature profile varies with length, and examples of the application of the two latter equations are given in 3.4 and 4.2.2.

It was shown that displacements derived using these equations correlated well with displacements measured in small scale experiments (Figures 4.13 and 4.15) and full scale experiments (Figure 4.35) on unrestrained steel I-section beams and columns respectively.

Figure 8.2 shows two different but typical temperature profiles across a steel I-section heated predominantly along one flange. Figure 8.2(a) is typical for a small section, such as the model sections described in this work since it displays no point of contraflexure in the curve. Figure 8.2(b) is typical of a full scale shelf angle floor beam or column-in-wall construction where contraflexure clearly occurs. A rigorous application of the simple theory of thermal bowing would require

a straight line to be best fitted to both curves ((a) and (b)) in order to obtain the appropriate value of $(T_2 - T_1)/d$. The best fits are shown by lines AB and EF. It is seen that AB is parallel to the line CD drawn between the surface temperatures. However, EF is not parallel to GH, but using GH has proved to give sufficiently good agreement in use (Figure 4.35) to make the inaccuracy acceptable. In other words the temperature difference (T_2-T_1) can be taken as the difference in the average temperature of the heated and unheated flanges and, of importance here, the actual profile of temperatures between the flanges is unimportant. Hence the designer has only to know (from a thermal analysis or by test) the heated and unheated flange temperatures in order to calculate the unrestrained thermal bowing.

The question may be asked 'Why does one want to calculate the thermal bow bearing in mind that the calculation assumes that no external load is acting and that there is no restraint to the bowing, if, in practice, most structural members are loaded and often restrained?' One answer is that a simple equation for the unrestrained thermal bow provides a useful diagnostic tool to aid an understanding of the displacement behaviour of a member. For instance the displacement time history of the design-loaded beam, Figure 6.9 and 6.12, could be broken down into several components - thermal bow, elastic displacement and plastic displacement. In a similar way a knowledge of the thermal bow time history for the design-loaded model columns, Figure 7.13 for example, indicates when elastic and plastic displacements become important.

An interesting practical example of the use of the thermal bowing equations for diagnostic purposes is as follows. The BSC and FRS

collaborated in the design of an experiment in which a single bay portal frame was to be exposed to fire[8.1]. The columns were fixed-base, bare, universal column sections with lightweight concrete blocks filling the void between the flanges. The beam was unprotected and joined to the columns with bolted connections designed to be moment resisting. The objective was to achieve a half hour fire resistance. The beam and both columns received non-uniform heating in the test such that temperature gradients were obtained across each member's section. The thermal bowing equations were used to calculate member rotations and resulting incompatibility of deformations at the beam-column joints and this led to an understanding of the composite behaviour.

Another reason for wishing to know the thermal bowing component of displacement of a member is that, should that component of displacement be detrimentally large, then measures to reduce it might be considered such as increasing the depth of section and/or reducing the temperature difference across the depth. Whereas it may not be practical to increase the depth of member, it may be possible to reduce the temperature difference by reducing T_2, the temperature of the 'hot zone', and the way in which this can be achieved for a vertical, diagonally braced structure of a tall fire wall, is shown in Figure 8.3. The temperature rise, T_2, of the heated channel section can be reduced by minimising conductive heat flow into it by interposing an insulating strip between the channel section and the exposed fire protecting membrane, and by reducing radiative heat flow (by reradiation from the unexposed face of the fire protecting membrane) by providing a back-up membrane of thermal insulation such as a suspended blanket of rockwool fibre. It is important to note that the horizontal movement at the top of a fixed-base

cantilever is proportional to the square of the height. If we assume, for example, that a fire wall is, say, 25 m high and that the 1 m depth of steel section is subjected to a temperature difference (T_2-T_1) equal to 400°C, then $\Delta = \alpha H^2(T_2-T_1)/2d = .000014 \times 25^2 \times 400/2 = 1.75$ m. Such a movement could have a detrimental effect upon the roof structure on the non-fire side of the wall, for example by placing purlins and cladding in compression possibly causing failure in the very zone where it is important to preserve the integrity of the roof against fire spread from above. Some applications of the thermal bowing equations to the design of tall fire walls have been described by Cooke elsewhere[8.2].

Knowledge of the thermal bowing equations is useful to the designer contemplating using the column-in-wall construction, shown in Figure 1.18. The designer has to bear two important points in mind. First, he should not apply the data summarised in Table 1.2 if (a) his design assumes that the masonry will not provide lateral stability (that is stability in the plane of the wall) to the web of the I-section, and if (b) the design load assumes failure about the major (xx) axis - the BSC data is based on failure about the minor (yy) axis which results in a lesser load. Second, he should consider the possible instability of both leaves of the masonry wall caused by the bowing of the steel I-section. In this context it would be necessary to leave a suitably large gap between the faces of the unexposed steel flange and the inner faces of both leaves of masonry. Having done this it would also be necessary, and here perhaps is an intractable practical problem, to provide a sliding joint between the I-section web and the vertical edges of the adjacent masonry such that movement of the web in the plane of the web did not cause unacceptably large out-of-plane movement of the exposed leaf of

masonry. The alternative approach is to key the masonry to the steel column and provide vertical steel members embedded within the masonry so that the double leaf construction moves with the column as a whole. A way of achieving this for a single leaf masonry wall is described in reference 8.2 and the same ideas could be used for a double leaf masonry wall.

The equation for end rotation of a member subjected to thermal bowing, $\theta = \alpha L(T_2-T_1)/2d$, which is Equation (b) in Figure 8.1, may be used in the structural analysis of frameworks incorporating member(s) subjected to thermal bowing, assuming the behaviour is elastic. Consider the simple case of a single bay fixed-base steel portal frame, Figure 8.4, of span L and height h in which column 12 is heated uniformly along its height but non-uniformly across its section such that it has a linear temperature profile across the section, while beam 23 and column 34 remain at ambient temperature. In the absence of externally applied loads, expansion of the heated column 12 would cause the frame to sway to the right if the temperature across the section was uniform, whereas column 12, being fixed at the base, would sway to the left due to thermal bowing. Intuitively it is not clear whether the combined and opposing effects of column expansion and thermal bowing result in sway to the left or right.

Using the force-displacement method of analysis developed by Smolira[8.3] and using the assumed displaced shape and direction of bending moments shown in Figure 8.4, equations for compatibility of deformation (Equations (8.1)-(8.4)) and equilibrium of forces (Equation (8.5) can be written as follows:

$$M_{12}\frac{h}{3E_1I_1} + M_{21}\frac{h}{6E_1I_1} = \theta_1 - \frac{\Delta_1}{h} \quad \ldots\ldots\ldots\ldots\ldots\ldots\ldots\ldots \quad (8.1)$$

$$M_{12}\frac{h}{6E_1I_1} + M_{21}\left(\frac{h}{3E_1I_1} + \frac{L}{3E_2I_2}\right) - M_{34}\frac{L}{6E_2I_2} = \frac{\lambda}{L} + \frac{\Delta_1}{h} + \theta_2 \quad \ldots \quad (8.2)$$

$$-M_{21}\frac{L}{6E_2I_2} + M_{34}\left(\frac{L}{3E_2I_2} + \frac{h}{3E_3I_3}\right) - M_{43}\frac{h}{6E_3I_3} = \frac{\Delta_1}{h} + \frac{\lambda}{L} \quad \ldots\ldots\ldots \quad (8.3)$$

$$-M_{34}\frac{h}{6E_3I_3} + M_{43}\frac{h}{3E_3I_3} = \frac{\Delta_1}{h} \quad \ldots\ldots\ldots\ldots\ldots\ldots\ldots\ldots \quad (8.4)$$

$$\frac{M_{12} - M_{21}}{h} - \frac{M_{43} + M_{34}}{h} = 0 \quad \ldots\ldots\ldots\ldots\ldots\ldots\ldots\ldots \quad (8.5)$$

where λ, the free expansion, is assumed to be the statically determinate quantity $\alpha hT/2$, where $T = T_2 - T_1$.

It should be noted that θ_1 and θ_2 in Equations (8.1) and (8.2) are the rotations at the ends of the column due solely to thermal bowing and are equal to $\alpha Th/2d$ where T = temperature difference across column, h = height of column and d = depth of column section in direction of heat flow.

Presenting the linear simultaneous equations in a matrix enables their solution which gives values for the unknowns, M_1, M_2, M_3, M_4 and Δ_1. The method of analysis has been illustrated and validated against model tests by the author elsewhere[8,4].

The fact that the modulus of elasticity is temperature dependent and therefore varies across the heated section means that either the theory is confined to temperature differences at temperature below say 300°C so that E can be assumed to be constant across the section, or an

'equivalent' E value is used to take account of temperature. Alternatively, finite elements using the stiffness method of analysis could be employed if a suitable computer program was available.

8.2 Application of simple theory of thermal bowing to non-metallic members

There is no reason in principle why the thermal bowing equations should not apply to members of non-metallic materials provided that i) the thermal expansion varies approximately linearly with temperature and that there are no phase changes in the material which greatly affect the coefficient of thermal expansion at temperatures in the range of interest and ii) an estimate of T_2 (the heated zone temperature) can be made, see later. Also the equations can be applied to other structural shapes, with the proviso that shear deformations in the structure are negligible (ie plane sections remain plane) and that the temperature difference across the section relates to the heated and unheated structural zones, as it does in the case of an I-section member in which the flanges are clearly the structural zones affecting bowing.

Can the thermal bowing equations be applied to elements of structure composed of, for example, brick or concrete? Such materials usually have a low thermal conductivity so that the temperature distribution near the heated face is markedly curvilinear, becoming almost asymptotic at the surface, Figure 8.5. As a result it is not obvious, at first sight, what temperature should be taken as T_2 (the 'hot zone' temperature). However since most non-metallic materials of structural interest, such as brick and concrete, lose strength at elevated temperatures it may be that good correlation of theory and experiment can be obtained if the first few

millimetres of heated face material are ignored (since it will have suffered loss of strength and will not contribute structurally) and T_2 is then taken to be the temperature those few millimetres below the surface. The writer is currently conducting thermal bowing tests on non-loaded, unrestrained vertical strips of clay brick and concrete blockwork and on horizontal concrete slabs of different thickness heated along one face with the objective of achieving good correlation of theory and experiment, but at the time of writing (August 1987) the test results have not been analysed.

CHAPTER 9. GENERAL CONCLUSIONS AND SUGGESTIONS FOR FURTHER RESEARCH

9.1 General conclusions

(i) Steel beams and columns may form part of fire separating elements such as floors and walls. Often the steelwork is fire protected by encasing it with board or spray material in which case large temperature differences across the section in the direction of the heat flow are unlikely to occur. There are, however, situations when the steel is not fire protected and where large temperature differences across the section can occur - 300°C for unprotected external columns and in excess of 800°C for an unprotected steel column forming part of a masonry fire wall within the building. These temperature differences cause differential expansion in the steel which, when unrestrained, causes thermal bowing toward the fire relative to the ends of the member. Thermal bowing in a column induces eccentric loading possibly leading to early failure especially in columns of large slenderness ratio. If thermal bowing is restrained, large forces or bending moments can be generated.

(ii) There is, as yet, no published guidance to suggest that the limiting temperature of 550°C for fully loaded steel columns heated uniformly across the section should, or should not, apply to columns which have large temperature differences across the section.

(iii) There has been a considerable amount of experimental and theoretical research into the fire performance of steel I-section members heated uniformly across the section. There has also been

experimental research aimed at establishing the thermal response of I-section steel members used outside the facade where they are subjected to predominantly one-sided heating by flames and hot gases emerging from openings in the facade. In contrast there has been, so far as the author is aware, little research into the structural response of such members heated from one side. One exception to this claim is experimental work by the British Steel Corporation on the fire resistance of full size I-section beams and columns partly built into adjoining masonry or concrete construction. Another is the experimental work on loaded pin-ended columns outside an opening in a fire compartment rig at CTICM in France. There has been, so far as the author is aware, no rigorous structural analysis of steel members heated non-uniformly. The Fire Committee of the European Convention for Constructional Steelwork (ECCS-T3) has stated that research is needed to rectify this imbalance.

(iv) Simple theories have been developed, based purely on geometry, for the unrestrained thermal bowing displacements of members having linear temperature gradients across the section. It is shown (3.2) that the central displacement Δ of a simply supported member of length L and depth d having a linear temperature gradient across the section resulting in a temperature difference T across the section for a material of constant coefficient of thermal expansion α, is given by $\Delta = \alpha TL^2/8d$ and the end rotation is $\theta = \alpha TL/2d$. Similarly, the linear displacement at the free end of a fixed-base cantilever is $\Delta = \alpha TL^2/2d$. A theory has also been derived (3.5) for linear and rotational

displacements of a member in which the temperature gradient varies along the length.

(v) For a member of fixed length and invariable coefficient of linear thermal expansion, the only way of reducing the amount of unrestrained thermal bowing is to increase the distance between heated and unheated faces, and reduce the temperature difference between them. An example of the improved design of a tall fire separating wall which uses this simple finding has been given in Chapter 8.

The effect of phase transformation in steel (Figure 2.2) was detected in the experiments on the unrestrained thermal bowing of a simply supported beam (Figures 4.13 and 4.15). However, in practice a steel member used in a building is likely to be carrying load and could therefore be expected to yield and fail by excessive displacement before the onset of phase transformation which occurs on heating at approximately 720°C. Thus it may be concluded that the effect of phase transformation is of little practical importance.

(vi) Displacements predicted using the theory given in (iv) above are shown to correlate well with displacements observed in small scale and full scale experiments on steel members heated along one face. Although the theory is strictly valid only for a linear temperature profile (whereas in practice the temperature profile is curvi-linear), the correlation between theory and experiment is good if a) a straight line is fitted to the curve

(Figures 4.13 and 4.15 for example) or, more conveniently, b) the temperature difference T is assumed to be independent of the shape of the temperature profile and is simply the difference between the heated and unheated face temperatures (Figure 4.35 for example).

(vii) Displacements, including and excluding the effect of phase transformation, for the unrestrained beam experiments, have been satisfactorily computed using the PAFEC suite of finite element programs. It was not possible to get the plasticity software to work properly, so that the computed displacements reported are based on elastic behaviour. A number of analyses were made to determine the sensitivity of the central displacement of the unrestrained test beam, when heated along the whole flange, to the value of α, size and shape of finite element, and relationship of elastic modulus to temperature. The effect of varying the latter two parameters was shown to be small (Figures 4.20 and 4.21). However a sensitivity analysis, for the test beam heated along half the flange, showed, Figure 4.26, that the choice of elastic modulus - temperature relationship had a marked effect on the computed central displacement at a late stage in the experiment.

The equations for unrestrained linear and rotational displacements can be used in writing equations for compatibility of deformation used in methods of analysis for framed structures having linear temperature profiles across the members, for example in Smolira's force-displacement method. This method is

suitable for framed structures behaving elastically and can therefore be used for determining displacements and forces (expansion forces for instance) arising in a heated steel frame before the yield point is reached. An example of this method is given in Chapter 8.

(viii) The simple theory of thermal bowing presented herein applies only to non-loaded, unrestrained members. In contrast, structural members in buildings are usually loaded and sometimes end-restrained. Nevertheless the theory provides a useful diagnostic tool for understanding the displacement behaviour of members heated along one face. It is, for instance, instructive to know what fraction of the total displacement of a loaded member is attributed to unrestrained thermal bowing, as shown in Figure 6.9. It is also essential to know the unrestrained thermal bowing displacement when calculating the force needed to prevent the displacement at mid-span of a simply supported beam heated along one face, and an example of the method, which assumes elastic behaviour and that the principle of superposition is valid, has been given, see 5.5 and Figure 5.8.

(ix) For conventionally loaded steel beams heated along one face it appears that the elastic component of displacement is small compared with plastic and thermal bowing components when the BS 476 limiting central displacement criteria of span/30 or span/20 are reached, Figure 6.9. This suggests that big differences in elastic modulus - temperature relationships (found from a comparison of BSC/Euronorm data and ECCS data for instance) have

only a small effect upon the total displacement of a loaded beam.

(x) Small scale steel members can be used to establish the structural response of full size I-section members heated along one flange since there are no problems of dimensional scaling. The high cost and lengthy time involved in full scale fire tests warrants the use of scaled models for research.

(xi) The steel models were made from small hot-rolled sections having tapered flanges, steel strip TIG welded together for the design-loaded beam, and by milling from a square steel billet for the design-loaded columns. TIG welding was shown to be acceptable for model beams, but milling from the solid was preferable for model columns where accuracy of section shape and the absence of residual stresses were considered important requirements. A modified portable spot welding machine proved ideal for the attachment of thermocouples where, in small I-sections, it is important to measure the surface temperature rather than the temperature at an uncertain depth which unfortunately attends the use of thermocouples peened into blind holes.

(xii) Several experiments have been successfully conducted using quarter scale I-section steel model members nominally 1.5 m long heated along one flange with high power electrical heating elements capable of heating the models to 1000°C and at a rate comparable to that in the full scale BS 476 : Part 8 fire

resistance test. The use of electrical heaters instead of the customary gas-fired furnace has the advantage of: facilitating easier and more accurate measurements of deformations and loads using displacement and load transducers; providing accurate control over the area of the specimen into which heat is conducted and giving control over the temperature gradients achieved; and allowing tests to be conducted easily and at low cost.

(xiii) It has been found that a simply supported model steel beam, heated along one flange and loaded at points span/4 apart (which is the loading arrangement commonly used in the UK when conducting BS 476 : Part 8 : 1972 fire resistance tests on full size steel beams), attained a central displacement of span/30 when the heated flange reached a temperature of 645°C. This is a lower temperature than that attained by the heated flange in full size steel shelf angle floor beams tested in the full size floor furnace; results of tests sponsored by the British Steel Corporation show that failure occurred at heated flange temperatures of over 900°C.

(xiv) One objective of the work was to compare the average temperature of the non-uniformly heated model members at failure with the so-called critical temperature of 550°C which assumes uniform heating across the section. The average temperature of the simply supported model beam at failure (assumed to occur when the mid-span displacement reached span/30), when subjected to the maximum permissible elastic design load (calculated according to

BS 449), was 462°C (6.10) which is lower than the critical temperature of 550°C. On the other hand the average temperatures of two pin-ended model columns at failure, assumed to occur when the specimen had regained its room temperature length after initial expansion and the contraction due to bowing, again when subjected to the maximum permissible elastic design load (calculated according to BS 449), were 570 and 610°C (7.9(iii)). There is clearly poor agreement between these failure temperatures and the 550°C criterion.

(xv) It might be thought that failure of an I-section steel member would occur when the temperature of the hottest flange reached the runaway displacement temperature (2.4.4) for uniaxial tension (Figure 2.11). However, at failure (judged to occur as in (xiv) above) the average heated flange temperature of the model beam was 645°C and the average heated flange temperatures of two model columns were 710 and 760°C. Again there is seen to be little agreement between the model beam and column test results, ie there is no single limiting heated flange temperature, and this can be explained by the fact that yielding of the heated flange merely results in the web carrying more of the load until it too progressively yields as its temperature increases. Sudden collapse is thereby avoided.

(xvi) Three model columns have been tested and in each case the phenomenon of reverse direction bowing (7.8.7) was observed (Figure 7.20 for example) even for the largest slenderness ratio of ℓ/r_{yy} of 138.

9.2 Suggestions for further research

1. Identify and validate computer program able to predict thermal response of different constructions subjected to non-uniform heating, eg column-in-wall and shelf-angle floor constructions.

2. Identify and validate user-friendly computer program able to predict the elastic/plastic behaviour of non-uniformly heated beams and columns, especially the displacement/time history for beams operating under different load levels.

3. Establish limiting heated and unheated flange temperatures and lower limit of ℓ/r ratio for the condition where reverse direction bowing does not occur in columns, and decide practical importance.

4. Conduct full scale fire resistance tests on pin-jointed steel columns in the column furnace in order to establish failure temperatures with and without uniform heating. This involves modification to the UK (FIRTO) column furnace to permit one-sided heating.

5. Validate the equations for unrestrained thermal bowing for a wider range of temperature profiles, structural shapes and explore validity for non- metallic materials.

6. Establish practical jointing systems for column-to-wall constructions to overcome or allow for incompatibility of deformation of column and wall.

7. Explore adaptation of the force-displacement method of elastic analysis for framed structures with members subjected to one-sided heating. This could be useful for analysing displacements and forces arising from expansion of a heated member before yielding occurs.

8. Establish heating rates and maximum temperatures possible using proprietary electrical heating elements with different thicknesses of steel to see if method is appropriate for heating full size I-sections with multiple heaters.

9. Undertake tests on model columns heated along one flange to explore the effect of eccentric loading.

REFERENCES

1.1 Department of the Environment. The Building Regulations 1985 : Fire. Approved Document B: Fire spread. London, HMSO, August 1985.

1.2 Read R E H, Adams F C and Cooke G M E. Guidelines for the construction of fire resisting structural elements. Building Research Establishment Report, London, HMSO, 1980 (Minor corrections 1982).

1.3 British Standards Institution. BS 5950 : Part 1 : 1985, Code of practice for design in simple and continuous construction: hot rolled sections. BSI, 1985.

1.4 British Standards Institution. BS 5950 : Draft Part 8, Code of practice for the fire protection of structural steelwork, (Document 85/12865), BSI, October 1985.

1.5 British Standards Institution. BS 476 Fire tests on building materials and structures, Part 8, Test methods and criteria for the fire resistance of elements of building construction, BSI, 1972.

1.6 British Standards Institution. BS 476 Fire tests on building materials and structures, Draft Part 20, Method for the determination of the fire resistance of elements of construction (general principles) (Part revision BS 476 : Part 8 : 1972), BSI Document 84/38456, BSI, 1984.

1.7 Association of Structural Fire Protection Contractors and Manufacturers Ltd and Constructional Steel Research and Development Organisation, Fire protection for structural steel in buildings. Constrado, April 1983.

1.8 Law Margaret. Fire-safe structural steel: a design guide. American Iron and Steel Institute, Washington, USA, March 1979.

1.9 Cooke G M E. New methods of fire protection for external steelwork. The Architect's Journal, 28 August 1974.

1.10 Bond G V L. Fire and steel construction: water cooled hollow columns. Constrado 1975.

1.11 Latham D J, Thomson G and Banks G. The influence of thermal and rotational restraint on the fire resistance of unprotected BS 4360 : Grade 43A steel beams, Confidential Contract Report RSC/2921/1/83, British Steel Corporation Sheffield Laboratories, 20 June 1983.

1.12 Kirby B R. Structural steelwork does not always need protection, researchers conclude. Fire, Sept 1986, p18,19.

1.13. Cooke G M E. Effect of end restraint on the bending of loaded steel beams heated to elevated temperatures. Private communication (N 92/85), Fire Research Station, July 1985.

1.14 Pettersson O, Magnusson S E and Thor J. Fire engineering design of steel structures. Swedish Institute of Steel Construction, Stockholm, 1976.

1.15 Cooke G M E. Problems in the development and application of new technologies for fire grading of buildings. Fire Prevention Science and Technology, No.12, July 1975.

1.16 Kirby B R. Developments in structural fire engineering design and its application to real buildings. Confidential Contract Report RSC/2921/19/84. British Steel Corporation Sheffield Laboratories, 13 February 1984.

1.17 Cooke G M E. Practical fire engineering: Part A: The context. National Structural Steel Conference 1984. "New developments in steel construction", held on 11/12 December 1984. British Constructional Steelwork Association Ltd, London.

1.18 Latham D J. Practical fire engineering: Part C: The use of unprotected steelwork in buildings. National Structural Steel Conference 1984. "New developments in steel construction", held on 11/12 December 1984. British Constructional Steelwork Association Ltd, London.

1.19 Newman G N. Practical fire engineering: Part B: Structural applications. National Structural Steel Conference 1984. "New developments in steel construction", held on 11/12 December 1984. British Constructional Steelwork Association Ltd, London.

1.20 Cooke G M E. Practical fire engineering: Part D: Applications of steel models research. National Structural Steel Conference 1984. "New developments in steel construction", held on 11/12 December 1984. British Constructional Steelwork Association Ltd, London.

1.21 Thomson G, Thomas I D and Smith C I. BS 476 : Part 8 : Fire tests on unprotected steel beams, Report T/RS/1189/17/81/A, British Steel Corporation Teesside Laboratories, 1981.

1.22 Thomson G, Hogan G and Smith C I. The fire resistance of a shelf angle floor construction, a BS 476 : Part 8 fire test carried out on 3rd November 1982. Confidential Report SH/RS/3664/1/83/B, British Steel Corporation Sheffield Laboratories, 4 July 1983.

1.23 Thomson G, Hogan G and Latham D J. The fire resistance of a shelf angle floor construction - a BS 476 : Part 8 Fire test carried out on 30 November 1983. Restricted Report SH/RS/3664/5/84/B, British Steel Corporation Swinden Laboratories, 18 June 1984.

1.24 Janss J and Minne R. Buckling of steel columns in fire conditions, Fire Safety Journal 4 (1981/82) 227-235, Elsevier Sequoia SA, Lausanne.

1.25 Olesen F B. Fire tests on steel columns, Institute of Building Technology and Structural Engineering, Aalborg, Denmark, 1980.

1.26 ECCS Technical Committee 3. European Recommendations for the Fire Safety of Steel Structures - Calculation of the fire resistance of load bearing elements and structural assemblies exposed to the standard fire. Elsevier Scientific Publishing Company, Oxford, 1983.

1.27 Butcher E G and Cooke G M E. Structural steel and fire, Conference on Steel in Architecture, held on Nov 24-26, 1969, British Constructional Steelwork Association.

1.28 Butcher E G, Chitty T B and Ashton L A. The temperature attained by steel in building fires. Fire Research Technical Paper No.15. London, 1966, HMSO.

1.29 Behaviour of structural steel in fire. Proceedings of the Symposium held at Fire Research Station on 24 January 1967. (Papers 1-4), 1968, HMSO.

1.30 Ove Arup and Partners. Design guide for fire safety of bare exterior structural steel: Technical reports (Theory and Validation, and State of the Art). American Iron and Steel Institute and Constrado. Jan 1977.

1.31 Kruppa J. Results of research ECSC: Behaviour of external steel columns in fire. Acier-stahl-steel, Vol 45, No.2, 1980, p66-74.

1.32 Kruppa J. Fire resistance of external steel columns. Report EUR 6731 EN, Commission of the European Communities, Luxembourg, 1981.

1.33 Smith C I, Thomson G and Chilvers N. The fire resistance of an unprotected steel column built into a fire resistant wall. Open Report No.T/RS/1189/28/82/C, British Steel Corporation Teesside Laboratories, 28 April 1982.

1.34 Thomson G, Hogan G and Latham D J. The influence of design stress on the performance of unprotected steel beams and columns built into a fire resistant wall. BSC Sheffield Laboratories, Restricted Report SH/RS/3664/3/83/B, 25 August 1983.

1.35 Thomson G, Hogan G and Latham D J. The fire resistance of a bare steel column built into a fire resistant wall. A BS 476 : Part 8 fire test carried out on 18 October 1983, BSC Swinden Laboratories Restricted Report SH/RS/3664/6/84/B, 4 July 1984.

1.36 Melinek S J. A thermal model of a column test furnace, Private communication (Table 2a, N32/85), Fire Research Station, March 1985.

1.37 Smith C I et al. The reinstatement of fire damaged steel framed structures. Open Report No.T/RS/1195/15/80/C. British Steel Corporation Teesside Laboratories, 31 March 1980.

2.1 Woolman J and Mottram R A The mechanical and physical properties of the British Standard En steels, (BS 970-1955), Volume 1, En 1 to En 20, Published on behalf of the British Iron and Steel Research Association by The Macmillan Company, New York, 1964.

2.2 Brebbia C A and Ferrante A J. Computational methods for the solution of engineering problems. Pentech Press Ltd, Plymouth, 1978.

2.3 Clark C L. High temperature alloys. Pitman, 1953.

2.4 Stirland C. British Steel Corporation Teesside Laboratories, letter dated 28 June 1982 and unpublished document entitled 'Appendix A, Proposed revision of Article 2 of the European recommendations for the design of steel structures exposed to the standard fire' dated 1980. Private communication.

2.5 White O M. Essentials of heat. Cleaver-Hume Press Ltd, London, 1961, p35.

2.6 The British Iron and Steel Research Association. Physical constants of some commercial steels at elevated temperatures. Butterworths Scientific Publications, London, 1953.

2.7 Gregory E and Simons E N. The structure of steel simply explained. Blackie and Son Ltd, London, 1942.

2.8 Walker J. The amateur scientist - in which heating a wire tells a lot about changes in the crystal structure of steel. Scientific American, May 1984, pp118-122.

2.9 Kennedy R et al. Dimensional changes in steels due to thermal cycling. Journal of the Iron and Steel Institute, London, June 1970, pp601-602.

2.10 Smith C I. Dilatometer curves for mild steel. British Steel Corporation, Teesside Laboratories, 23 July 1982. (Private communication).

2.11 Salmon E H. Materials and Structures. Longmans, 1931.

2.12 BS 3688 : Part 1 : 1963. Methods for mechanical testing of metals at elevated temperatures, Part 1, Tensile testing. BSI, 1963.

2.13 Skinner D H. Determination of high temperature properties of steel. BHP Technical Bulletin, Vol 16, No.2, Australia, 1972.

2.14 Witteveen J and Twilt L. Behaviour of steel columns under fire action. Proceedings of the International Colloquium on Column Strength, (International Association for Bridge and Structural Engineering) Paris, Nov 23-24, 1972.

2.15 Witteveen J, Twilt L and Bijaard B. The stability of braced and unbraced frames at elevated temperatures. Proceedings, Stability of Steel Structures, Liege, April 13-15, 1977.

2.16 Anderberg V. Effect of fire on steel. Rilem Committee 4-PHT, Draft papers II and III. March and November 1980.

2.17 Harmathy T Z and Stanzak W W. Elevated temperature tensile and creep properties of some structural and prestressing steels. National Research Council of Canada Research Paper No 424 of the Division of Building Research, Ottawa, Jan 1970.

2.18 Crook R N. The elevated temperature properties of reinforced concrete. PhD Thesis, University of Aston, 1980.

2.19 Holmes M, Anchor R D, Cooke G M E and Crook R N. The effects of elevated temperatures on the strength properties of reinforcing and prestressing steels. The Structural Engineer, March 1982, pp7-13.

2.20 Stirland C. British Steel Corporation Teesside Laboratories, letter dated 28 June 1982 and unpublished document entitled 'The temperature dependence of Young's Modulus (modulus of elasticity) for structural steel' dated 21 July 1980. Private Communication.

2.21 Jerath V, Cole K J and Smith C I. Elevated temperature tensile properties of structural steels manufactured by the British Steel Corporation. Report T/RS/1189/11/80/C British Steel Corporation Teesside Laboratories, 24 July 1980.

2.22 Kirby B. The behaviour of structural steels manufactured by BSC under stress controlled anisothermal creep conditions. Restricted report SH/RS/3664/4/83/B, BSC Sheffield Laboratories, 12 Oct 1983.

2.23 Kirby B and Thomas I. Anisothermal creep tests on structural steels manufactured by BSC - preliminary results. Confidential Report T/RS/1380/36/82/D, 7 April 1982.

2.24 Schleich J B. Computer assisted analysis of the fire resistance of steel and composite concrete-steel structures. Final report (from 1/7/1982 to 30/6/85) under CEC Agreement Number 7210-SA/502, (ECCS-3-1986/4/Lux), Arbed Recherches, 14/3/1986.

2.25 Thomson G, Smith C I and Bunyan R. BS 476 fire test on an unprotected steel beam - 3rd report, Report No T/RS/1189/4/80/C, British Steel Corporation Teesside Laboratories, 2 June 1980.

4.1 Cooke G M E. The thermal bowing of steel members at elevated temperatures. Private communication (Appendix 2, N 81/83), Fire Research Station, June 1983.

4.2 Latham D J, Kirby B R et al. The temperatures attained by unprotected structural steelwork in natural fires, Confidential Contract Report, RSC/7281/10/86, British Steel Corporation Swinden Laboratories, 5 February 1986.

5.1 British Standards Institution, BS 4360 : 1979. Specification for weldable structural steels, BSI, 1979.

5.2 British Standards Institution, BS 18 : Part 2 : 1971. Methods for tensile testing of metals - steel (general), BSI, 1971.

7.1 Litle W A and Foster D C. Fabrication techniques for small-scale models, Structural behaviour of small-scale steel models, Bulletin No.10, American Iron and Steel Institute, April 1968.

7.2 Mills R S et al. Model tests on earthquake simulators - development and implementation of experimental procedures, undertaken by The John A Blume Earthquake Engineering Centre, Stanford University, June 1979, p.79-89.

7.3 Kusakabe T and Mihara Y. Effects of residual stresses in H-shapes on performance, Transactions ISIJ, Vol 20, 1980.

7.4 Babb A S. Likely residual stresses in an air-cooled 78 mm square steel billet, British Steel Corporation Sheffield Laboratories, private communication, 14 October 1982.

7.5 British Standards Institution, BS 449 : Part 2 : 1969. The use of structural steel in building, Part 2, Metric units, BSI, 1969.

8.1 Cooke G M E and Latham D J. The inherent fire resistance of a loaded steel framework, Steel Construction Today, 1987, 1, 49-58.

8.2 Cooke G M E. Fire engineering of tall separating walls, Fire Surveyor; Part 1, June 1987, p13-29; Part 2, August 1987, p19-29.

8.3 Smolira M. Analyses of tall buildings by the force-displacement method, McGraw Hill Book Company (UK) Ltd, London, 1975.

8.4 Cooke G M E. The structural response of steel portal frames with one column heated to elevated temperatures, Private communication (BRE N 142/82), Fire Research Station, October 1982.

TABLES

Element	Limiting temperature °C	Time (min) to reach limiting temperature for P/A ratios (m^{-1}) of:			
		60	120	200	300
Beam (i)	500	34	20.8	14.5	10.9
	700	51.2	33.5	24.5	19.1
Column (ii)	500	25.4	17	12.2	9.4
	700	38.5	27.5	20.3	15.9

Notes. (i) Beam is supporting a dense concrete slab, hence heated on 3 sides
(ii) Column is heated on all 4 sides

TABLE 1.1 Heating rates for bare steel I-section beams and columns exposed to the BS 476 : Part 8 : 1972 heating exposure (taken from draft BS 5950 : Part 8)

Test No (BSC Report ref) I-section size Grade of steel	Configuration	Effective length (i)	$\frac{\ell}{r_{yy}}$	$\frac{\ell}{r_{xx}}$	P_c (N/mm²)	Test load (kn) and % allowable	Average heated flange temp (°C)	Average unheated flange temp (°C)	Measured maximum mid-span lateral displacement: Toward fire	Measured maximum mid-span lateral displacement: Away from fire, at end of test
Test 1 (T/RS/1189/28/82/C) 203 x 203 x 52 kg/m BS 4360 : Grade 43A	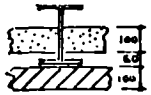	0.85L about xx		28.7			473°C at 18 min 1000°C at 103 min	45.8°C at 18 min 250°C at 103 min	25 mm at 18 min	40 mm at 103 min
		0.75L about yy	43.6		137	476 52.4%				
Test 2 (SH/RS/3664/3/83/B) 203 x 203 x 52 kg/m BS 4360 : Grade 43A	〃	1.2L about xx		40.4			359°C at 15 min 742°C at 30 min	31°C at 15 min 88°C at 30 min	16 mm at 15 min	58 mm at 30 min
		1.0L about yy	58.14		127	970 115%				115 mm at 34 min
Test 3 (SH/RS/3664/3/83/B) 356 x 171 x 67 kg/m BS 4360 : Grade 50	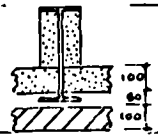	1.0L about yy	75.2		140	470 40%	519°C at 25 min 1048°C at 180 min	13°C at 25 min 162°C at 180 min	20 mm at 25 min	115 mm at 180 min
Test 4 (SH/RS/3664/6/84/B) 203 x 203 x 52 kg/m BS 4360 : Grade 43A		1.2L about xx		40.4			507°C at 18 min 922°C at 63 min	58°C at 18 min 170°C at 63 min	10 mm at 18 min	100 mm at 63 min
		1.0L about yy	58.14		127	843 100%				

(i) L = span between end plates = 3 m. Effective length factors are BSC estimates since end restraint conditions in wall furnace are uncertain

TABLE 1.2 Summary of data for BSC column-in-wall fire resistance tests

BSC column-in-wall test number	T (°C) (i)	d (mm)	Calculated Δ (mm) (ii)	Measured Δ (mm)
1	427	203	33	25
2	328	203	25.5	16
3	506	356	22.4	20
4	449	203	34.8	10

(i) T = average heated flange temp - average unheated flange temperature, taken from Table 1.2

(ii) $\Delta = \frac{.000014\ TL^2}{8d}$ where L = 3000 mm. Applies to non-loaded member.

TABLE 1.3. Comparison of experimental and theoretical mid-height thermal bowing displacements for BSC column-in-wall tests

Temperature °C	Elastic modulus lb/in^2	Shear modulus lb/in^2	Poisson's ratio
20	30.8×10^6	11.9×10^6	0.288
95	30.3	11.7	0.290
205	29.2	11.2	0.293
425	26.7	10.2	0.300
595	24.1	9.2	0.306
650	22.8	8.75	0.311

TABLE 2.1. Variation of Poisson's ratio of steel with temperature

Material	Coefficient of linear expansion per °C x 10^6
Aluminium	22.2
Iron	12.0
Steel	11.0
Invar	1.0
Brick	9.5
Silica	0.42

TABLE 2.2 Some indicative values of coefficients of linear thermal expansion for different materials at room temperature

	Mean coefficient of expansion (X 10^6/°C) over temperature range (°C) of:											
Steel	0-100	0-200	0-300	0-400	0-500	0-600	0-700	0-800	0-900	0-1000	0-1100	0-1200
1	12.62	13.08	13.46	13.83	14.25	14.65	15.00	14.72	12.89	13.79	14.65	15.37
2	12.18	12.66	13.08	13.47	13.92	14.41	14.88	12.64	12.41	13.37	14.16	14.81
3	11.21	12.14	13.00	13.58	14.05	14.58	14.85	11.84	12.65	13.59	14.36	15.00

TABLE 2.3 Mean coefficients of thermal expansion of carbon steels over different temperature ranges

Steel	C %	Si %	Mn %	S %	P %	Cr %	Ni %	Mo %	Cu %	Al %	As %
1	0.06	0.01	0.38	0.035	0.017	0.022	0.055	0.030	0.08	0.001	0.039
2	0.23	0.11	0.635	0.034	0.034	Trace	0.074	Nil	0.13	0.010	0.036
4	0.415	0.11	0.643	0.029	0.031	Trace	0.063	Nil	0.12	0.006	0.033

TABLE 2.4 Chemical composition of carbon steels featured in Table 2.3

$\frac{\sigma_{applied}}{\sigma_{yield\ at\ 20°C}}$	Temperature (°C) at 1% strain*	
	BHP data	BSC data
0.66	571-574	545
0.33	670-676	644
0.17	745	721

*For a heating rate of 10°C/minute

TABLE 2.5. 1% total strain temperatures for different stress levels for structural steels

Non dimensional parameter	Temperature of steel, °C								
	20	100	200	300	400	500	600	700	800
$\frac{\sigma_{elev.temp}}{\sigma_{yield\ at\ 20°C}}$	.575	.562	.519	.490	.418	.299	.177	.065	.055
$\frac{E_{elev.temp}}{E_{20°C}}$	1	.977	.903	.852	.727	.520	.308	.113	.095

Notes

Yield strength at 20°C assumed to be 275 N/mm² in accordance with BS 5950 : Part 1 : 1985, assuming steel thickness is less than 16 mm.

Stress data are for a strain of 0.08% for Grade 43 steel taken from draft BS 5950 : Part 8.

TABLE 2.6. Anisothermal elastic modulus data derived from BSC results (draft BS 5950 : Part 8 data)

Distance up from heated face (mm)	Average of temperatures at 12 stations (°C) at times (min) of:								
	0	6	12	18	24	30	36	42	48
100	14	16.84	30.18	105.4	164.8	210.2	238.1	258.3	272.7
75		19.525	60.25	130.9	197.2	244.6	274.8	296.9	312.4
50	14	25.725	89.99	186.0	271.14	327.2	365.6	394.3	415.1
25	14	36.55	136.95	277.8	401.9	482.9	547.0	596.0	633.2
9	14	49.99	188.97	381.1	552.1	664.4	778	856.9	915.5
T/d (°C/mm)	0	0.351	1.675	2.95	4.131	4.831	5.683	6.283	6.742
Δ = 3.049 T/d (mm)	0	1.0702	5.107	8.994	12.59	14.73	17.32	19.16	20.55

TABLE 4.1 Average temperature, best-fit slopes and calculated central displacements for unrestrained test beam heated along whole flange

Duration of Heating (min)	Best-fit T/d values at 12 stations corresponding to thermocouple numbers:												Computed Central Displacement (mm)
	1-5	6-10	11-15	16-20	21-25	26-30	31-35	36-40	41-45	46-50	51-55	56-60	
8	.02043	.02053	.02136	.0230	.0251	.07099	.5198	.8478	.7743	.7791	.7701	.8735	0.4997
16	.01447	.01506	.01621	.0165	.0259	.1816	1.592	3.064	2.868	2.994	2.788	2.641	3.091
24	.01453	.01467	.01407	.01394	.0375	.3381	2.487	4.888	4.723	4.814	4.601	4.103	5.1692
40	.01196	.00985	.00988	.01701	.06674	.5382	3.521	7.010	7.064	7.079	6.238	5.570	7.6368
48	.0103	.00814	.00807	.01879	.0822	.6618	3.866	7.487	7.627	7.594	6.514	6.068	8.232

TABLE 4.2 Best-fit T/d data at 12 stations and calculated central displacements for unrestrained test beam heated along half of flange

Thermo-couple Number	Temperature (°C) at time of heating (min) of:							
	6	12	18	24	30	36	42	48
2	22.5	62.6	121.6	164.6	211.6	240.0	259.5	271.7
7	20.1	63.6	140.5	210.4	257.9	287.7	309.2	323.9
12	19.3	63.4	142.2	214.4	262.2	291.5	313.1	325.8
17	19.8	64.4	142.3	213.6	261.0	289.7	310.4	324.9
22	19.3	60.9	134.1	202.6	250.5	278.8	300.3	312.8
27	17.6	46.4	101.0	162.9	213.8	250.9	279.3	295.9
32	17.9	47.5	103.1	167.1	219.6	256.4	286.1	308.6
37	19.4	62.6	137.2	207.7	256.7	287.4	310.6	326.1
42	19.4	65.4	144.9	217.7	264.8	294.8	316.8	332
47	19.5	65.7	145.6	218.4	265.5	294.5	316.4	331.7
52	20.4	65.3	141.9	211.4	257.2	286.1	306.3	322.4
57	19.1	55.3	116.9	175.6	215.1	240.5	256.8	272.9
Ave temp	19.52	60.25	130.9	197.2	244.6	274.8	296.9	312.4

TABLE 4.3. Data used in obtaining average temperature 25 mm from unheated flange at different times for unrestrained test beam heated along whole flange

Distance up from heated face (mm)	Average of thermocouple temperatures (°C) at 12 stations at times (min) of:								
	0	6	12	18	24	30	36	42	48
100	14	16.84	30.18	105.4	164.8	210.2	238.1	258.3	272.7
75	14	19.525	60.25	130.9	197.2	244.6	274.8	296.9	312.4
50	14	25.725	89.99	186.0	271.14	327.2	365.6	394.3	415.1
25	14	36.55	136.95	277.8	401.9	482.9	547.0	596.0	633.2
9	14	49.99	188.97	381.1	552.1	664.4	778	856.9	915.5

TABLE 4.4 Average steel temperatures at each horizontal line of thermocouples for unrestrained test beam heated along whole flange

Analysis Number	Value of α /°C 10^6	Phase Transformation Allowed for:		Mesh Geometry			Modulus of Elasticity	
				Number of Elements		Max'm Element Aspect Ratio	Constant at 209E9	Variable
		Yes	No	Across Depth	Along Half Length			
130	14.0	✓		4	10	11	✓	
130a	14.0		✓	4	10	11	✓	
130b	14.8648		✓	4	10	11	✓	
131	14.8648	✓		4	10	11	✓	
132	14.8648	✓		7	40	5.48	✓	
133	14.8648	✓		7	40	5.48		✓ (i)
233A-H	14.8648	✓		7	40	5.48		✓ (ii)

Notes: Temps specified only at corner nodes (not at mid-side nodes).
(i) BSC/Euronorm E
(ii) Arbed E

TABLE 4.5 Bases of PAFEC elastic analyses for unrestrained test beam heated along whole flange

Analysis Number	Central displacement (mm) of beam at duration of heating (min) of:							
	6	12	18	24	30	36	42	48
130	1.2073	5.3097	9.6142	13.625	15.126	14.073	15.445	17.361
130a	1.2118	5.3256	9.6478	13.677	15.869	19.224	21.215	23.136
130b	1.2867	5.6545	10.243	14.522	16.849	20.412	22.527	24.565
131	1.2820	5.6377	10.208	14.470	16.087	15.118	16.593	18.630
132	1.2444	5.5252	9.9524	14.123	15.616	14.646	16.4443	18.145
133	-	5.5692	9.8792	13.924	15.345	14.799	15.994	17.331
233A-H	1.2534	5.5468	9.8674	13.460	14.417	13.916	13.95	13.772
Experiment Value	0.7	3.9	8.7	13	13.95	15.5	16.35	16.8

TABLE 4.6 Central displacements obtained from PAFEC analyses for unrestrained test beam heated along whole flange

Thermocouple Number	Temperature (°C) at time (min) of						
	6	12	18	24	30	36	42
36	24.3	58.3	124.5	185.9	226.5	252.1	270.1
41	23.7	58.2	128.4	193.9	235.9	261.5	279.6
46	23.3	58.7	130.8	195.6	236.5	261.2	278.6
51	23.2	59.9	130.3	192.7	232.9	256.2	272.8
56	22.9	55.8	115.4	170.0	205.9	225.9	238.9
Average	23.48	58.18	125.88	187.6	227.54	251.4	267.98
37	28.2	75.7	154.2	221.6	263.2	290.7	309.6
42	26.9	74.2	156.6	228.6	272.1	300.4	320.0
47	26.7	75.4	159.7	230.8	272.8	300.1	318.7
52	26.8	77.5	160.3	229.9	269.9	295.5	313.5
57	26.7	70.9	140.3	199.5	237.1	258.4	272.9
Average	27.06	74.76	154.22	221.9	263.02	289.02	306.94
38	36.1	112.0	219.1	304.9	354.4	390.1	416.2
43	34.0	108.0	218.0	308.5	359.9	398.8	423.9
48	34.1	111.0	224.1	312.9	362.8	400.0	424.9
53	34.9	114.4	226.0	311.5	359.2	393.3	416.9
58	36.0	105.4	198.8	273.9	319.1	345.4	365.2
Average	35.02	110.1	217.2	302.34	351.1	385.3	409.4
39	49.9	170.4	330.3	458.8	533.5	597.9	643.9
44	46.4+	165.0+	330.0	460.9	540.8	610.9	656.7
49	46.4	167.6	332.7	465.5	541.1	609.5	657.8
54	47.0+	165.0+	334.0+	466.3	537.7	598.8	610.0+
59	51.7	159.0	295.0	404.2	473.0	515.2	549.8
Average	48.28	165.4	324.4	451.14	525.2	586.5	623.6
40	66.7	238.2	463.0	647.9	763.4	884.9	961.3
45	59.8	219.2	443.0	638.6	763.6	896.3	973.7
50	60.9	230.5	458.6	649.7	768.8	895.1	975.3
55	60.3	223.0	444.8	618.1	718.7	818.6	883.7
60	70.3	217.6	401.5	553.7	653.2	718.3	782.2
Average	63.6	225.7	442.18	621.6	733.5	842.6	915.24

+ Interpolated values

TABLE 4.7 Thermocouple temperatures and their averages for heated portion of unrestrained test beam heated along half of flange

Analysis Number	Phase Transformation Allowed For		Modulus of Elasticity	
	Yes	No	Constant	Variable
133X		✓	✓	
133Z	✓		✓	
134 A-E	✓			✓ (i)
135 A-E	✓			✓ (ii)

Notes i) BSC/Euronorm data
ii) Arbed data

TABLE 4.8 Bases of PAFEC elastic analyses for unrestrained test beam heated along half of flange

Analysis number	Central displacement* (mm) of beam at time of heating (min) of:						
	6	12	18	24	30	36	42
133X	.75598	2.8698	5.33	7.2609	8.8483	11.77	11.734
133Z	.75604	2.870	5.3302	7.2607	7.2367	9.0829	9.5503
134A-E		2.8634	5.2982	7.1789	7.1786	8.3827	9.2198
135A-E		2.8644	5.2573	6.9198	6.9194	7.4512	7.6634
Experiment value	0.4	0.8	3.0	5.25	5.75	6.7	7.2

*Node number 4

TABLE 4.9 Central displacements obtained from PAFEC analyses for unrestrained test beam heated along half of flange

Duration of test, minutes		0	4	8	12	16	20
Test 1	Average heated flange temperature °C	23.46	93.48	174.28	234.56	278.4	275.53
	Average unheated flange temperature °C	22.28	22.48	23.3	25.82	30.38	35.85
	Temperature difference °C	1.18	7.1	150.98	208.74	248.02	239.68
	Bowing displacement mm	.058	.352	7.488	10.353	12.3	11.89
Test 2	Average heated flange temperature °C	22.83	88.18	220.17	319.28	417.4	450.78
	Average unheated flange temperature °C	22.03	22.08	22.75	25.82	31.76	41.05
	Temperature difference °C	0.8	66.1	197.42	293.46	385.64	409.73
	Bowing displacement mm	.039	3.28	9.79	14.55	19.13	20.32

TABLE 4.10 Calculated mid-height bowing displacements of column-in-wall in Cardington compartment fires, Tests 1 and 2

Test 1	Duration of test, min							
	5	7	8	11	13	16	21	26
Bowing displacement mm	3	6	8	11	13	15	15	13.50

a) Test 1

Test 2	Duration of test, min					
	4	5	6½	9	12	14½
Bowing displacement mm	2.5	5	7	11	15	19

b) Test 2

TABLE 4.11 Measured mid-height bowing displacements of column-in-wall in Cardington compartment fires, Tests 1 and 2

Element	C	S_i	M_n	S	P	N_i	C_r	M_b	T_i	N_b	V	C_u	A_l
%	.21	.05	.57	.039	.014	<.01	.01	<.01	<0.01	<.01	<.01	.01	<.005
													Total

TABLE 5.1. Chemical composition of steel used in 2-span model beam

Sample	Yield stress N/mm^2	Tensile strength N/mm^2	Elongation %	Reduction in area %
Unheated	315	463	37	63
Heated	223	428	37	60

TABLE 5.2 Strength properties of steel used in 2-span model beam

Duration of heating (min)	Half flange heated		Whole flange heated	
	Load transducer output (mV)	Load (kN) (1)	Load transducer output (mV)	Load (kN) (1)
0	0	0	0	0
2	0.03	.1029	.05	0.1715
4	0.03	1.029	.41	1.4063
6	0.90	3.087	1.15	3.944
8	1.71	5.8653	2.21	7.5803
10	2.75	9.432	3.67	12.588
12	4.01	13.754	5.39	18.4877
14	5.31	18.213	7.02	24.078
16	6.0	20.58	6.97	23.907
18	6.29	21.575	7.01	24.044
20	6.06	20.875	7.11	24.387
22	4.96	17.013	6.75	23.152
24	4.21	14.44	5.89	20.202
26	3.39	11.627	5.26	18.042
28	2.61	8.952	4.46	15.298
30	2.29	7.854	3.42	11.73
32	2.25	7.717	2.92	10.015
34	2.26	7.572	2.56	8.781
36	2.09	7.168		
38	1.93	6.619		

Notes (1) Obtained by multiplying mV by 3.43 kN/mV

TABLE 5.3. Measured load transducer outputs and corresponding loads for 2-span test beam heated along the flange

Distance down from unheated face (mm)	Average of temperatures (°C) at 12 stations at times (min) of								
	0	4	8	12	16	20	24	28	32
0	20	21.67	25.25	45.6	78.36	116.86	154.88	185.17	210.11
26	20	22.15	31.62	57.36	98.32	143.86	186.48	220.47	246.88
52	20	23.25	41.08	82.01	140.15	182.74	256.23	300.06	332.43
78	20	25.88	56.57	120.63	202.29	290.86	378.43	439.69	482.26
95	20	29.17	73.27	160.49	276.24	397.6	510.1	604.2	674.7

TABLE 5.4. Average temperatures at thermocouple levels in 2-span model steel beam heated along whole flange

	Parameter	Notes	Value of parameter at time (min) of: 0	4	8	12	16	20	24	28	32	Data row
Experimental temperature data, °C	Average temp of unheated flange	i	20	22	26	46	79	117	155	186	210	1
	Average temp of heated flange	ii	20	30	80	180	310	440	570	690	770	2
	Average temperature difference between flanges	iii	0	8	54	134	231	323	415	504	560	3
	Average temperature of beam	iv	20	26	53	113	194	278	362	443	490	4
E (kN/mm²) and P (kN) using Euronorm E data	E, assuming average temp of beam	v	210	210	210	205	200	195	188	180	175	5
	E, assuming average temp of heated flange	vi	210	210	205	200	192	178	170	155	145	6
	Calculated P, assuming average temp of beam	vii	0	1.542	10.41	25.22	42.41	57.82	71.62	83.28	89.96	7
	Calculated P, assuming ave. temp of heated flange	viii	0	1.542	10.16	24.60	40.71	52.78	64.76	71.71	74.54	8

NB. For notes i - viii see after Table

TABLE 5.5. Data used in analyses of mid-support restraint forces for 2-span model beam heated along whole flange

	Parameter	Notes	Value of parameter at time (min) of: 0	4	8	12	16	20	24	28	32	Data row
E (kN/mm²) and P (kN) using Arbed E data	E, assuming average temp of beam	ix	210	210	210	209	205	197	188	166	149	9
	E, assuming average temp of heated flange	x	210	210	210	205	193	164	125	84	70	10
	Calculated P, assuming average temp of beam	xi	0	1.54	10.41	25.71	43.47	58.41	71.62	76.80	76.60	11
	Calculated P, assuming ave. temp of heated flange	xii	0	1.54	10.41	25.22	40.93	48.62	47.62	38.86	35.98	12
Experimental P data and derived E and σ	Experimental restraint force P (kN)	xiii	0	1.41	7.60	18.5	23.9	24.4	20.2	15.3	10.0	13
	Effective E (kN/mm²)	xiv	210	192	153	150	105	77	50	31	18	14
	Maximum elastic flexural stress (N/mm²)	xv	0	171	922	2245	2901	2962	2452	1857	1214	15

NB. For notes ix - xv see after Table

TABLE 5.5 continued. Data used in analyses of mid-support restraint forces for 2-span model beam heated along whole flange

i From Table 5.4 rounded up to nearest whole number

ii Average temperature at mid-depth of equivalent flange thickness for heated flange, taken from Figure 5.4

iii Row 2-row 1

iv Row 1 + $\frac{\text{row 3}}{2}$

v E value taken from Figure 2.9 using the average temp of beam

vi " " " " " " " heated flange temp

vii 9.18×10^{-4} x E (from row 5) x T (from row 3). This is Equation (5.2)

viii 9.18×10^{-4} x E (from row 6) x T (from row 3). This is Equation (5.2)

ix E value taken from Figure 2.13 using the average temp of beam

x " " " " " " " heated flange temp

xi 9.18×10^{-4} x E (from row 9) x T (from row 3). This is Equation (5.2)

xii 9.18×10^{-4} x E (from row 10) x T (from row 3). This is Equation (5.2)

xiii Taken from Table 5.3

xiv P (from row 13) ÷ (9.18×10^{-4} x T (from row 3)). This is Equation (5.3)

xv 0.1214 x P (from row 13). This is Equation (5.4).

Notes to Table 5.5

Rating tonnes	Model Number	Stroke mm	Cylinder effective area cm^2	Cylinder outside diameter mm	Collapsed height mm	Maximum cylinder capacity kN
4.5	RC-55	133	6.41	38	216	44.8

TABLE 6.1 Design details of Enerpac jacks

Distance from heated face (mm)		Average temperature (°C) at middle 6 stations at time (min) of:								
		0	4	8	12	16	20	24	28	32
0	(1)	23.8	54.4	150.3	256.5	363.5	465.0	555.1	618.3	672.5
5	(2)	23.8	52.0	143.1	249.4	355.2	457.0	548.0	610.0	662.3
20	(3)	23.6	43.5	115.7	202.3	289.4	373.0	449.0	501.6	546.3
40	(4)	23.4	35.4	87.7	156.9	228.2	296.3	359.1	402.0	438.5
60	(5)	23.5	30.2	65.8	118.0	173.1	225.8	274.4	308.4	352.6
75	(6)	23.4	26.9	51.8	94.0	140.5	186.5	229.6	260.6	285.4
80	(7)	23.6	27.4	54.0	98.1	146.9	195.0	240.2	272.3	298.1

Notes: (1) Average of thermocouple numbers 8, 15, 22, 29, 36, 43
(2) " " " " 9, 16, 23, 30, 37, 44
(3) " " " " 10, 17, 24, 31, 38, 45
(4) " " " " 11, 18, 25, 32, 39, 46
(5) " " " " 12, 19, 26, 33, 40, 47
(6) " " " " 13, 20, 27, 34, 41, 48
(7) " " " " 14, 21, 28, 35, 42, 49

TABLE 6.2. Average of thermocouple temperatures for design-loaded model beam heated along one flange

Distance from	Average temperature (°C) at middle 6 stations heated face at time (min) of:								
(mm)	0	4	8	12	16	20	24	28	32
0	23.8	54.4	150.3	256.5	363.5	465	555	618	680
5	23.8	52.0	143.1	249.4	355.2	440	530	590	645
20	23.6	43.5	115.7	202.5	289.4	373	449	502	555
40	23.4	35.4	87.7	157.0	228	296	359	402	445
60	23.5	30.2	65.8	118.0	173	226	275	308	355
75	23.4	26.9	51.8	100	150	195	235	260	310
80	23.6	27.4	54.0	98	147	185	225	250	298

TABLE 6.3. Average temperatures taken from profiles for design-loaded model beam heated along one flange

Displacement transducer	Displacement of transducer shaft (mm) at time (min) of:															
	0	2	4	6	8	10	12	14	16	18	20	22	24	26	28	30	32
A	0	0.339	1.432	3.166	5.238	7.254	9.647	12.210	14.471	16.751	18.918	21.556	24.51	27.90	35.52	48.95	67.42
B	0	0.302	1.379	3.060	5.082	6.915	9.296	11.449	13.546	15.682	17.722	20.235	23.05	26.53	34.42	45.79	64.99
Average $(\frac{A+B}{2})$	0	0.3205	1.4055	3.113	5.16	7.085	9.472	11.83	14.018	16.217	18.32	20.896	23.78	27.21	34.97	47.37	66.2

TABLE 6.4 Transducer displacements for design-loaded model beam heated along one flange

Mid-span displacement (mm) at time (min) of:																
0	2	4	6	8	10	12	14	16	18	20	22	24	26	28	30	32
0	.3205	1.405	3.113	5.16	7.085	9.472	11.75	13.918	16.097	18.18	20.75	23.63	27.16	35.57	49.27	66.2

Note: Mid-span displacement = average transducer displacement - (end displacement[+] ÷ 2)

[+]End displacement is obtained from dial gauge readings

TABLE 6.5 Corrected transducer displacements for design-loaded model beam heated along one flange

Duration of heating, min	24	26	28	30
Rate, mm/min	1.6	2.687	5.094	7.76

TABLE 6.6 Rate of displacement for design-loaded model beam heated along one flange

Duration of heating, min	4	8	12	16	20	24	28	32
Difference in temperature between heated and unheated flanges °C	27	96.3	158.4	216.6	270	314.9	346	374.4
Mid-span displacement due to thermal bowing, mm	1.329	4.739	7.796	10.66	13.29	15.498	17.03	18.42

TABLE 6.7. Thermal bowing data for design-loaded model beam heated along one flange

Dimensional parameter		Specified	Actual average	Tolerance*	Actual maximum
Flange width	(in)	0.669	0.670	+.04/-.03	±.004
Depth	(in)	1.005	1.006	±.02	±.007
Web thickness	(in)	0.041	0.040	-	±.004
Flange thickness	(in)	0.047	0.047	-	±.007
Area of section	(in^2)	0.1002	0.1028	±.003	±.005
I_x	(in^4)	0.01712	0.01768	-	-
Camber	(in)	-	-	.025	.02
Sweep	(in)	-	-	.05	.01
Flange out of square	(in)	-	-	.04	.01

*Tolerances are scaled values from standard mill practice, AISC Steel Construction Manual

TABLE 7.1 Dimensional data for American model I-section beams fabricated by milling from the solid

Section Parameter	Flange width, mm 40	50	60
Area, mm^2	672	792	912
I_{xx}, mm^4	388224	476064	563904
I_{yy}, mm^4	64256	125256	216256
r_{xx}, mm	24.0356	24.5171	24.86
r_{yy}, mm	9.7785	12.576	15.3988
ℓ/r_{xx}	56.166	55.0636	54.304
ℓ/r_{yy}	138.058	107.37	87.669

Table 7.2 Section properties of model columns

Test Number	Column flange width (mm)	$\frac{\ell}{r_{yy}}$	η	C_o (N/mm²)	D	B	F	p_c (N/mm²)	A (mm²)	Calculated design load, P. (kN)	(lbf)	P (kN) for BS 4360 Grade: 43	50
1	40	138.58	.5718	99.83	251.4	34541	82.10	48.296	672	32.45	7,293	31.58	34.94
2	50	107.37	.3457	165.12	284.1	57131	130.5	76.786	792	60.81	13,670	57.02	64.94
3	60	87.67	.2630	247.57	329.3	85659	178.37	104.92	912	95.69	21,510	86.18	103.97

Notes:

i) $D = \frac{\sigma_s + (\eta + 1)}{2} C_o$; $B = \sigma_s C_o$; $F = D - \sqrt{(D^2 - B)}$; $p_c = \frac{F}{1.7}$; P = design load

ii) $\frac{\ell}{r_{yy}}$ and A are taken from Table 7.2

iii) σ_s = 346 N/mm²; E = 192.8 kN/mm² from tensile test, except for last two columns of data which assume σ_s of 250 and 350 N/mm² for BS 4360 grade 43 and 50 steel respectively and E = 210 kN/mm²

iv) P for BS 4360 Grades 43 and 50 was calculated using Tables 17a and 17b respectively of BS 449

TABLE 7.3 Data for calculation of model column test loads, assuming failure about the minor (yy) axis

Calibration pressure (lb/in^2)	1000	2000	3000	4000	5000	6000	7000	8000	9000	10000
Indicated pressure (lb/in^2)	1040	2030	3025	4030	5030	6030	7025	8020	9010	10000

TABLE 7.4 Calibration data for hydraulic pressure gauge

Rating (tonnes)	Model Number	Stroke (mm)	Cylinder effective area (cm^2)	Cylinder outside diameter (mm)	Collapsed height (mm)	Maximum cylinder capacity (kN)
10	RC-104	105	14.43	57	172	101
15	RC-152	51	20.3	70	149	140
25	RC-252	51	33.2	85	165	229

TABLE 7.5 Details of Enerpac jacks used in model column tests

	Thermocouple Number	Duration of Heating (Mins):										
		6	12	18	24	30	36	42	48	54	60	66
Maximum Steel Temperature (°C)	11	32.0	105.2	229.8	380.5	525.9	610.3	656.3	690.7	729.5	747.2	763.1
	17	29.1	96.0	219.3	380.3	532.0	620.9	667.4	702.7	740.5	758.1	774.7
	23	33.2	104.5	228.8	381.5	534.6	621.4	665.3	700.0	739.2	751.3	765.5
	29	30.0	87.7	200.7	334.9	473.6	556.3	596.6	626.4	658.4	677.4	687.4
	35	27.1	90.1	203.2	338.1	475.7	562.9	605.1	635.9	665.3	684.8	691.5
	41	31.8	118.9	254.2	400.0	531.0	612.2	656.0	686.0	718.9	735.9	744.1
	47	29.8	98.8	229.3	388.4	538.8	620.0	662.2	692.9	727.1	745.6	757.1
i	55	29.1	97.2	223.2	376.3	516.9	593.3	631.1	658.9	692.0	712.0	722.5
Minimum Steel Temperature (°C)	6	20.9	49.1	116.7	215.7	318.3	398.8	440.0	455.8	473.3	488.6	496.6
	12	21.1	47.3	116.5	221.8	330.7	416.6	450.9	466.9	485.1	498.6	508.2
	18	21.4	48.6	117.4	221.0	334.1	421.6	458.0	474.5	495.2	507.5	515.0
	24	21.1	44.7	107.1	198.7	302.2	381.7	419.2	435.3	448.7	463.6	469.0
	30	20.1	44.0	109.0	204.6	303.4	387.7	428.9	444.0	458.7	470.0	472.4
	36	20.6	53.1	129.7	234.2	339.3	422.5	458.0	471.6	489.8	501.1	505.6
	42	20.4	46.9	118.8	225.9	338.9	424.5	456.5	470.9	486.5	500.6	507.2
i	48	21.4	45.7	111.4	212.0	317.1	394.5	430.5	446.4	463.9	474.9	479.9
Average Maximum Steel Temp. (°C)		30.26	99.8	223.56	372.47	516.06	599.66	642.5	674.18	708.36	726.53	738.23
Average Minimum Steel Temp. (°C)		20.87	47.42	115.82	216.7	323	406	442.75	458.17	475.15	488.11	494.23
Average Temperature difference (°C)	ii	9.37	52.38	107.7	155.71	193.06	193.68	199.75	216	233.2	238.4	244
Average Temperature rise (°C)	iii	5.565	32.1	149.5	274	399.5	482.5	522	546	571	587	596
Calculated central horizontal deflection (mm)	iv	.5053	2.803	5.810	8.392	10.403	10.440	10.766	11.64	12.56	12.85	13.16
Calculated axial deflection (mm)	v	0.106	0.61	2.84	5.21	7.59	9.17	9.93	10.37	10.86	11.15	11.32

Notes: i except thermocouples at ends of specimen where temperatures are unrepresentative due to large heat losses.
ii average maximum steel temp. - average minimum steel temp.
iii (average max. steel temp + average min. steel temp.)/2 - initial temp.
iv 0.0539 x average temp. difference
v 0.0190 x average temp. rise

TABLE 7.6 Temperature and calculated displacement data for model column, Test 1.

	Thermocouple Number	Duration of Heating (Min): 4	8	12	20	24	28	32	35	46	51	55	59
Maximum Steel Temperature (°C)	11	42.8	118.6	251.0	495.7	584.8	642.7	681.7	702.4	737.4	743.4	752.3	733.5
	17	37.9	106.9	240.3	507.7	604.9	667.0	704.1	725.7	767.7	779.1	786.8	782.5
	23	47.1	121.5	252.7	507.2	602.8	664.8	703.9	725.9	768+	780+	786+	782+
	29	44.2	125.3	220.1	424.4	532.7	587.6	624.5	644.9	688+	700+	710+	720+
	35	41.0	103.8	193.4	392.9	511.0	587.4	637.3	660.1	704.6	721.8	733.6	744.4
	41	35.0	98.1	198.2	443.3	565.9	639.9	688.9	713.4	757.4	775.0	785.3	790.9
	47	34.7	97.6	199.7	454.7	578.0	650.8	697.2	721.1	764.1	779.6	786.3	794.1
	55 i	41.0	110.9	212.7	445.4	553.9	621.2	665.3	688.6	731.9	742.0	748.2	756.9
Minimum Steel Temperature (°C)	6	21.6	45.4	107.1	249.5	324.0	380.3	419.2	436.0	460.8	462.2	460.1	460.8
	12	21.4	43.7	107.9	265.8	349.1	414.0	449.7	464.1	486.5	488.4	477.5	469.0
	18	21.4	44.2	106.4	257.5	339.8	401.2	438.4	453.7	473+	473+	468+	458+
	24	21.6	42.5	97.6	299.6	299.8	363.8	400.9	416.8	441+	450+	452+	450+
	30	19.4	38.1	77.2	201.7	274.7	345.3	396.0	418.2	443.6	452.1	455.8	453.2
	36	19.1	37.9	81.3	222.2	306.0	376.7	425.5	443.3	464.6	472.8	473.5	464.3
	42	19.1	38.4	83.2	228.1	313.7	385.0	431.5	449.7	471.9	478.5	477.8	471.4
	48 i	19.6	41.3	86.0	217.6	288.5	350.1	394.5	415.7	445.0	451.3	452.1	453.5
Average Maximum Steel Temp. (°C)		40.46	110.3	221.0	395.5	566.7	632.6	675.4	697.7	740	753	761	763
Average Minimum Steel Temp. (°C)		20.4	41.4	93.3	234	312	377	419	437	461	466	465	460
Average Temperature difference (°C) ii		20.1	68.9	135	161.5	254.7	255.6	256.4	260.7	279	287	296	303
Average Temperature rise (°C) iii		10.73	56.85	137.4	295	419.6	485.1	527.5	522	580.7	589.8	593.3	591.8
Calculated central horizontal deflection (mm) iv		1.084	3.714	7.276	8.705	13.73	13.77	13.82	14.05	15.04	15.47	15.95	16.33
Calculated axial deflection (mm) v		0.204	1.080	2.611	5.606	7.973	9.217	10.02	9.918	11.03	11.206	11.27	11.24

Notes: i except thermocouples at ends of specimen where temperatures are unrepresentative due to large heat losses.
ii average maximum steel temp. - average minimum steel temp.
iii (average max. steel temp + average min. steel temp.)/2 - initial temp (19.7°C)
iv 0.0539 x average temp. difference
v 0.0190 x average temp. rise
\+ interpolated data

TABLE 7.7 Temperature and calculated displacement data for model column, Test 2

	Thermocouple Number	Duration of Heating (Min): 4	8	12	16	20	24	28	32	36	40	44
Maximum Steel Temperature (°C)	11	38.1	112.6	225.9	345.8	486.5	585.5	645.8	683.6	709.9	728.9	643.4
	17	35.5	101.0	211.5	338.1	501.8	610.5	670.7	707.7	735.0	752.5	765.8
	23	43.5	120.5	230.3	358.2	505.1	604.4	665.5	713.9	746.3	779.1	802.1
	29	38.4	107.1	208.1	282.0	371.5	473.5	578.9	676.0	747.5	815.0	859.8
	35	46.4	120.3	213.5	277.9	346.0	434.1	539.3	639.7	712.3	745.1	768.9
	41	47.1	128.7	232.5	344.6	482.5	574.2	639.2	683.4	720.1	739.1	756.6
	47	37.9	108.5	215.9	338.4	492.2	595.0	659.6	703.2	729.7	745.6	764.1
i	53	48.0	154.9	261.2	371.5	489.4	576.6	637.3	673.6	702.4	715	730
Minimum Steel Temperature (°C)	6	21.6	40.3	85.1	145.2	220.5	297.1	357.9	397.4	419.7	430.1	434.6
	12	21.6	37.7	80.6	143.5	229.1	316.6	381.7	419.0	539.5	444.5	439.1
	18	21.6	39.8	83.6	144.7	226.7	303.9	367.7	409.0	434.8	443.6	442.9
	24	21.9	40.1	81.5	132.6	185.8	237.1	289.2	347.9	408.3	456.8	501.8
	30	21.6	41.5	82.9	131.6	180.8	226.2	275.0	331.7	393.4	446.1	493.1
	36	21.4	42.0	86.7	147.0	222.8	295.2	358.4	403.3	430.1	444.3	452.8
	42	22.9	42.5	87.4	149.7	230.5	313.2	337.0	417.3	436.0	445.7	452.3
i	48	22	49.8	96.0	154.1	224.9	291.3	347.2	389.8	409.7	419.9	428.7
Average Maximum Steel Temp. (°C)		41.9	119.2	224.9	332	459.4	556.7	628.3	685.1	725.4	685	681
Average Minimum Steel Temp. (°C)		21.82	41.7	85.47	143.5	215.1	285	339.2	389.4	421.4	441.3	455.6
Average Temperature difference (°C)	ii	20.08	69.4	139.4	188.5	244.3	271.7	289.1	295.7	304	243.7	225.4
Average Temperature rise (°C)	iii	11.86	60.45	135.25	217.5	317	400.8	463.5	470	553	543	548
Calculated central horizontal deflection (mm)	iv	1.08	3.74	7.513	10.16	13.167	14.64	15.58	15.94	16.38	13.13	12.15
Calculated axial deflection (mm)	v	0.225	1.15	2.57	4.14	6.02	7.62	8.81	8.93	10.51	10.32	10.41

Notes: i except thermocouples at ends of specimen where temperatures are unrepresentative due to large heat losses.
ii average maximum steel temp. - average minimum steel temp.
iii (average max. steel temp + average min. steel temp.)/2 - initial temp
iv 0.0539 x average temp. difference
v 0.0190 x average temp. rise

TABLE 7.8 Temperature and calculated displacement data for model column, Test 3

Test No	Average temperature* °C	Time min
1	550	42
2	580	36
3	540	32

*Average temperature = (heated flange temp + unheated flange temp)/2 taken from Figures 7.13, 7.14 or 7.15 as appropriate

TABLE 7.9 Average temperature of model columns when thermal bowing ceased being dominant

Δ_N, mm	0	5	10	15	20	25	30
Δ_L, mm	0	0.05	0.196	0.441	0.784	1.225	1.765

TABLE 7.10 Shortening of model column in terms of bowing displacement

Test No	Average temperature °C (i)	Heated flange temperature °C (ii)	Time min
2	610	760	59
3	570	710	48

i) Average temperature = (heated flange temp + unheated flange temp)/2 taken from Figures 7.14 and 7.15

ii) Heated flange temperature taken from Figures 7.14 and 7.15

TABLE 7.11 Average and heated flange temperatures when initial length of model columns regained

Test No	Applied test load kN	Percentage error in load assuming Grade:- 43	50
1	32.45	-2.7	+7.67
2	60.81	-6.23	+6.79
3	95.69	-9.94	+8.65

TABLE 7.12 Percentage errors in model column test loads based on yield stress according to BS 4360 Grades 43 and 50

ILLUSTRATIONS

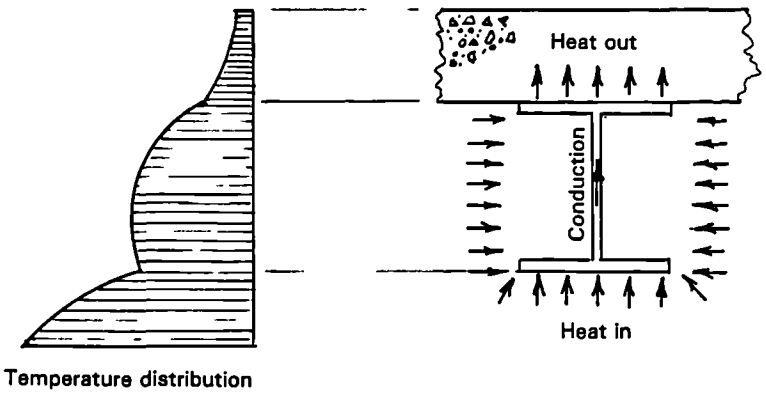

FIGURE 1.1 Heat flow processes for a steel I-section next to a heat sink

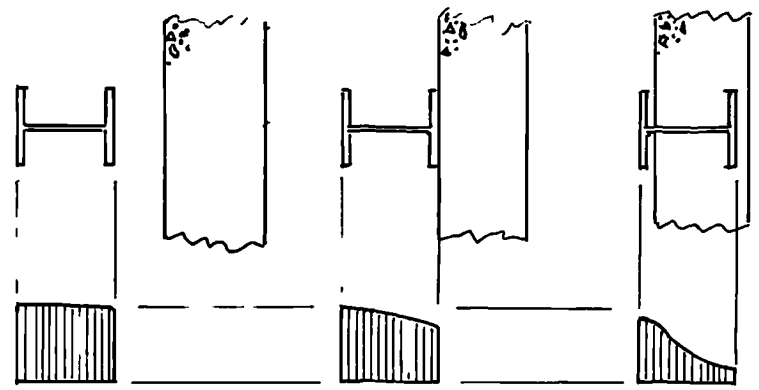

FIGURE 1.2 Effect of heat sink location on temperature profile in steel I-sections

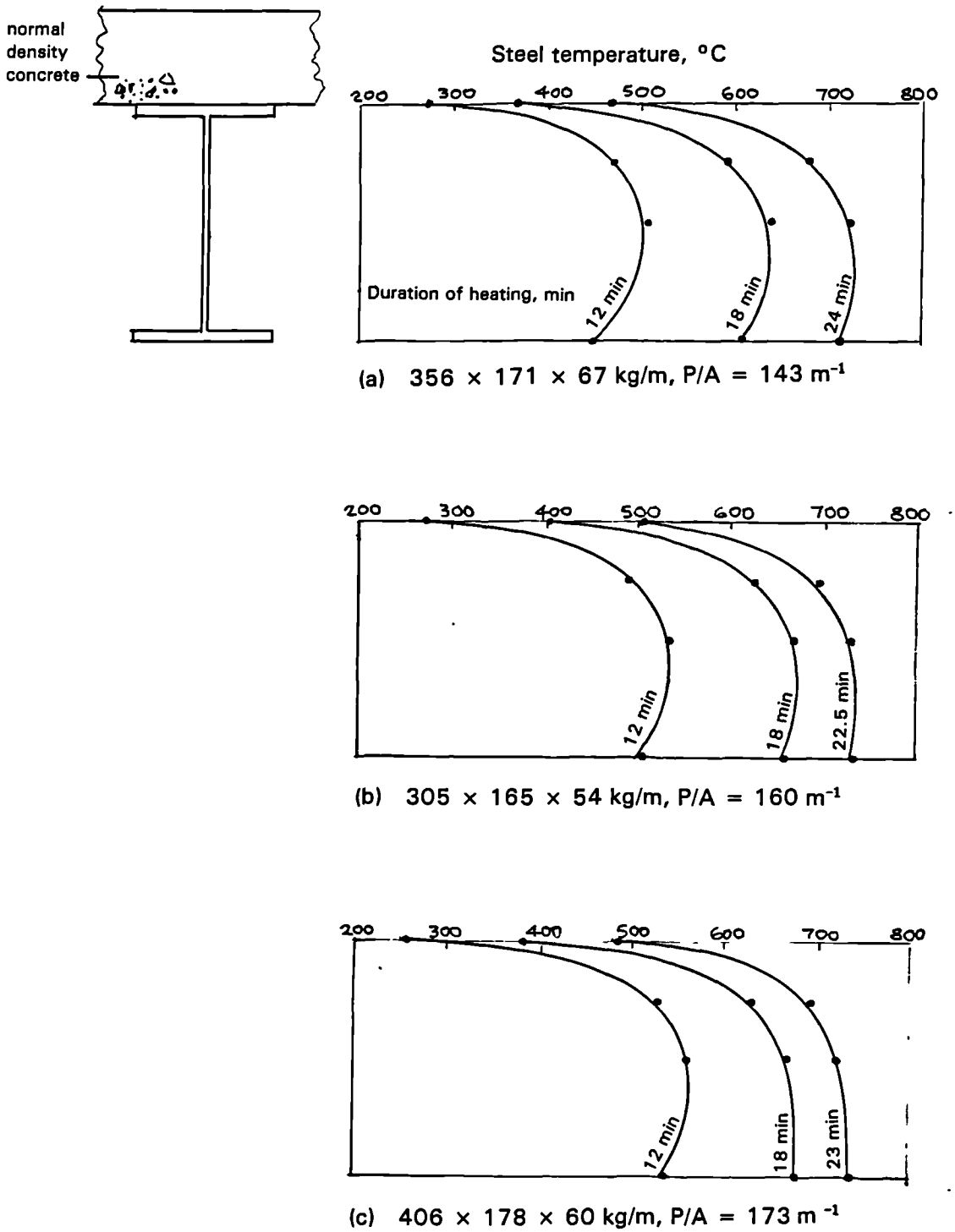

FIGURE 1.3 Temperature profiles in unprotected steel I-section beams supporting a concrete slab when exposed to BS 476 : Part 8 heating

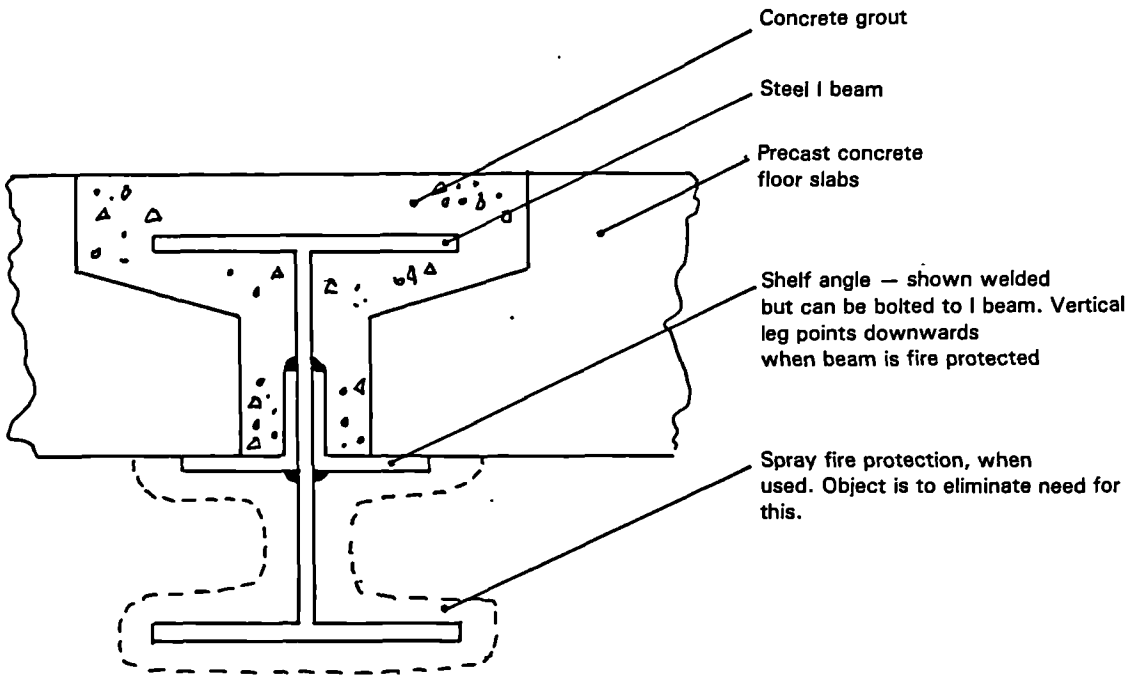

FIGURE 1.4 Shelf angle floor beam design

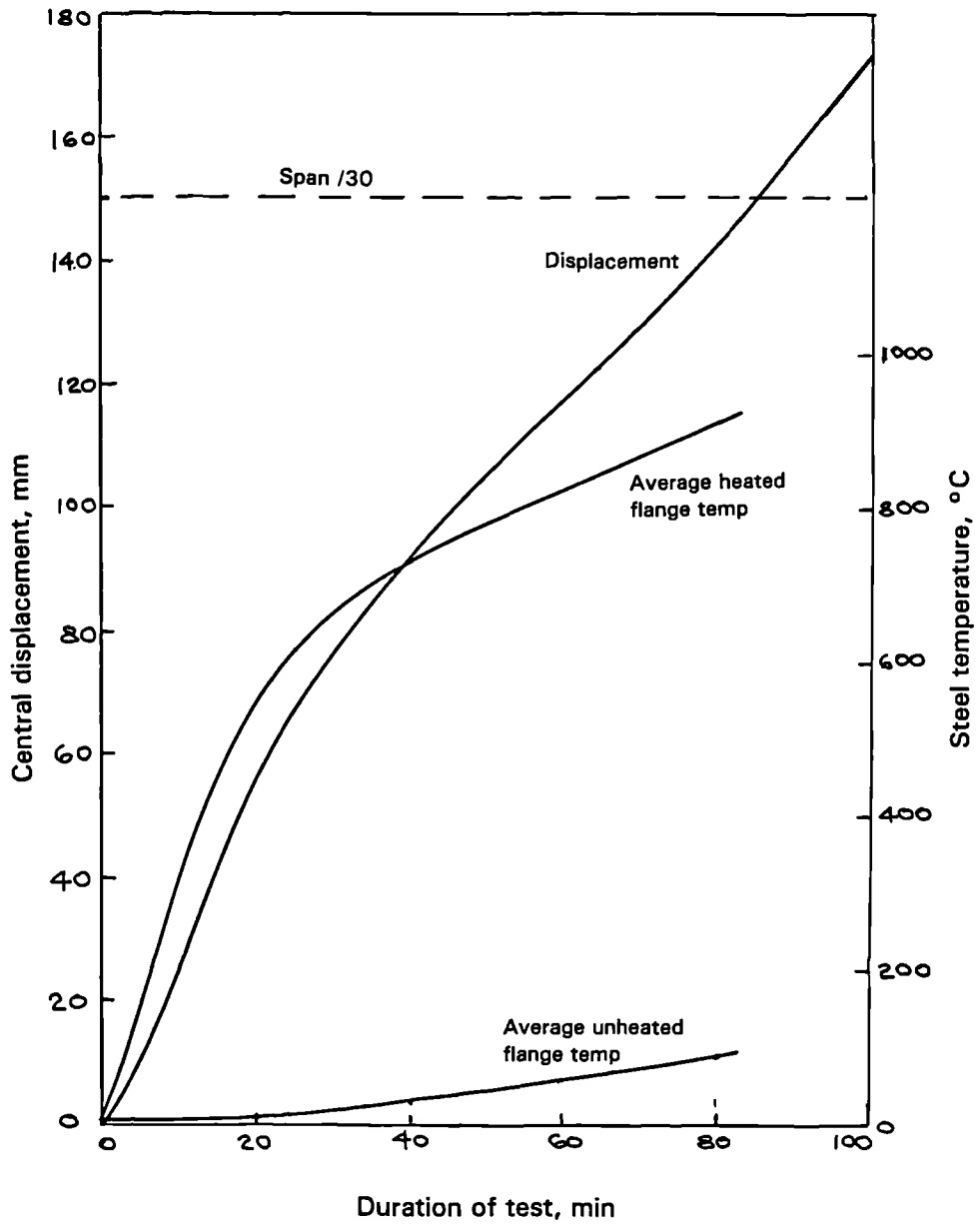

FIGURE 1.5 Variation of central displacement and flange temperatures with time for a 305 mm deep shelf angle floor beam exposed to BS 476 : Part 8 heating

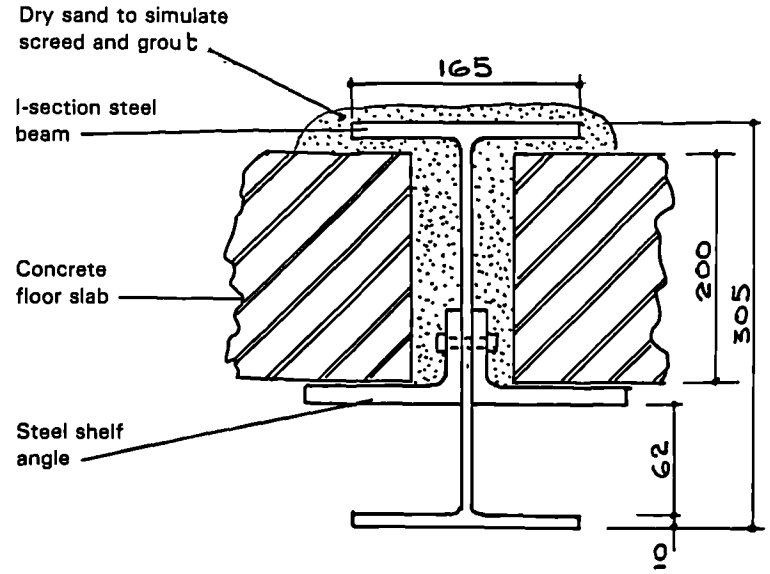

FIGURE 1.6 Section through 305 mm deep shelf angle floor beam

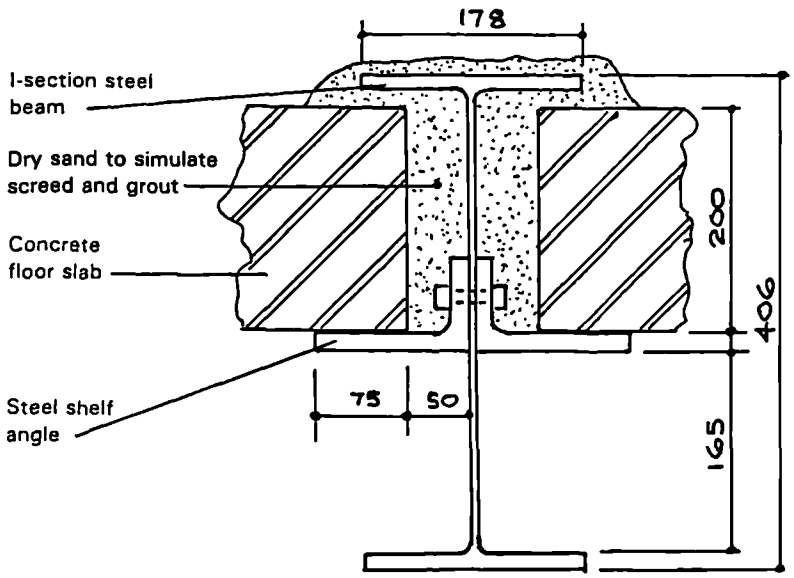

FIGURE 1.8 Section through 406 mm deep shelf angle floor beam

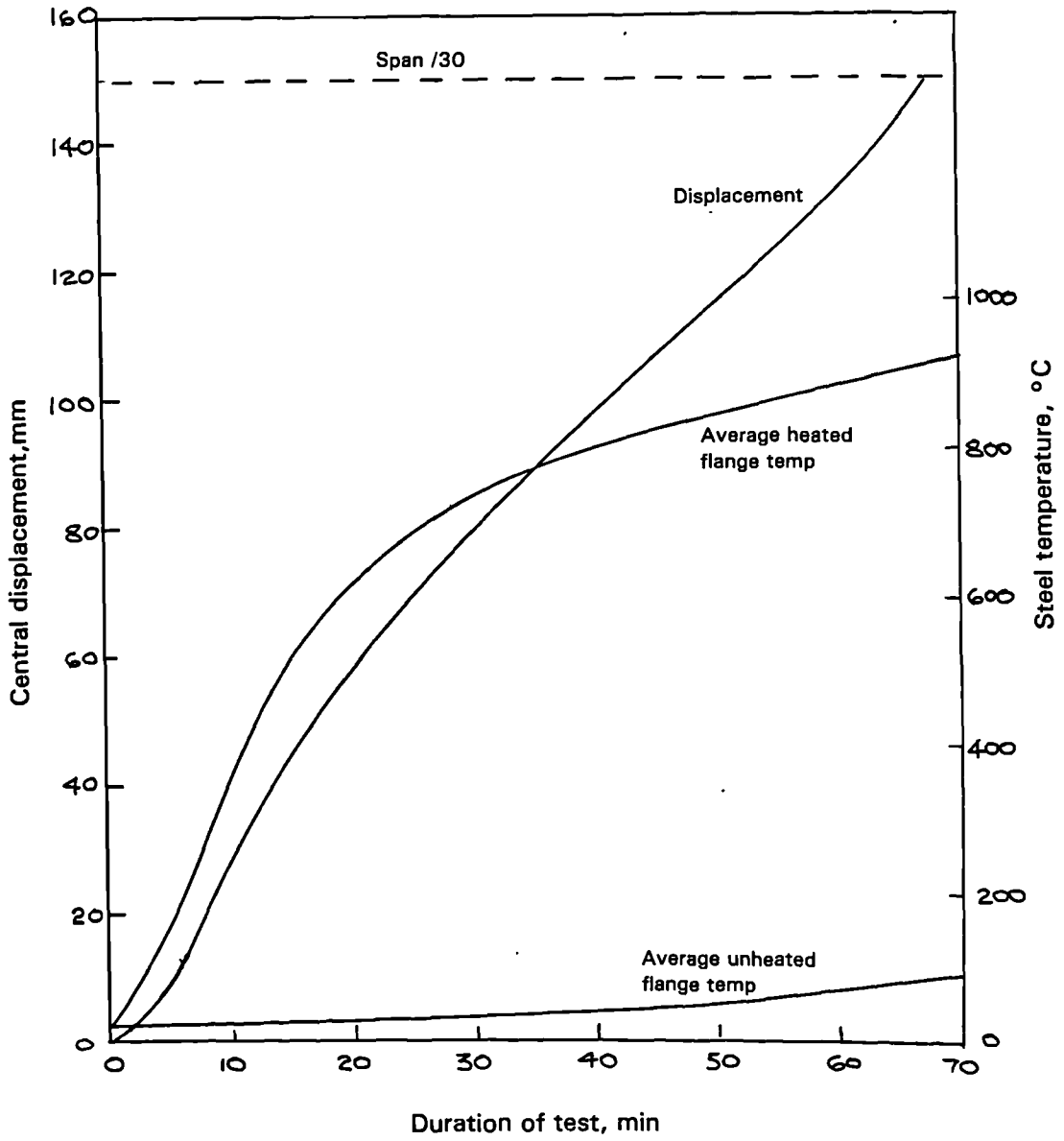

FIGURE 1.7 Variation of central displacement and flange temperatures with time for a 406 mm deep shelf angle floor beam exposed to BS 476 : Part 8 heating

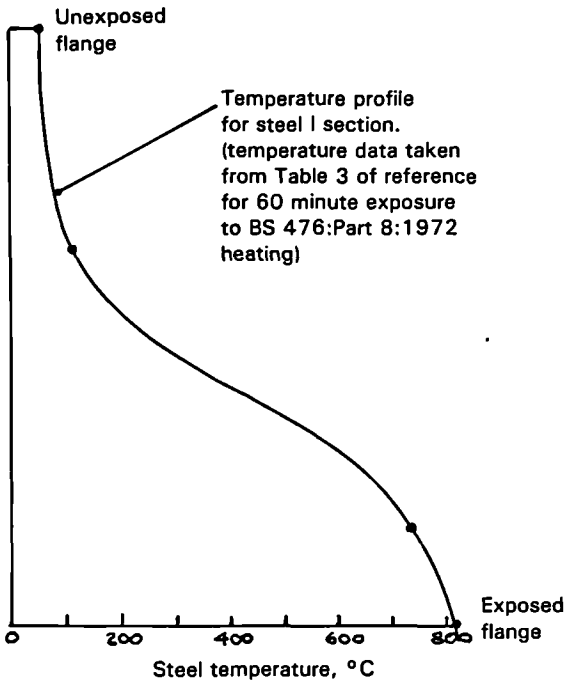

FIGURE 1.9 Temperature profile for a 305 mm deep shelf angle floor beam after 60 minute exposure to BS 476 : Part 8 heating

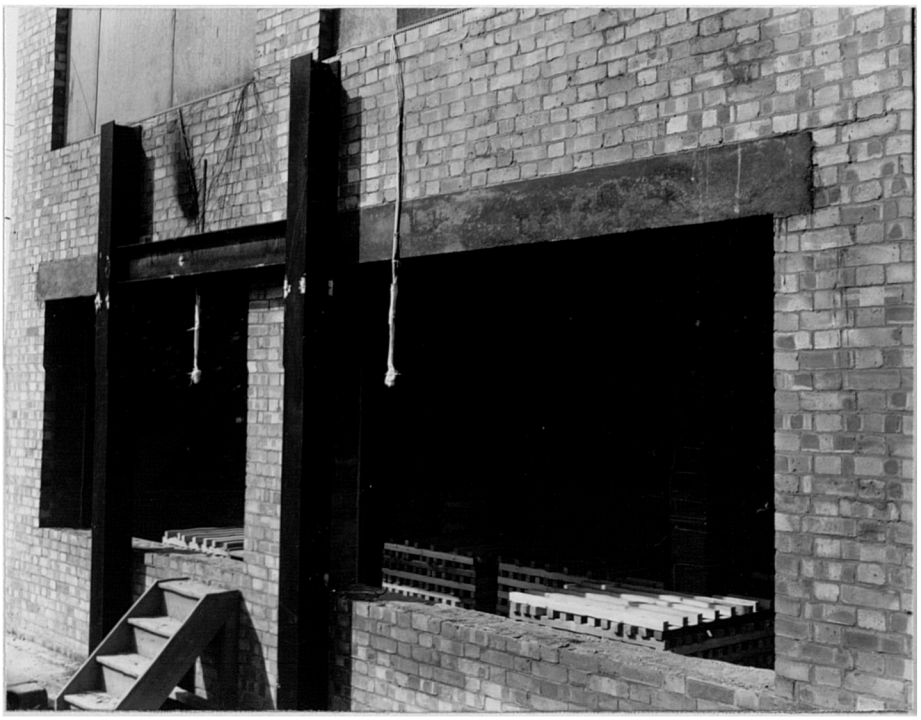

FIGURE 1.10 FRS fire compartment rig showing timber crib fire load and steelwork

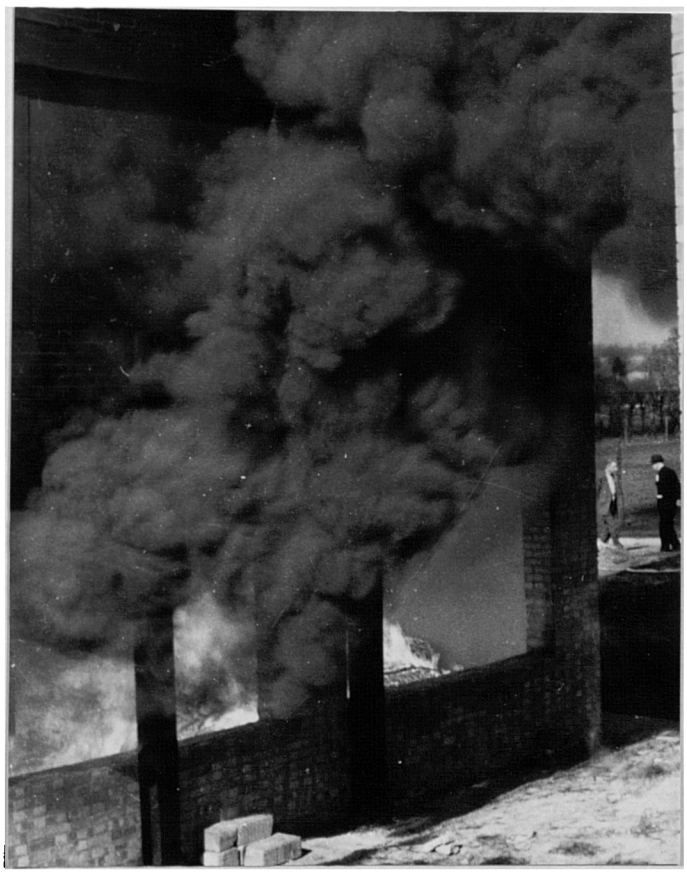

FIGURE 1.11 Fully developed fire in progress in FRS fire compartment rig

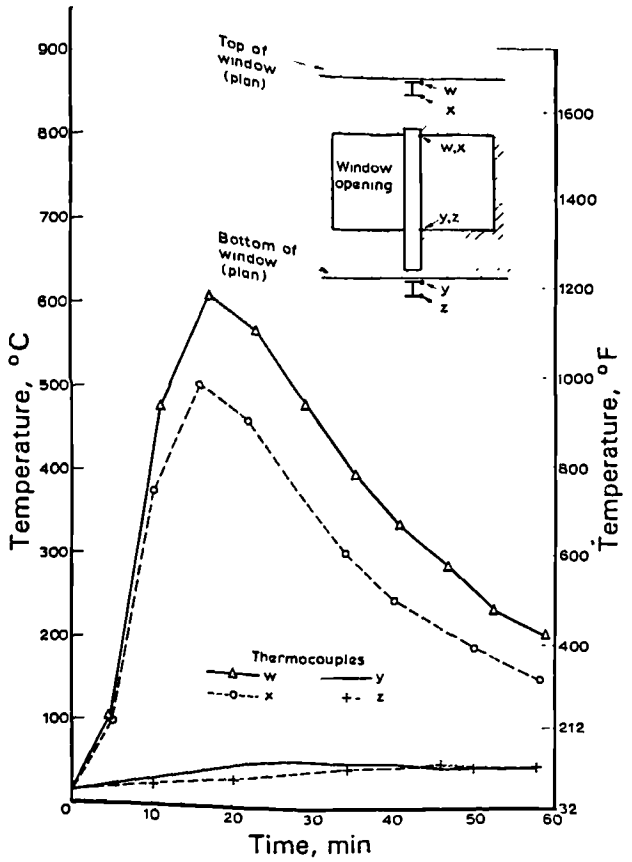

FIGURE 1.12 Temperatures attained in a bare external steel column (30 kg/m² fire load density, ½ ventilation)

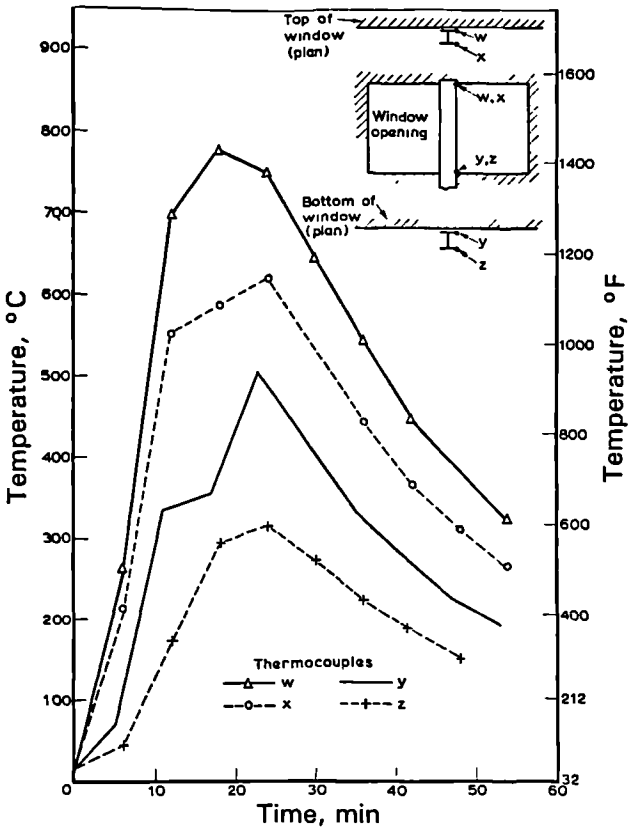

FIGURE 1.13 Temperatures attained in a bare external steel column (30 kg/m² fire load density, ¼ ventilation)

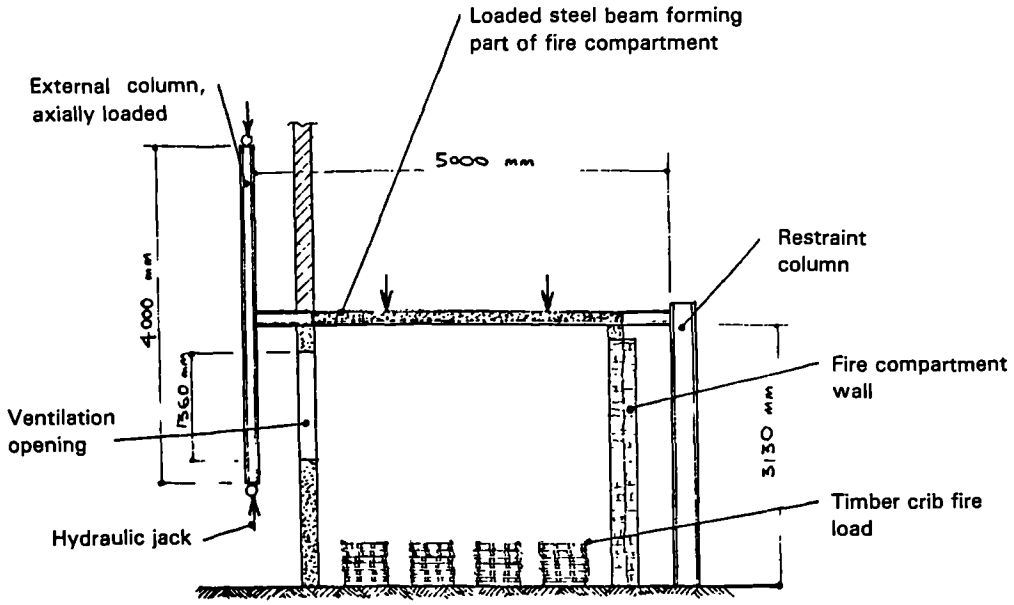

FIGURE 1.14 Section through CTICM fire test structure

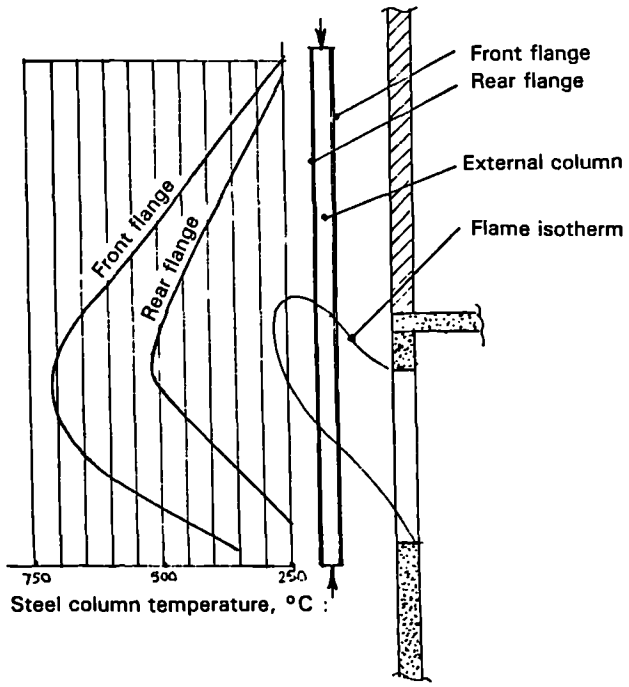

FIGURE 1.15 Typical temperature profiles in external steel column in CTICM test

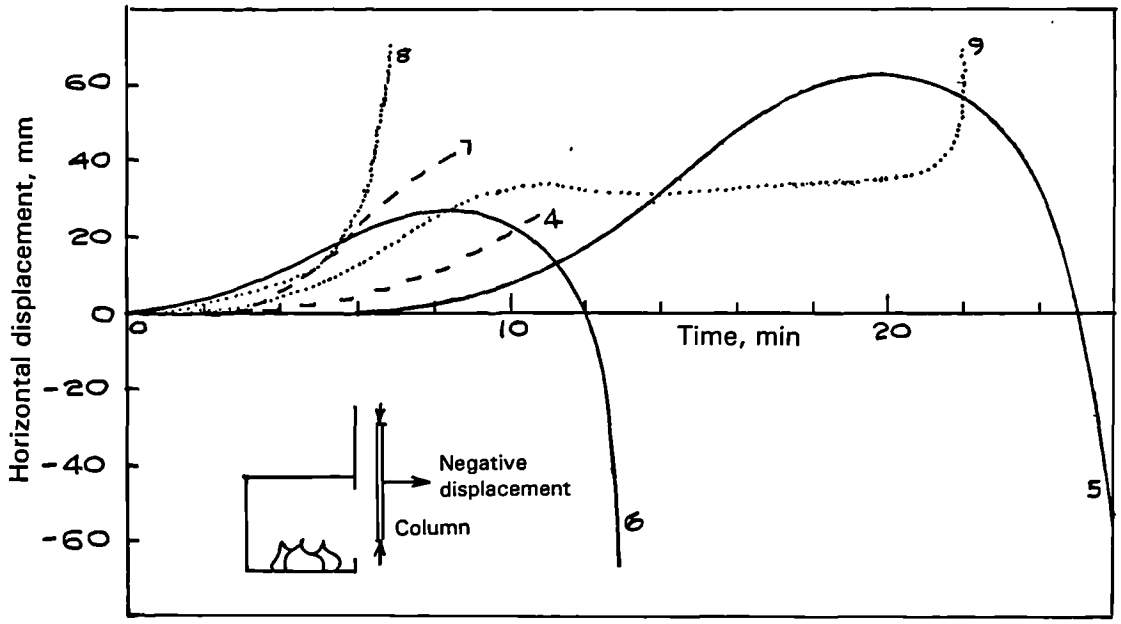

FIGURE 1.16 Mid-height displacements of external column perpendicular to facade in CTICM tests

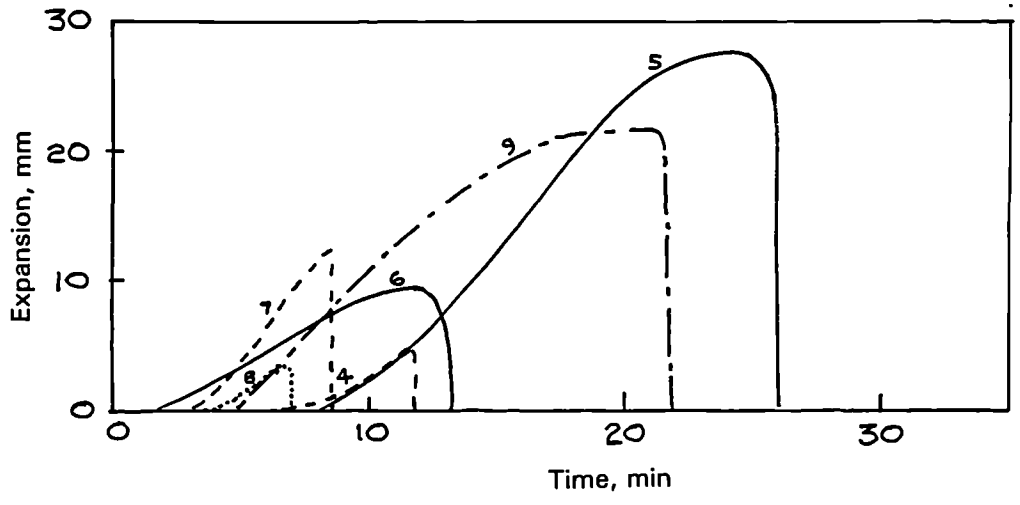

FIGURE 1.17 Axial displacements of external columns in CTICM tests

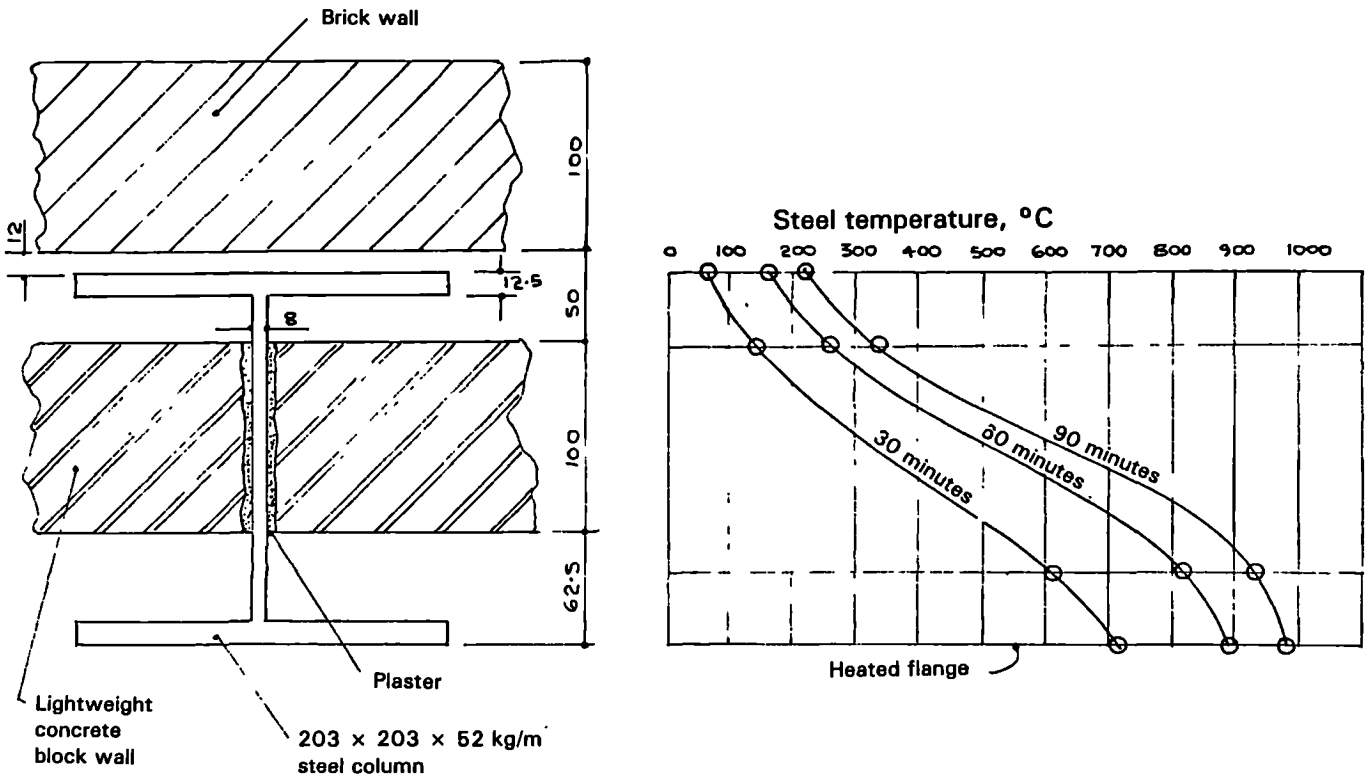

FIGURE 1.18 Section through an unprotected steel I-section column partly built into a cavity wall, and temperature profiles for BS 476 : Part 8 heating

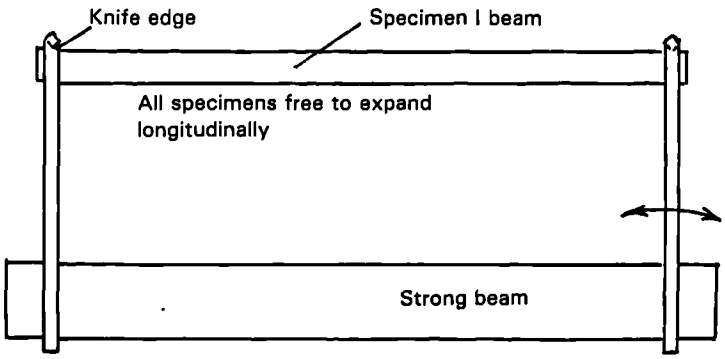

Restraint frame supporting or holding down end of specimen

Restraint frame can rotate about bottom of strong beam allowing free expansion of specimen

(a) Concept of test rig

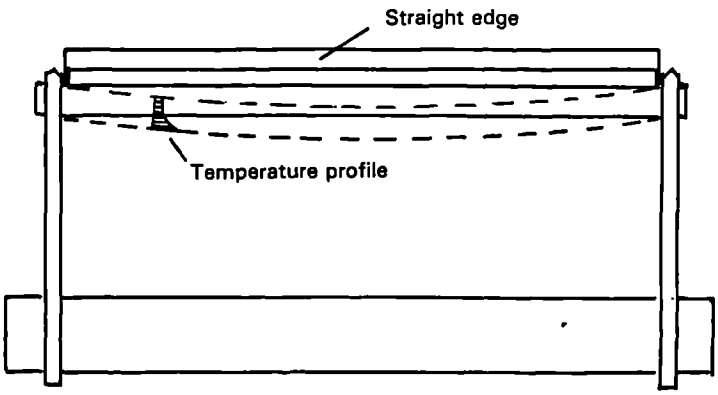

Central displacement measured relative to ends of specimen

(b) Unrestrained thermal bowing experiments

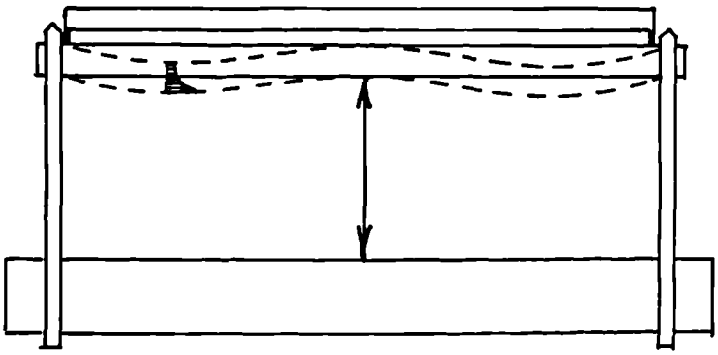

Central displacement kept zero relative to ends of specimen

Load transducer measures variable compressive load, and screw jack adjusted to maintain zero deflection

(c) Restrained thermal bowing experiments

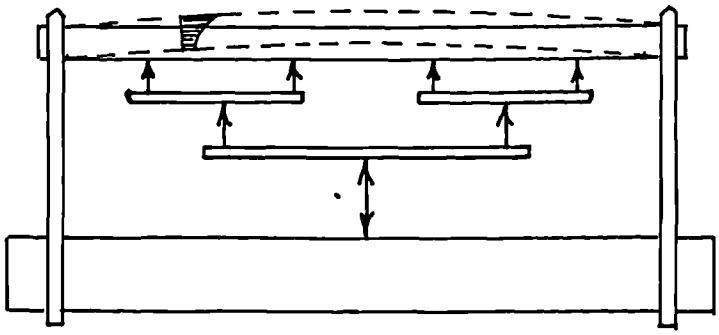

Central displacement measured

Compression jack load kept constant

(d) Constant design load experiments

FIGURE 1.19 Concept of model beam test rig and beam experiments

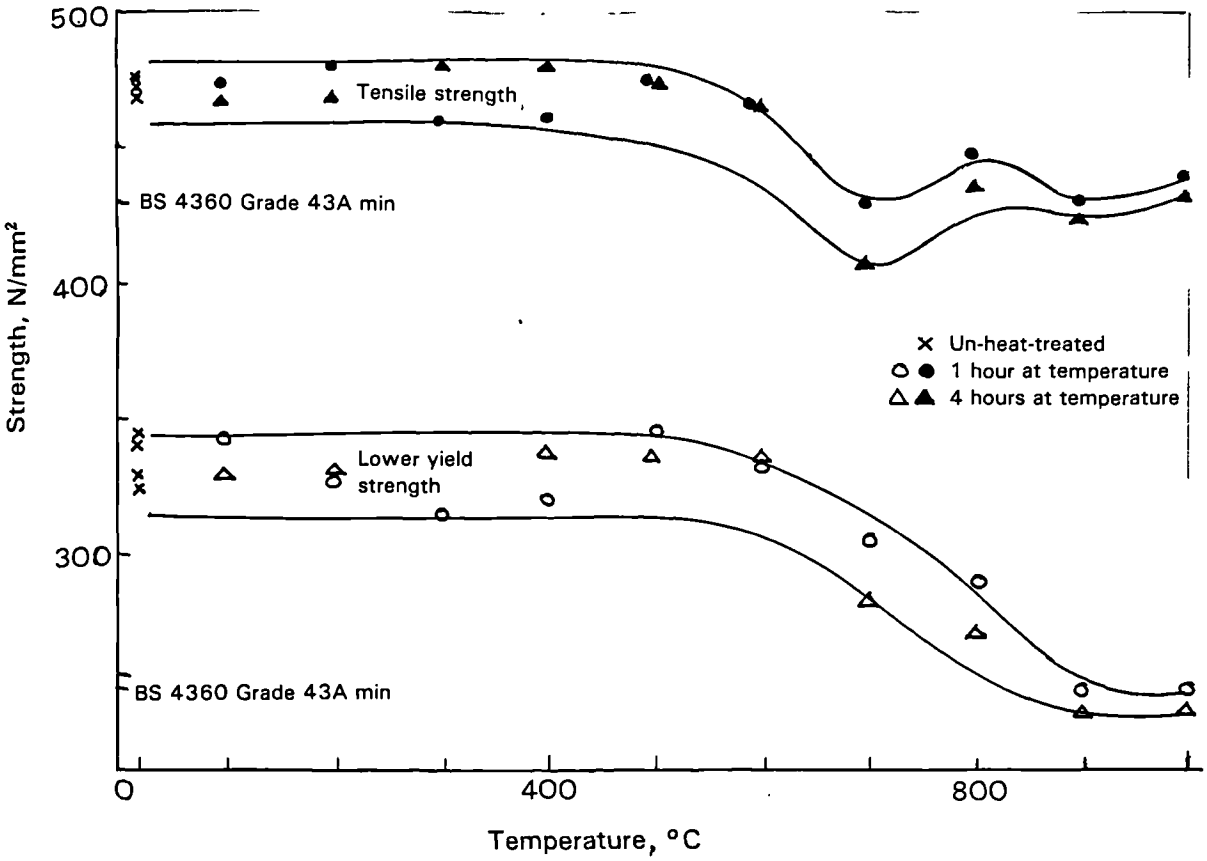

FIGURE 1.20 Room-temperature strengths of BS 4360 : Grade 43A steel after heating to elevated temperatures

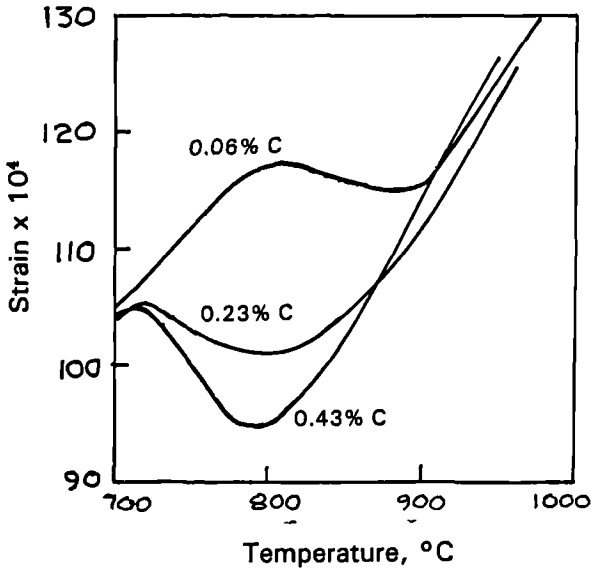

FIGURE 2.1 Thermal expansion-temperature curves for low and medium carbon steels in the phase transformation range

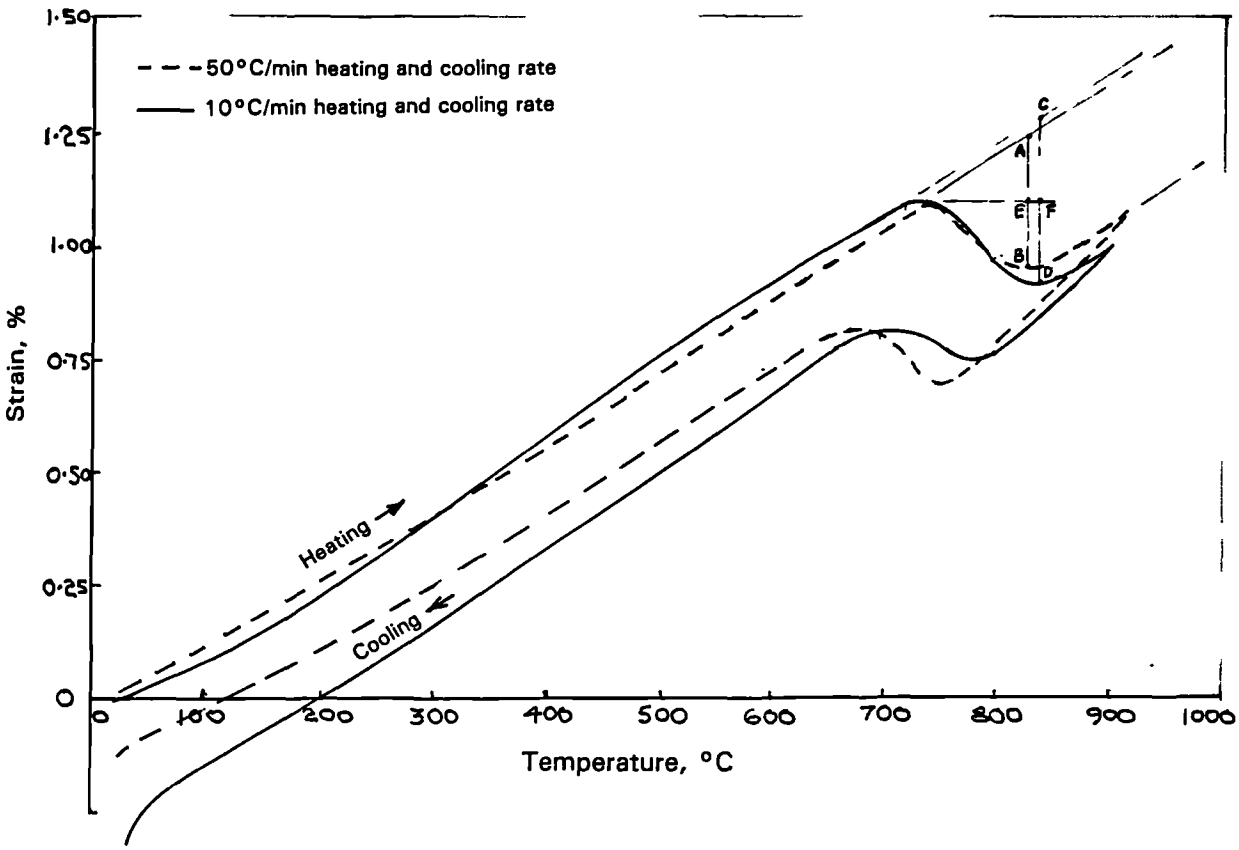

FIGURE 2.2 Dilatometer curves for a mild steel showing effect of different heating and cooling rates

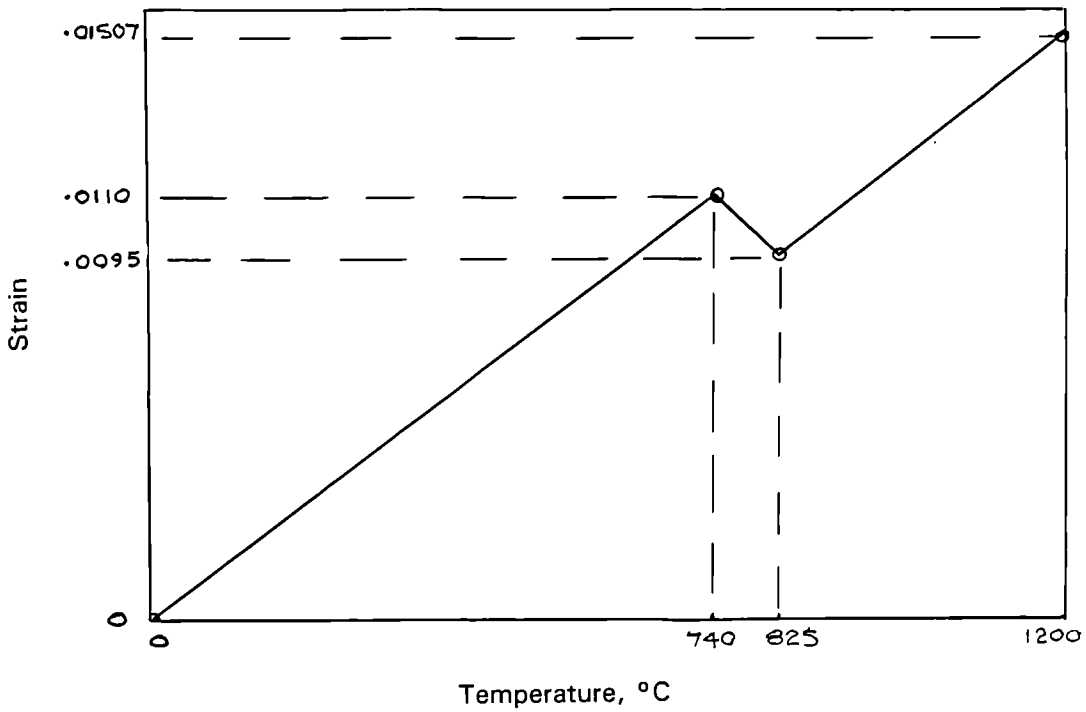

FIGURE 2.3 Tri-linear idealisation of thermal expansion-temperature curve used for finite element analyses

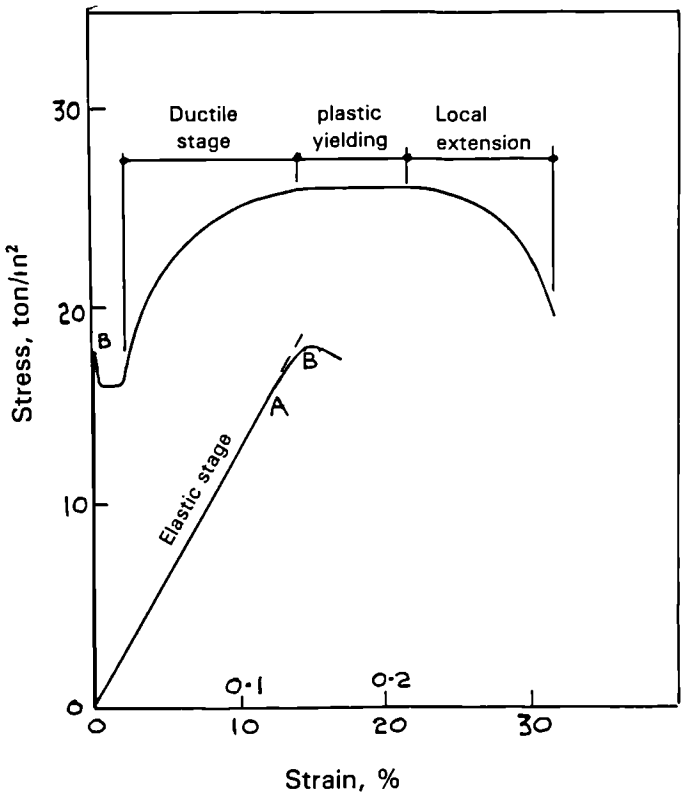

FIGURE 2.4 Stress-strain curve for mild steel taken to failure at 20°C

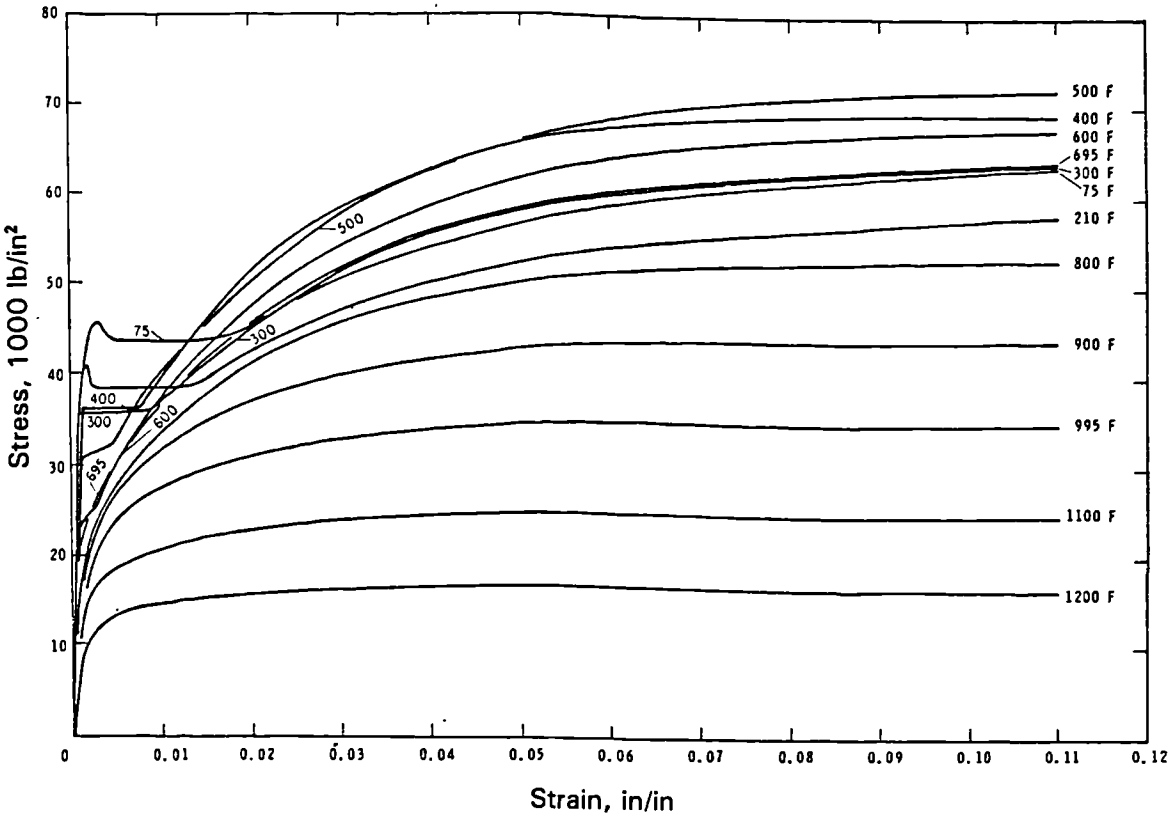

FIGURE 2.5 Stress-strain curves for an ASTME36 structural steel at different elevated temperatures

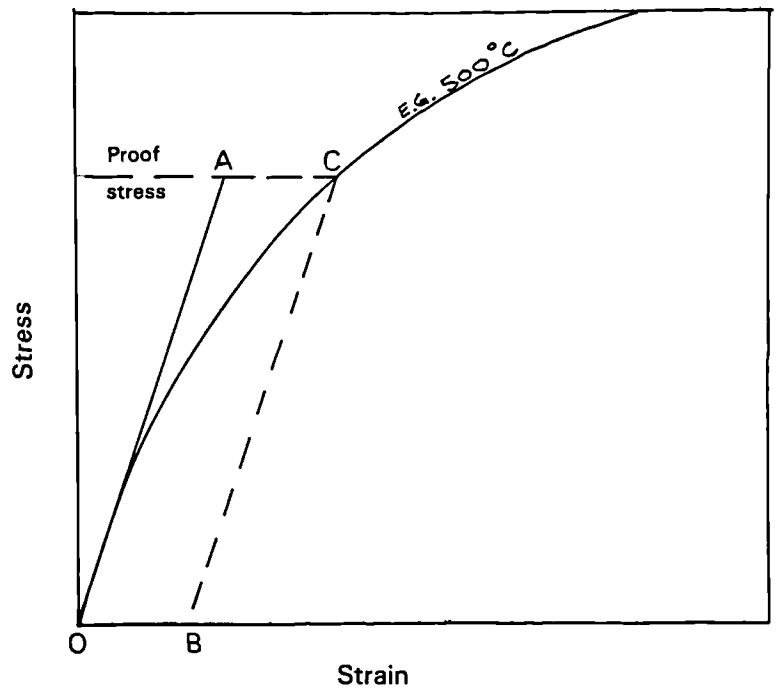

FIGURE 2.6 Concept of proof stress

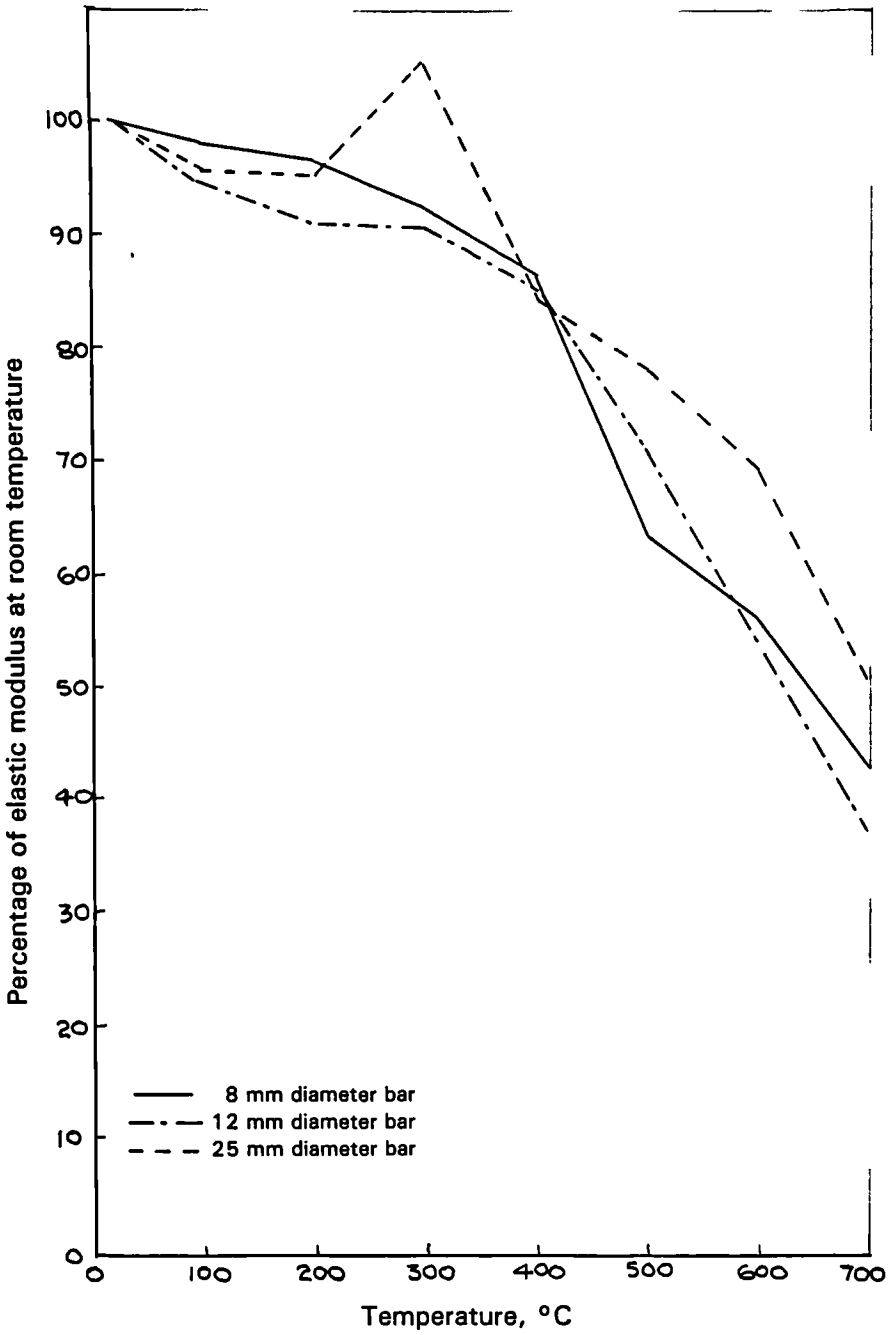

FIGURE 2.7 Elastic modulus-temperature curves for hot rolled mild steel reinforcing bars, Crook data

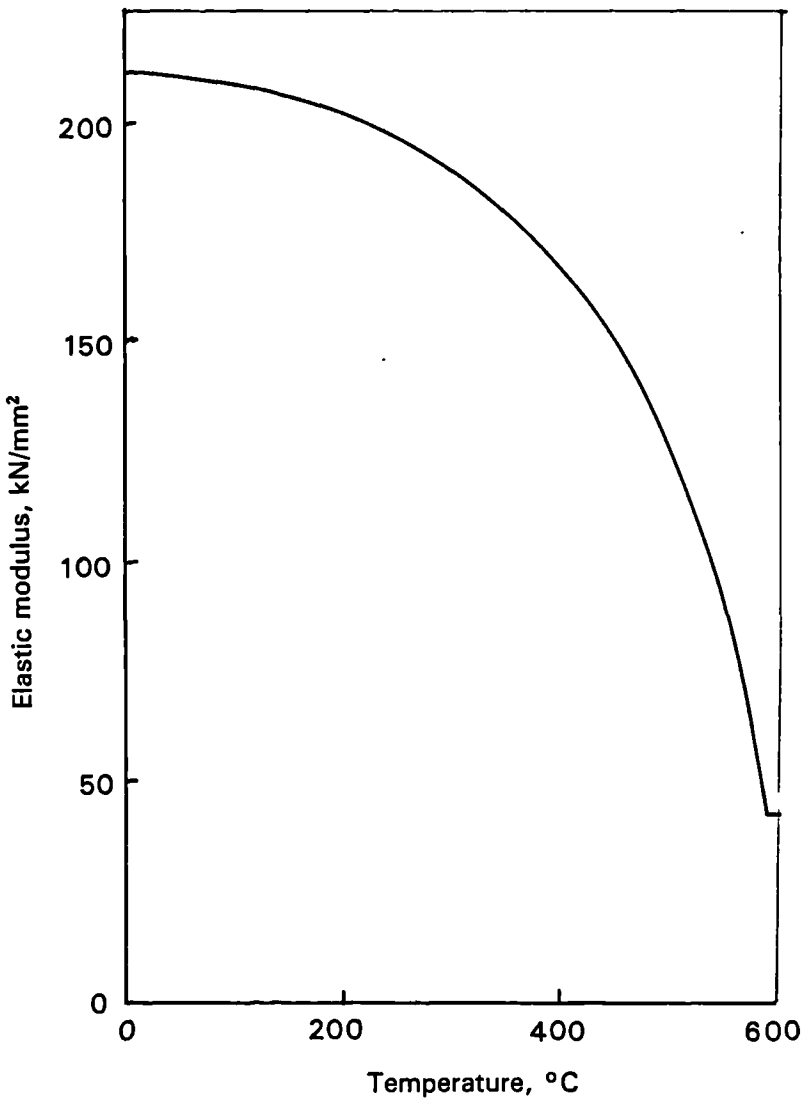

FIGURE 2.8 Elastic modulus-temperature curve for structural steel ECCS Recommendation

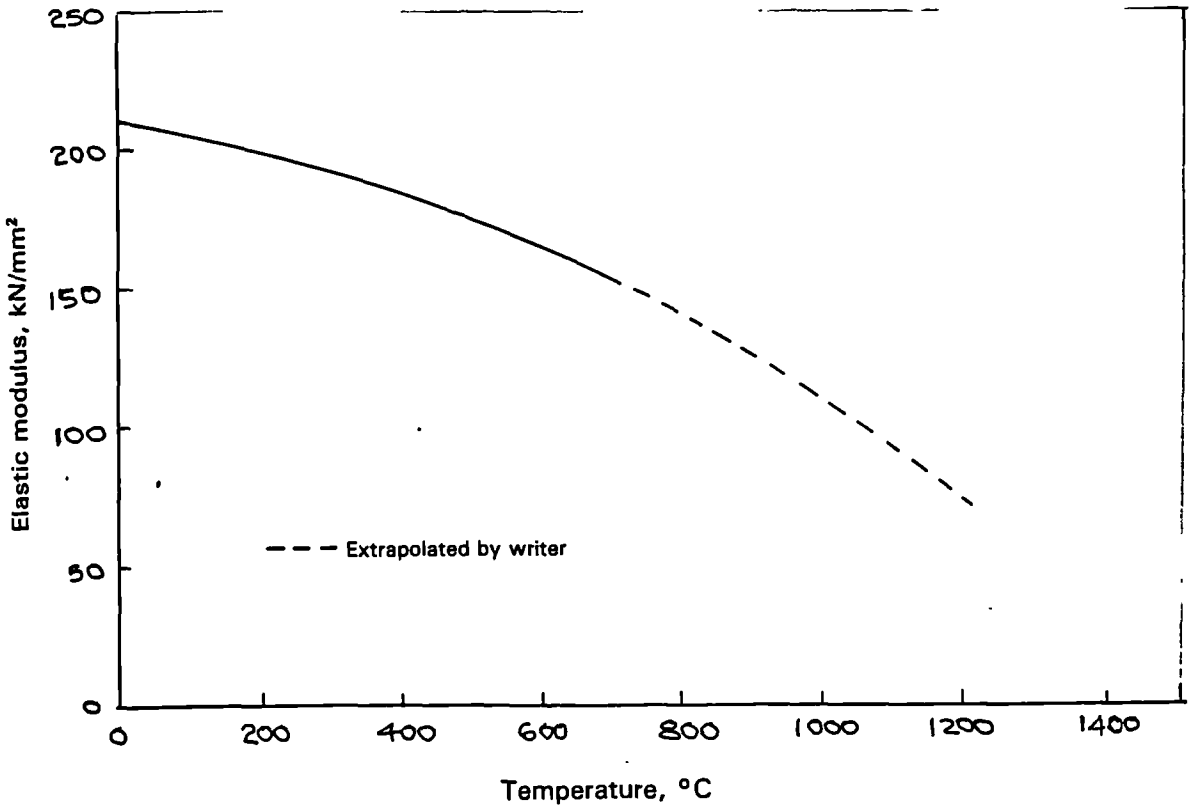

FIGURE 2.9 Elastic modulus-temperature curve for mild steel extrapolated BSC/Euronorm data

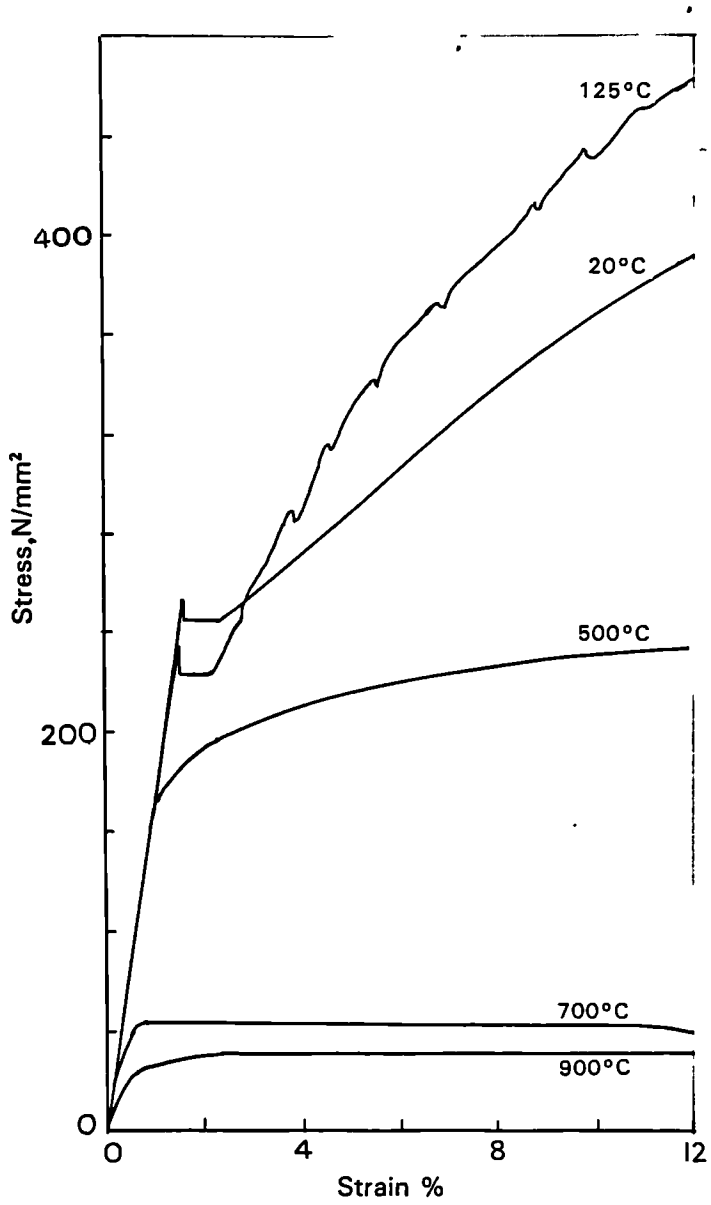

FIGURE 2.10 Elevated temperature stress-strain curves for BS 4360 : Grade 43A steel, recent BSC isothermal data

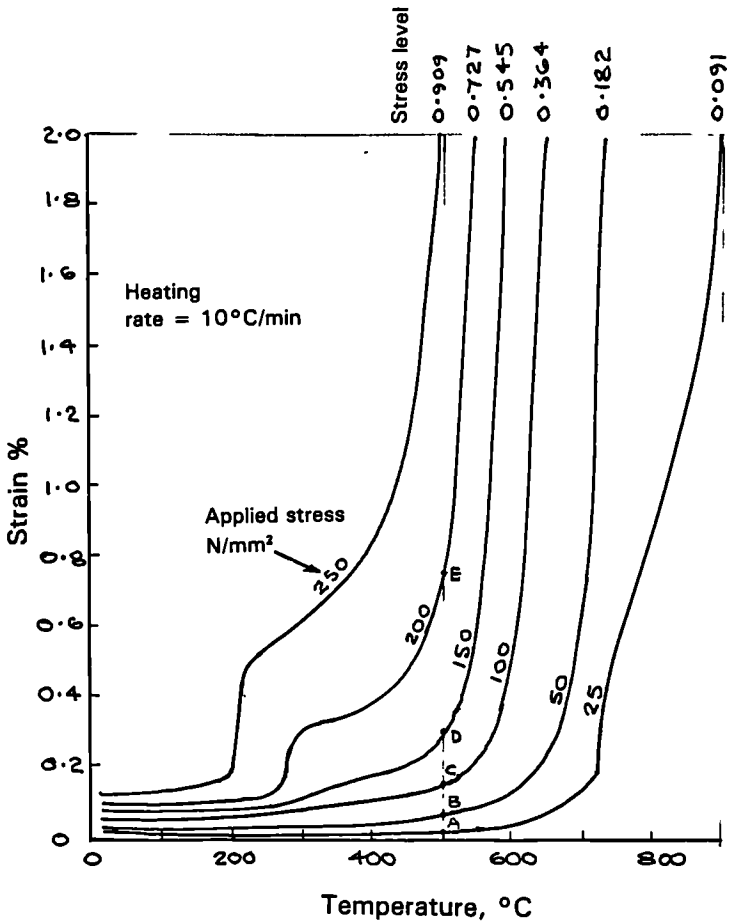

FIGURE 2.11 Elevated temperature anisothermal strain-temperature curves for BS 4360 : Grade 43A steel, recent BSC data

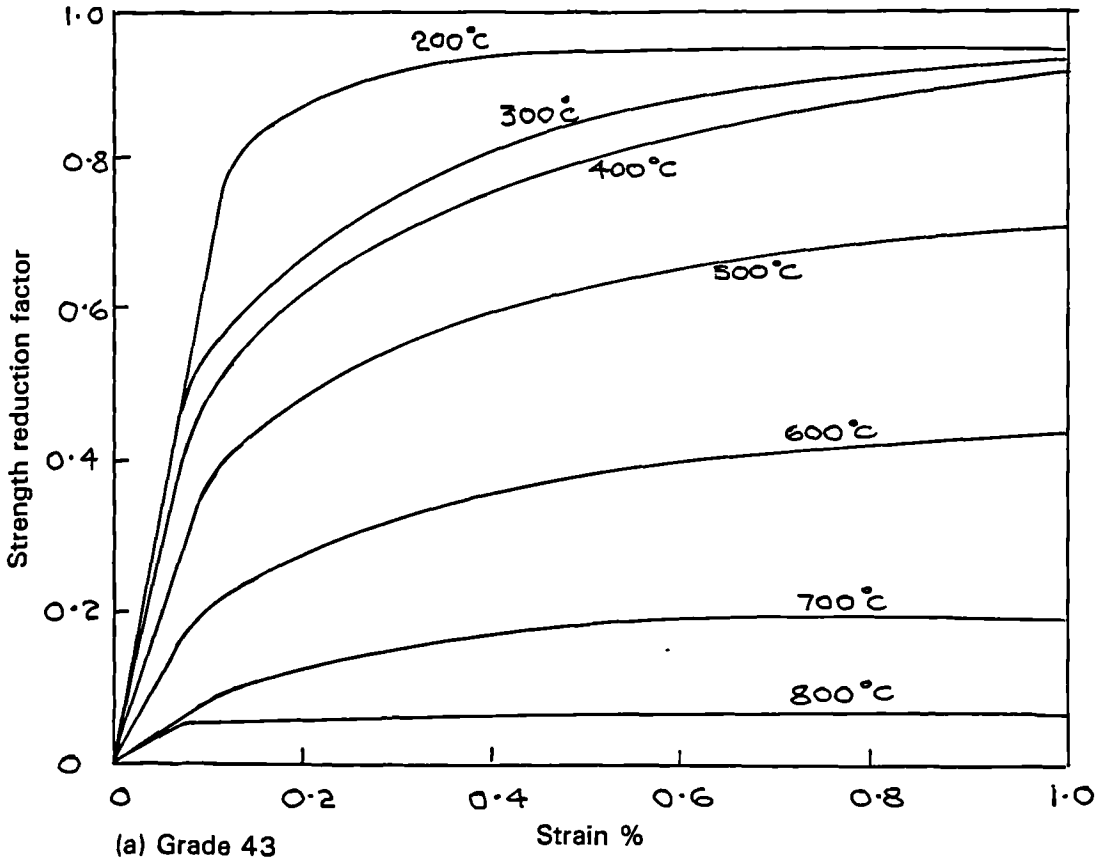

(a) Grade 43

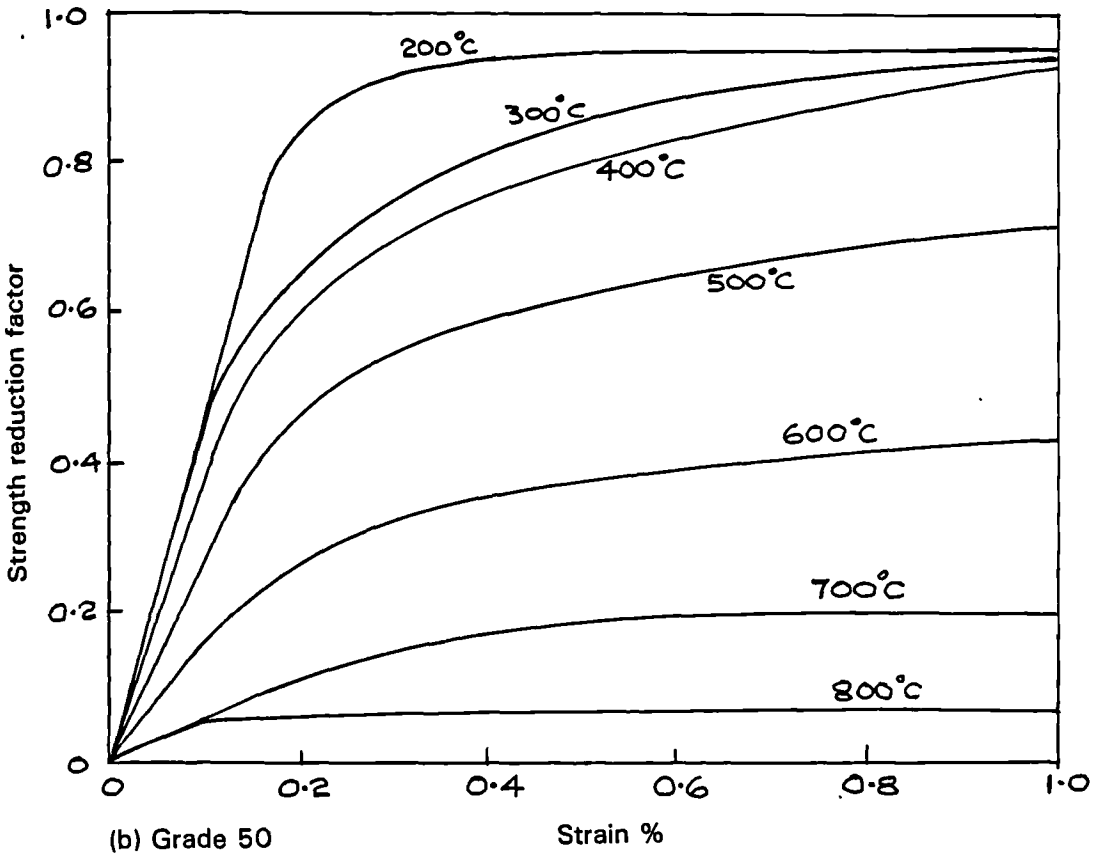

(b) Grade 50

FIGURE 2.12 Elevated temperature anisothermal strength reduction factor-strain curves for BS 4360 : Grade 43 and 50 steels, draft BS 5950 : Part 8 data

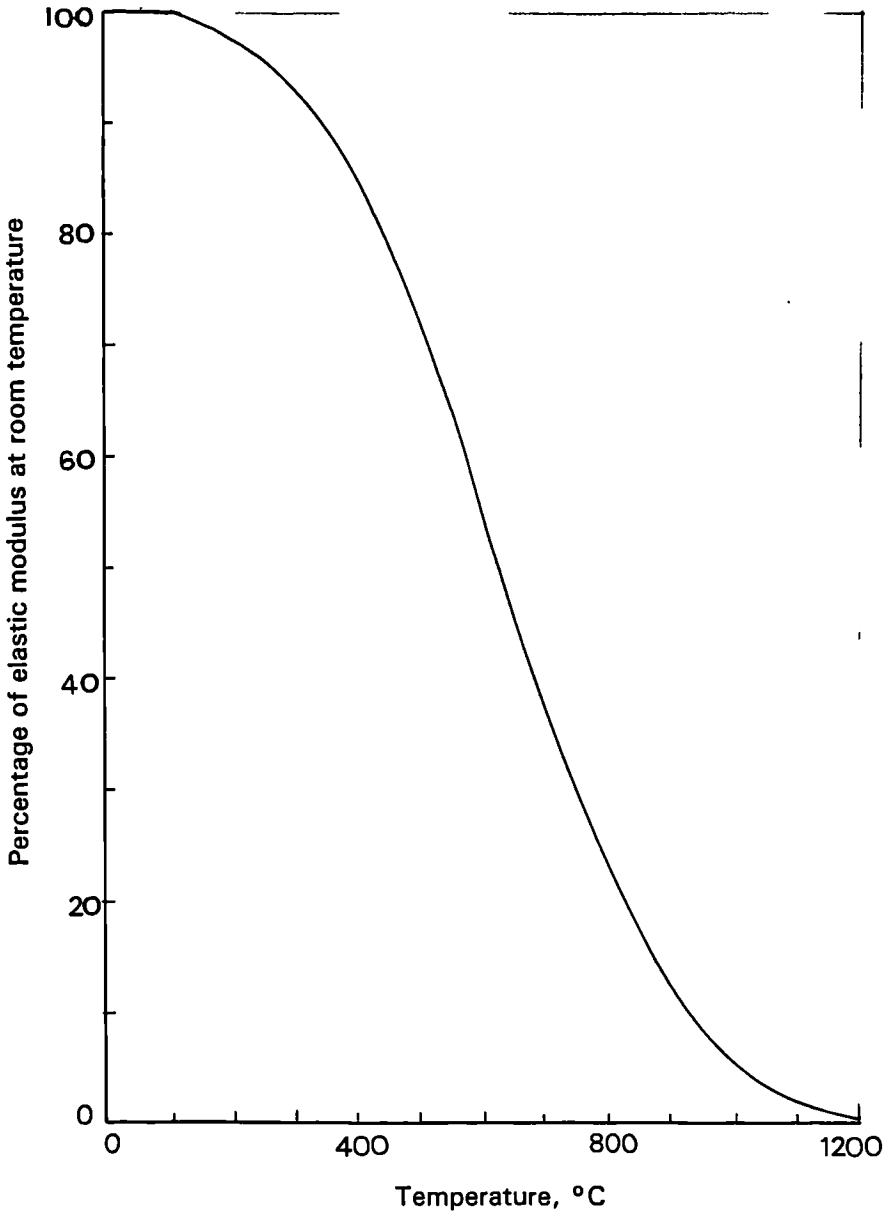

FIGURE 2.13 Elastic modulus-temperature curve for a structural steel, Arbed data

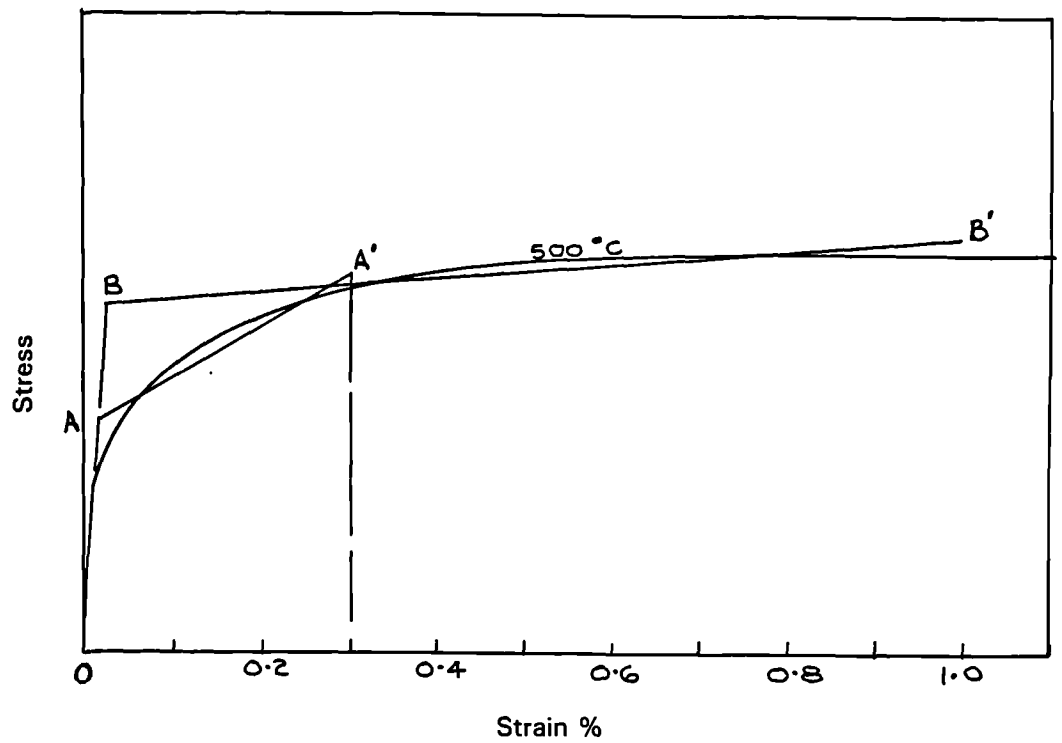

FIGURE 2.14 Possible alternative bi-linear idealisations of a stress-strain curve used for computing purposes

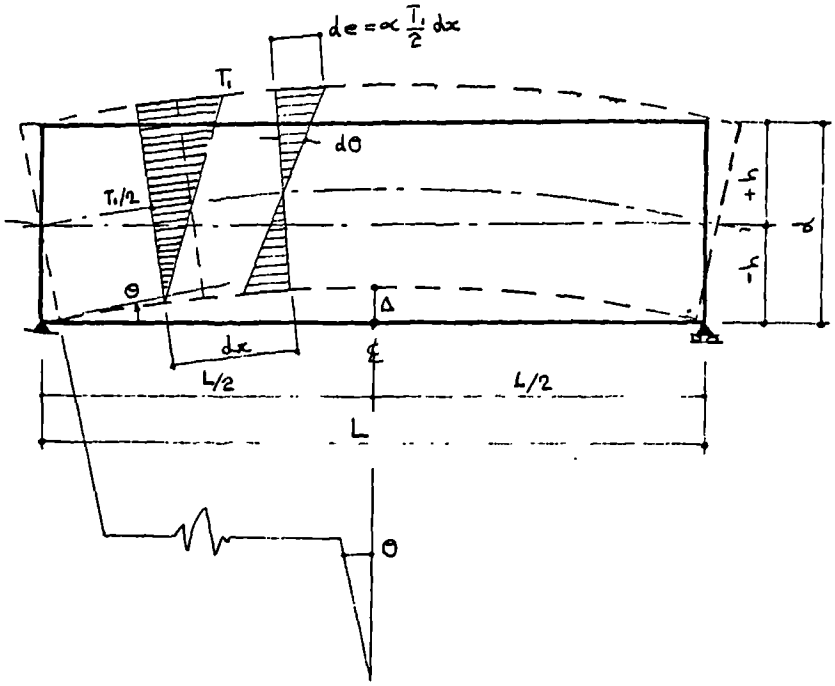

FIGURE 3.1 Displacements of a non-loaded, simply supported beam having a linear temperature profile across its depth which does not vary with length

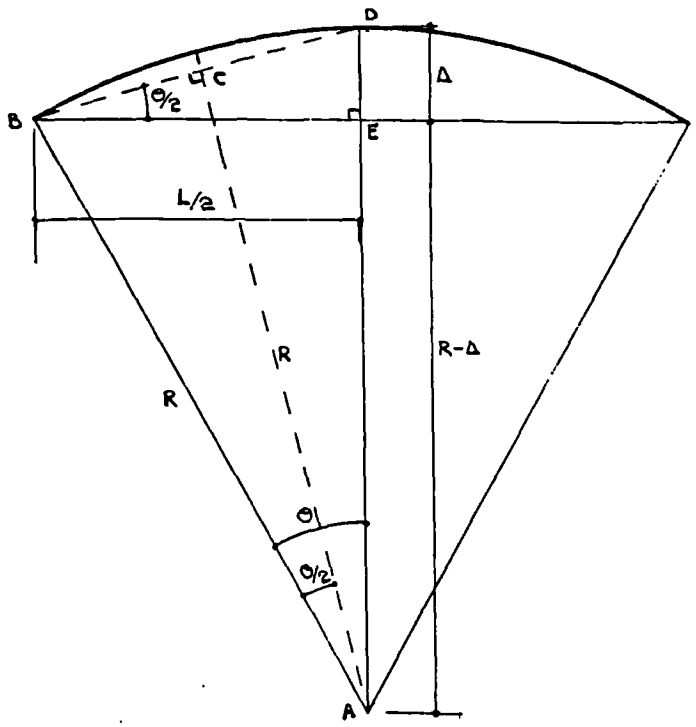

FIGURE 3.2 Diagram relating θ to R and Δ

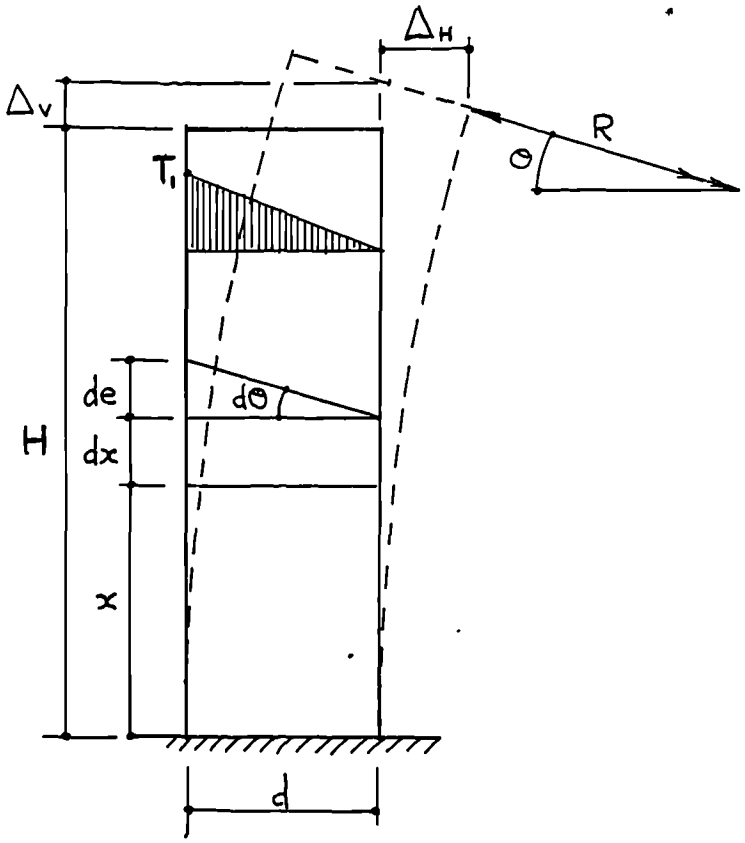

FIGURE 3.3 Displacements of a non-loaded vertical cantilever having a linear temperature profile across its section which does not vary with height

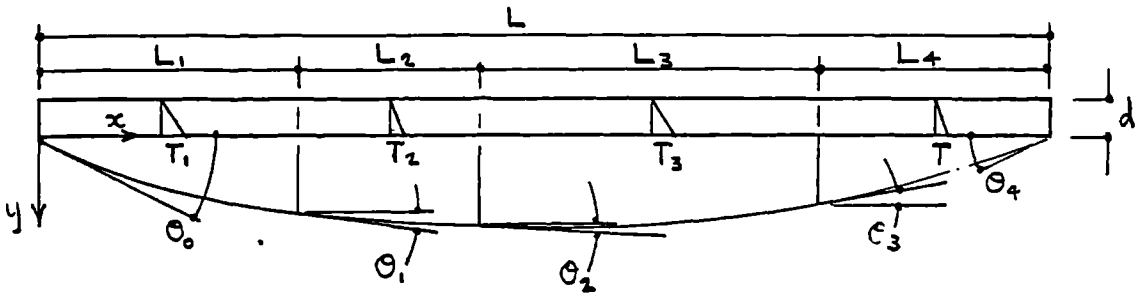

FIGURE 3.4 Displacements of a non-loaded, simply supported beam having linear temperature profiles across depth of section which vary with length

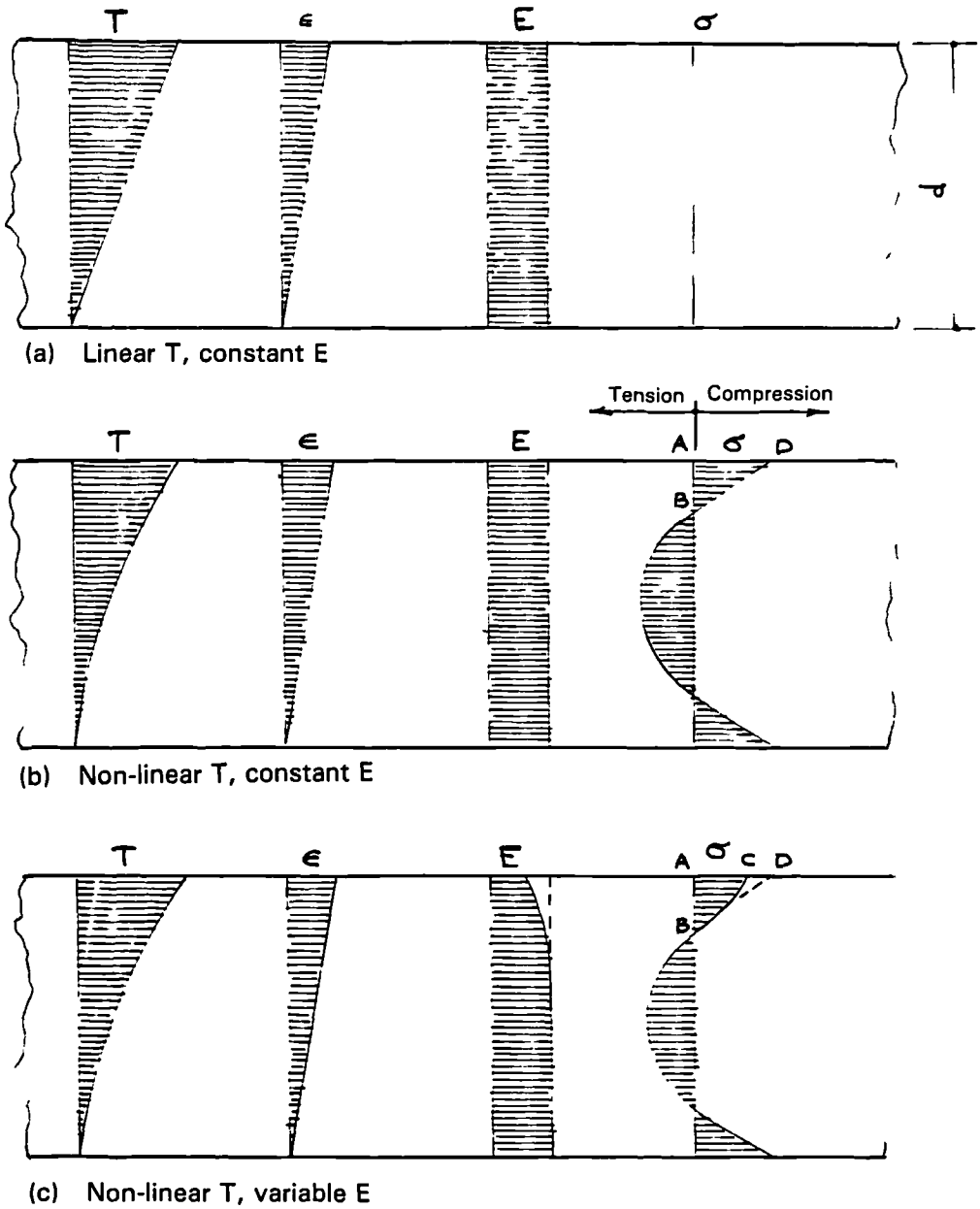

FIGURE 3.5 Dependence of stress on elastic modulus and temperature profile for a member free to bow

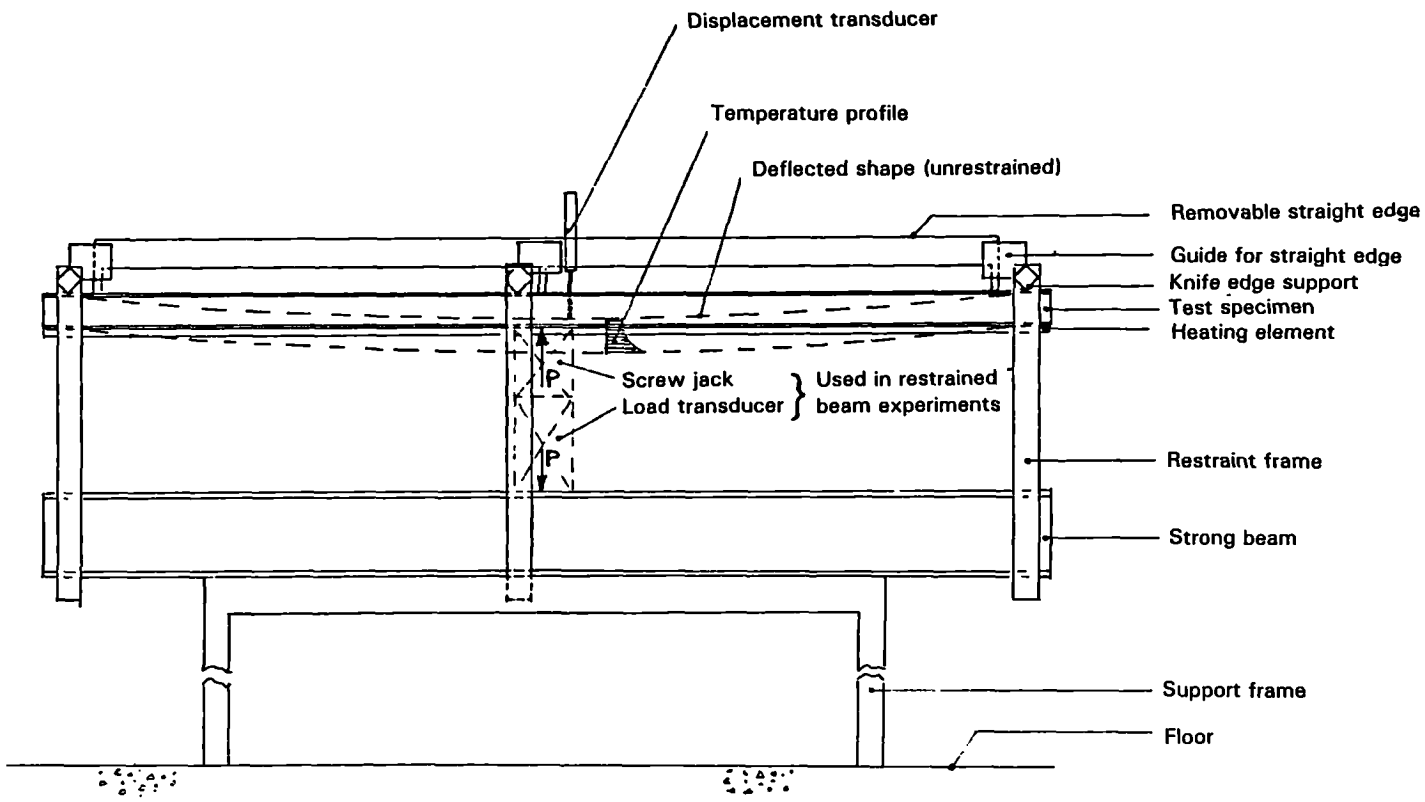

FIGURE 4.1 Apparatus used to measure unrestrained thermal bowing of model beams heated along one flange

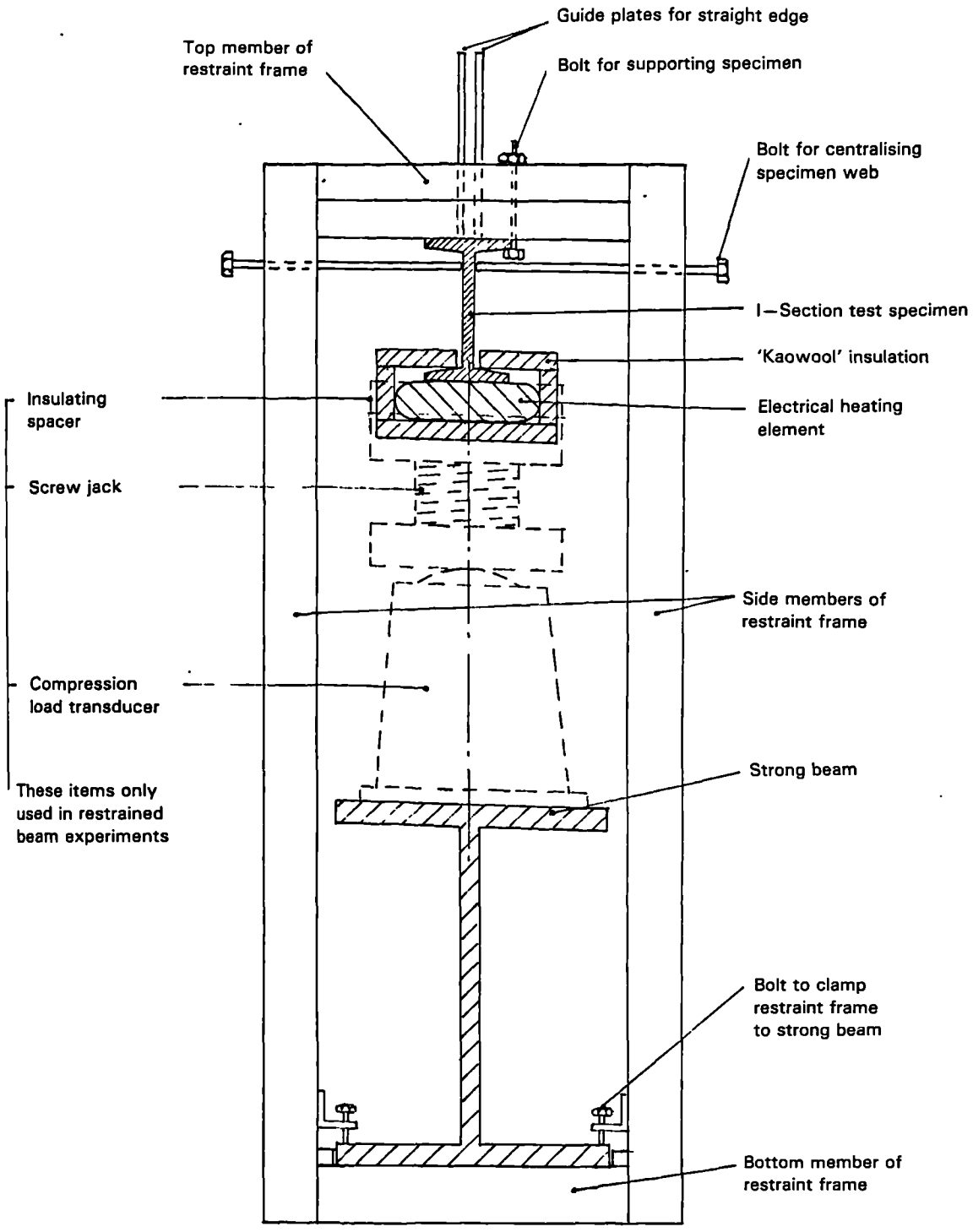

FIGURE 4.2 Section through beam test apparatus

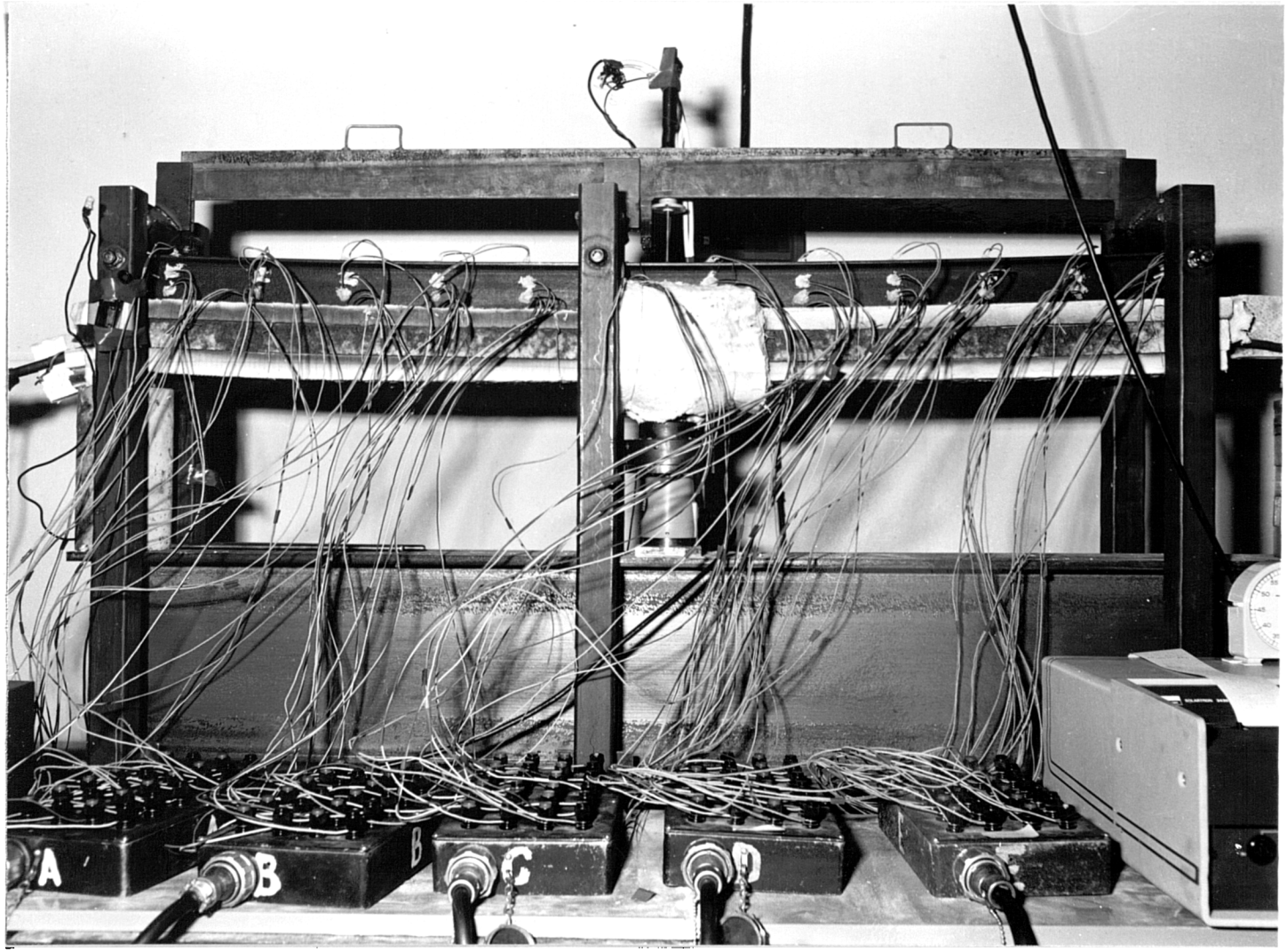

FIGURE 4.3 General view of beam test apparatus with straight-edge in position during a test

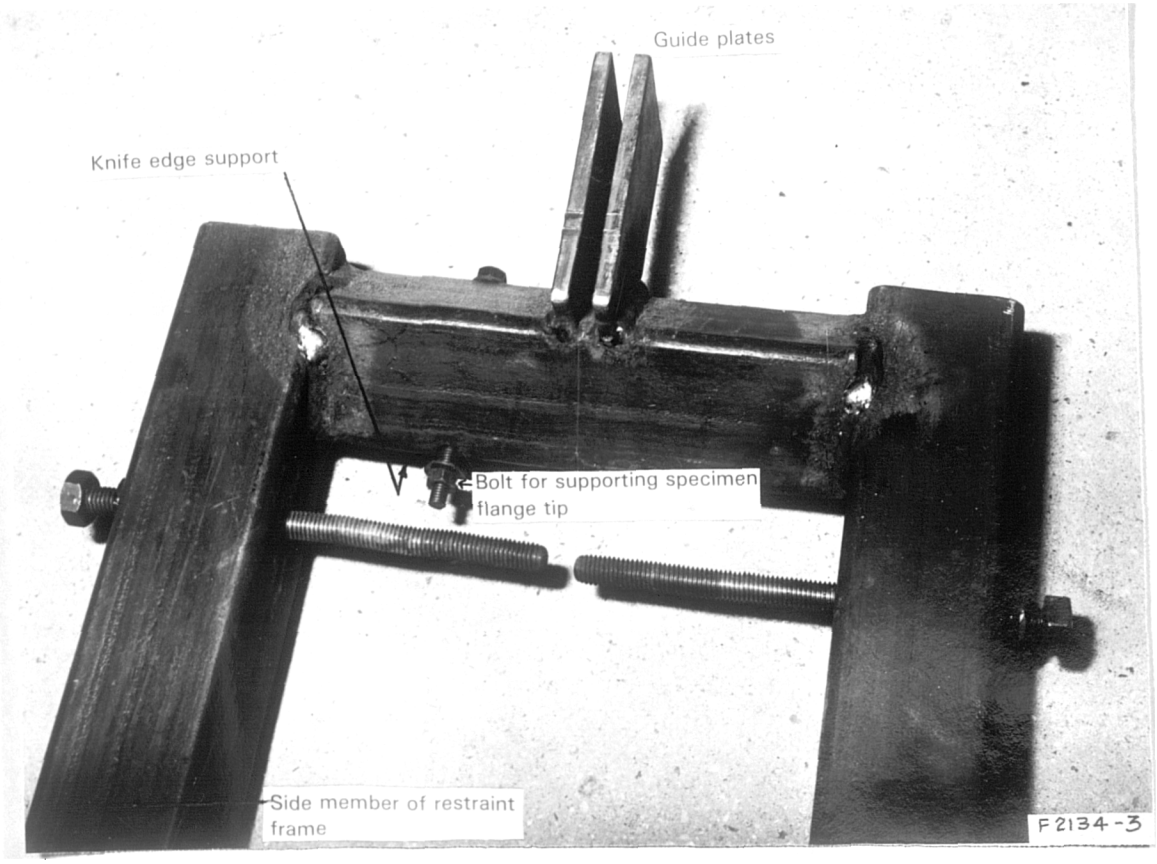

FIGURE 4.4 Top of beam test restraint frame

FIGURE 4.5 Electrical heating element

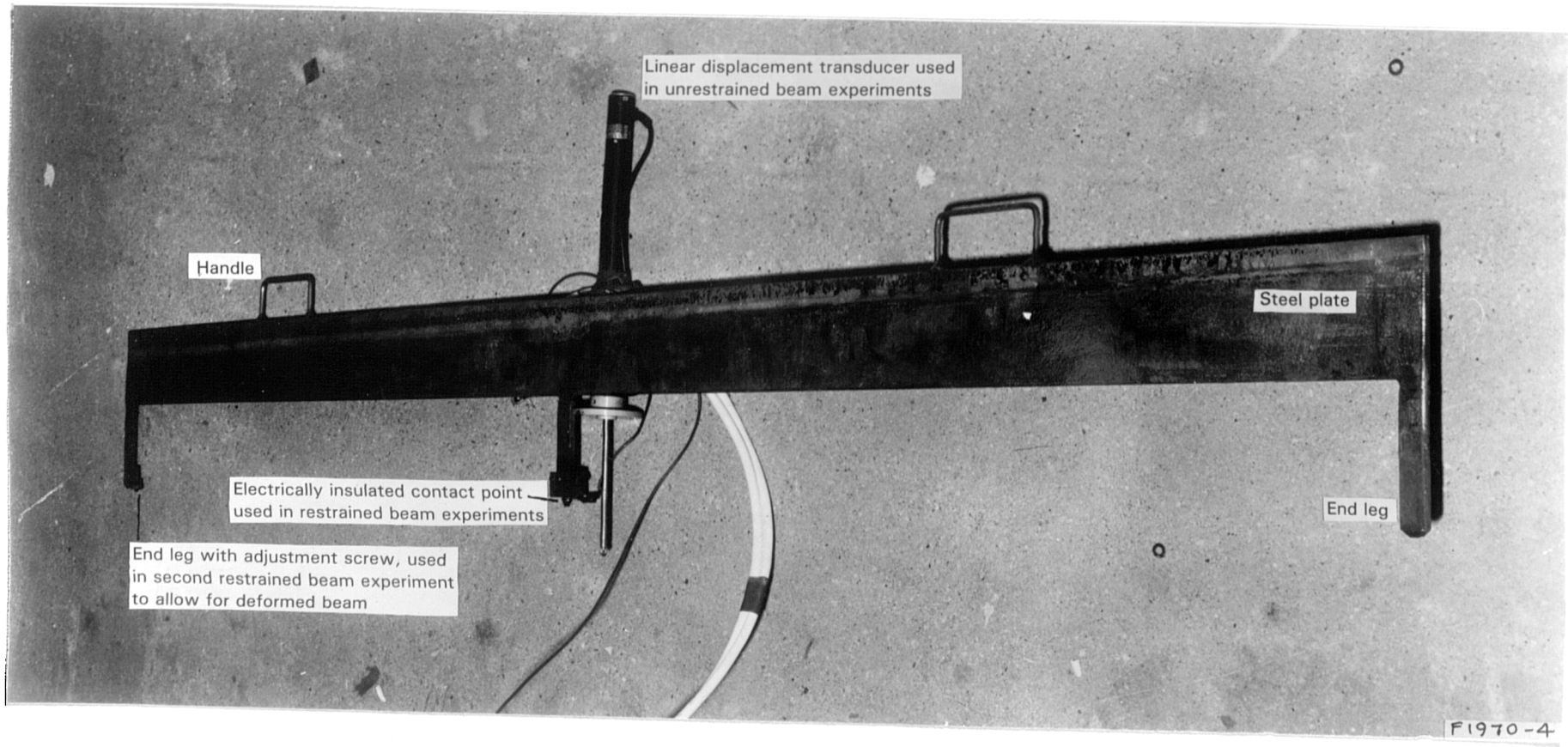

FIGURE 4.6 View of straight-edge of beam test apparatus

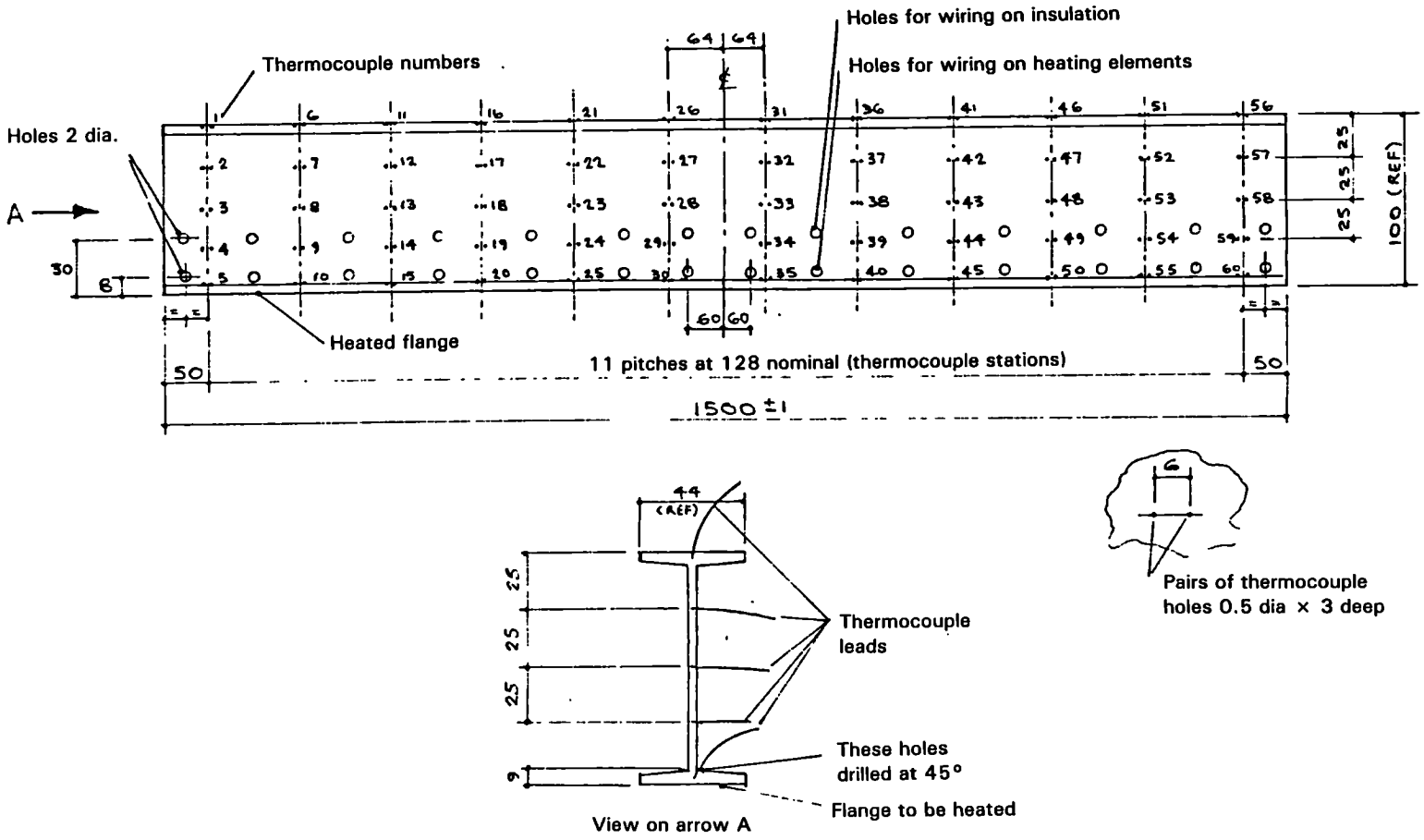

FIGURE 4.7 Details of specimen beam and thermocouples

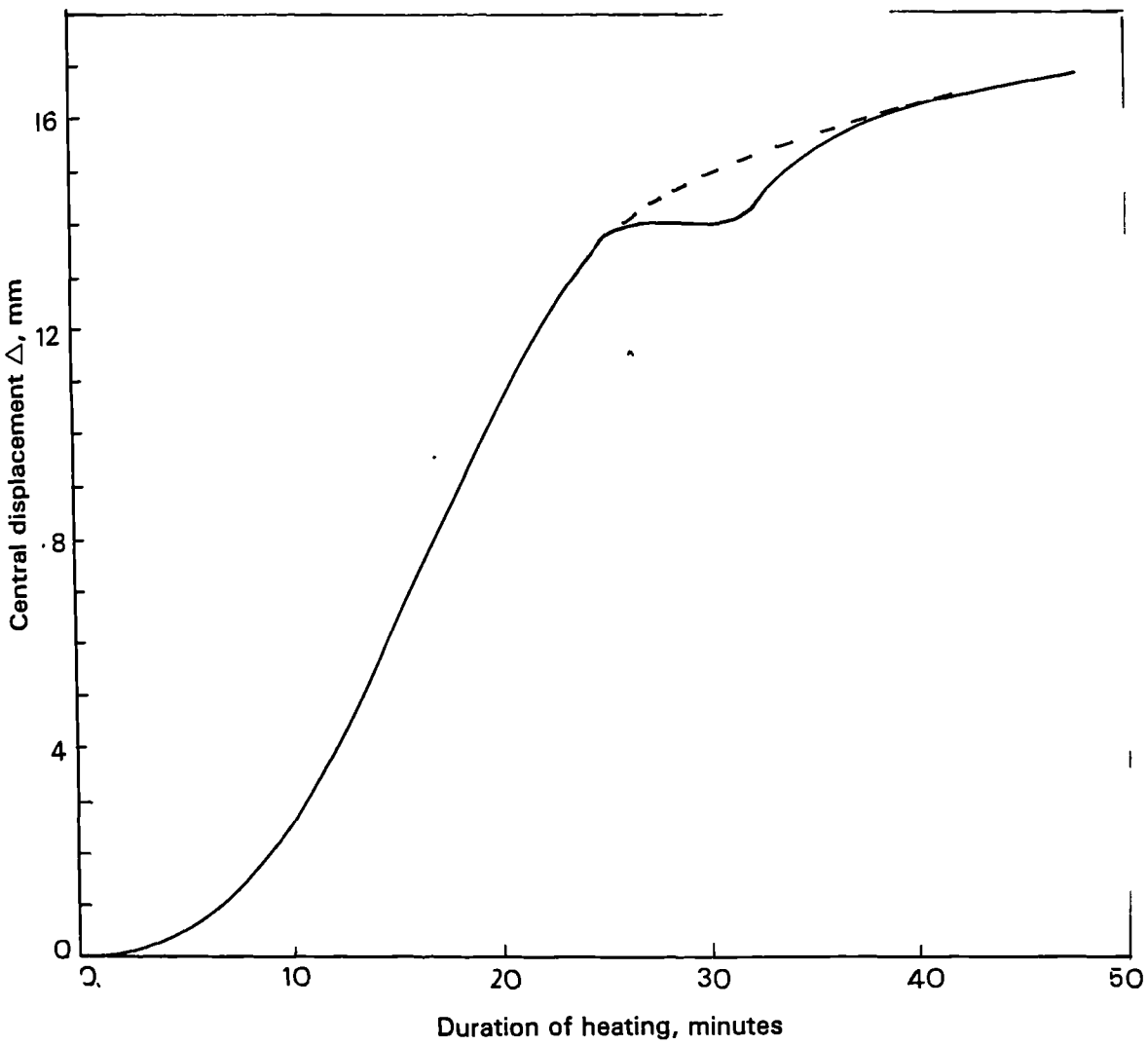

FIGURE 4.8 Central displacement of unrestrained test beam heated along whole flange

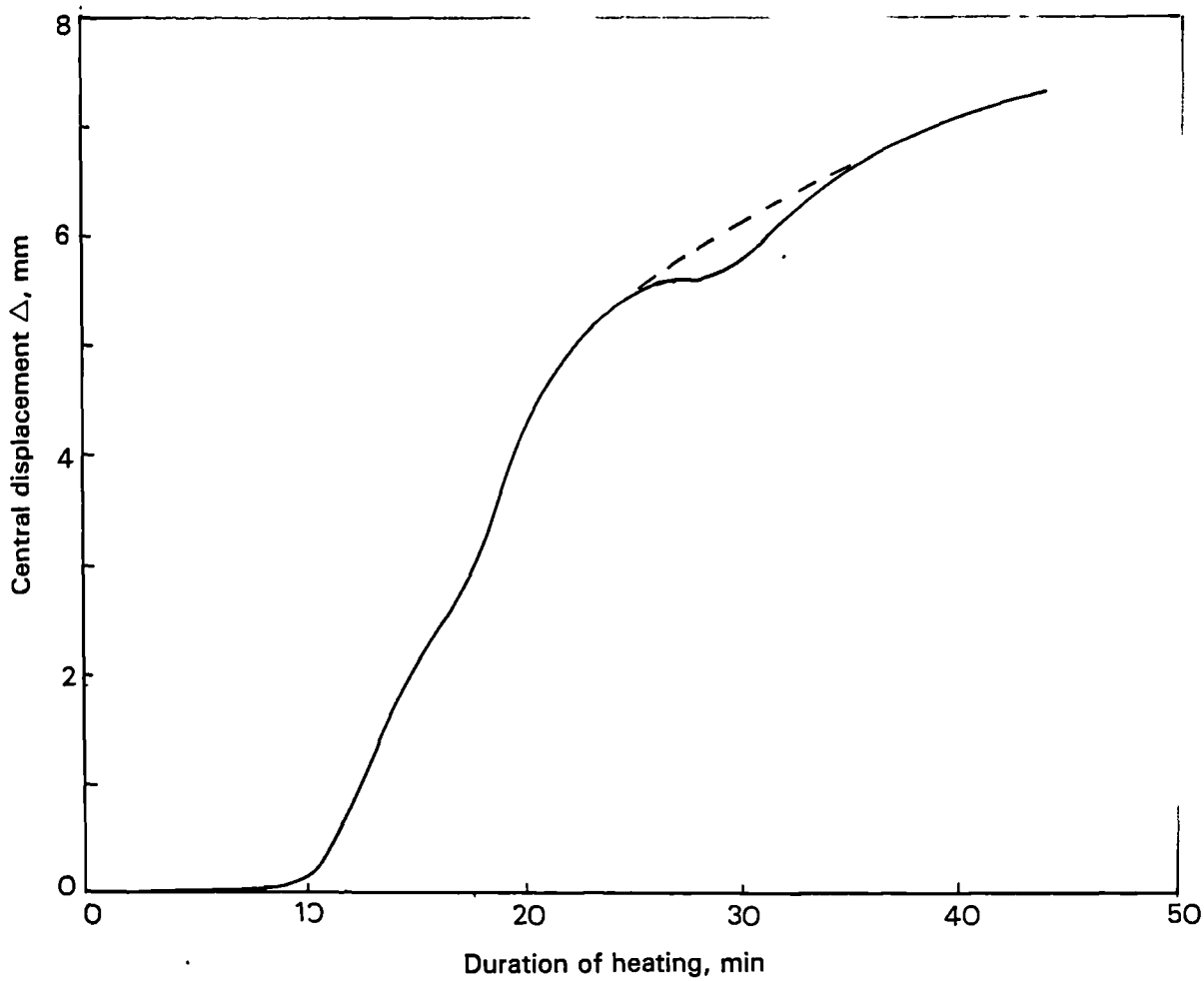

FIGURE 4.9 Central displacement of unrestrained test beam heated along half of flange

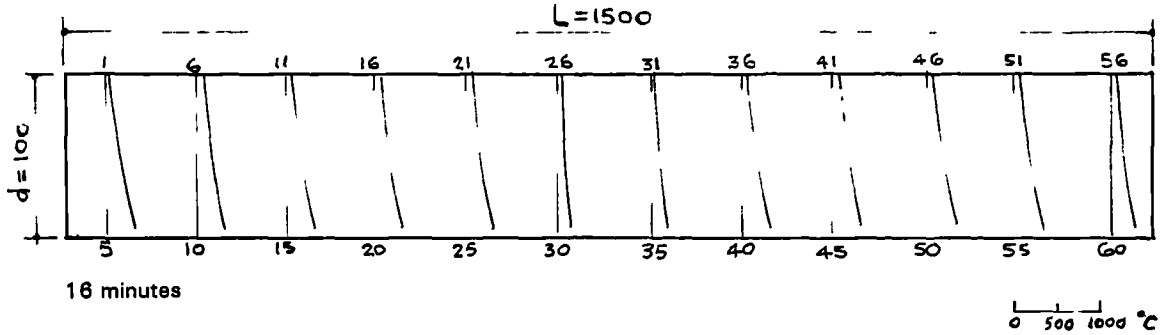

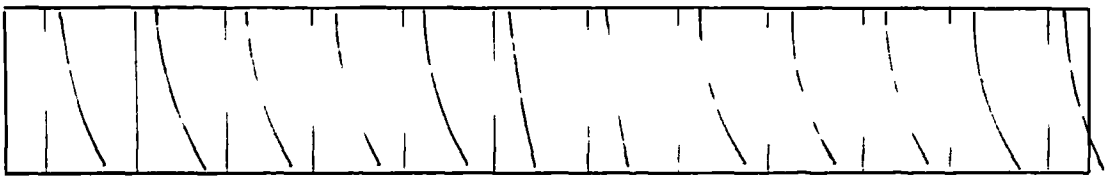

32 minutes

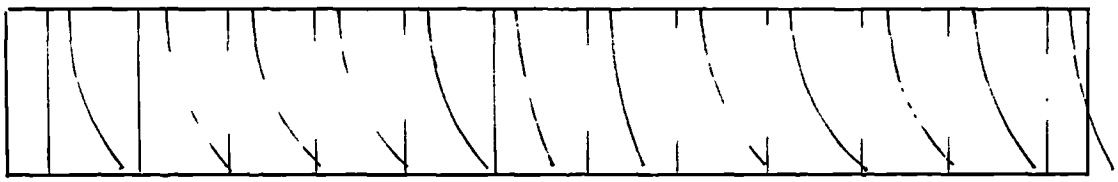

48 minutes

FIGURE 4.10 Temperature profiles in unrestrained test beam heated along whole flange

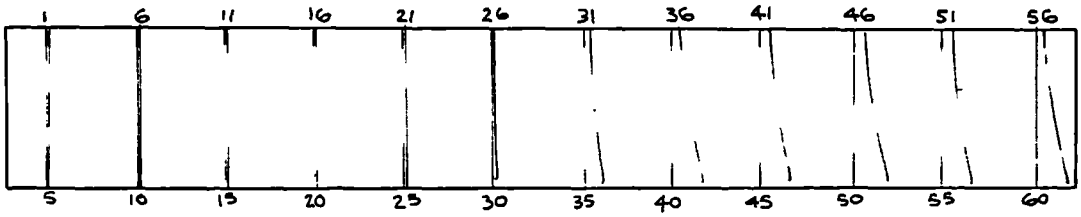

16 minutes

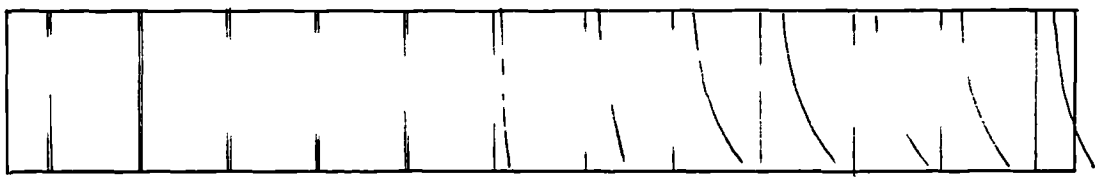

32 minutes

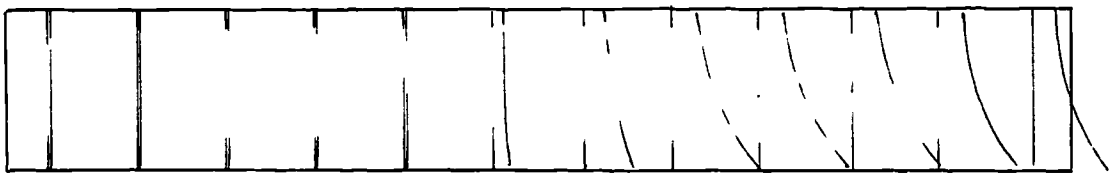

48 minutes

FIGURE 4.11 Temperature profiles in unrestrained test beam heated along half of flange

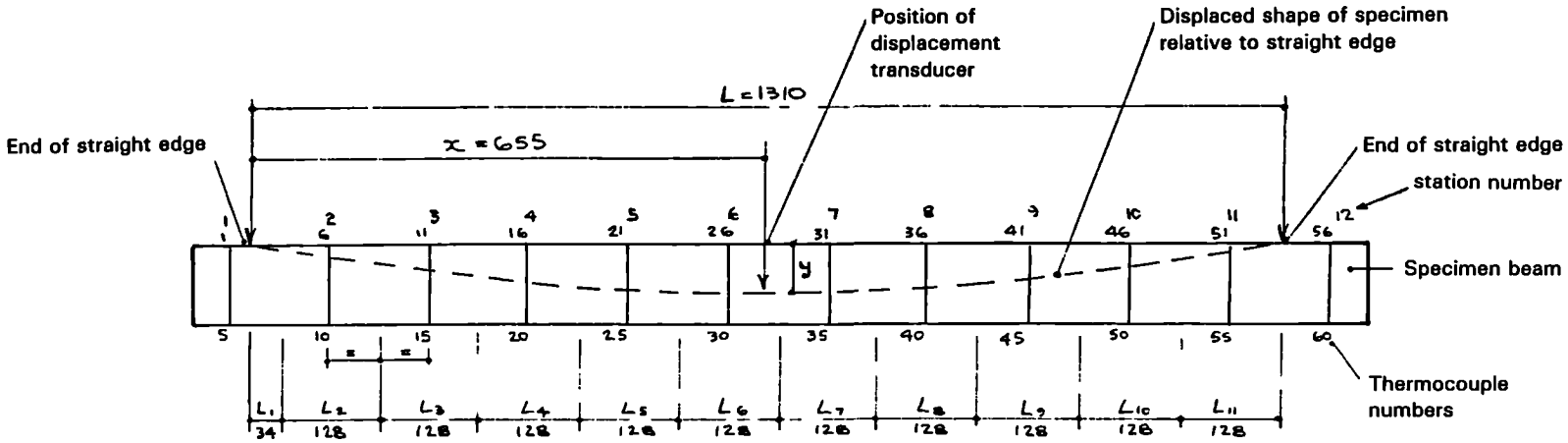

FIGURE 4.12 Dimensions used in computation of displacement of unrestrained test beam heated along half of flange

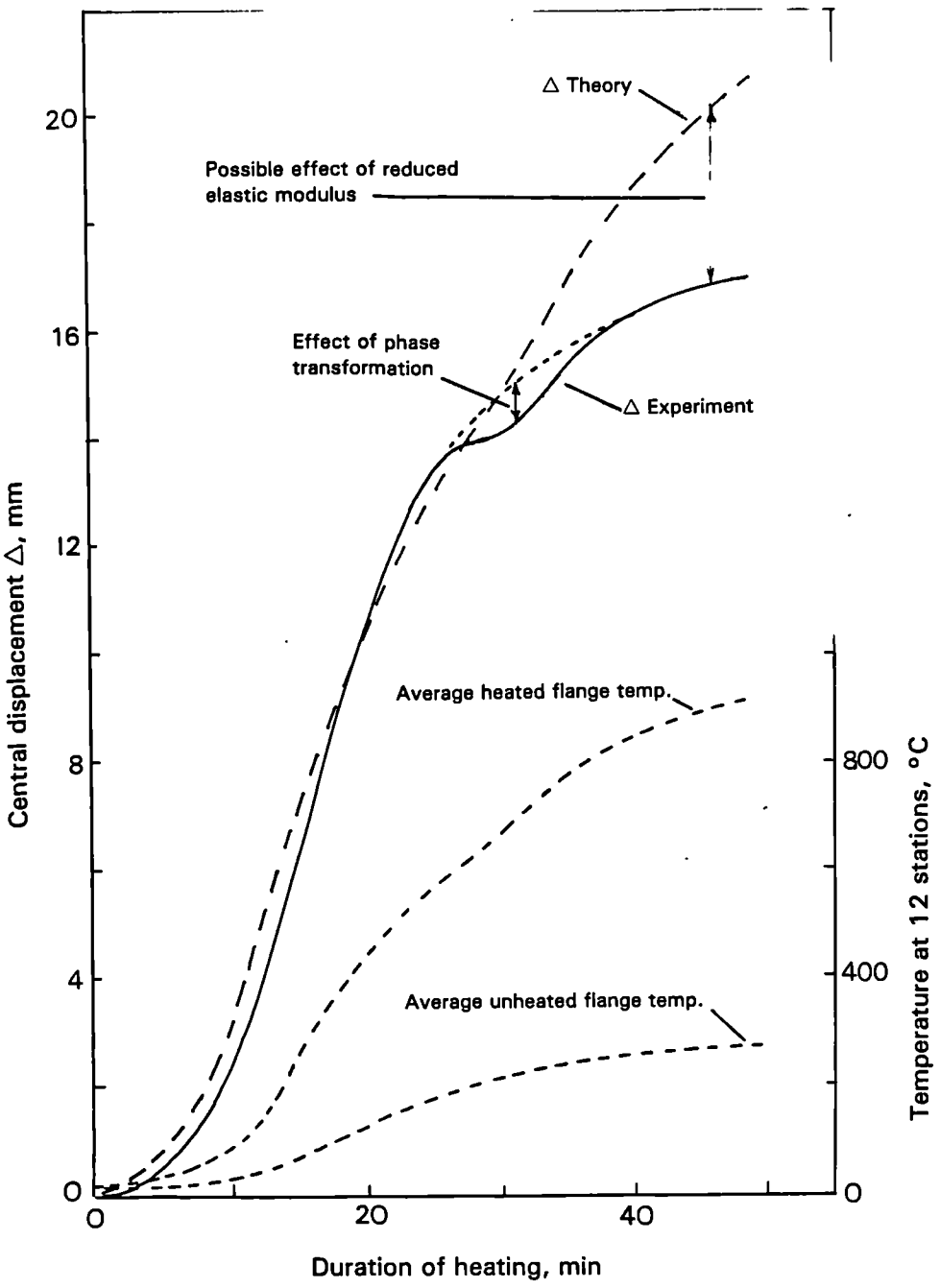

FIGURE 4.13 Comparison of computed and experimental central displacements of unrestrained test beam heated along whole flange

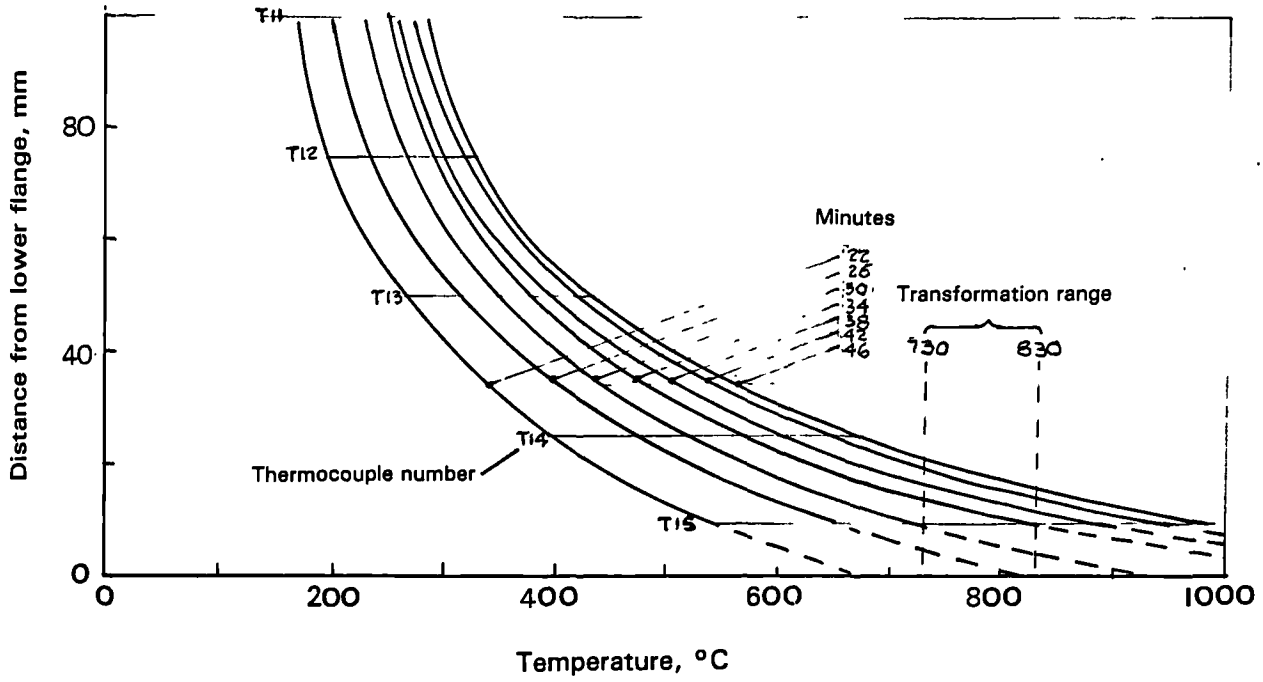

FIGURE 4.14 Temperature profiles at one station for different times

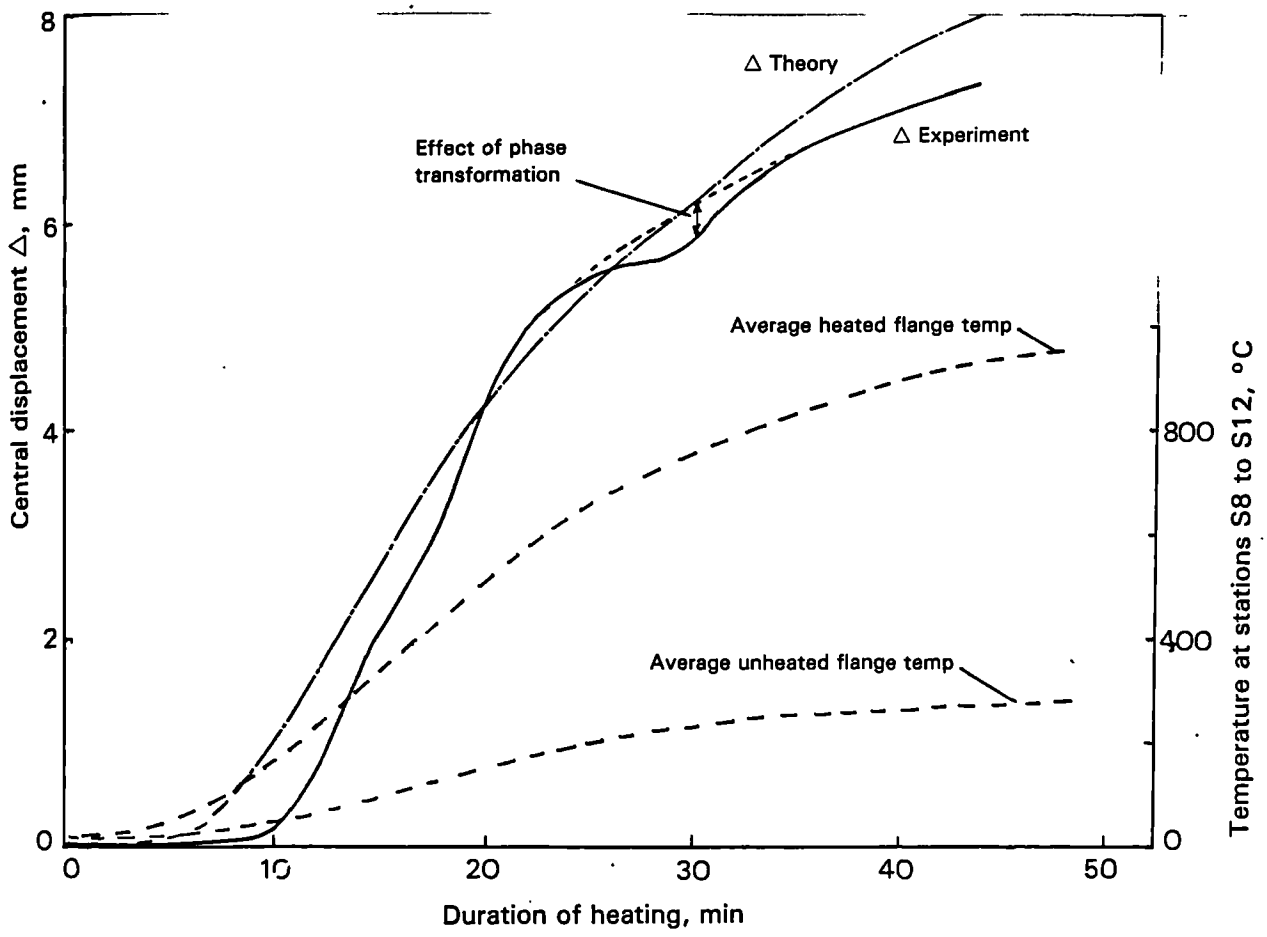

FIGURE 4.15 Comparison of computed and experimental central displacements of unrestrained test beam heated along half of flange

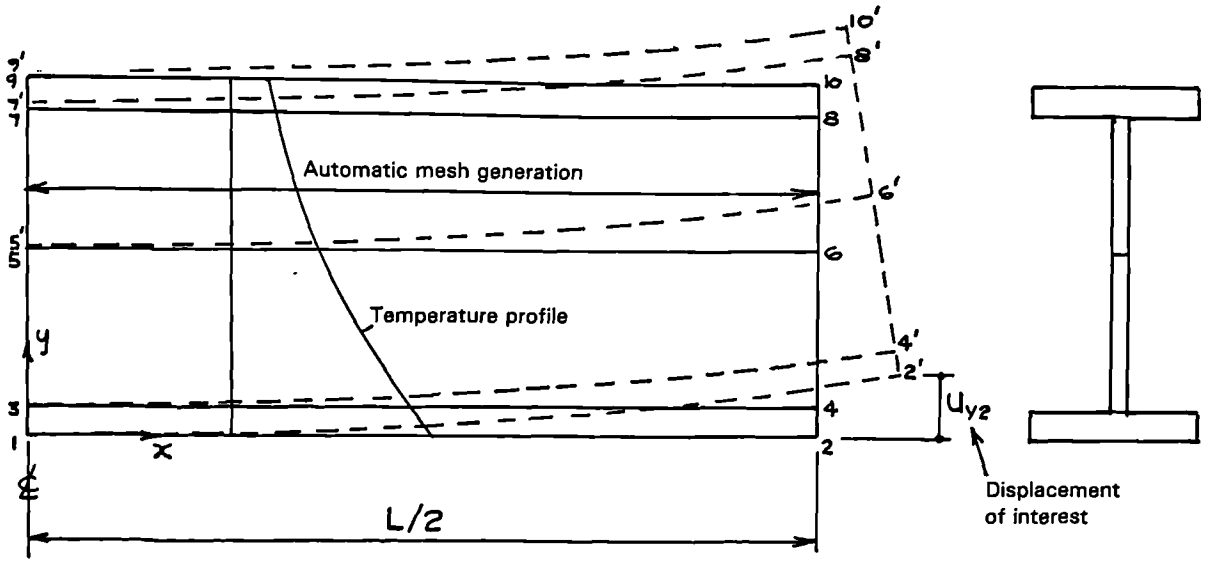

FIGURE 4.16 Finite element mesh model of unrestrained test beam, whole flange heated

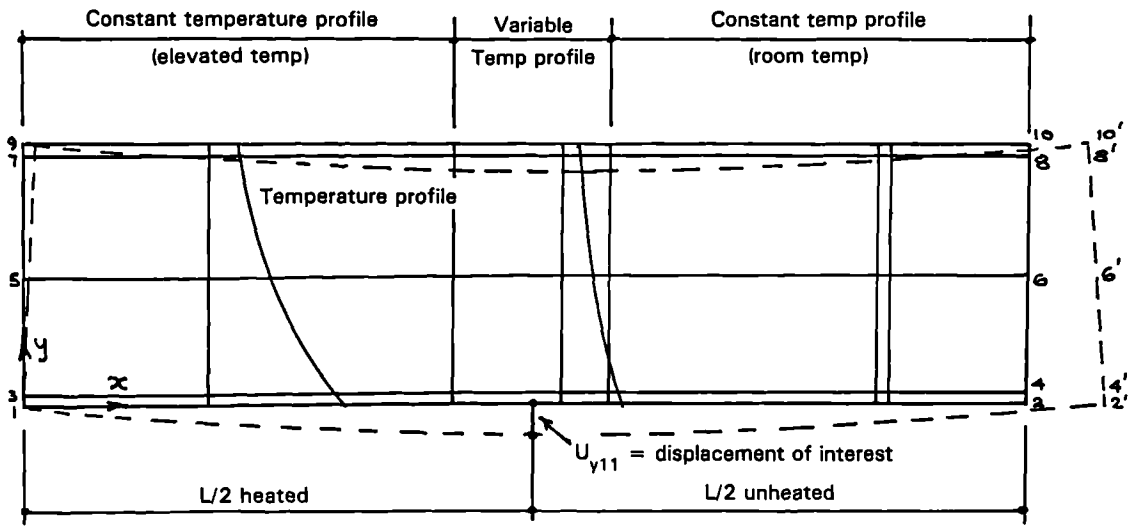

FIGURE 4.17 Finite element mesh model of unrestrained test beam, half of flange heated

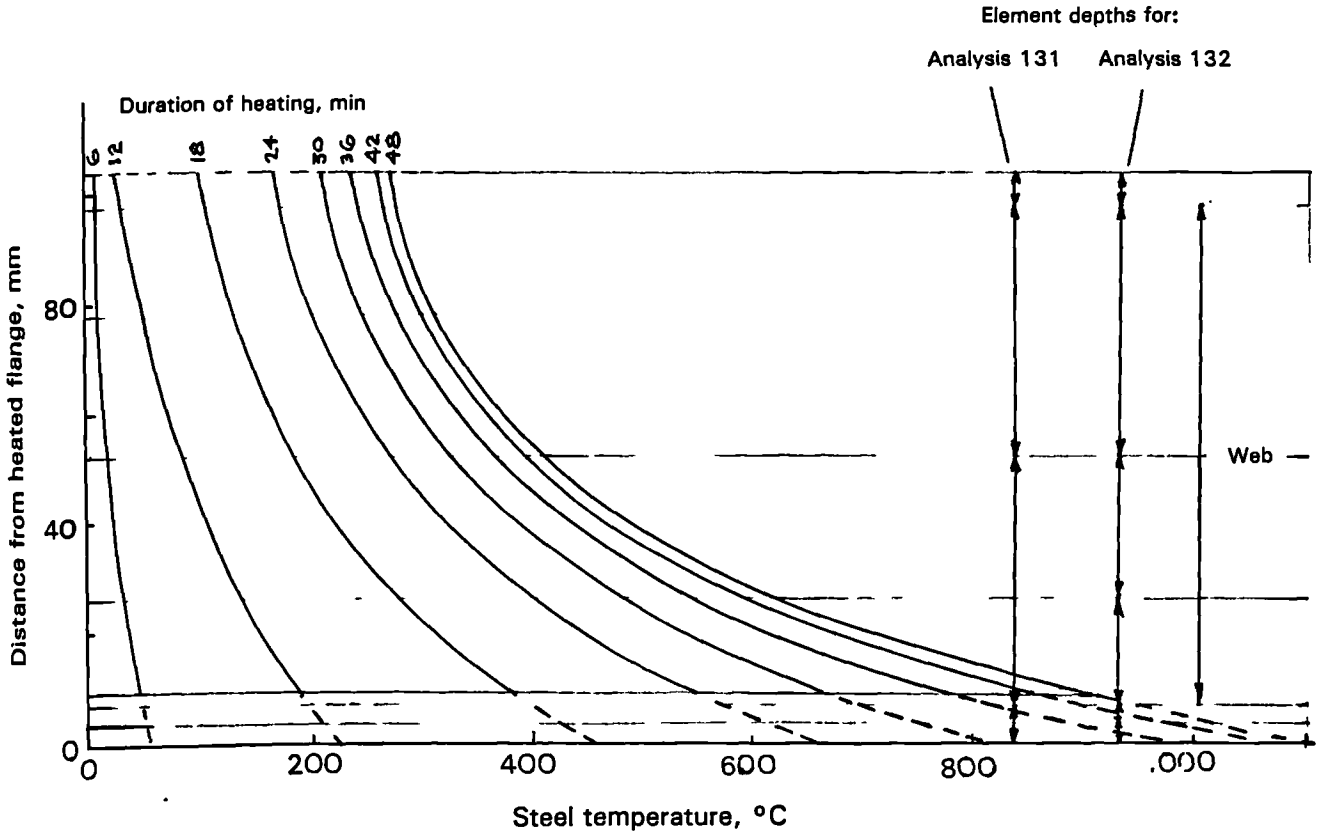

FIGURE 4.18 Profiles of averaged temperatures and element sizes for unrestrained test beam heated along whole flange

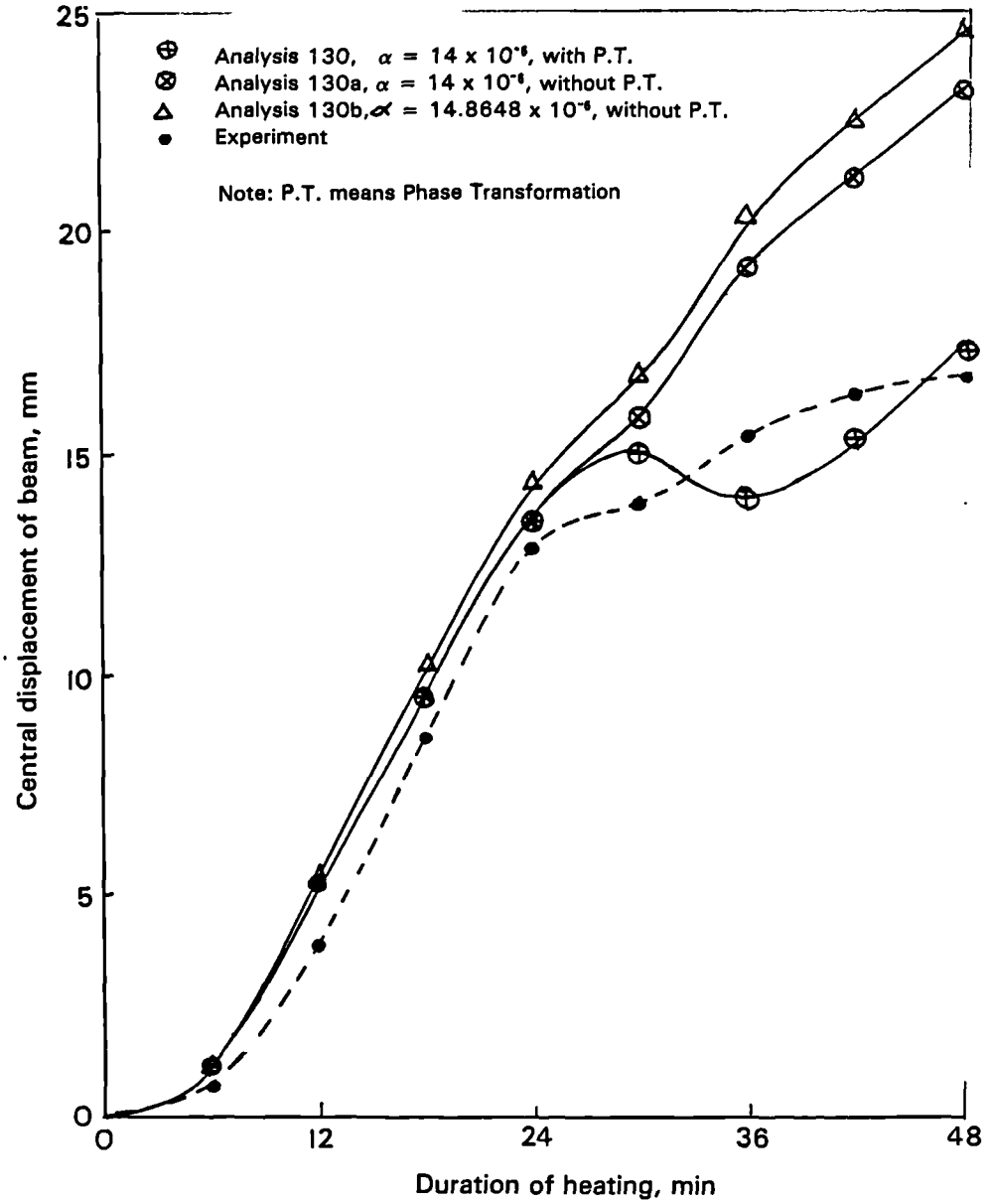

FIGURE 4.19 PAFEC-computed central displacements of unrestrained test beam heated along whole flange showing effect of α value and phase transformation

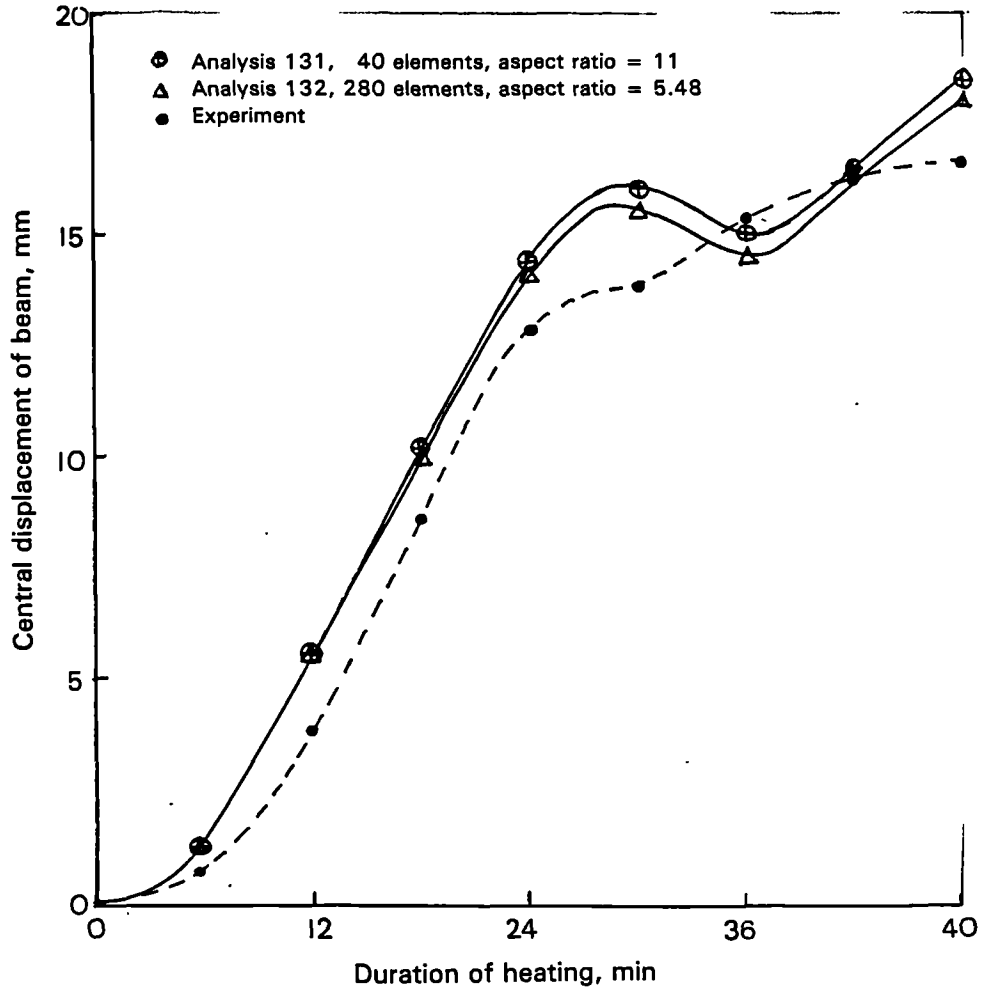

FIGURE 4.20 PAFEC-computed central displacements of unrestrained test beam heated along whole flange showing effect of varying the size and shape of finite elements

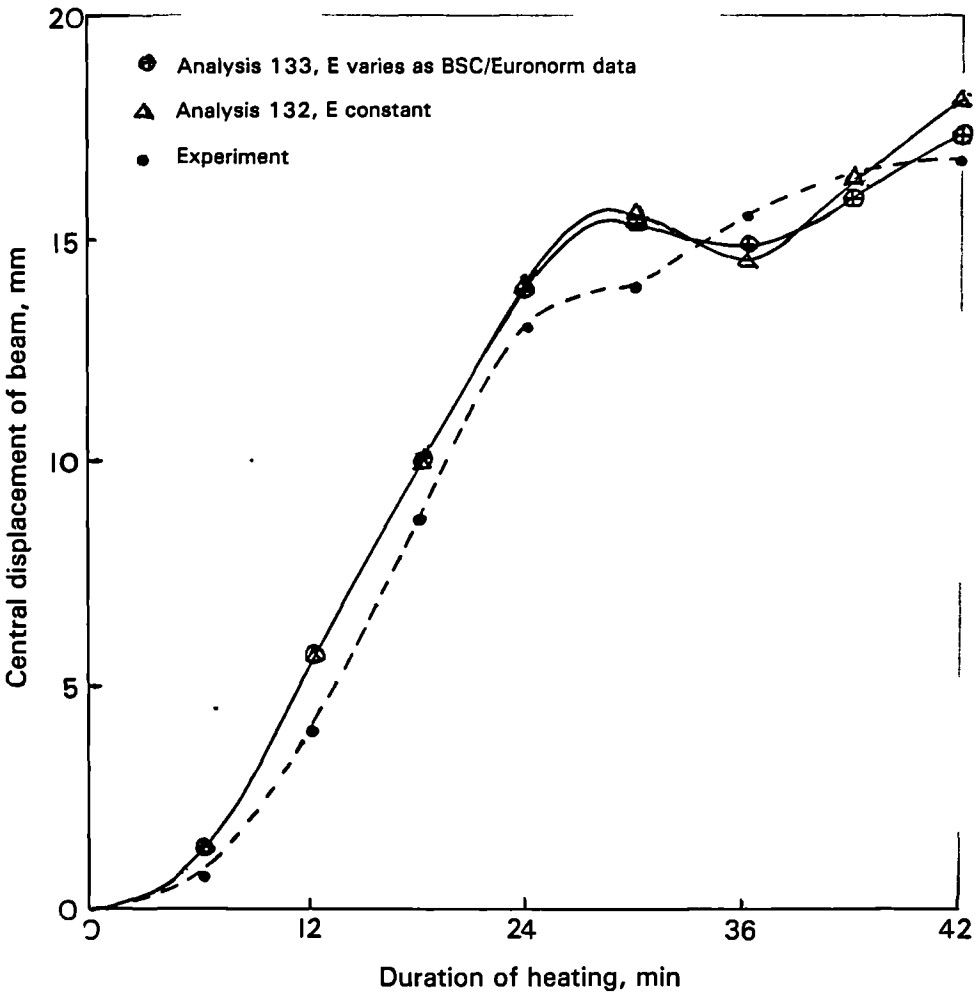

FIGURE 4.21 PAFEC-computed central displacements of unrestrained test beam heated along whole flange showing effect of variable elastic modulus

FIGURE 4.22 PAFEC-graphic of displaced shape of unrestrained test beam heated along whole flange

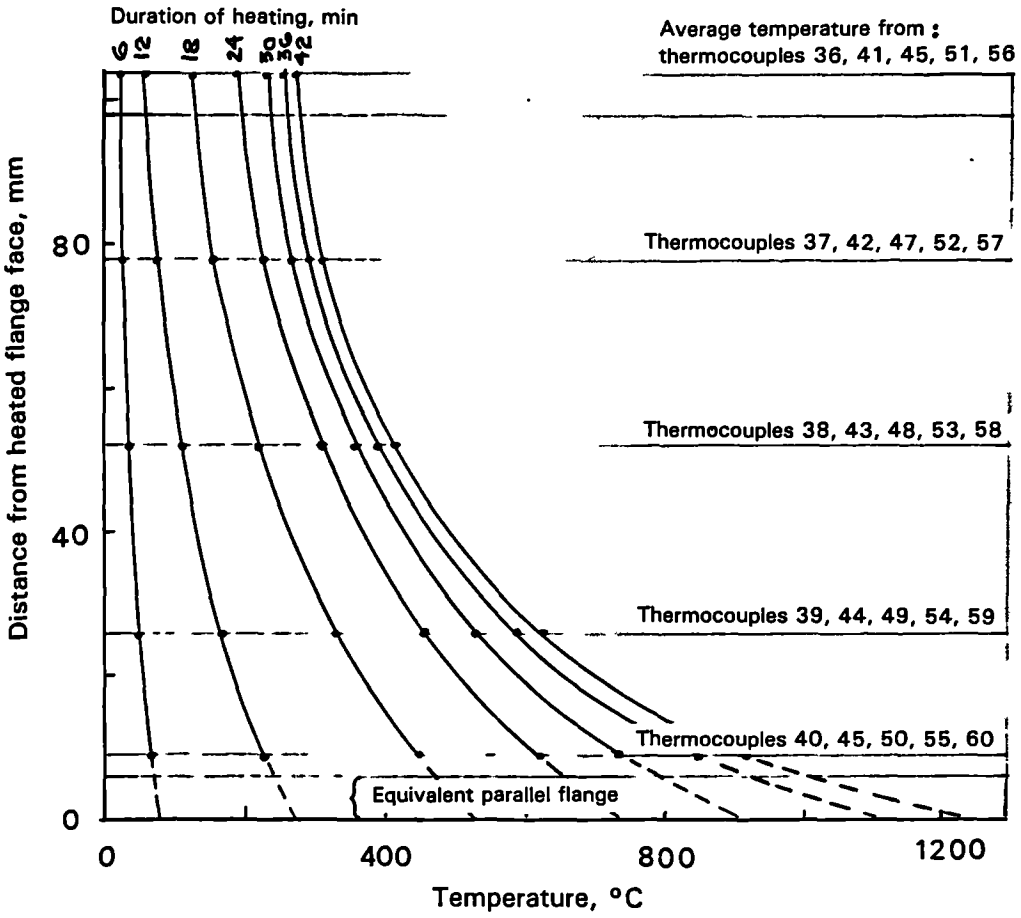

FIGURE 4.23 Profiles of averaged temperatures for heated portion of unrestrained test beam heated along half of flange

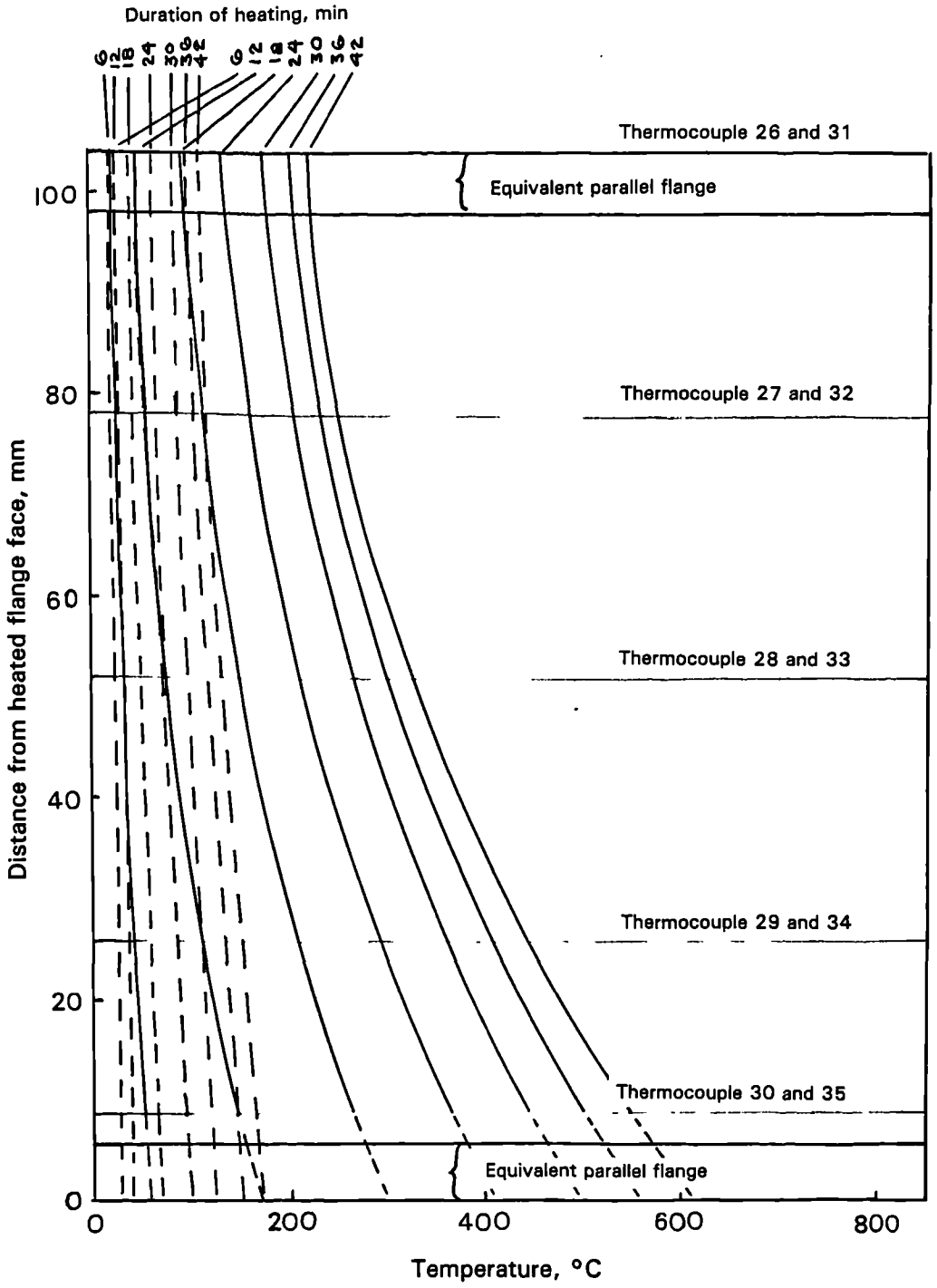

FIGURE 4.24 Temperature profiles at mid-span of unrestrained test beam heated along half of flange

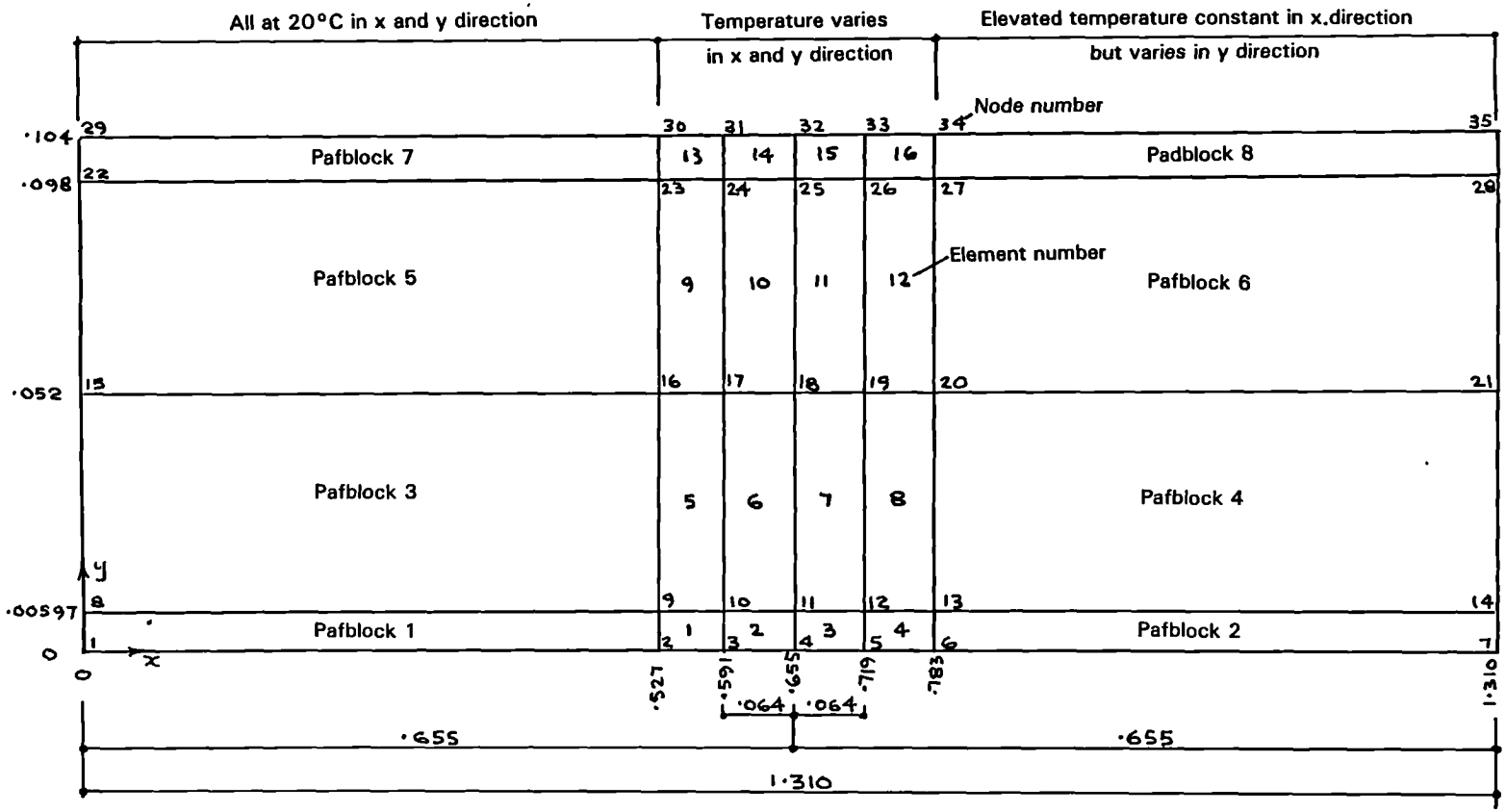

FIGURE 4.25 Finite element mesh model of unrestrained test beam heated along half of flange

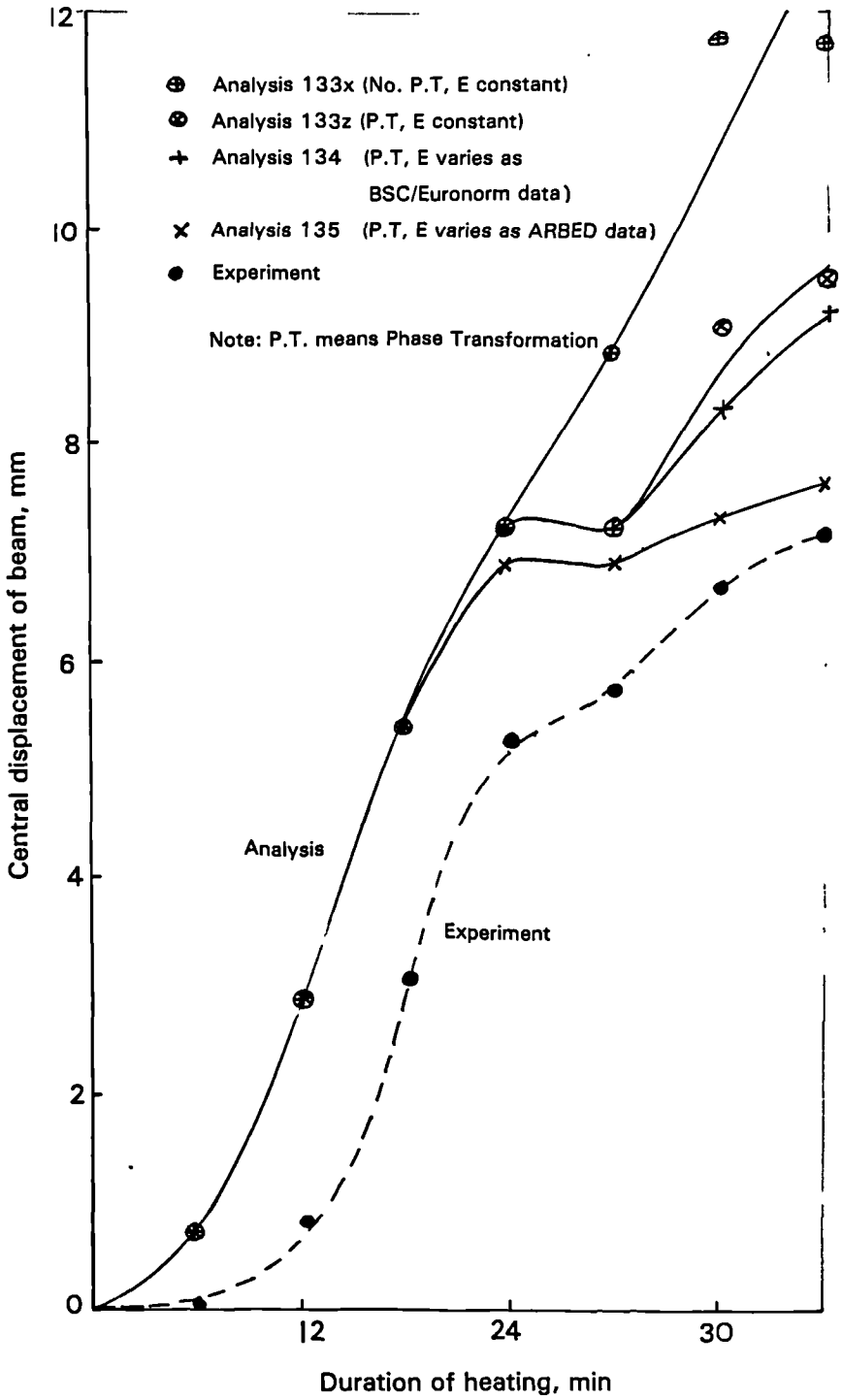

FIGURE 4.26 PAFEC-computed central displacements of unrestrained test beam heated along half of flange showing effect of phase transformation and varying elastic modulus

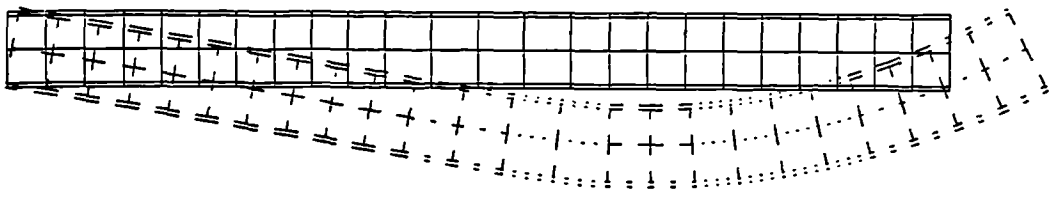

FIGURE 4.27 PAFEC-graphic of displaced shape of unrestrained test beam heated along half of flange

FIGURE 4.28 Fire in progress in Cardington test rig

FIGURE 4.29 Interior view of Cardington test rig showing bare steel columns and timber crib fire load

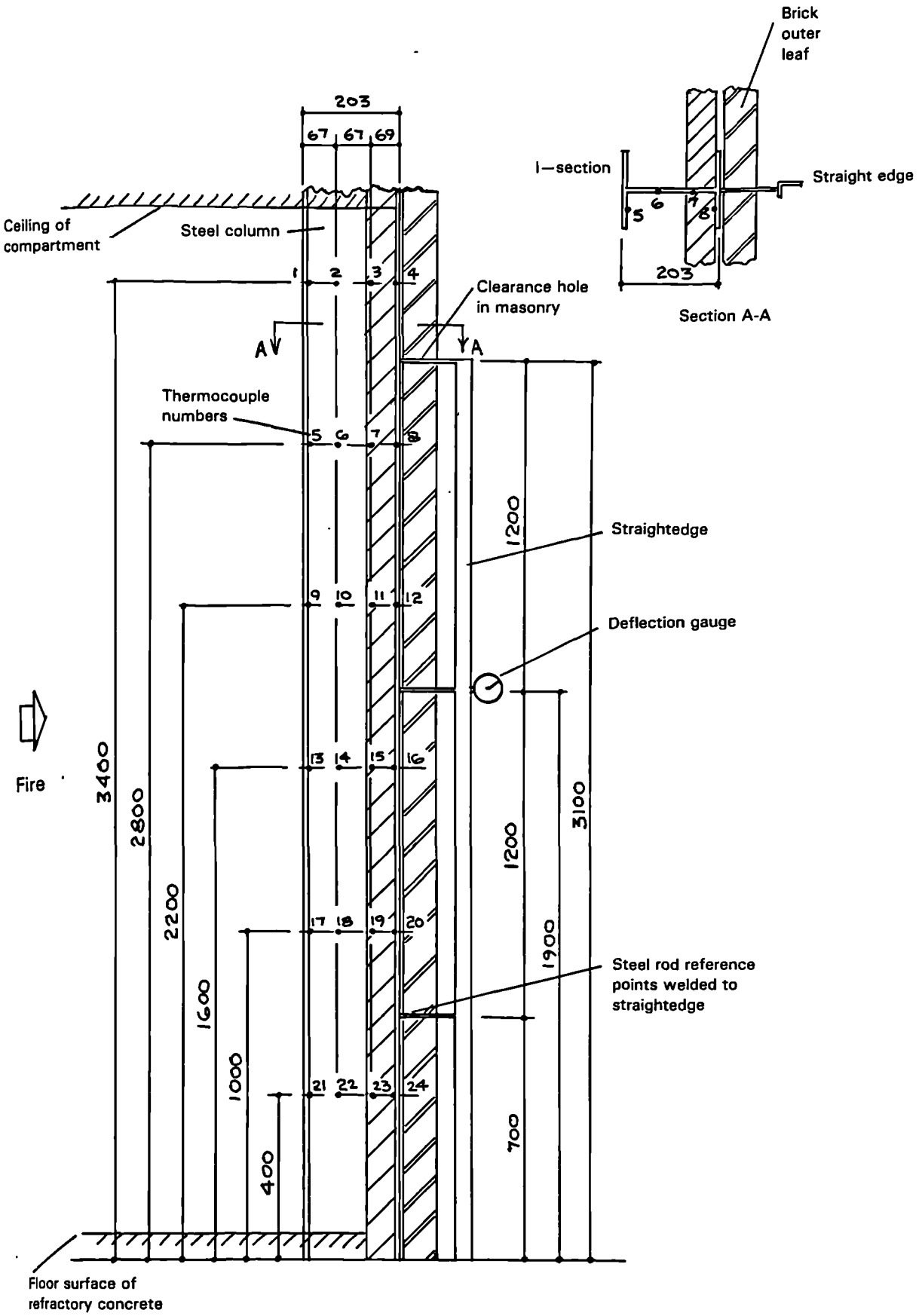

FIGURE 4.30 Vertical section through Cardington column-in-wall showing details of straight-edge and thermocouple positions

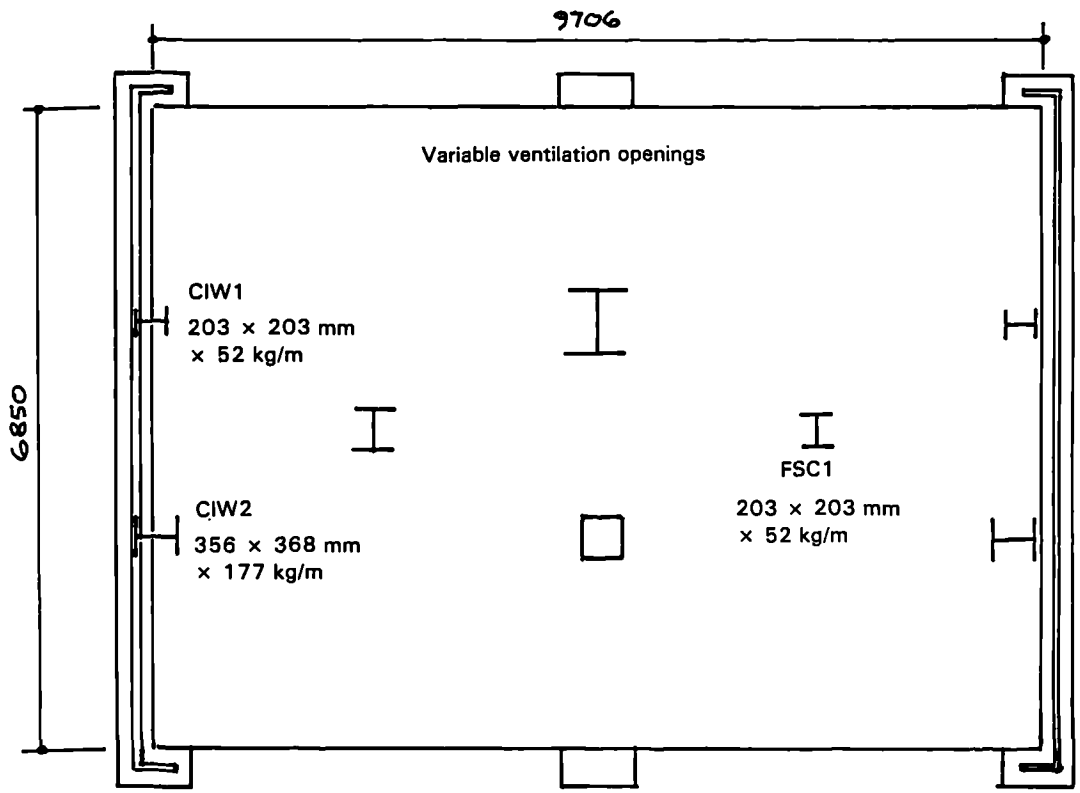

FIGURE 4.31 Plan of Cardington test rig showing positions of columns

FIGURE 4.32 Two columns partly built into wall of Cardington test rig

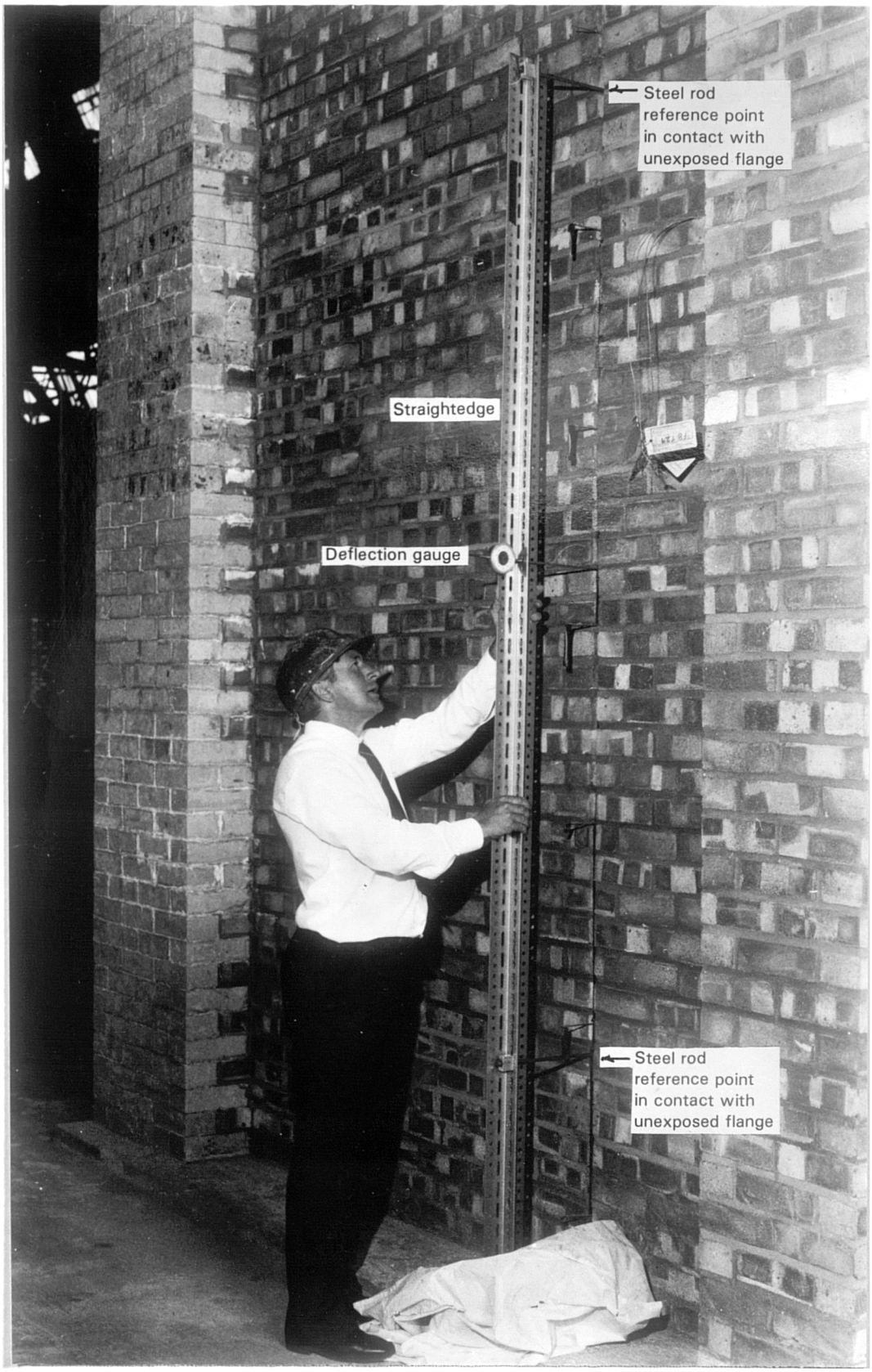

FIGURE 4.33 Use of straight-edge for measuring thermal bowing of Cardington column-in-wall

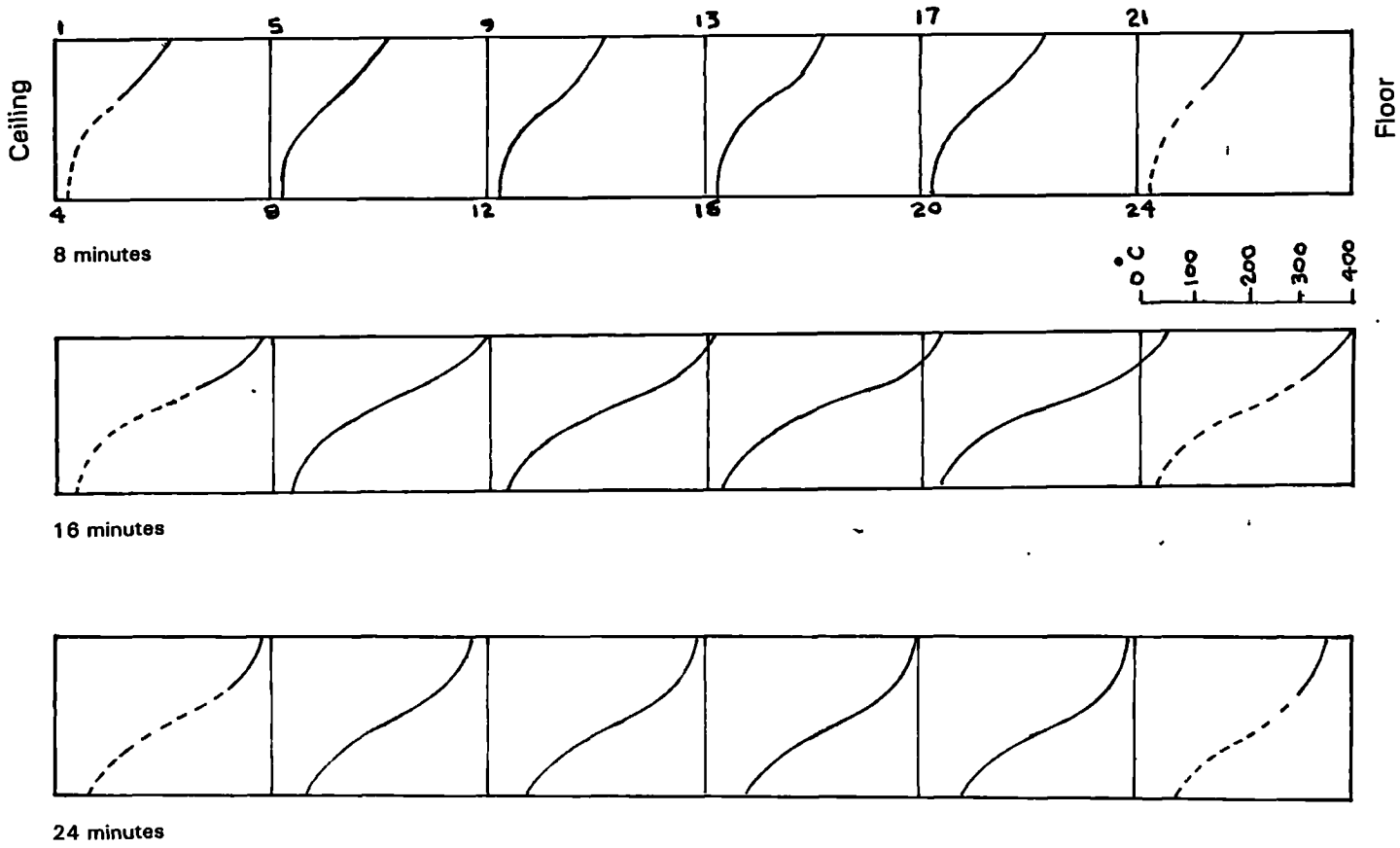

FIGURE 4.34 Temperature profiles in Cardington column-in-wall at three different times in a compartment fire test

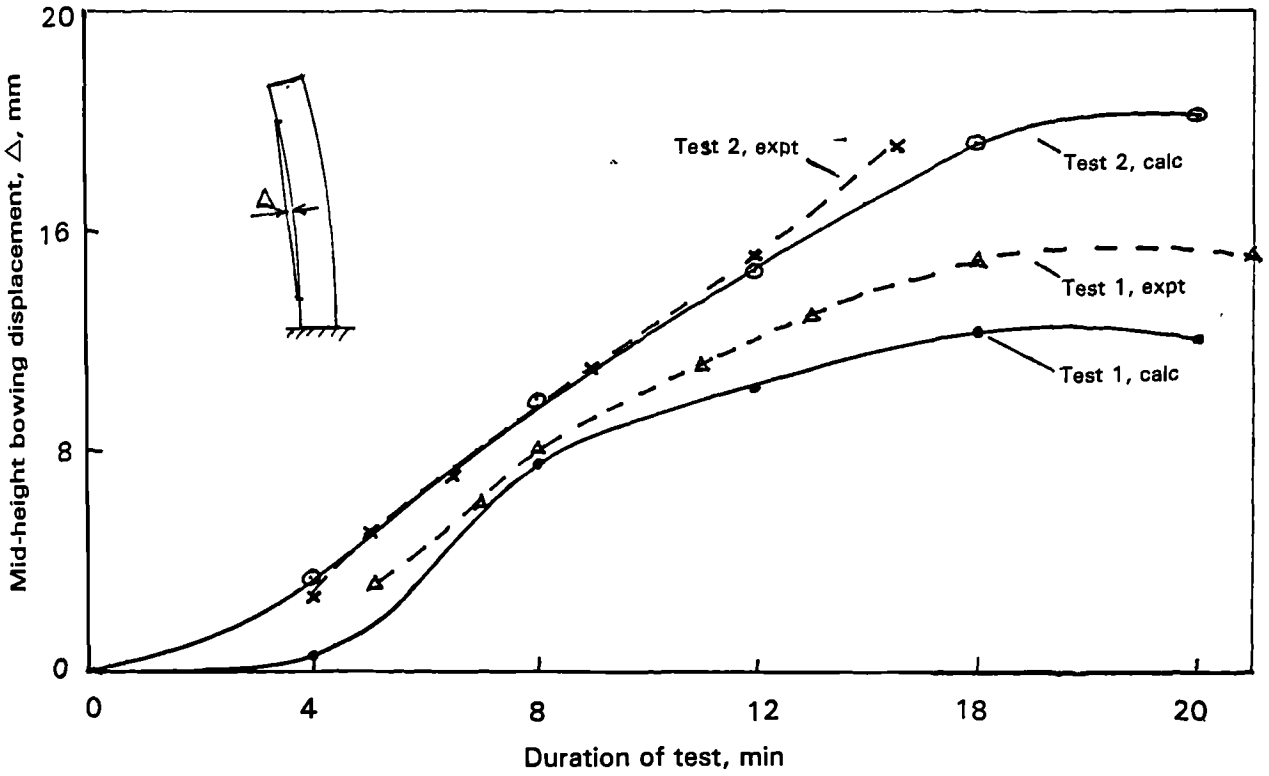

FIGURE 4.35 Comparison of experimental and calculated mid-height bowing displacements of Cardington column-in-wall for Tests 1 and 2

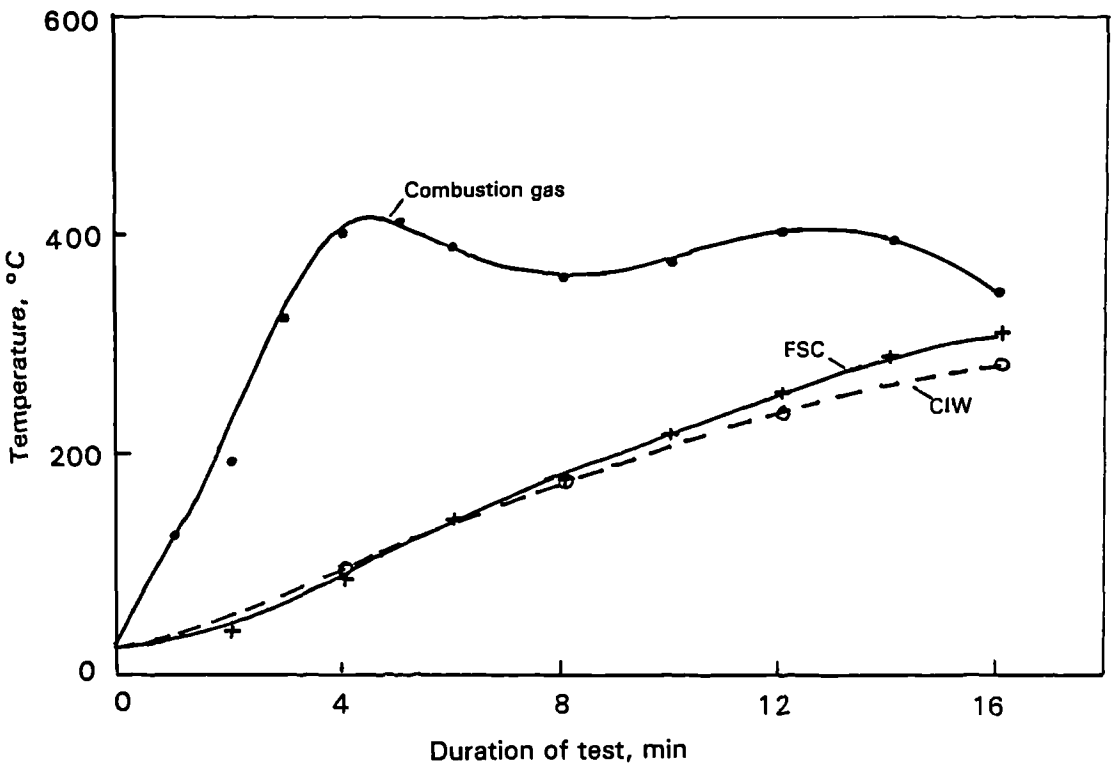

FIGURE 4.36 Comparison of temperatures attained by heated flange of free standing column and column-in-wall having identical I-sections exposed to Cardington compartment fire, Test 1

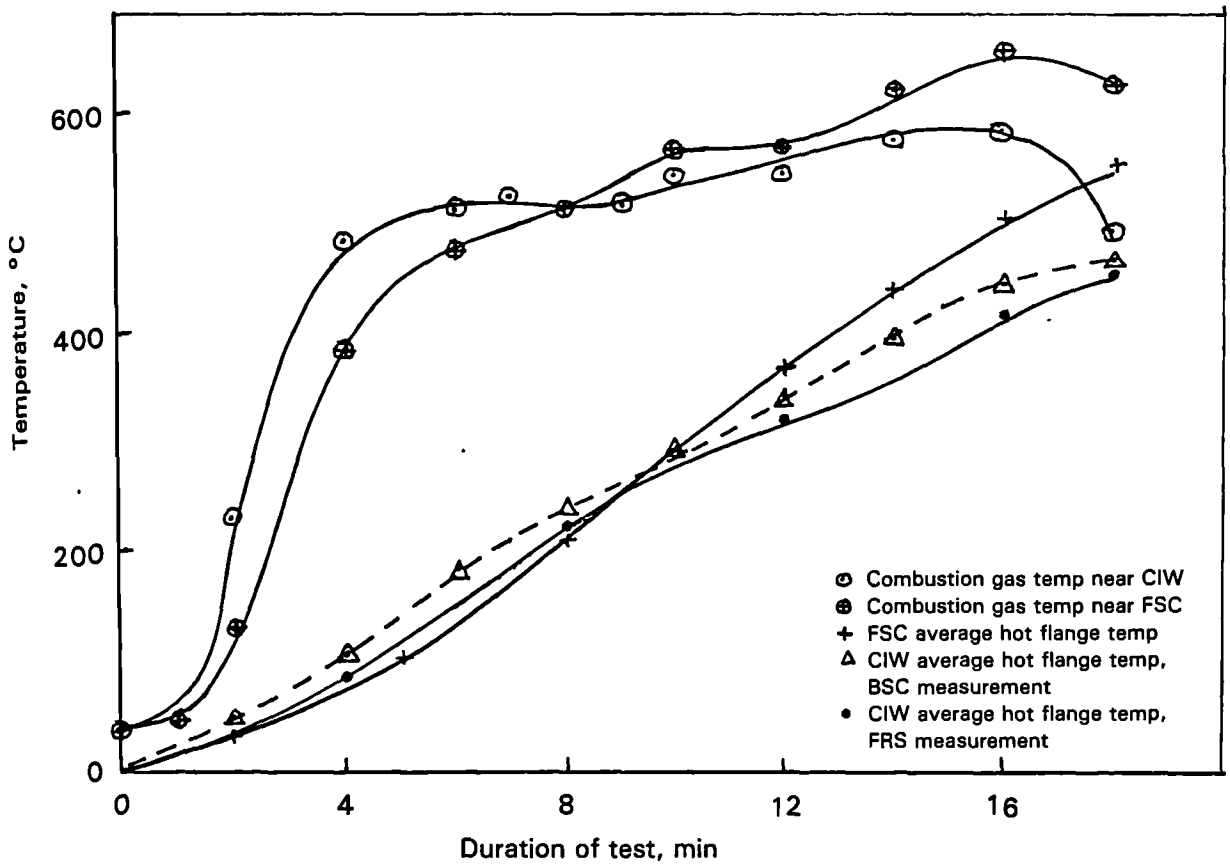

FIGURE 4.37 Comparison of temperatures attained by heated flange of free-standing column and column-in-wall having identical I-sections exposed to Cardington compartment fire, Test 2

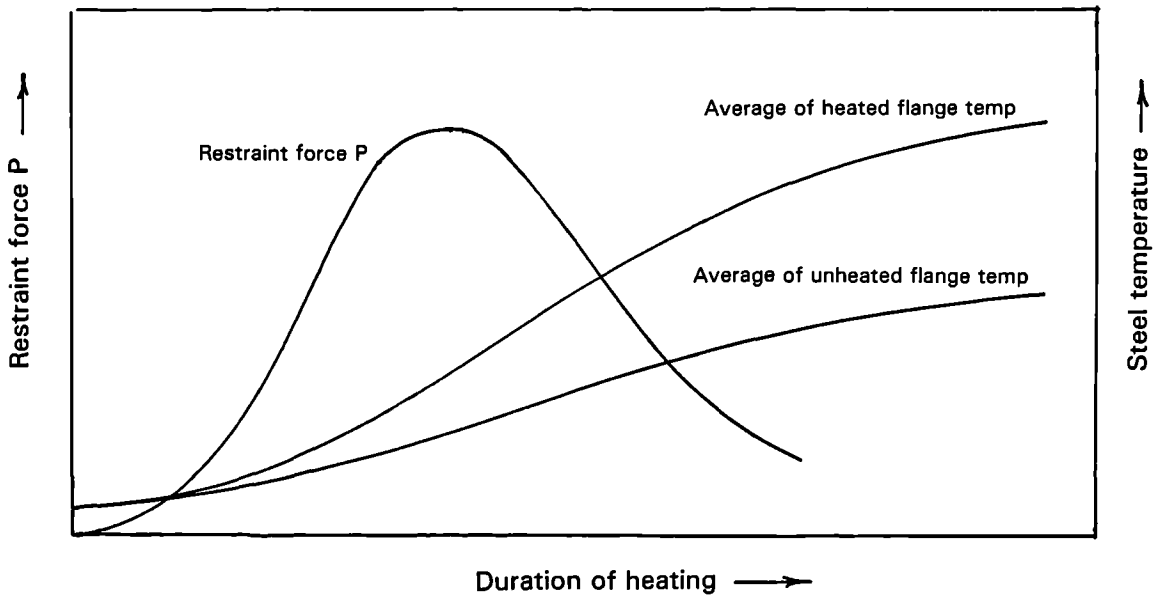

FIGURE 5.1 Qualitative prediction of relationship between mid-support restraint force and temperature for a 2-span beam heated along one flange

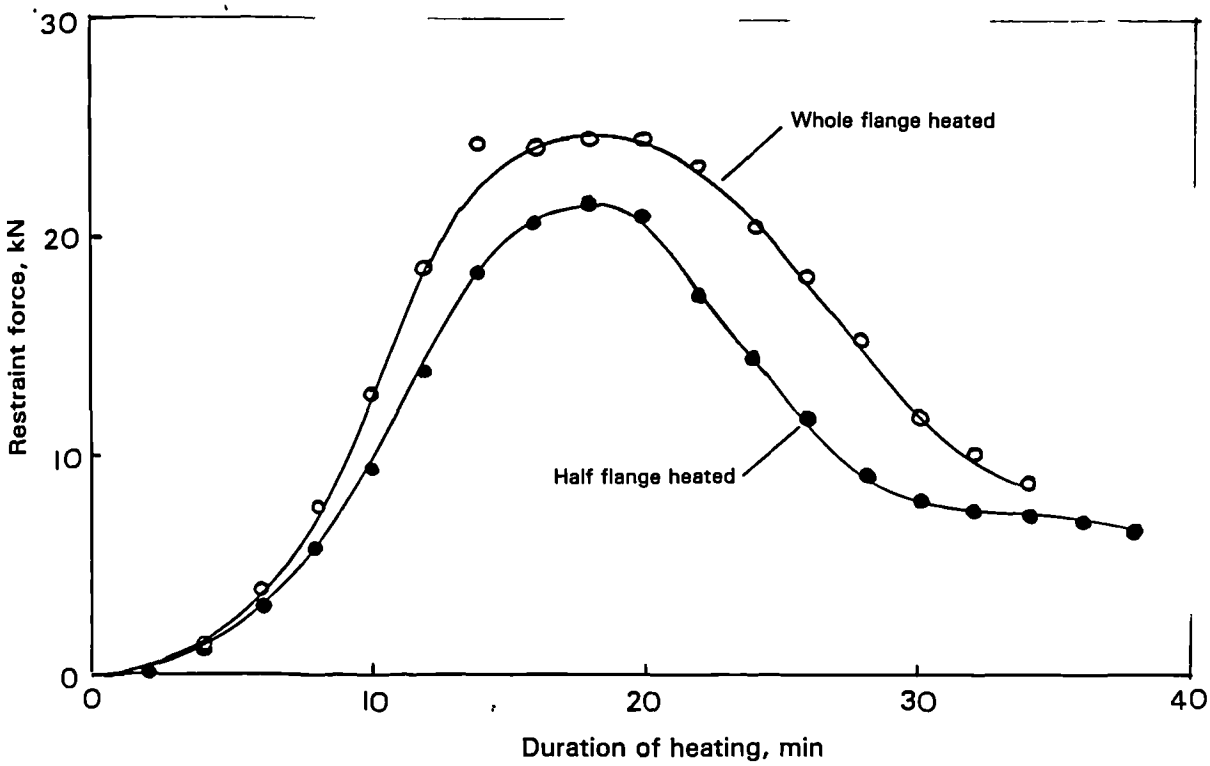

FIGURE 5.2 Variation of mid-support restraint force with time for 2-span test beam heated along whole and half of one flange

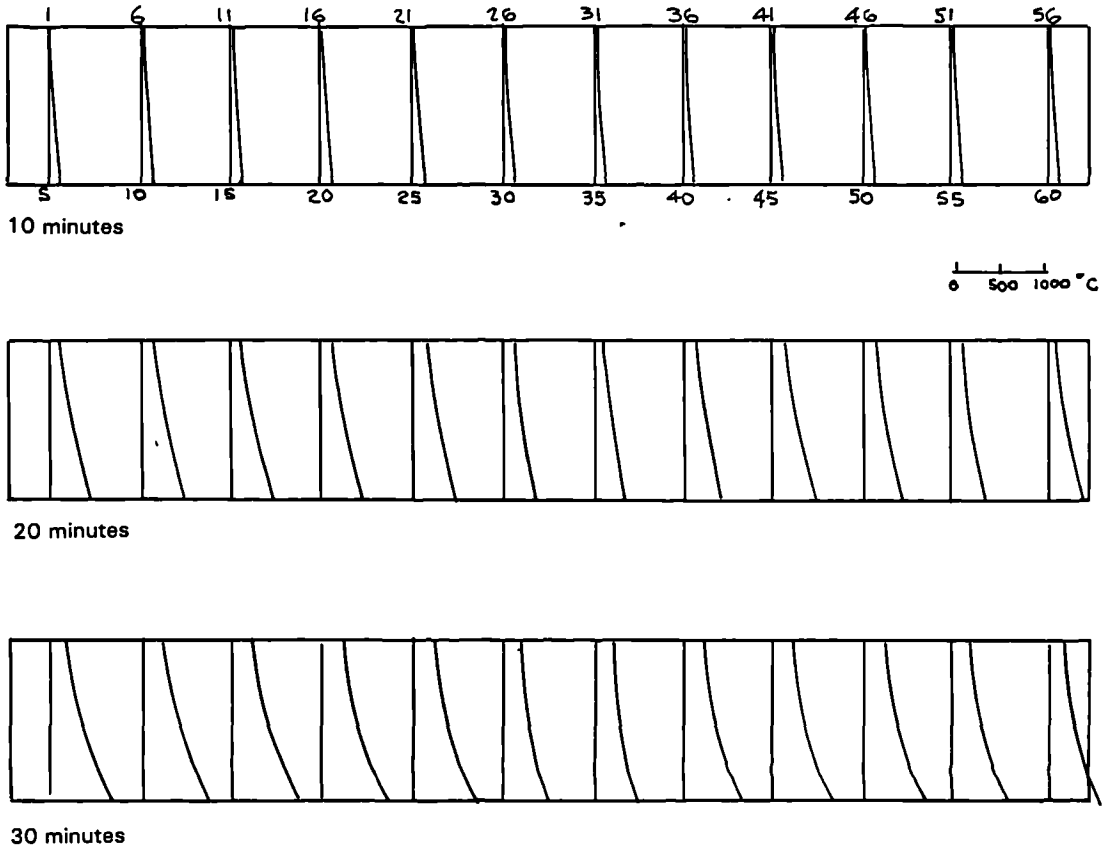

FIGURE 5.3 Temperature profiles along the length of restrained 2-span test beam heated along whole flange at three different times

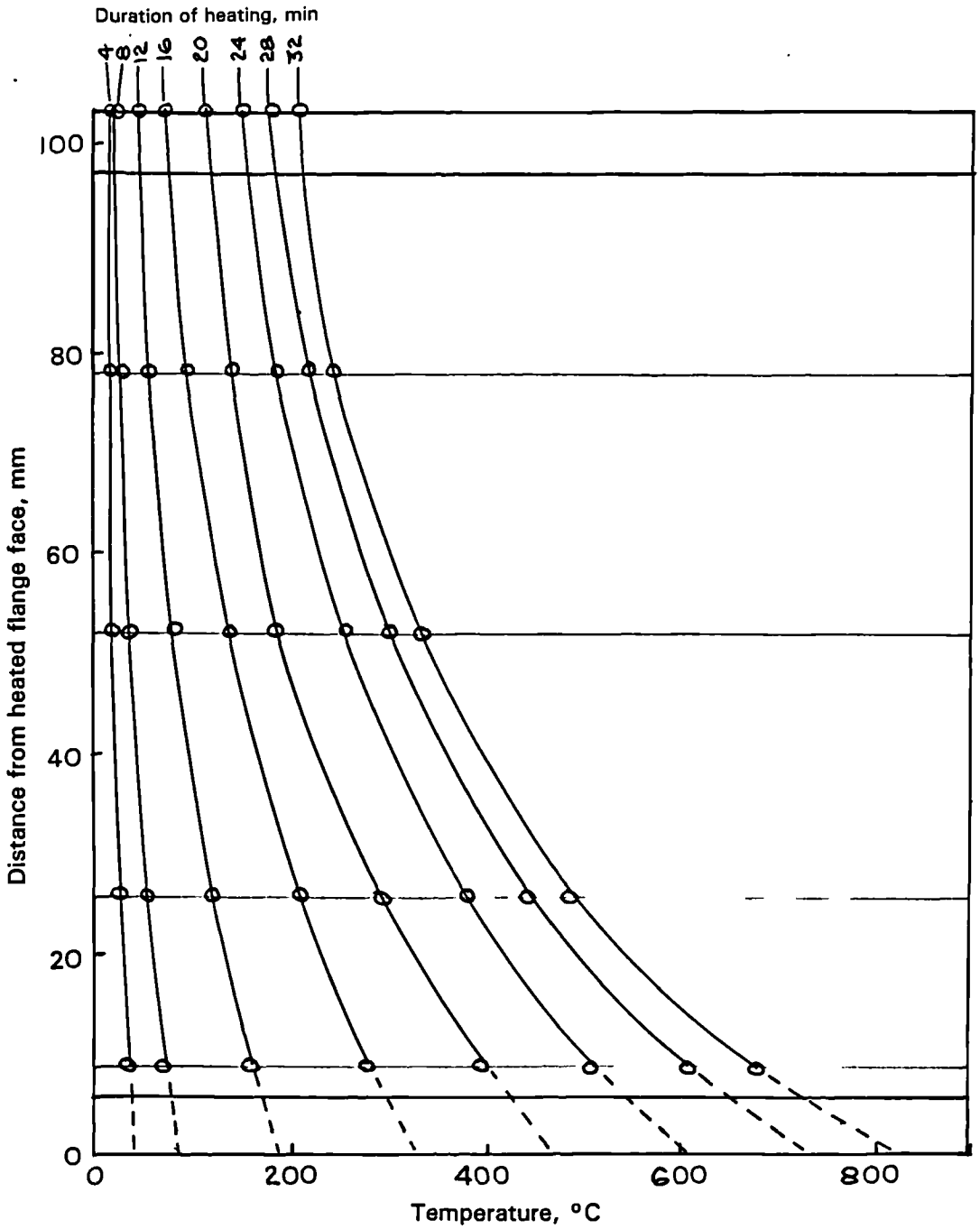

FIGURE 5.4 Profiles of average temperatures in restrained 2-span test beam heated along whole flange

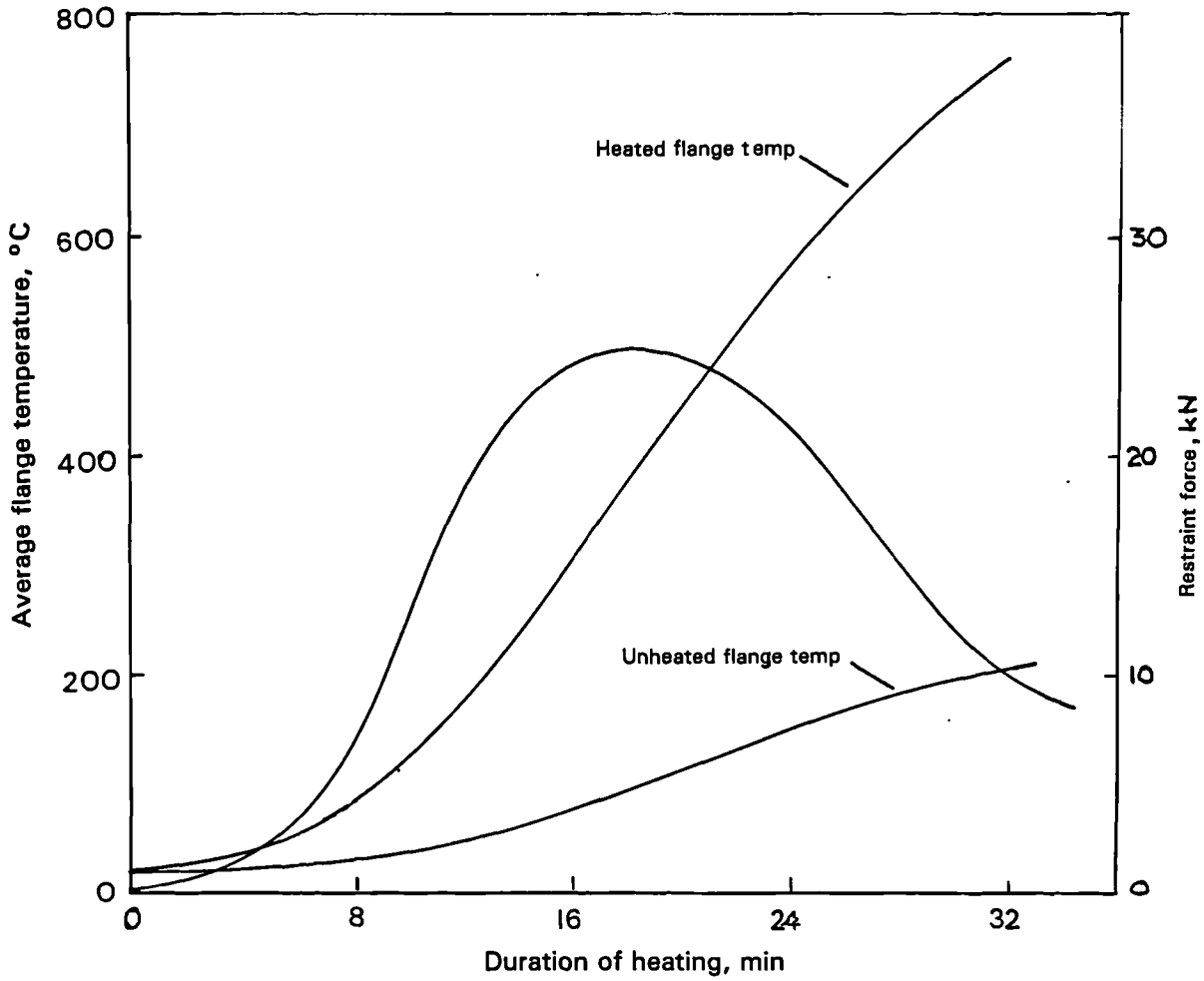

FIGURE 5.5 Variation of mid-support restraint force and flange temperature for 2-span test beam heated along whole flange

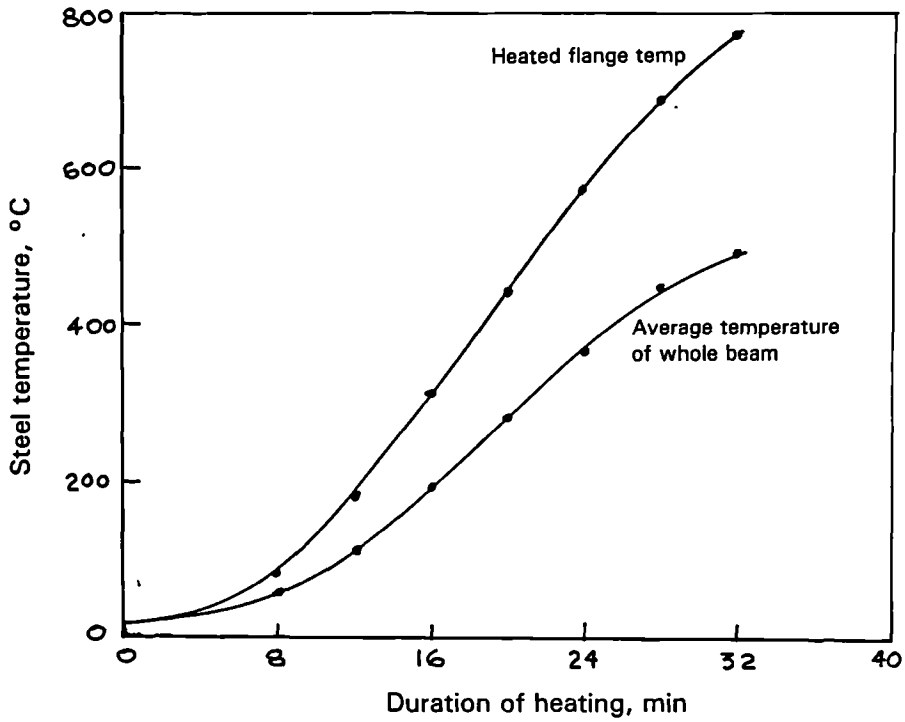

FIGURE 5.6 Comparison of heated flange temperature and average temperature of whole beam for 2-span test beam heated along whole flange

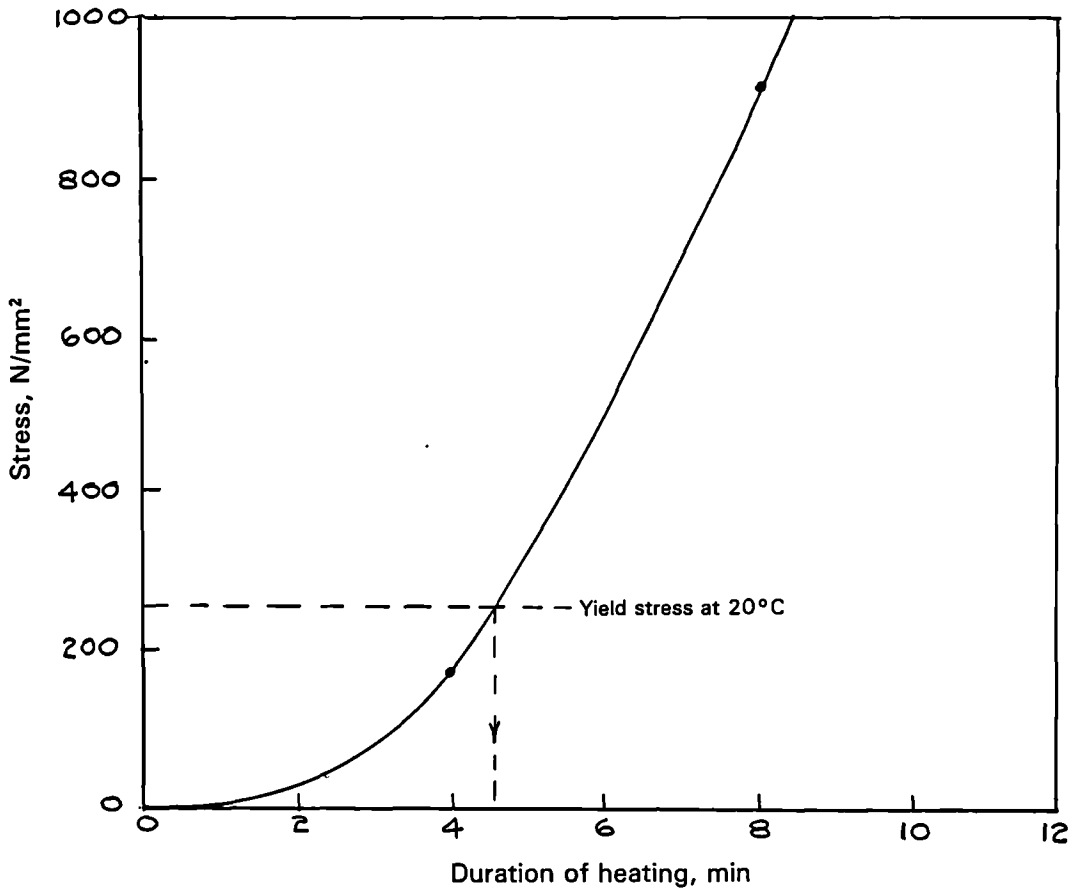

FIGURE 5.7 Variation of elastic stress in flange with time for 2-span test beam heated along whole flange

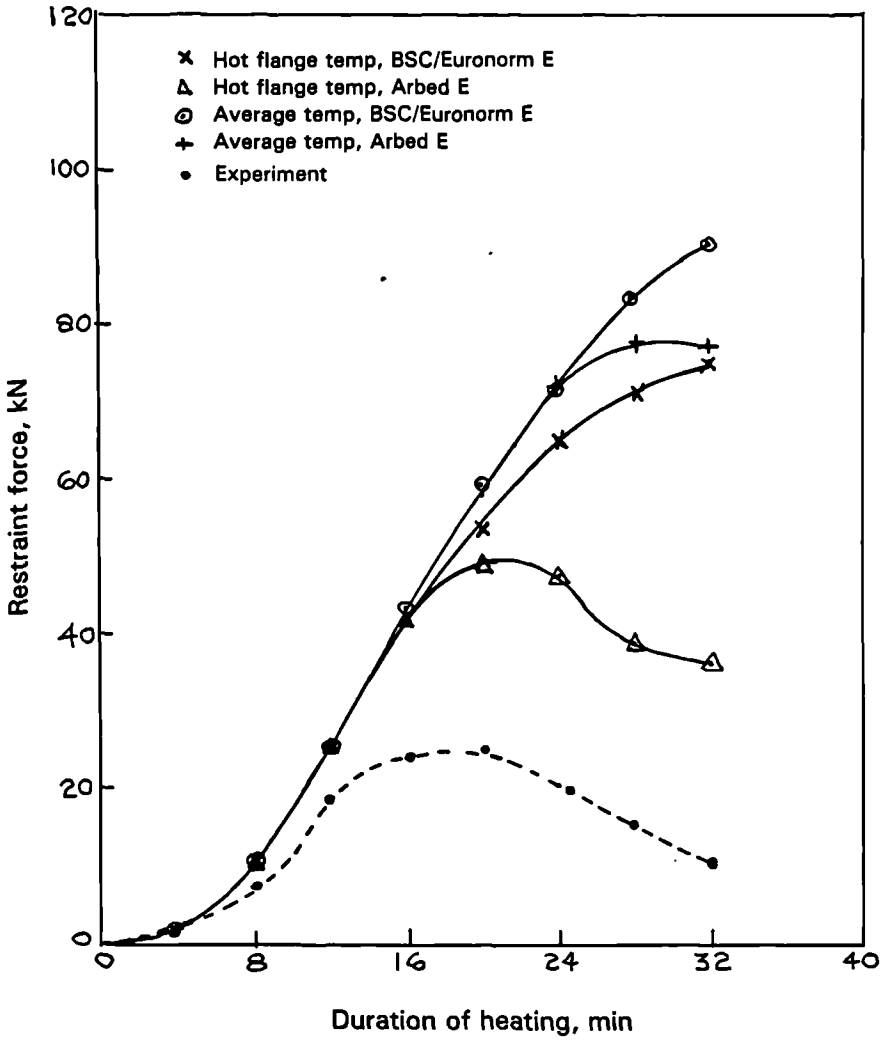

FIGURE 5.8 Variation of calculated elastic restraint force with time for 2-span test beam heated along whole flange

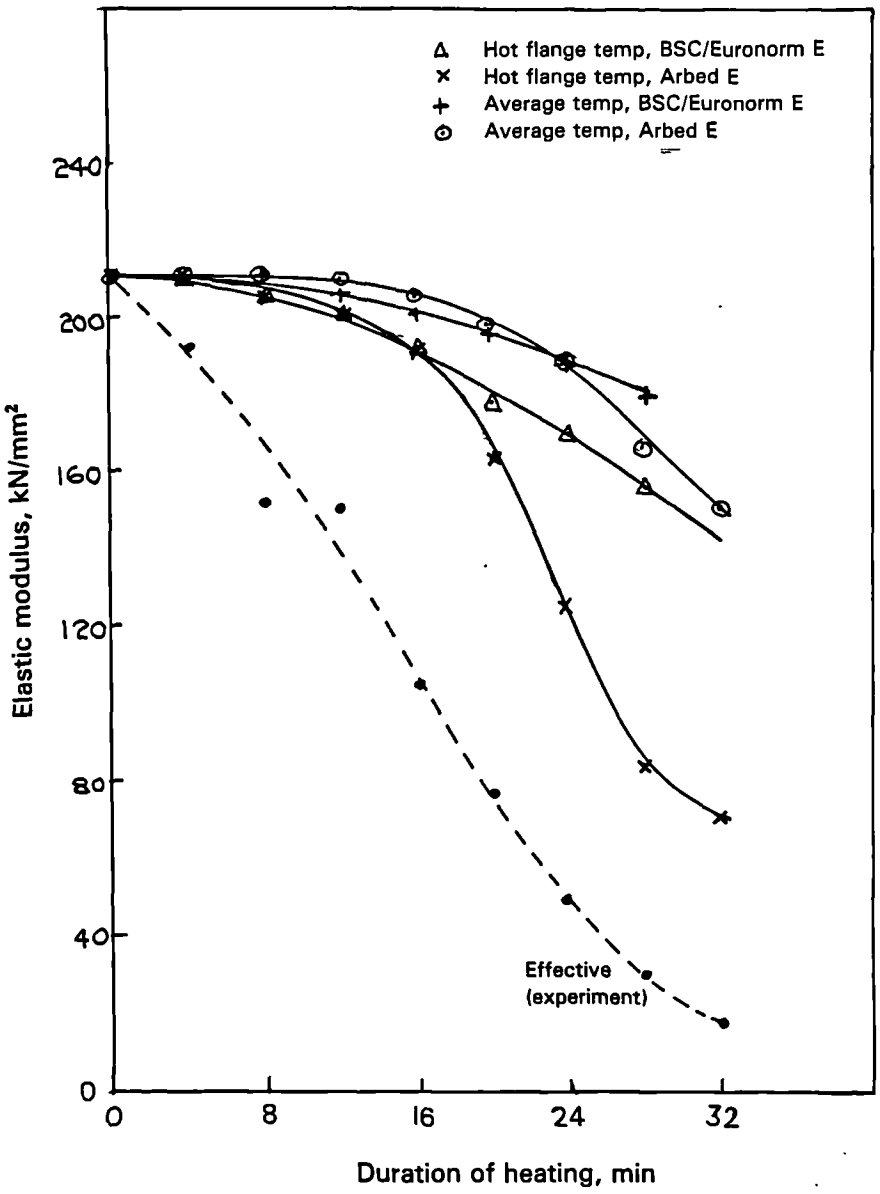

FIGURE 5.9 Variation of derived elastic modulus values with time for 2-span test beam heated along whole flange

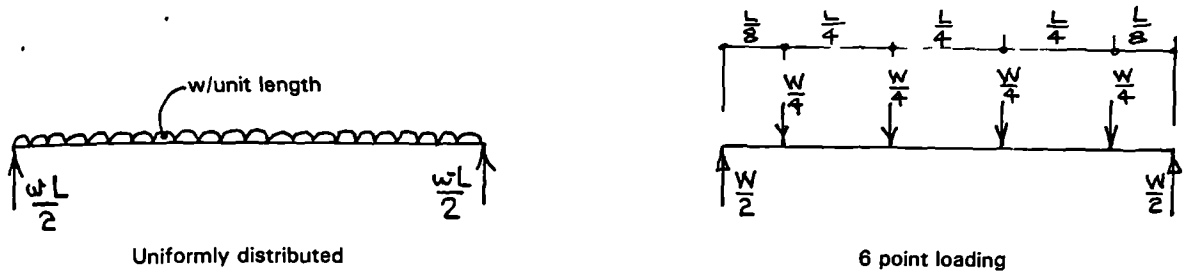

FIGURE 6.1 Equivalent load configuration for design-loaded test beam

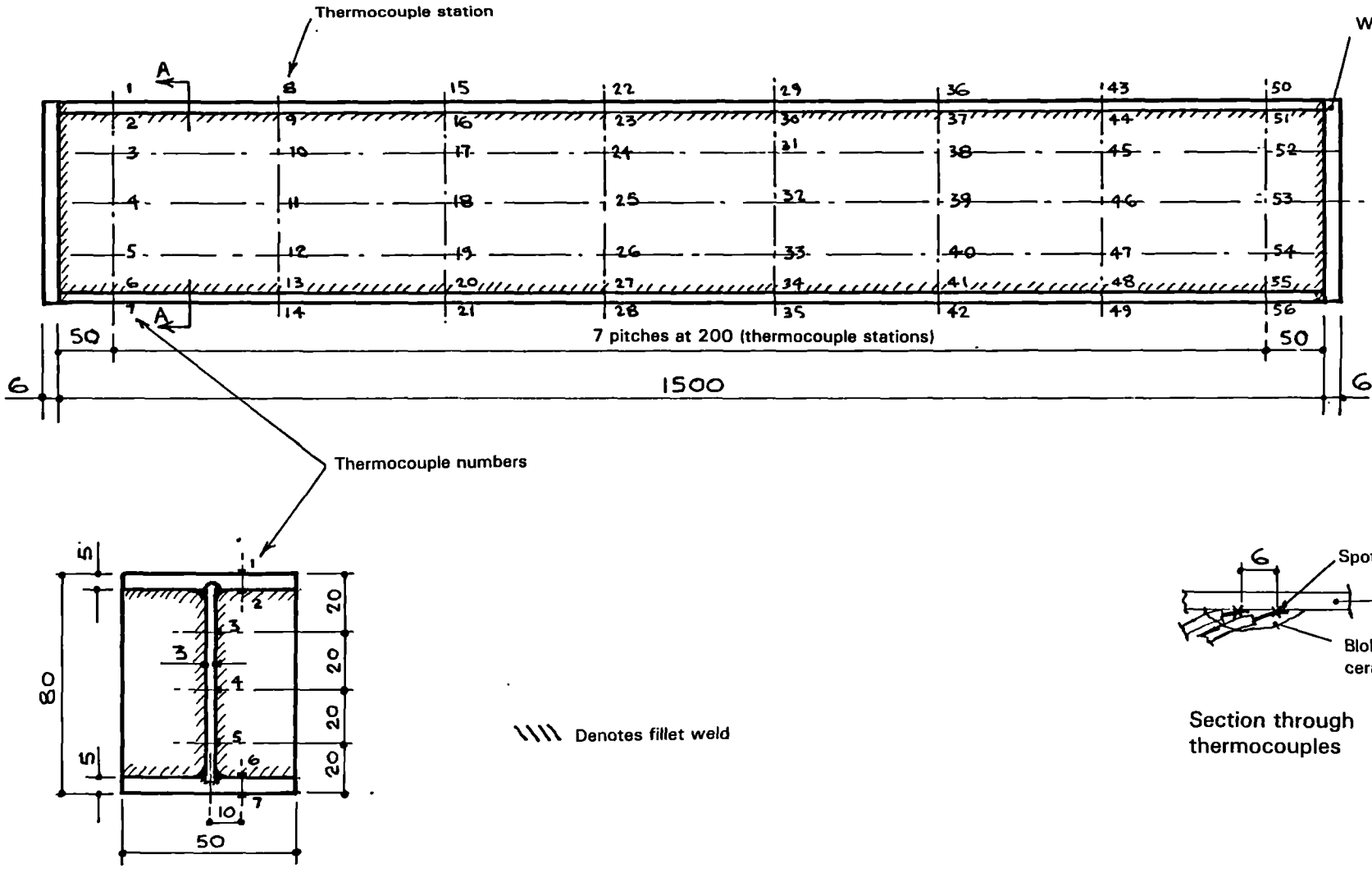

FIGURE 6.2 Fabrication and thermocouple details for design-loaded test beam

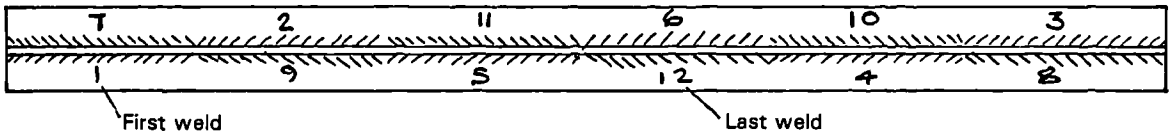

FIGURE 6.3 Welding sequence for design-loaded test beam

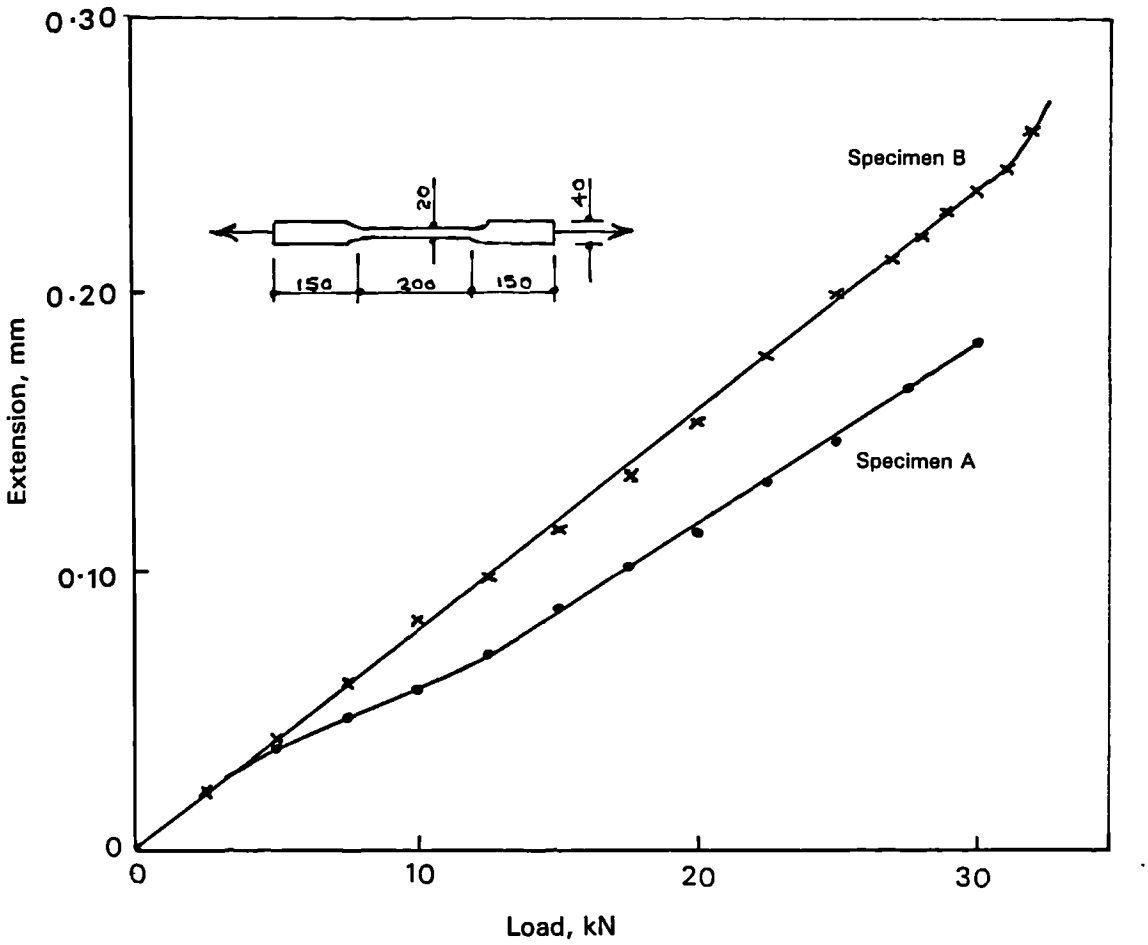

FIGURE 6.4 Tensile test results for flange steel used in design-loaded beam heated along one flange

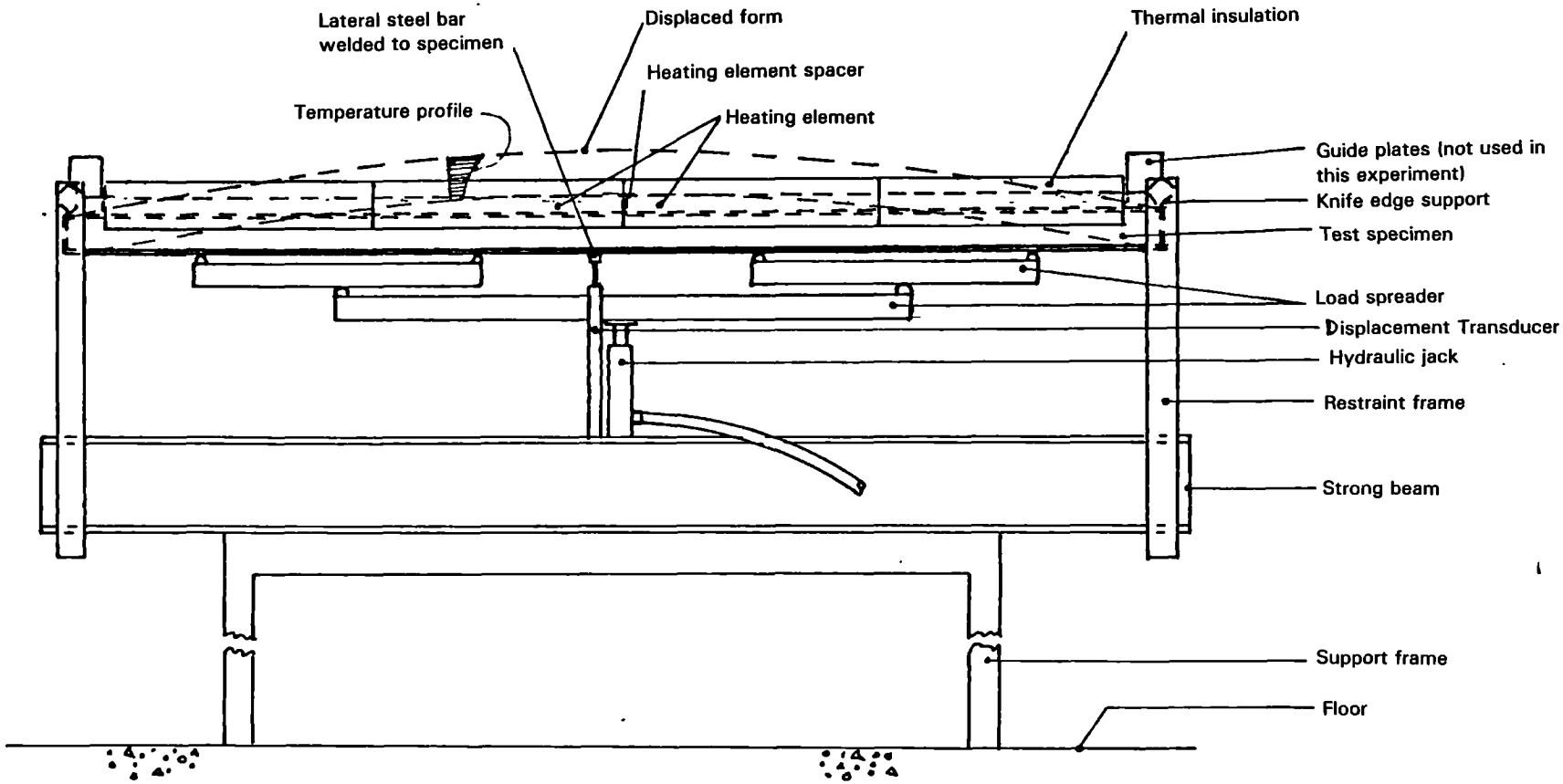

FIGURE 6.5 Details of test apparatus for design-loaded beam heated along one flange

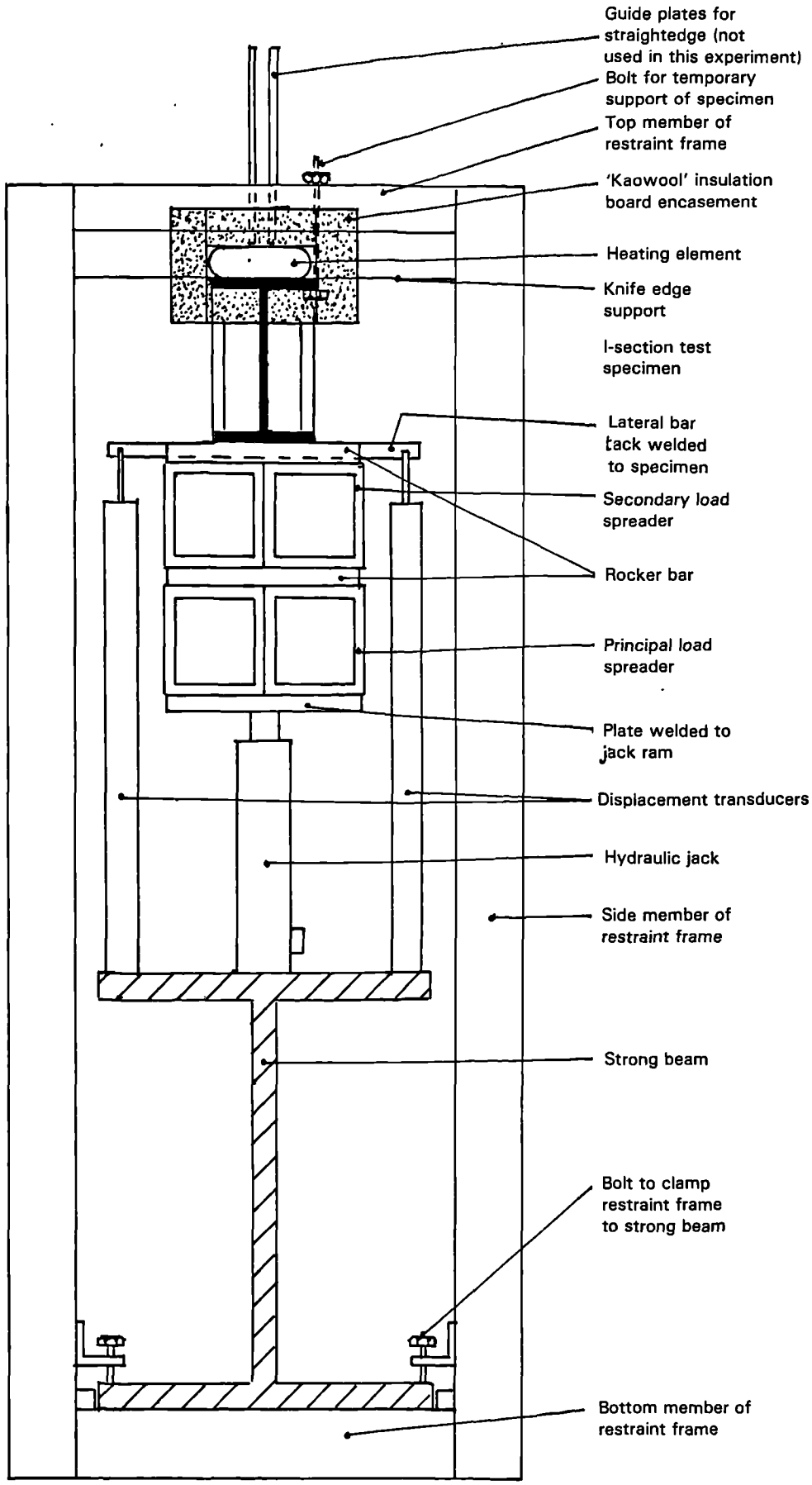

FIGURE 6.6 Section through test apparatus for design-loaded beam heated along one flange

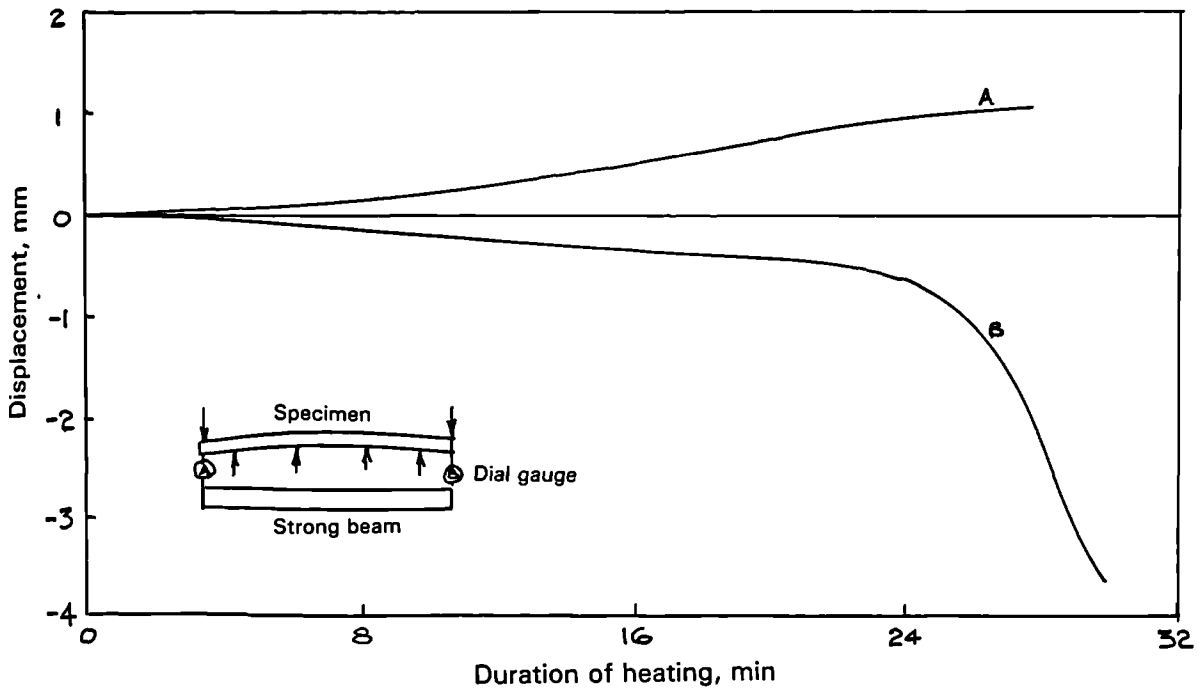

FIGURE 6.7 Displacement of ends of design-loaded beam heated along one flange

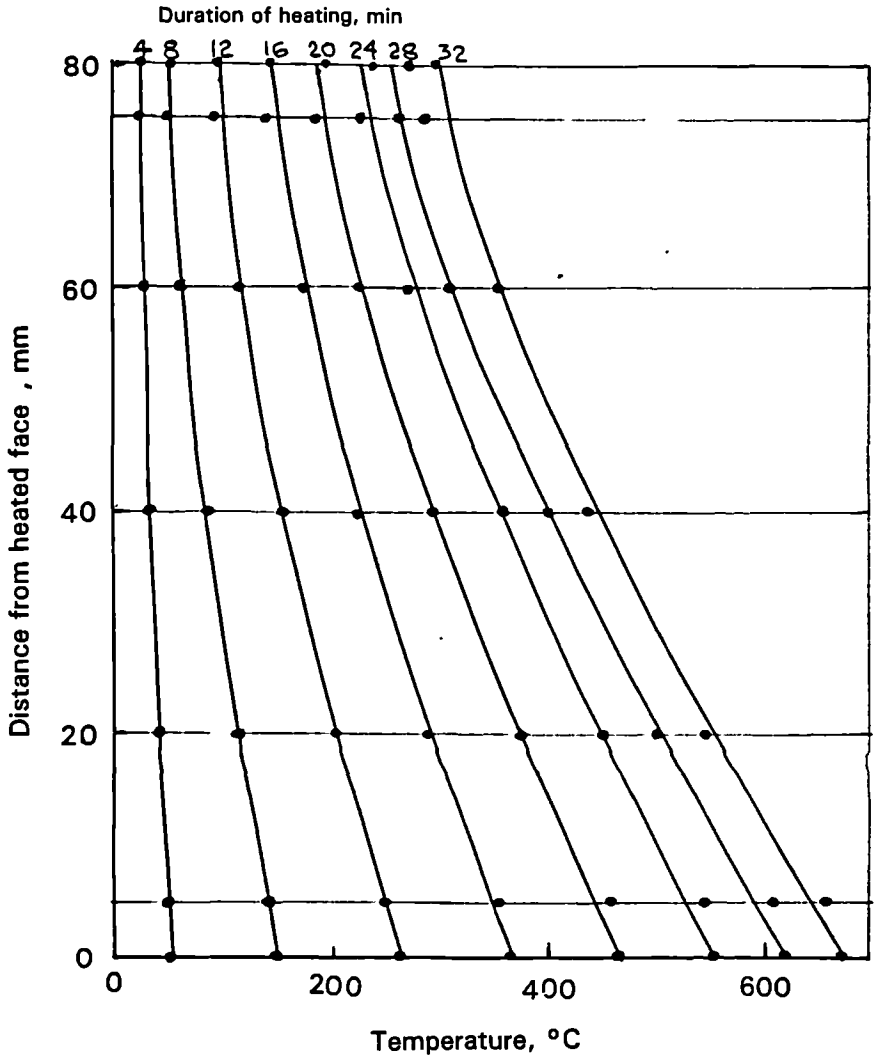

FIGURE 6.8 Profiles of average temperatures in design-loaded beam heated along one flange

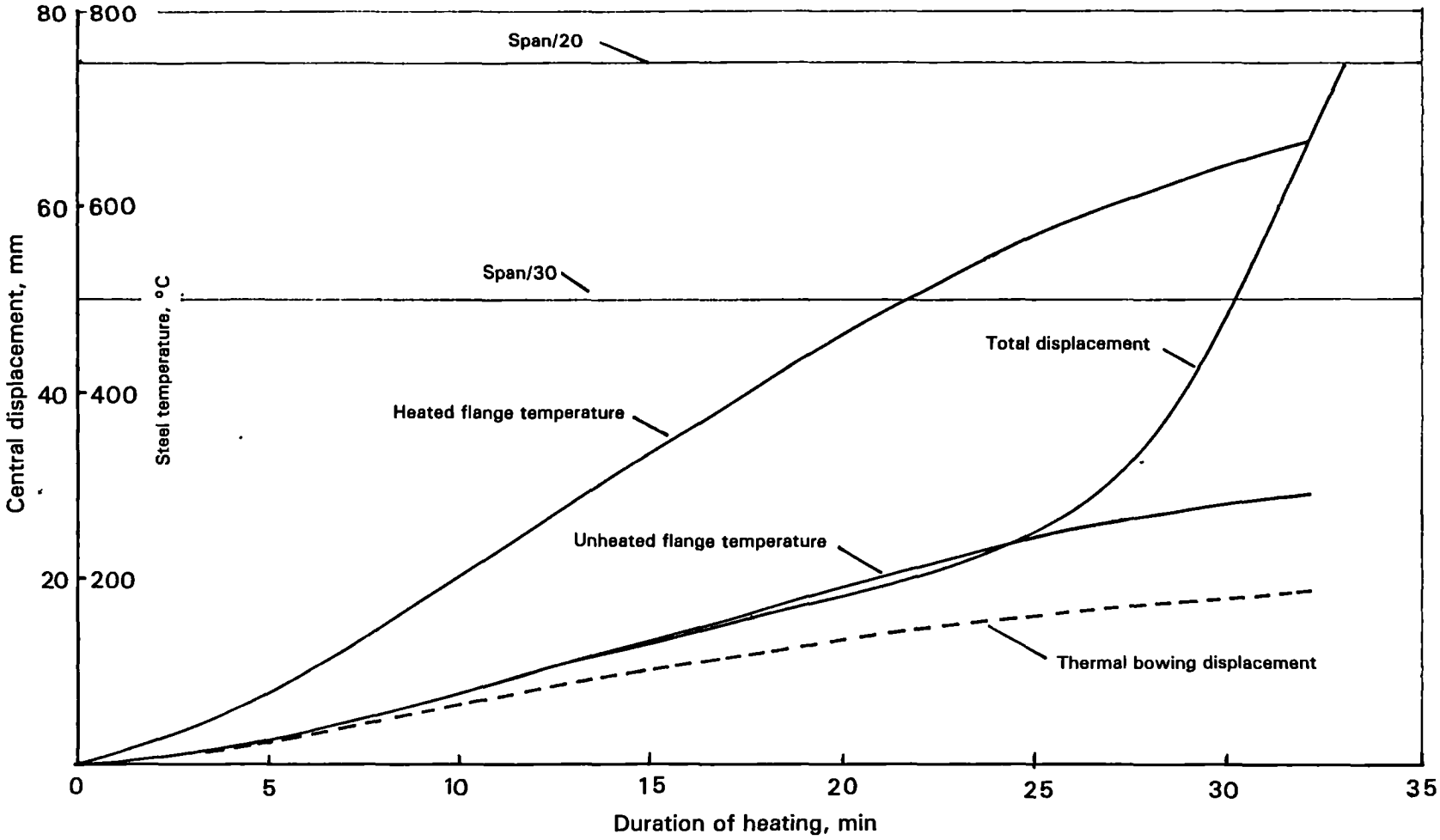

FIGURE 6.9 Variation of central displacement and flange temperatures with time for design-loaded beam in first heating test

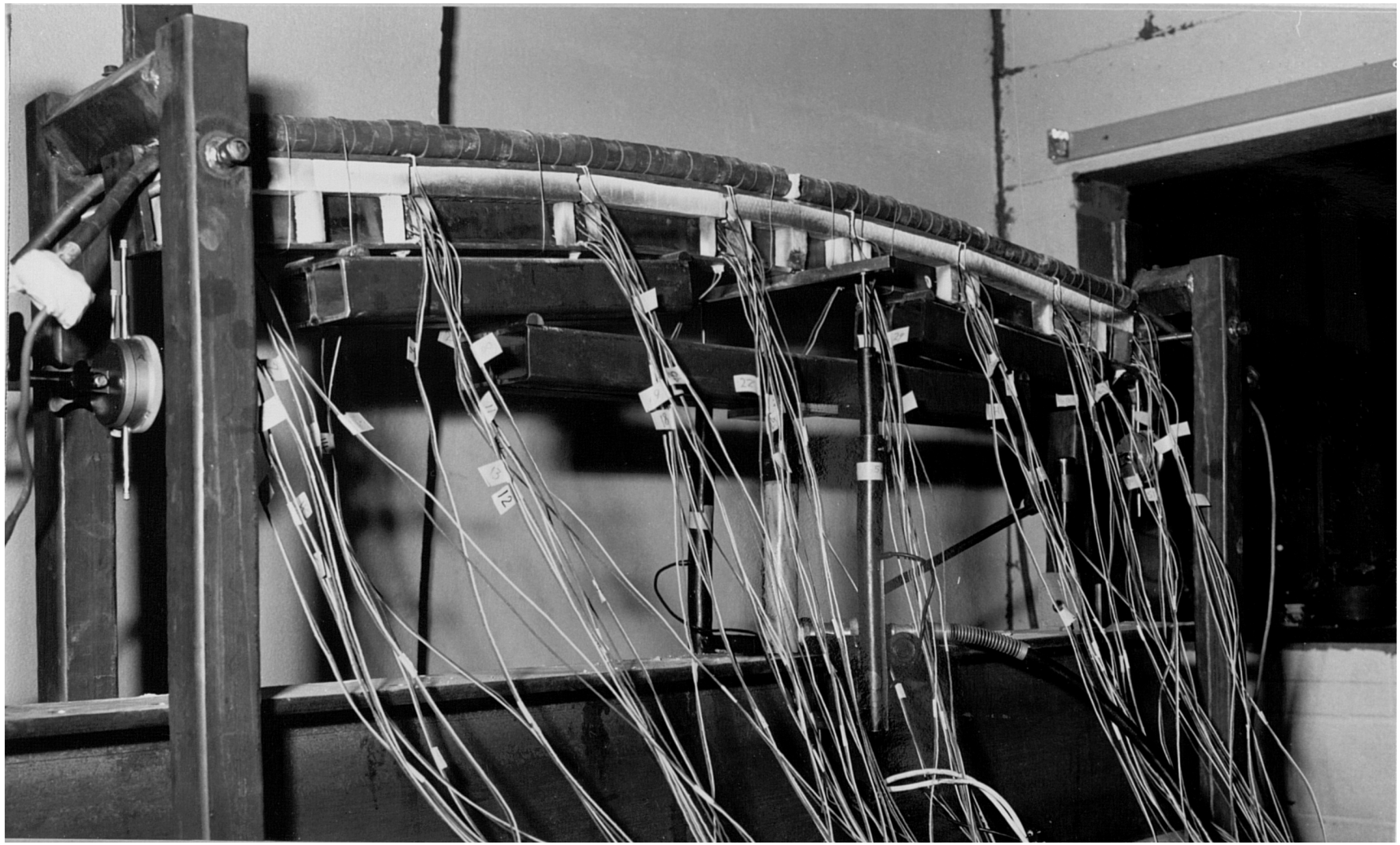

FIGURE 6.10 View of design-loaded beam in apparatus after first heating test

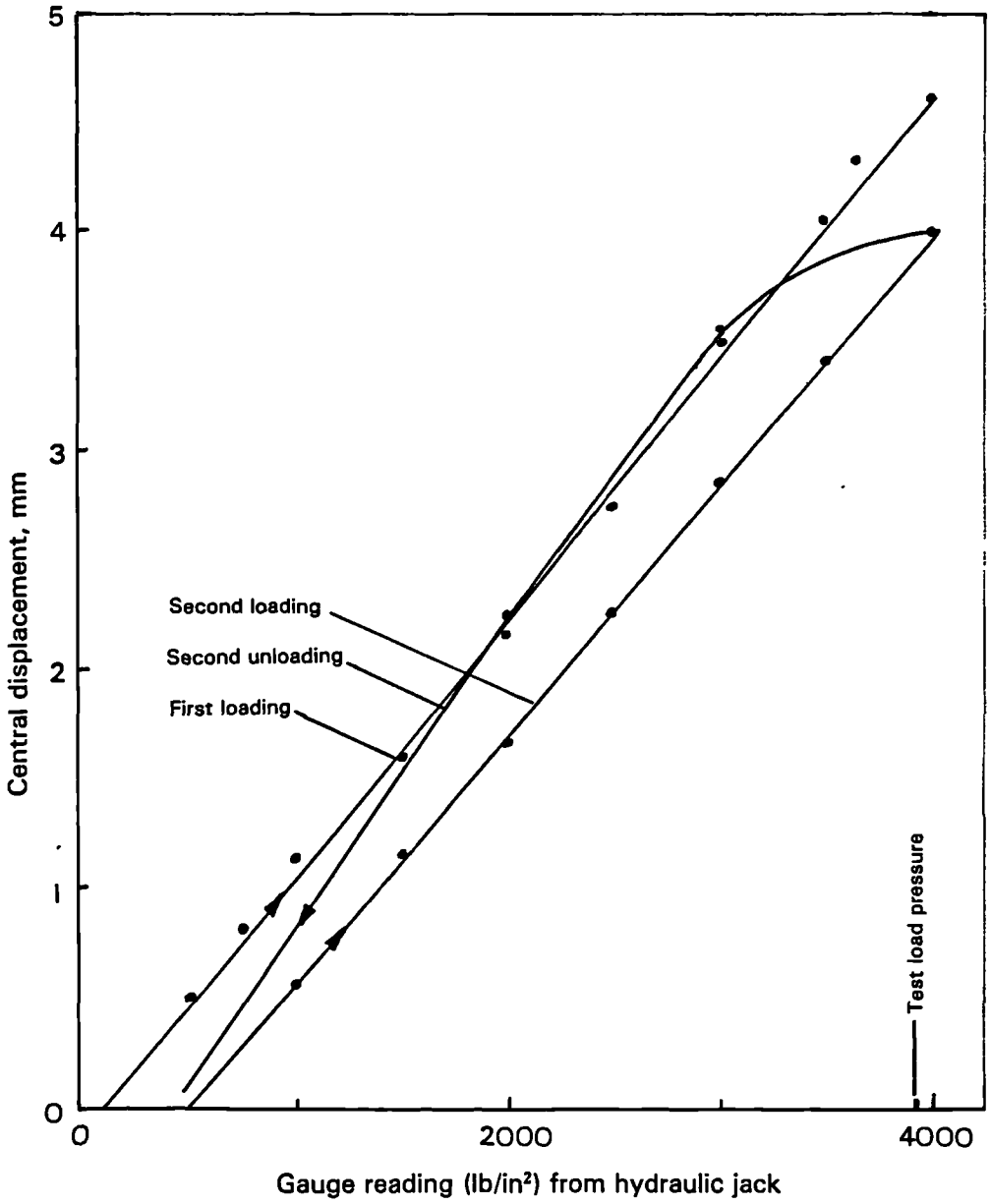

FIGURE 6.11 Room temperature load-displacement curves for design-loaded beam after first heating test

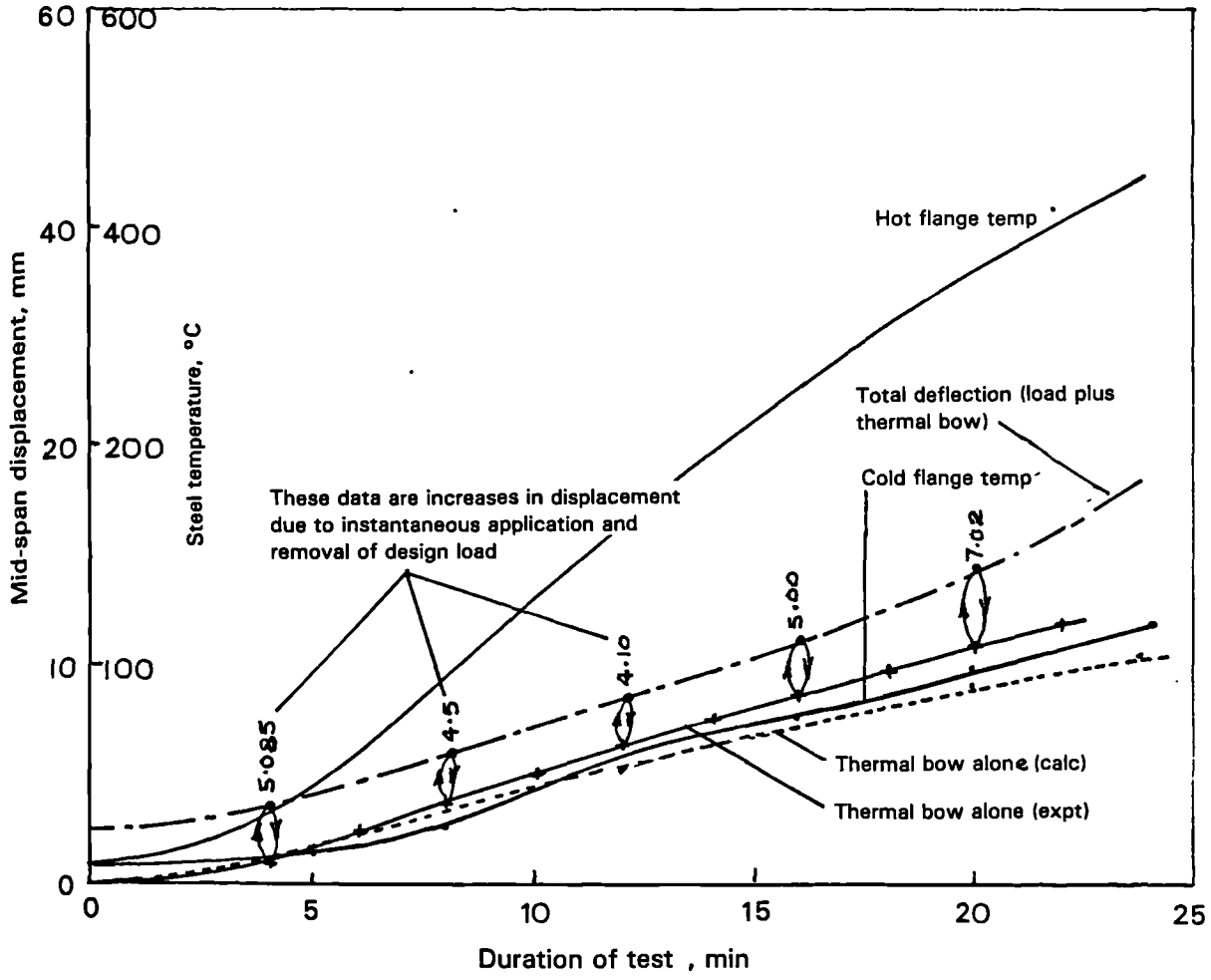

FIGURE 6.12 Variation of central displacement and flange temperatures with time for design-loaded beam in second heating test

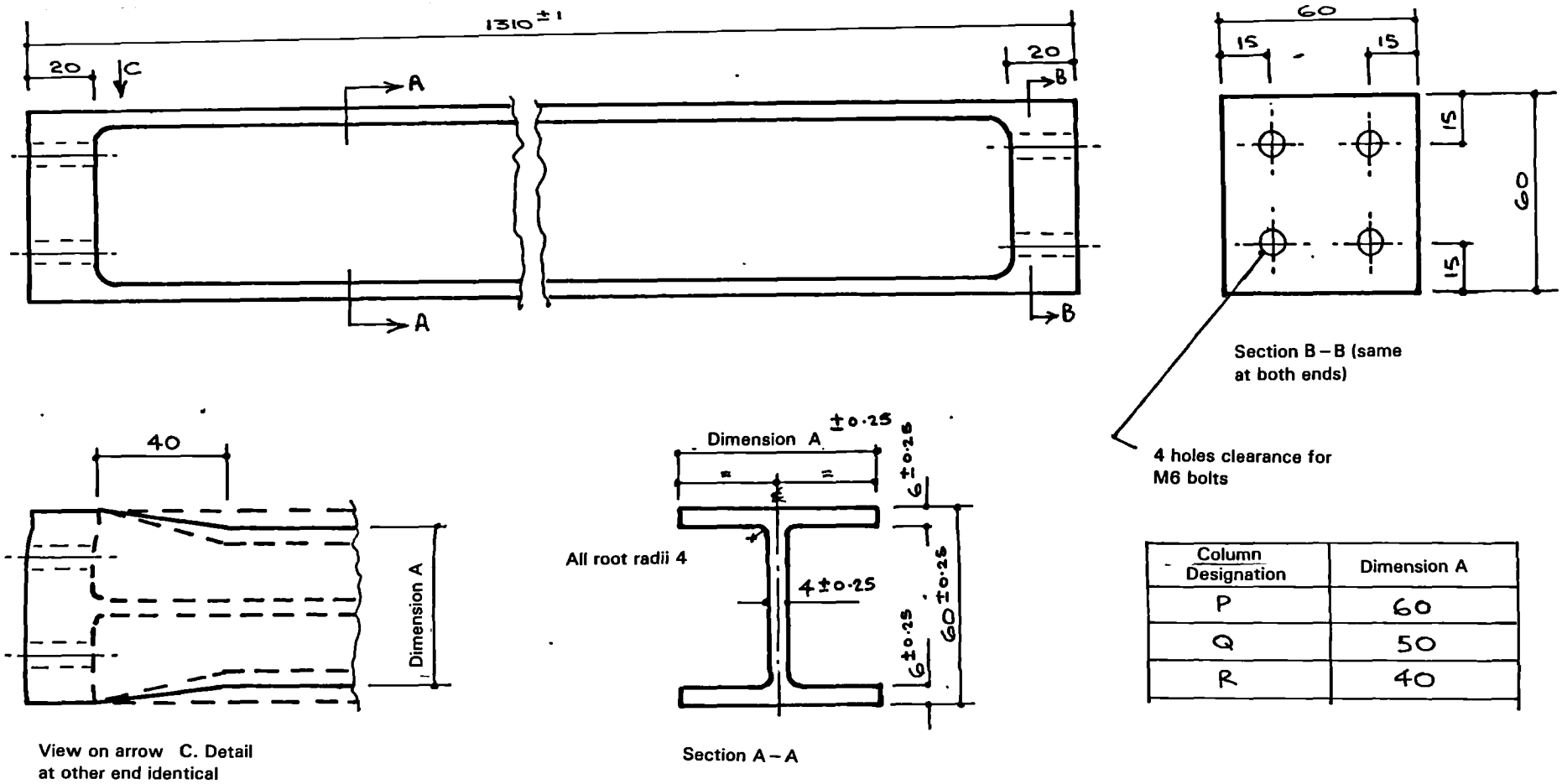

Column Designation	Dimension A
P	60
Q	50
R	40

FIGURE 7.1 Design of model test columns

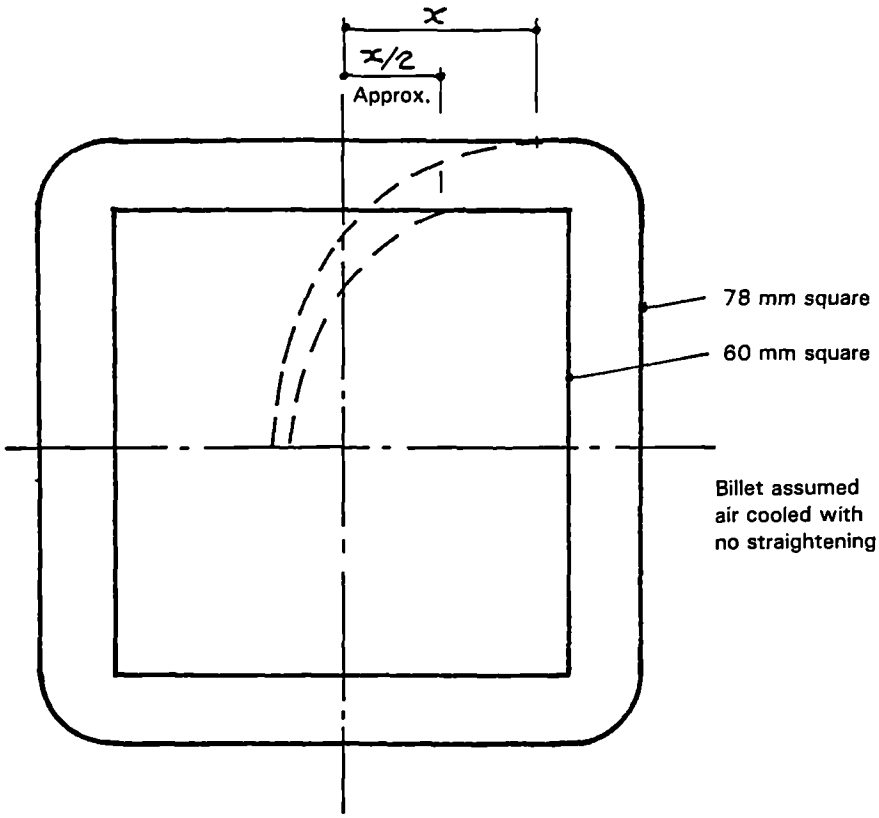

FIGURE 7.2 Estimated residual stress distribution in a steel billet before and after machining, assuming air cooled and no roll-straightening

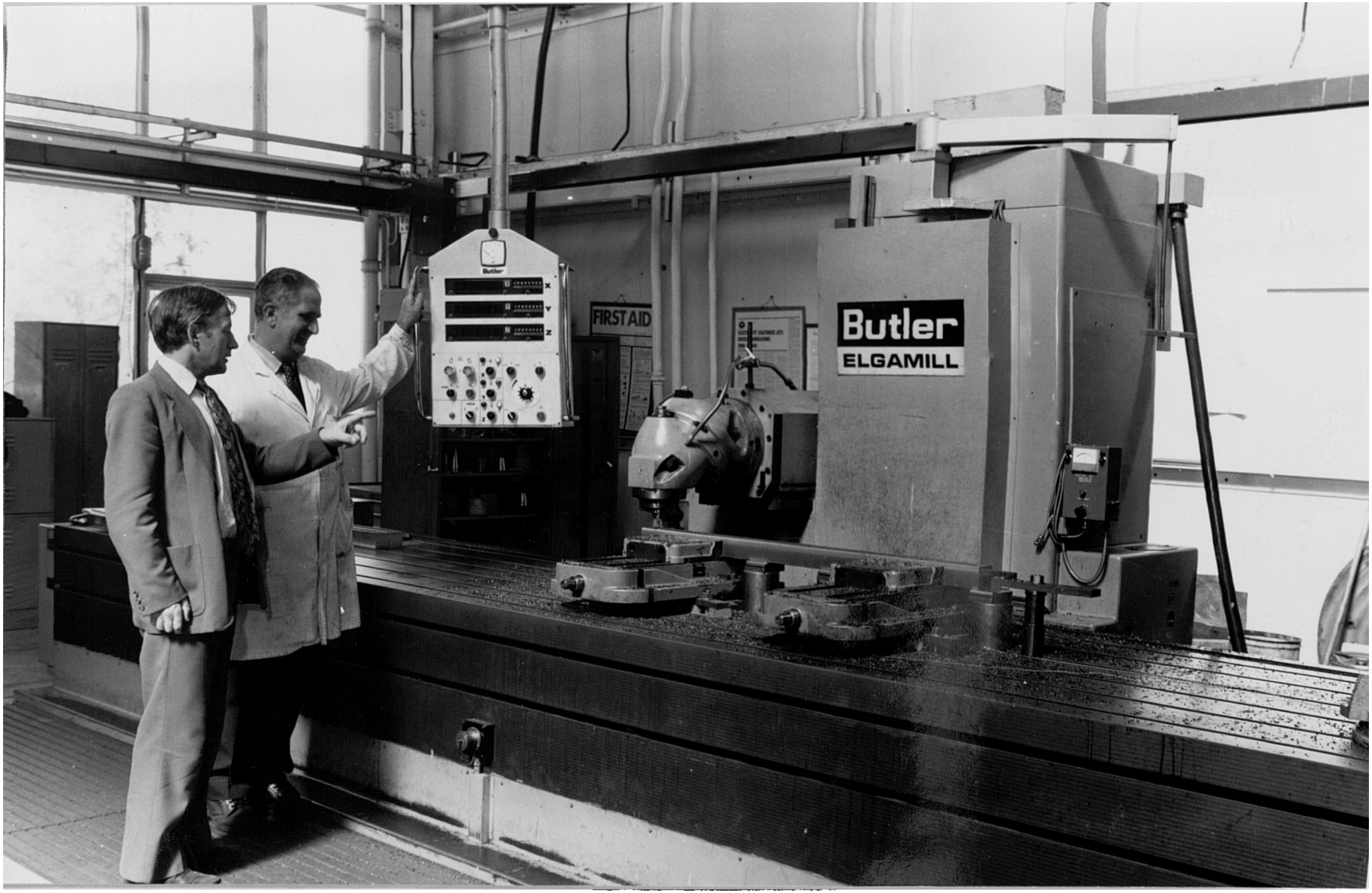

FIGURE 7.3 View of Elgamill used to mill model steel columns

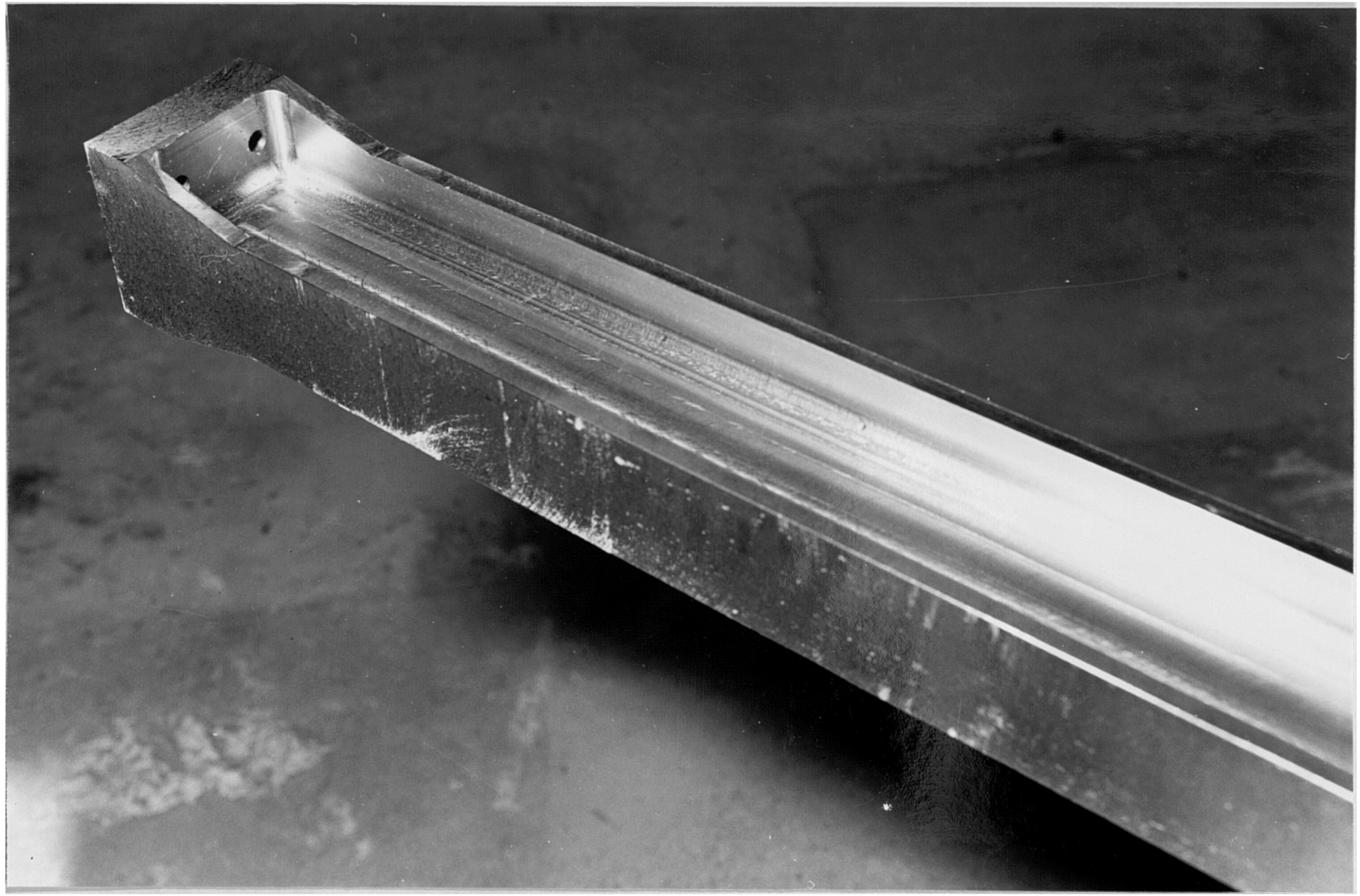

FIGURE 7.4 View of portion of model column after machining

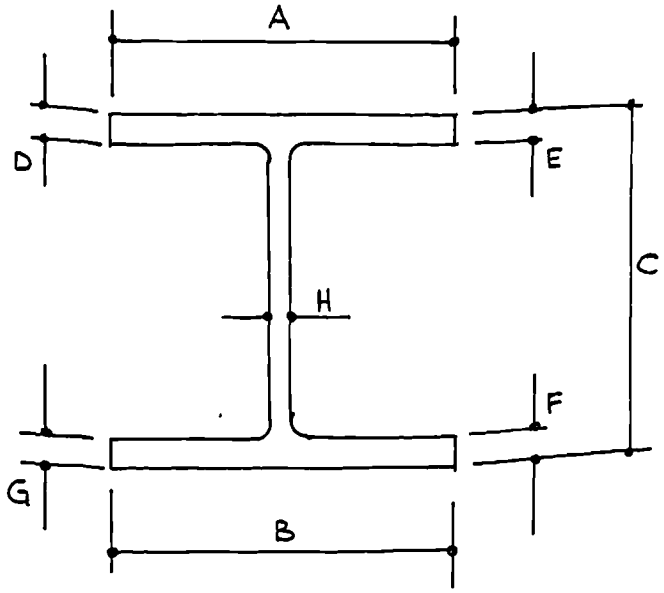

Section dimensions

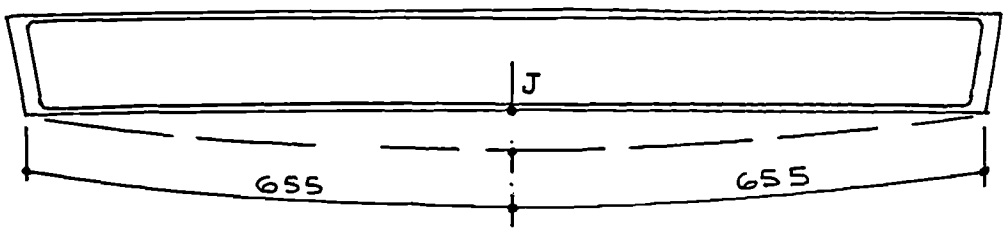

Out-of-straightness, measured in plane of web

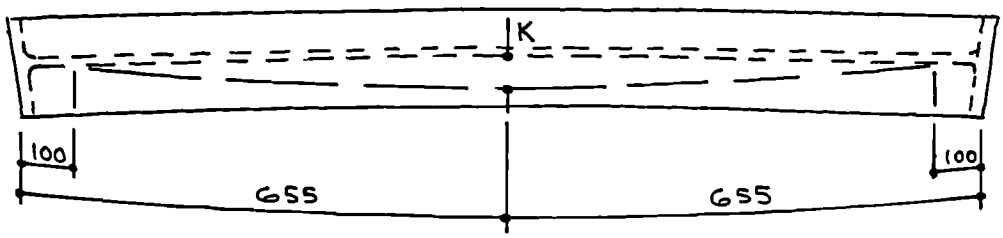

Out-of-straightness, measured in plane of flanges

Notes

i Section dimensions measured at 100 from each end and at centre to accuracy of ± 0.02

ii Dimensions J and K measured at centre of section to accuracy ± 0.1

FIGURE 7.5 Dimensional parameters for test columns

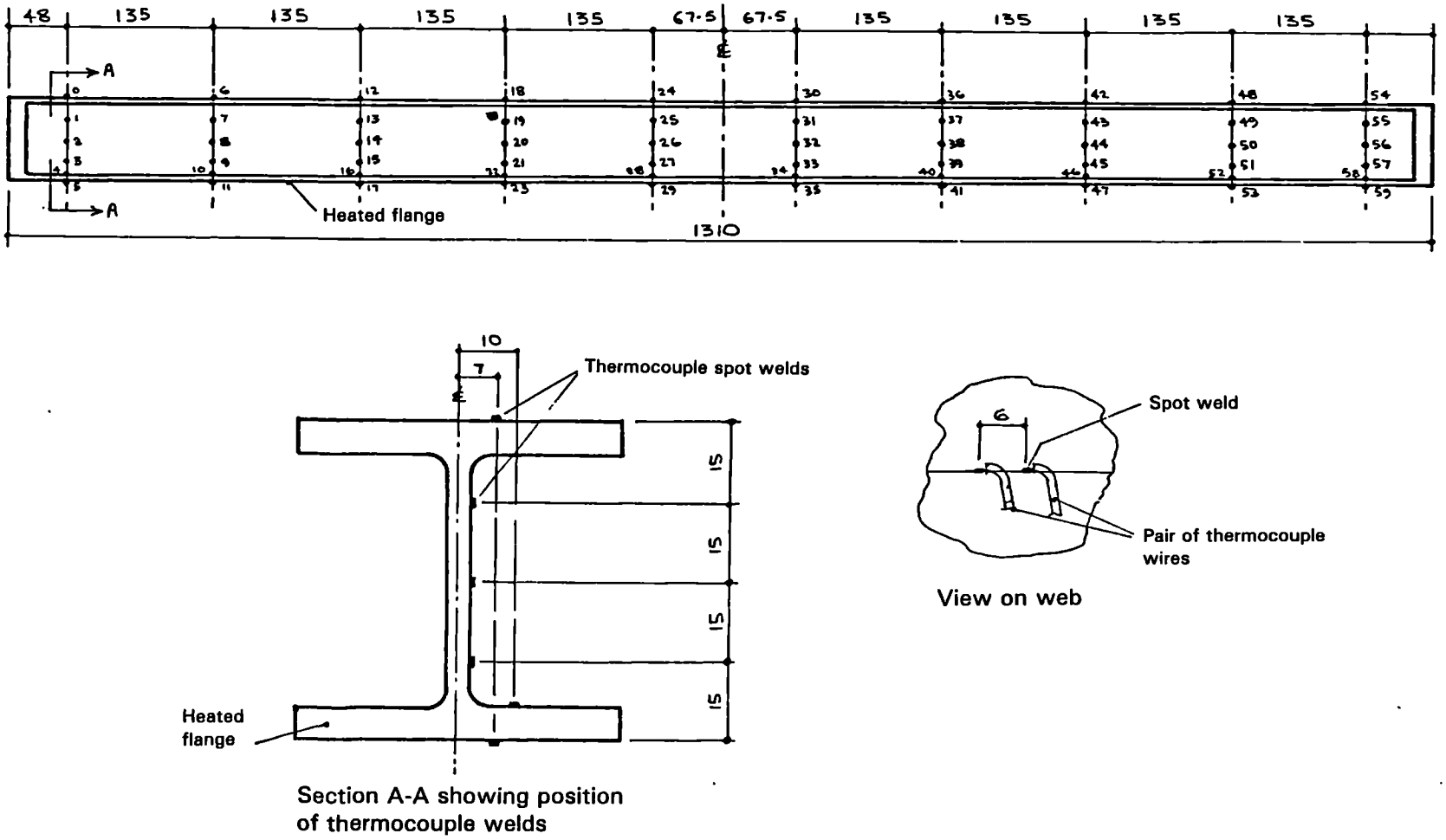

FIGURE 7.6 Positioning and numbering of thermocouples for test columns

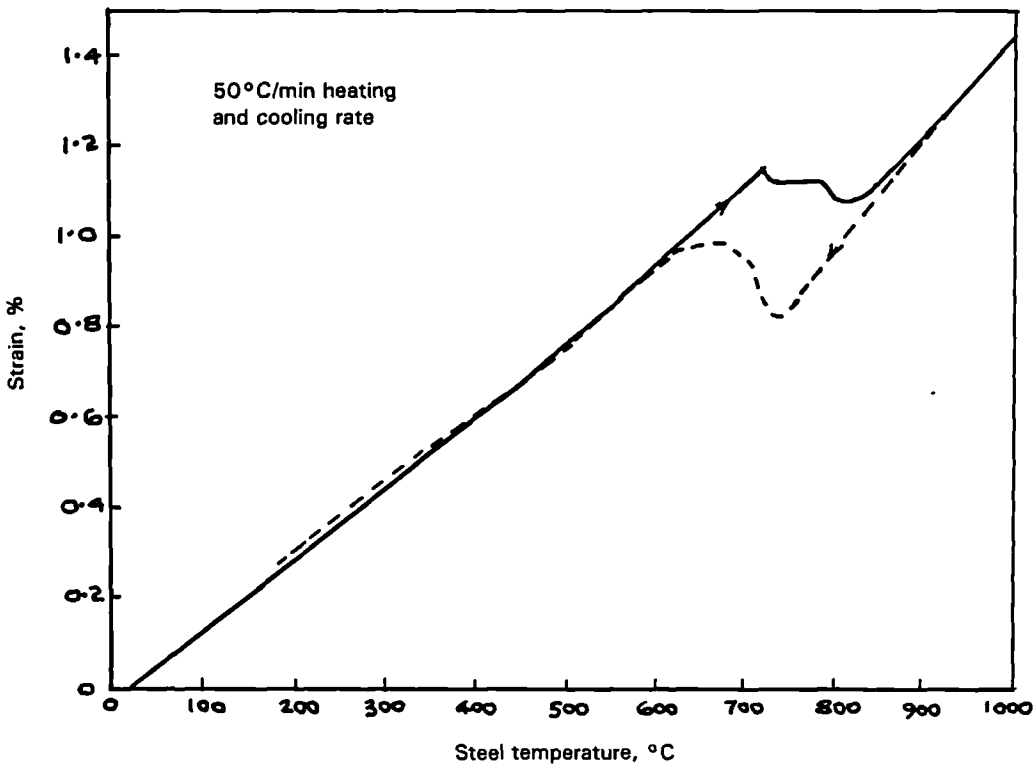

FIGURE 7.7 Dilatometer curves for steel used in test columns

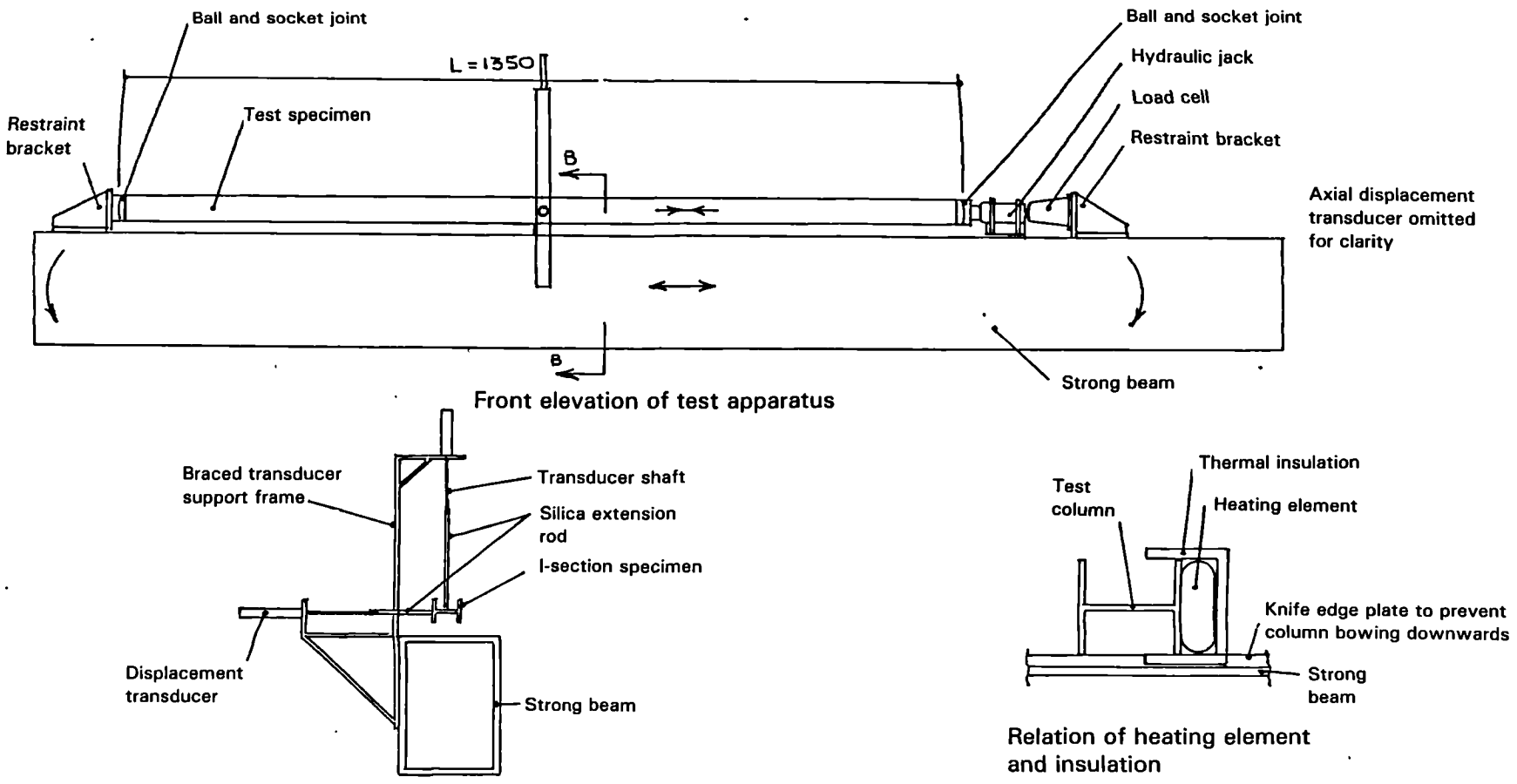

FIGURE 7.8 General arrangement of column test apparatus

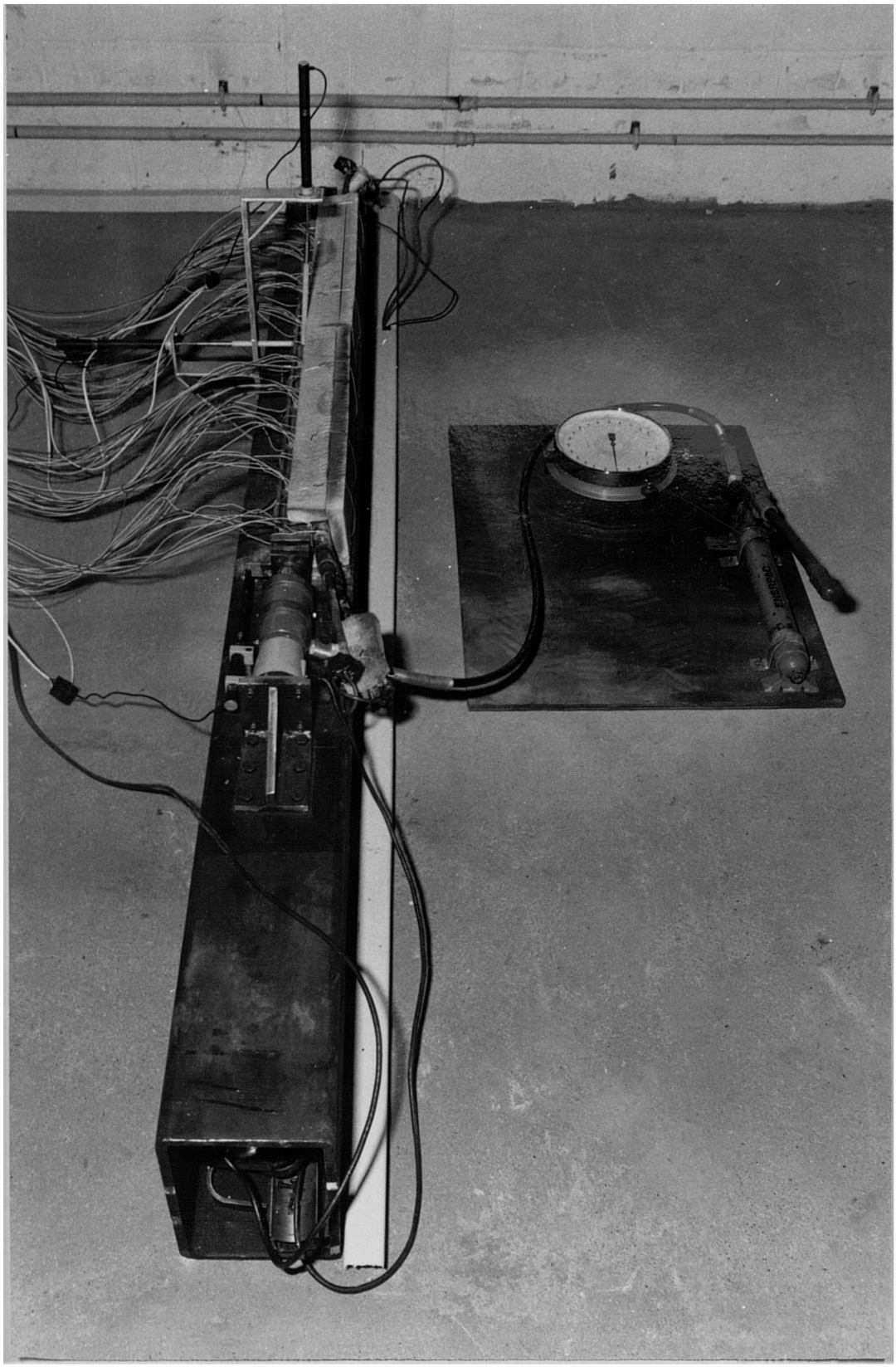

FIGURE 7.9 General view of apparatus with column test in progress

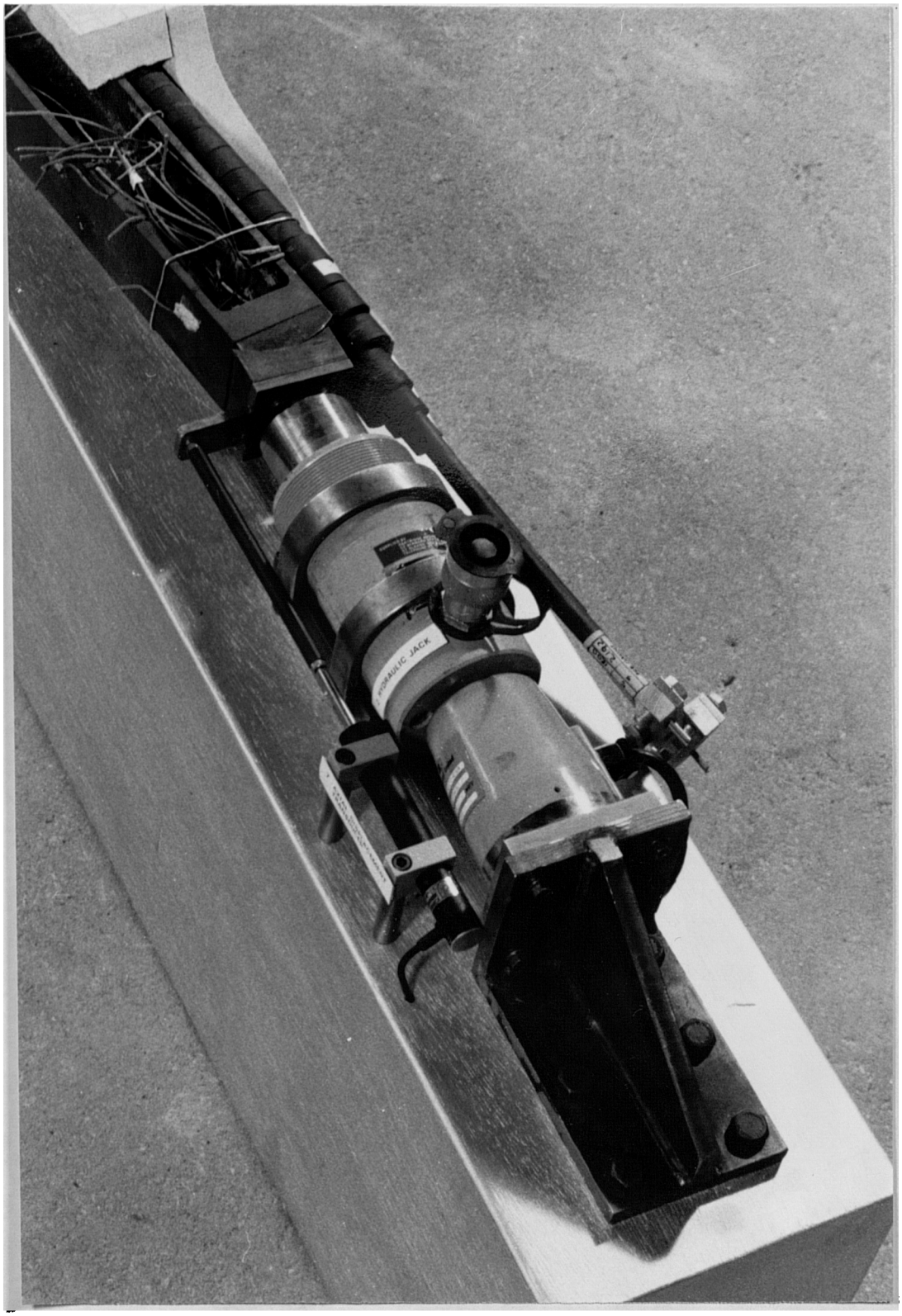

FIGURE 7.10 View of modified axial transducer assembly

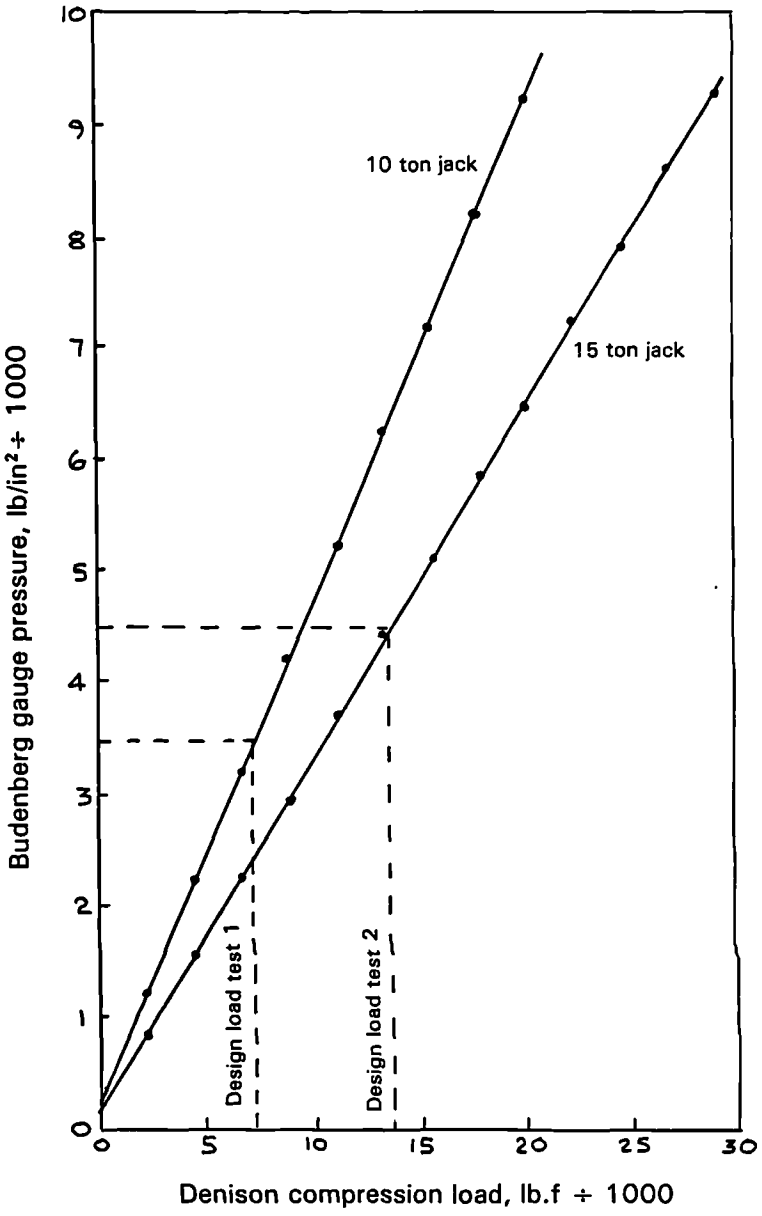

FIGURE 7.11 Calibration curves for hydraulic jacks

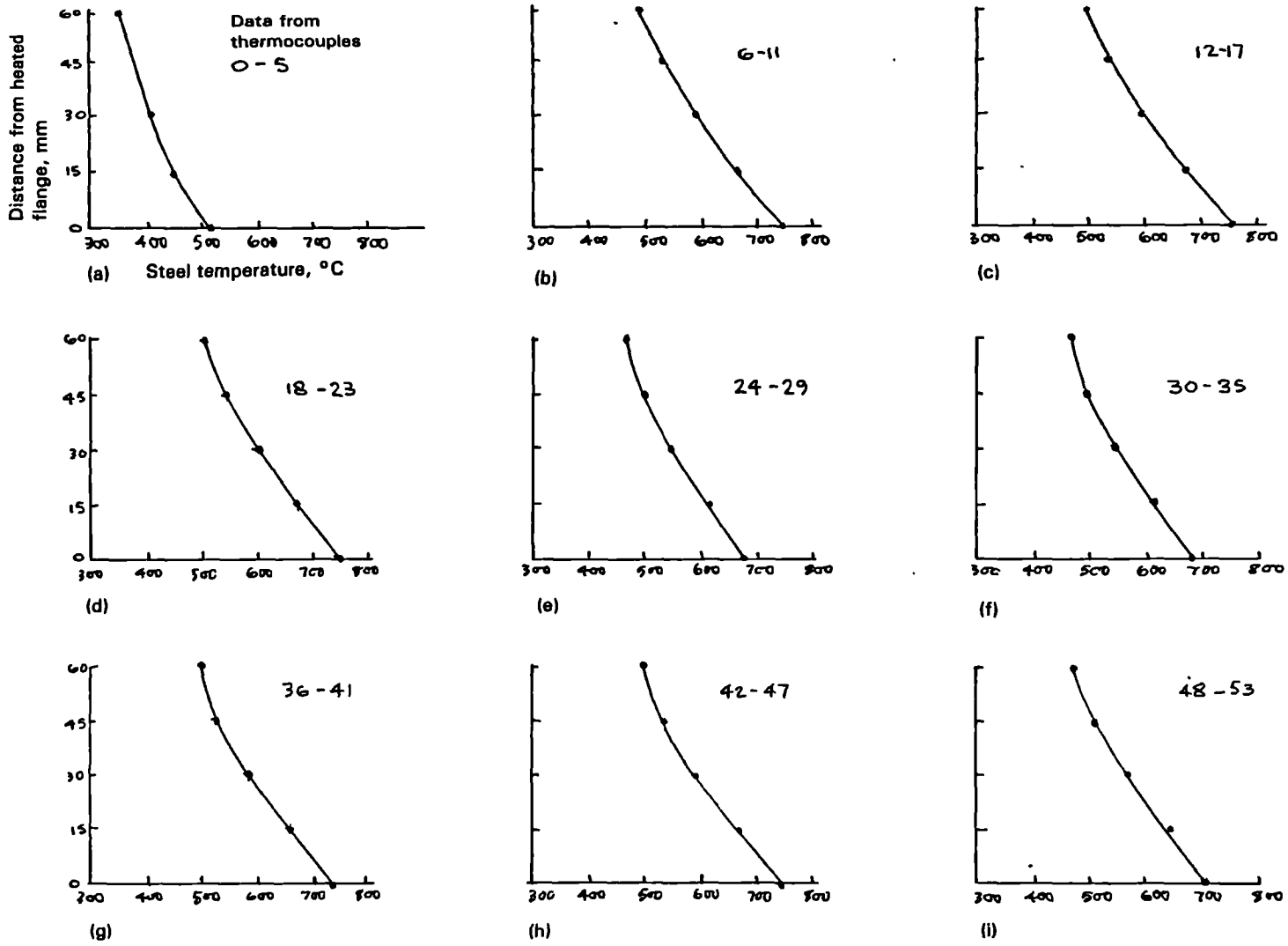

FIGURE 7.12 Temperature profiles in column at 60 minutes, Test 1

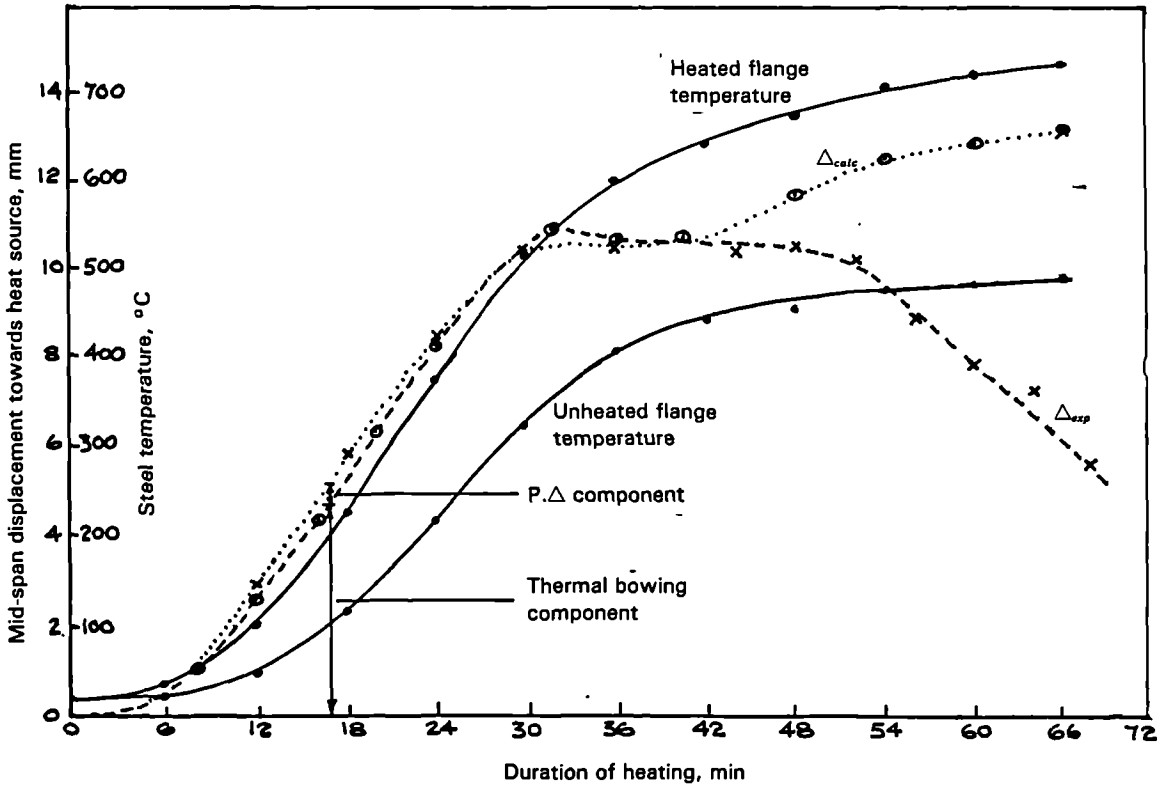

FIGURE 7.13 Comparison of experimental and calculated bowing displacements with flange temperature for column, Test 1

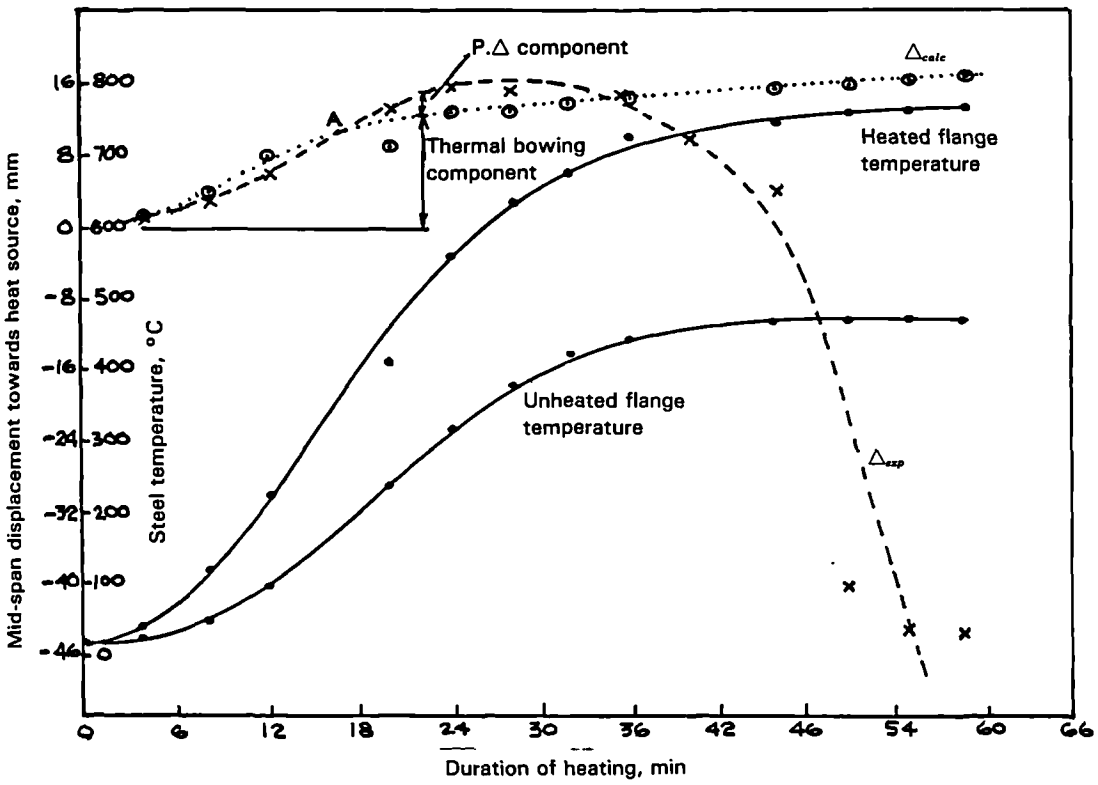

FIGURE 7.14 Comparison of experimental and calculated bowing displacements with flange temperature for column, Test 2

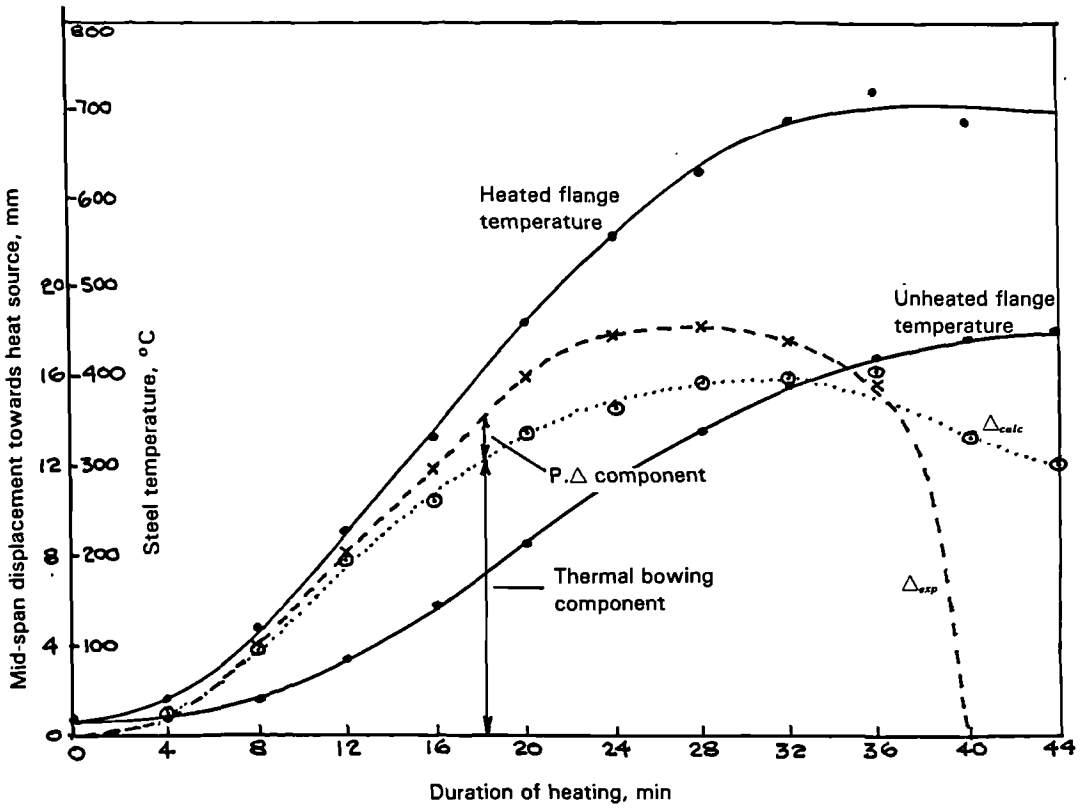

FIGURE 7.15 Comparison of experimental and calculated bowing displacements with flange temperature for column, Test 3

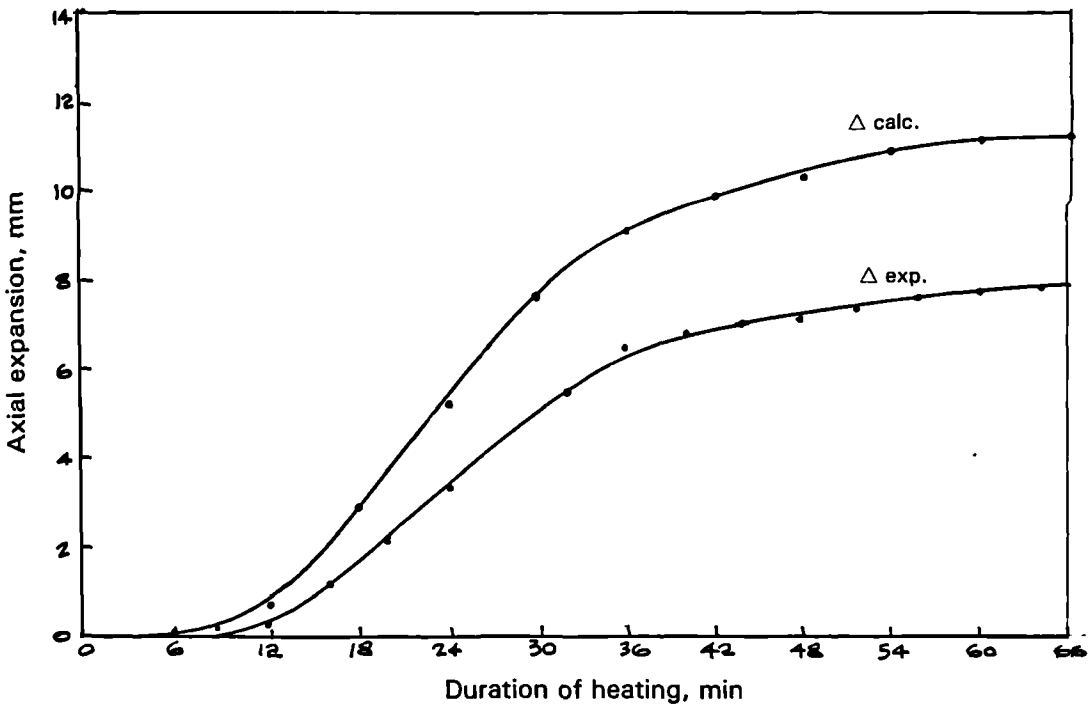

FIGURE 7.16 Comparison of experimental and calculated axial displacements for column, Test 1

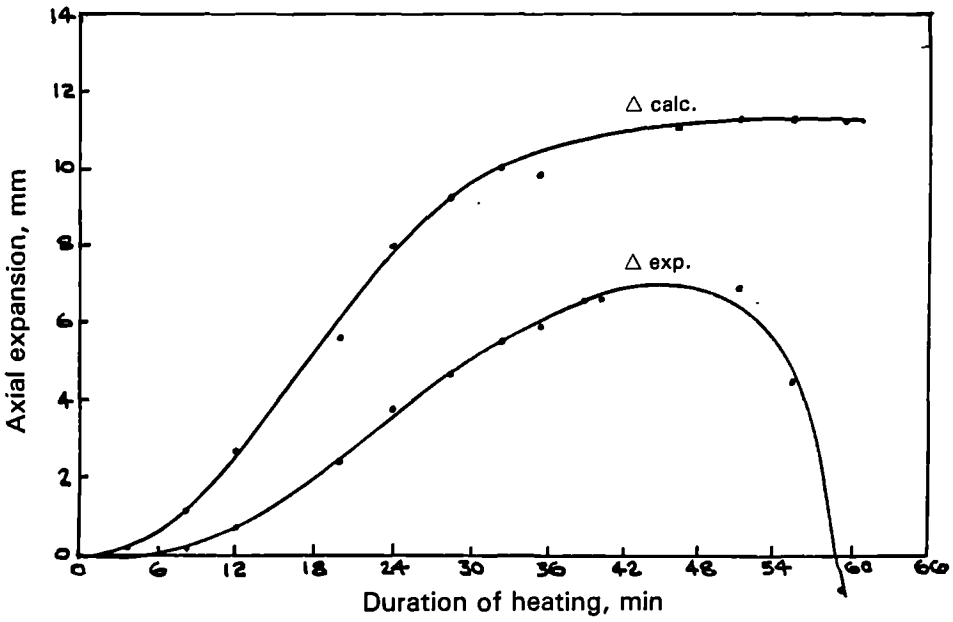

FIGURE 7.17 Comparison of experimental and calculated axial displacements for column, Test 2

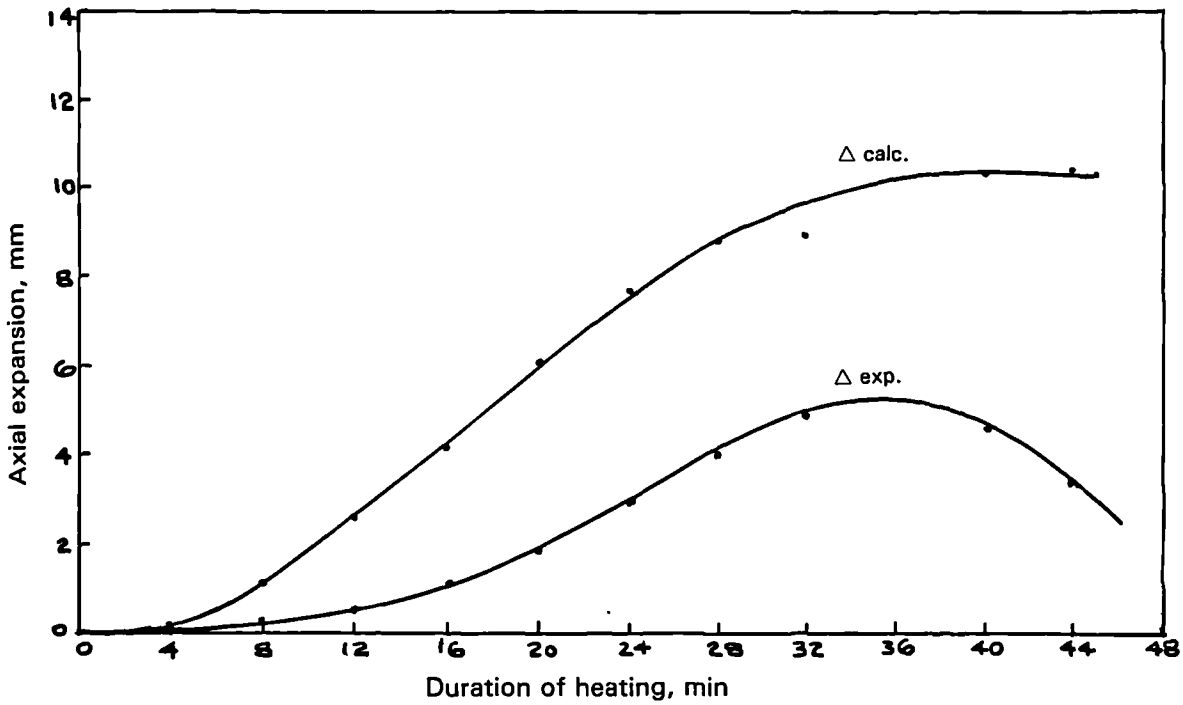

FIGURE 7.18 Comparison of experimental and calculated axial displacements for column, Test 3

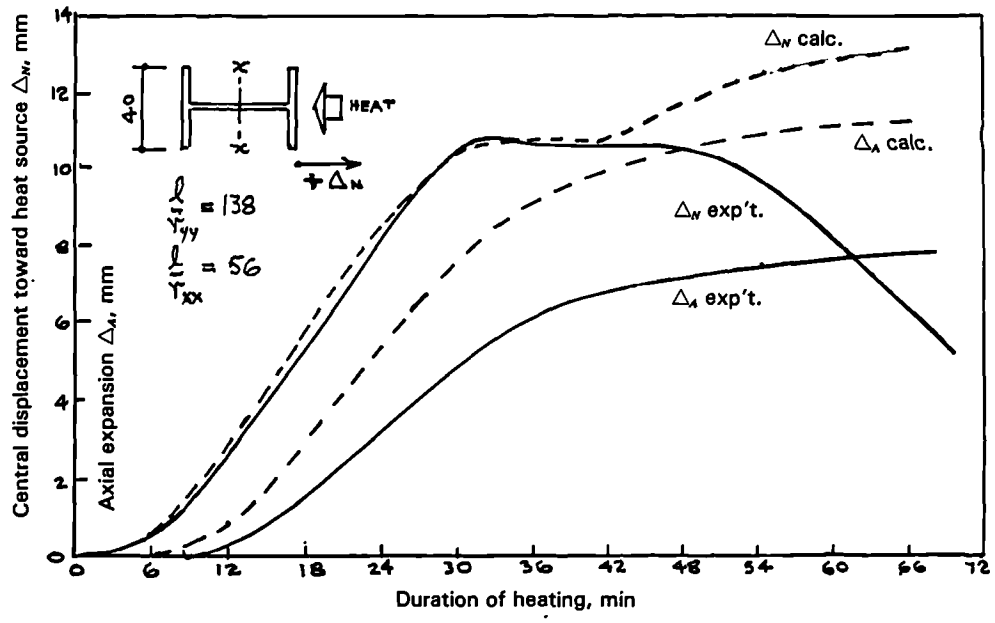

FIGURE 7.19 Comparison of bowing and axial displacements for column, Test 1

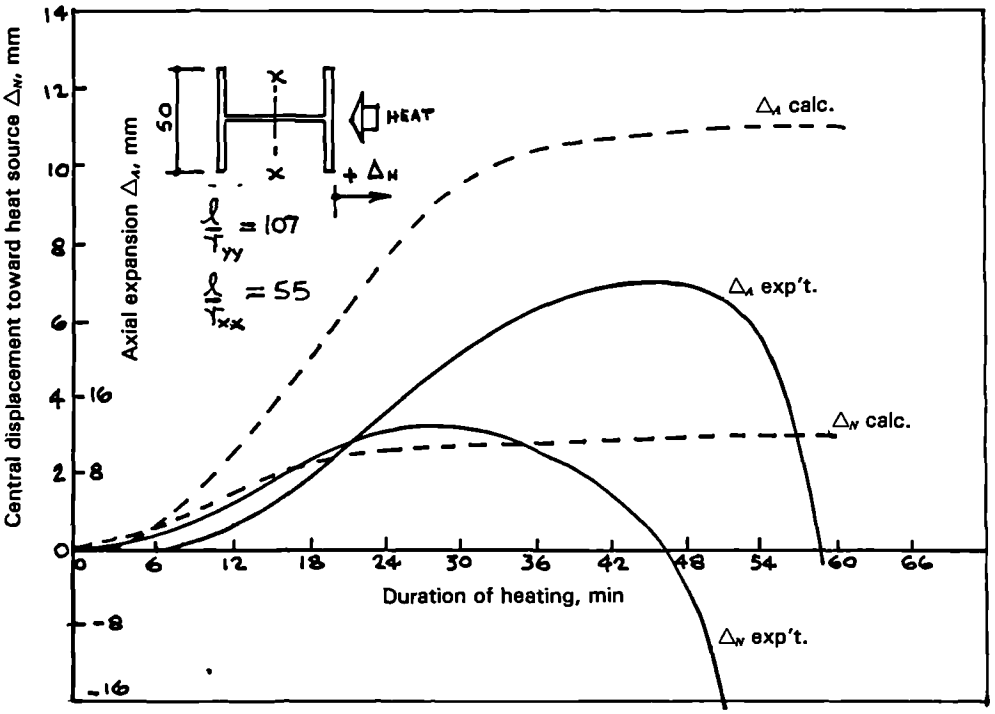

FIGURE 7.20 Comparison of bowing and axial displacements for column, Test 2

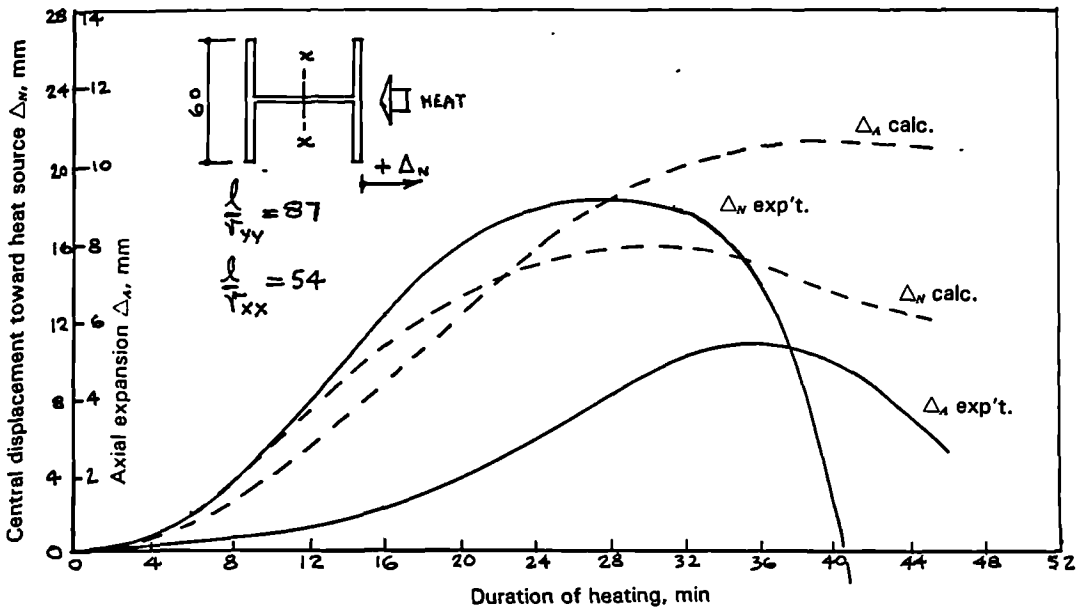

FIGURE 7.21 Comparison of bowing and axial displacements for column, Test 3

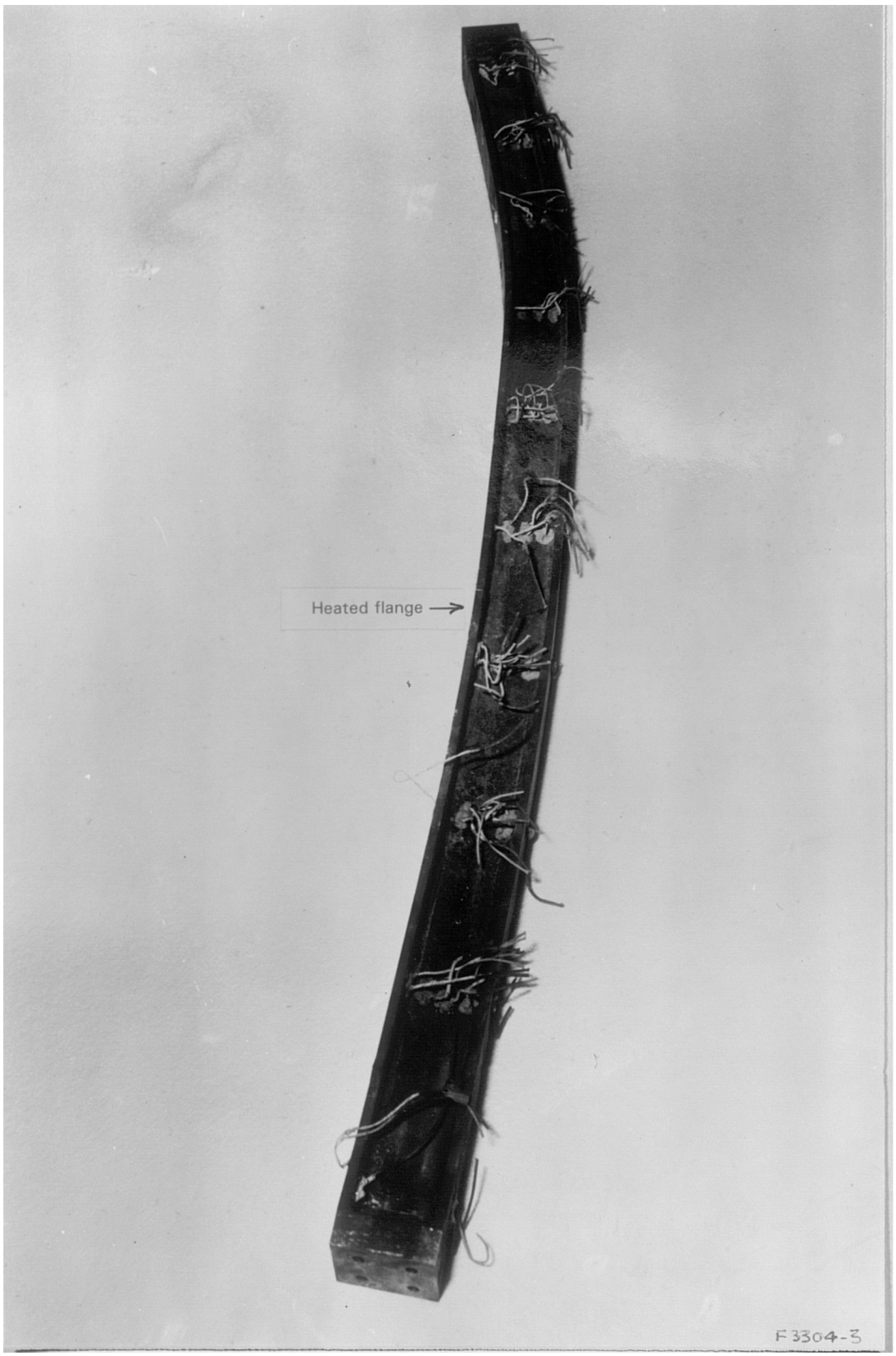

FIGURE 7.22 Deformed shape of model column after test showing reverse direction bow

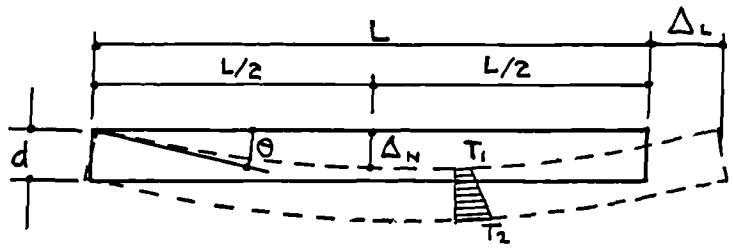

$$\Delta_N = \frac{\alpha L^2(T_2-T_1)}{8d} \qquad (a)$$

$$\Theta = \frac{\alpha L(T_2-T_1)}{2d} \qquad (b)$$

$$\Delta_L = \alpha L \left(\frac{T_1+T_2}{2}\right) \qquad (c)$$

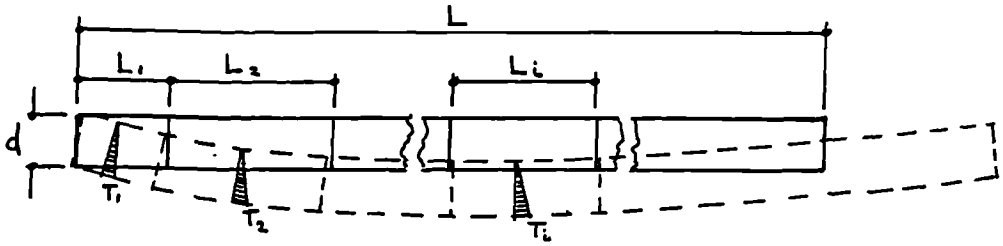

$$y = \Theta_o x + \frac{\alpha}{2d} \sum (T_i - T_{i-1})\left(x - \sum_1^{i-1} L_i\right)^2 \qquad (d)$$

$$\text{for } \sum_1^{i-1} L_i < x < \sum_1^{i} L_i$$

$$\Theta_o = -\frac{\alpha}{2dL} \sum (T_i - T_{i-1})\left(L - \sum_i^{i-1} L_i\right) \qquad (e)$$

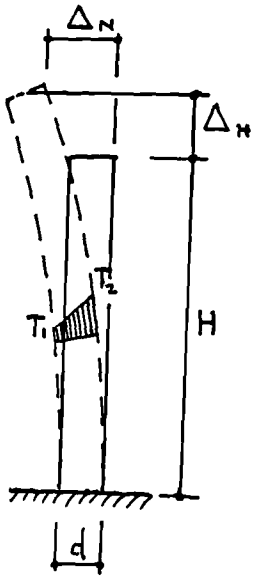

$$\Delta_N = \frac{\alpha H^2(T_2-T_1)}{2d} \qquad (f)$$

$$\Delta_H = \alpha H \left(\frac{T_1+T_2}{2}\right) \qquad (g)$$

FIGURE 8.1 Summary of thermal bowing relationships

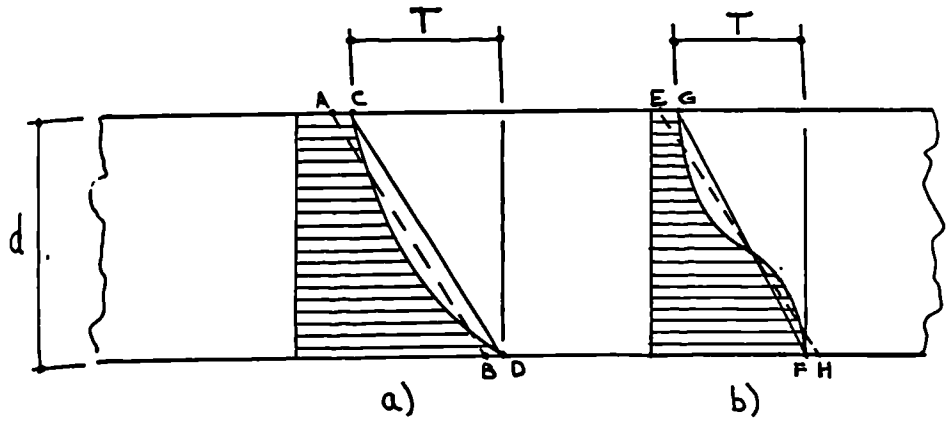

FIGURE 8.2 Comparison, for different curvi-linear temperature profiles across member section, of line drawn between surface temperatures and best-fit line.

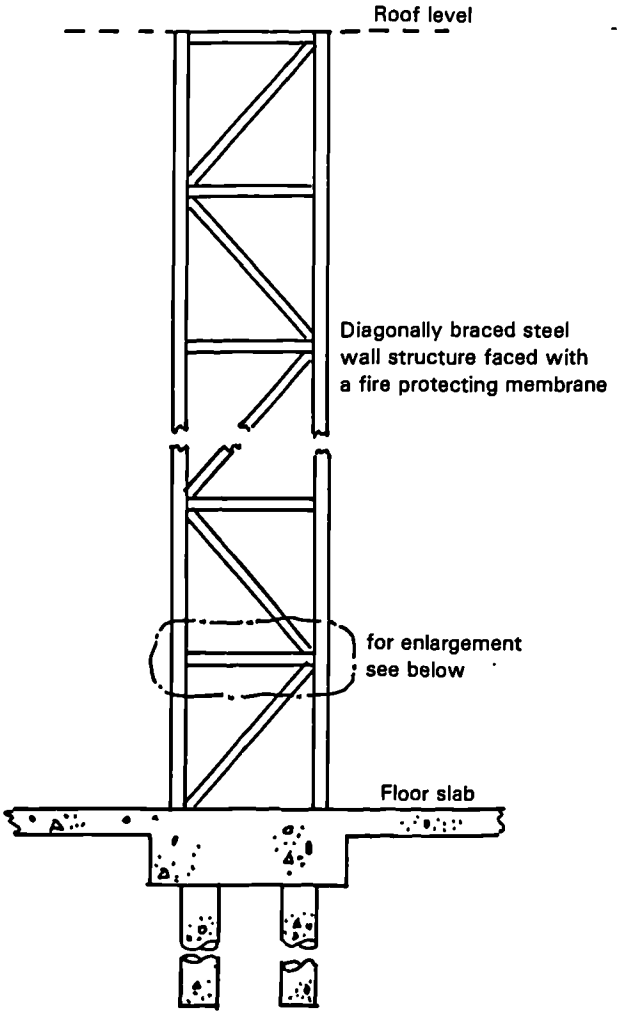

a) Vertical section through tall fire wall structure.

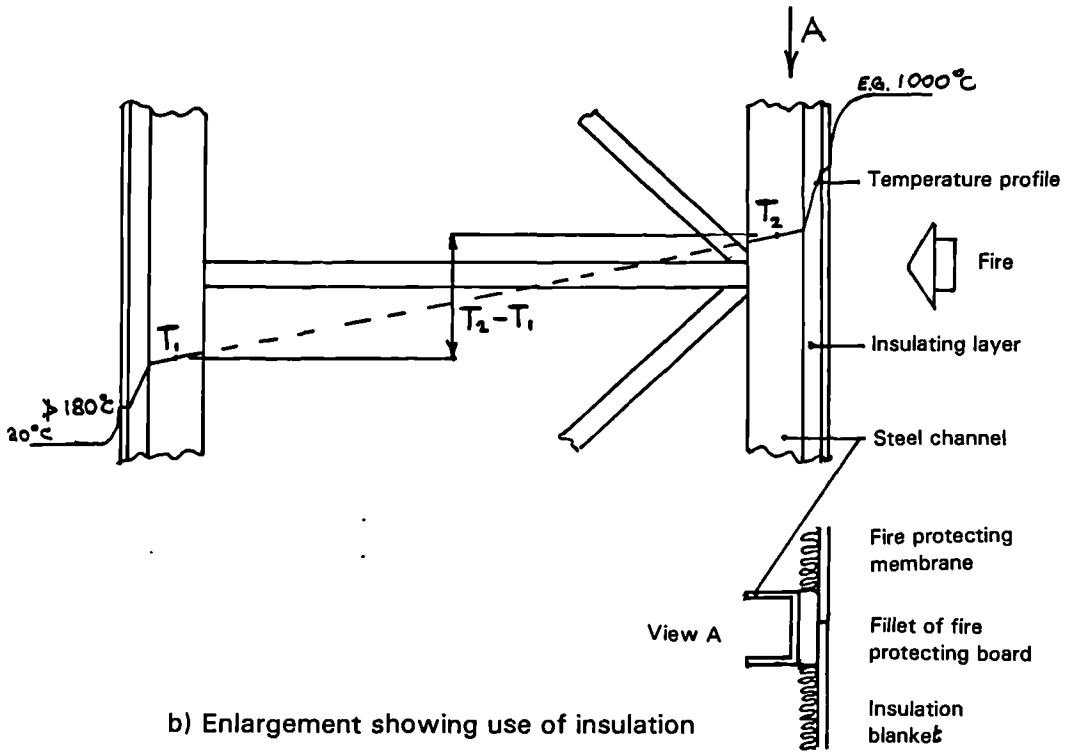

b) Enlargement showing use of insulation

FIGURE 8.3 Reduction of thermal bowing of a tall fire wall structure

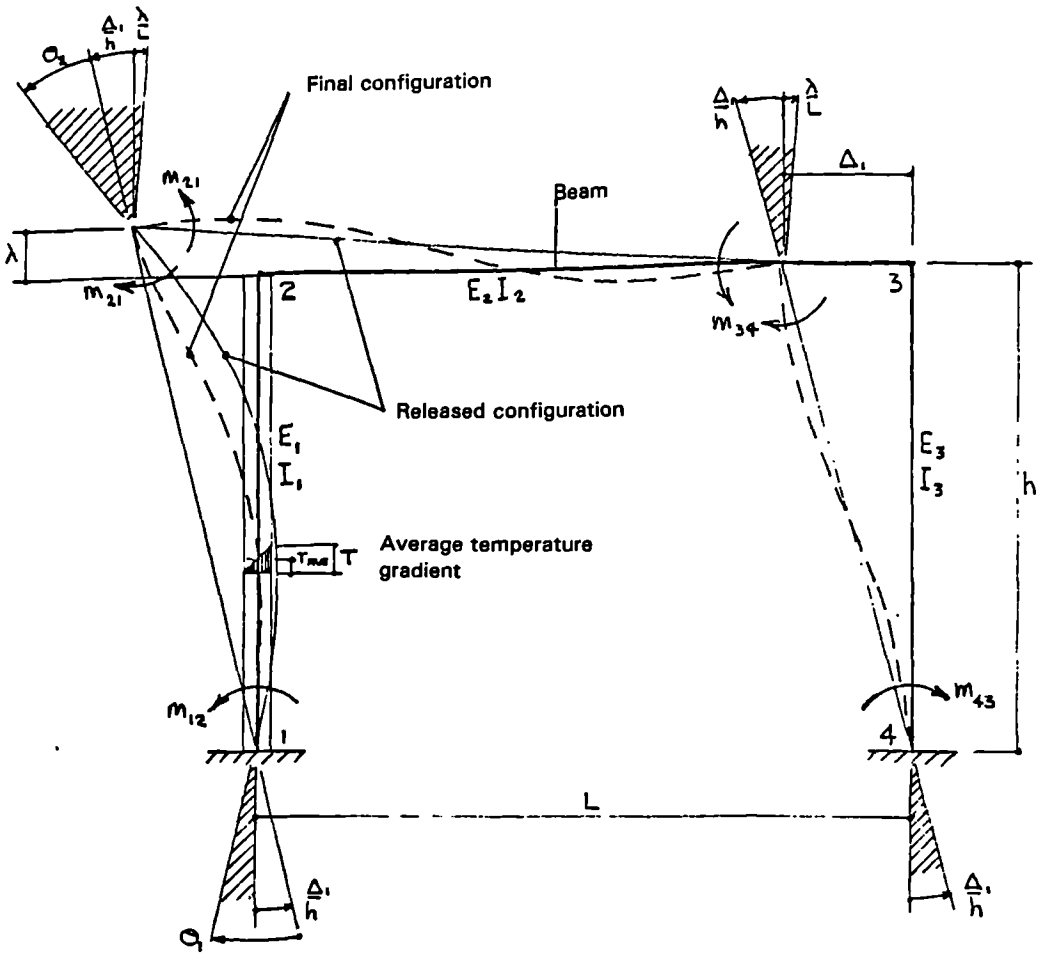

FIGURE 8.4 Configuration of a portal frame with one column having a temperature gradient across its section

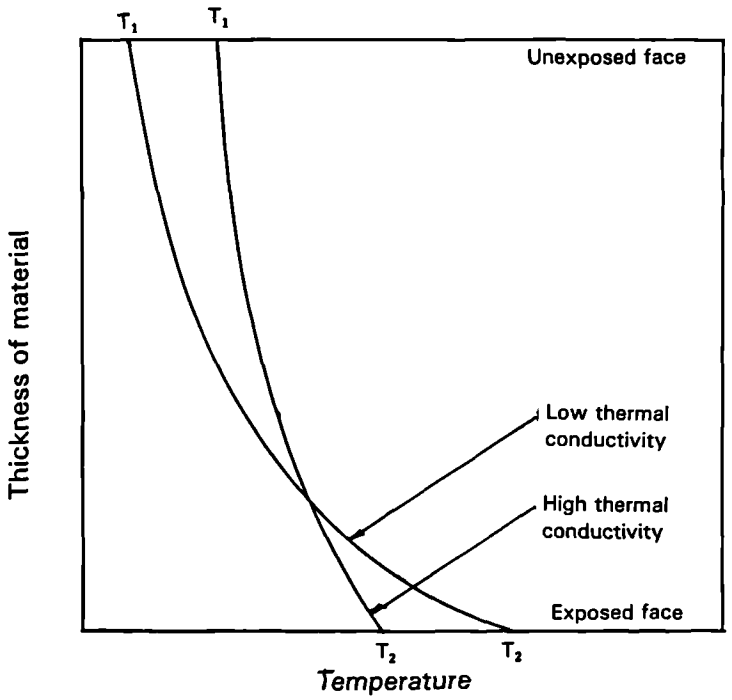

FIGURE 8.5 Temperature profiles in materials having different values of thermal conductivity when heated on one face

APPENDIX 1

NOTES ON THE 'PAFEC' FINITE ELEMENT PROGRAM, AND VALIDATION OF THE PHASE TRANSFORMATION SOFTWARE

In this Appendix the limitations of simple theory applied to the experiments covered in this thesis are summarised. The advantages of the finite element method (FEM) are then stated, and reasons given for the adoption of a commercial FEM program called PAFEC. After describing the PAFEC suite of programs, the reasons for extending the capability of PAFEC are given, together with a validation of the phase transformation software.

1.1 Limitations in the application of simple theory

It has been shown (3.2 and 4.3.1) that the overall displacements of a steel member, free of external loads and restraints but heated so that it attains a curvi-linear temperature distribution across its section which does not vary with length, can be calculated with reasonable accuracy using a simple formula if the temperatures of the heated and unheated faces are known. However, the application of the simple theory to steel members with temperature gradients which vary along the length has been shown to be tedious (4.2.2).

It has also been shown that the elastic displacements of a loaded steel beam at elevated temperature can be calculated from simple bending theory using an appropriate reduced elastic modulus (6.8.6). Where a frame attains different temperatures along the length of each member it is again possible to predict elastic displacements by considering each member as a number of finite lengths each having a temperature gradient

which is uniform along the finite length, although an example of the method is not given herein.

However the range of problems that can be solved using the simple theories mentioned above are limited. For example, to predict the displacement-time history of a steel beam progressively heated from room temperature to near its melting point it is necessary to consider displacements due to plasticity and creep in addition to elastic, and, if appropriate, thermal bowing displacements. Since, even in a simply supported beam, the bending and shear stresses vary across and along the section, it follows that any analysis which takes account of plasticity and creep must be made assuming that the member may be divided into small (finite) relatively simple shapes (elements) each having simple loading and simple stresses so that equations for equilibrium of forces and compatibility of displacement at the boundaries of these elements can be solved. This is the basis of the FEM.

1.2 The choice of the PAFEC finite element program

For a member whose geometrical and mechanical properties are changing with temperature and time, and, more importantly, where the mechanical properties are, at any instant, different across the section and along the length of the member, a suitably rigorous and valid theoretical approach is one based on the use of finite elements. It was considered not feasible nor desirable to develop a program from scratch since this would require many man hours of effort and seemed, at the time, pointless in view of the existence of commercially available programs.

It was desirable that any commercially available program should be 'user friendly' so that time taken for data input should be minimised and the

interpretation of output data made easy. For a number of reasons it would be desirable to have access to a program already installed on the main frame computers at the Building Research Station (BRS) of the Building Research Establishment. It was found that colleagues at BRS were already using the PAFEC program where there were good reports on its ease of use for structural analyses at ambient temperatures.

PAFEC is a finite element computer program developed by PAFEC Ltd, Strelley Hall, Strelley, Nottingham. The software was initially installed on PRIME main frame computers at BRS Garston but it now runs on the VAX computers. Access to it at Fire Research Station, several miles away, is via a Modem dataline.

The theoretical basis of PAFEC is given in the 'PAFEC 75' Theory and Results Manual published in 1975. The instructions on data preparation are given in the 'PAFEC 75 Data Preparation Manual' published in 1975 which was updated in 1982 with a 'PAFEC Data Preparation User Manual: Supplement for Level 4'. A new level was introduced in 1985 for which a new manual 'Data Preparation User Manual Level 5' was produced.

Apart from minor editing of subroutines in PAFEC, the user is not allowed to make modifications/additions to the program - such activities are undertaken by the PAFEC development team, either as part of the general development of PAFEC for the good of all users, or on a contract basis if the timescales are short or the development work is of narrow application.

Upon examining the capability of PAFEC for application to structural problems at elevated temperatures it was found that whilst it could

tackle problems in the elastic range in which material properties, such as modulus of elasticity and coefficient of linear expansion, varied continuously with temperature, the standard software could not be used for (a) plasticity analyses where stress/strain relationships varied with temperature, and (b) discontinous variation of thermal expansion which occurs with steel above 720°C. A contract was therefore placed with PAFEC Ltd to provide program modifications which would:

(a) allow the plasticity facility to be used on input of yield stress and plastic slope data which varied with temperature and

(b) allow the phenomenon of phase transformation to be catered for by input of thermal strain and temperature coordinate data (for use in elastic analyses).

1.3 The PAFEC suite of programs

The PAFEC finite element suite consists of 10 separate computer programs which, when executed sequentially, gives a complete engineering analysis. Each of these programs is known as a phase of PAFEC and Table 1 gives a synopsis of the operations undertaken by them.

Table 1 shows that some phases are clearly more important, from the view point of obtaining printed results, than others. Phase 1, used for reading-in and data expansion, is an essential part of the whole process. Phases 4, 6 and 7 can be seen to play an equally important role. These four phases form the minimum requirements for any analysis where the structure is fully defined. The remaining six provide the many extra facilities available such as a complete passive graphics capability, automatic mesh generation and element stressing where required.

Phase	Short description	Detailed description
1	Read	Data modules are read in, default values are inserted and the modules are placed onto backing store. The NODES module is expanded so that all mid-side nodes are included.
2	PAFBLOCKS	Any PAFBLOCK data is replaced by the full nodal coordinate and topological description of the complete mesh of elements.
3	IN.DRAW structure	The structure itself is drawn. At this stage it is not possible to show any results such as displacements, stresses or temperatures since these have not yet been evaluated.
4	Pre-solution housekeeping	In this phase the constraints on the problem are considered and a numbering system for the degrees of freedom is derived.
5	IN.DRAW constraints	This phase is very similar to phase 3 except the constraints which have been applied are shown. Conversely the degrees of freedom can be indicated on a drawing.
6	Elements	The stiffness (or other such as conductivity, mass etc) matrices of all the elements are found and put onto backing store.
7	Solution	The system equations are solved for displacements, temperatures or whatever happens to be the primary unknowns in the problem being tackled.
8	OUT.DRAW displace-ments	The primary unknowns in the problem (ie displacements or temperatures) are drawn.
9	STRESS	The stresses are found.
10	OUT.DRAW	Stress contour, stress vector plots etc are produced.

Table 1 Summary of operations for each of the PAFEC phases

Since phases 1, 4, 6 and 7 are essential, these are automatically included. If, however, there is no DATA module present describing any loading conditions, the run will not continue beyond phase 4. For phase 2 to be entered automatically a PAFBLOCKS module must be present; for phases 3 and 5 an IN.DRAW module has to appear; for phases 8 and 10 and OUT.DRAW or GRAPH module and lastly, for phase 9, a STRESS.ELEMENTS module.

As indicated above the data file comprises a number of input data modules. Their use is fully explained in the Data Preparation Manuals.

In addition a CONTROL module is needed. This guides a job through from beginning to end. It begins with the word CONTROL and ends with CONTROL.END. In between, CONTROL statements may be included which either describe the type of problem to be solved, eg PLASTIC, or control and sequence the calculations.

For a prismatic member such as an I section beam the use of the PAFBLOCKS module, which automatically generates the mesh, is particularly useful.

PAFEC is programmed to work with SI units. In the present analyses units of N and m are consistently used.

PAFEC permits the use of 10 sets of standard material properties. For example, Material Number 1 identifies mild steel having the following properties relevant to static analyses; Modulus of Elasticity = 209E9 N/m^2, Poisson's ratio = 0.3, coefficient of thermal expansion

= 11E-6 per °C. However it is possible to input other values in the MATERIAL module by using a MATERIAL.NUMBER greater than 10, and this has been necessary in the analyses reported herein because the coefficient of thermal expansion for steel at elevated temperatures is nominally 14E-6 per °C.

It is also possible to input material properties which are dependent upon a single parameter such as temperature. In this case the VARIABLE.MATERIAL module is used in which the VARIABLE.MATERIAL.NUMBER has to be greater than 10 and be different to the MATERIAL.NUMBER in the MATERIAL module. The VARIABLE.MATERIAL module calls up a TABLE module in which the values of the dependent variable (such as E) are given for values of the independent variable (such as temperature).

Because the stiffness matrix changes if the material properties change (as with temperature for instance), it follows that an analysis which incorporates say 3 load cases (where for example each load case represents a different set of temperatures) must be run as 3 separate jobs so as to take account of the 3 different stiffness matrices.

1.4 Choice of element size and type

In general it can be said that the larger the element, the smaller the number of elements in the member and the lower the CPU time. Conversely, the smaller the element the more accurate the result. A balance has to be achieved between the two.

It was considered reasonable to assume that problems could be treated as two-dimensional plane stress problems. Hence, in the case of an I

section member heated along one flange for instance, variation of temperature and stress across a flange width did not exist in theory, and was probably small and of little consequence in the experiments with which the theory would be compared. This simplification (from a 3-D to a 2-D analysis) brought benefits in terms of simpler data input and shorter computer runs, and was justified by the simple (prismatic) shape of the members and the absence of 3-D heat flow.

In all the present analyses PAFEC eight noded isoparametric curvilinear quadrilateral plate elements (Type 36210) were used.

Clearly a 2 dimensional element must have a constant thickness so this dictates the use of different elements either side of a flange/web intersection in an I section member for example. Another important criterion is a limit on the length to width ratio of a quadrilateral element - the aspect ratio - and in PAFEC a warning is printed in Phase 2 output when the length of longest side ÷ length of shortest side is greater than 5 but less than 15 whereas an error is printed out and the program terminates if the aspect ratio is equal to or greater than 15. The maximum aspect ratio allowed in the present analyses is 12. This means that severe distortion of the element is avoided while at the same time reducing the size of the stiffness matrix to be solved. It should be noted that in an I section member the length of the shortest side of an element is governed by the flange thickness (assuming the flange thickness is not represented by 2 or more elements). Adopting an aspect ratio of 12 for instance therefore means that the length of the longest side of an element in the flange zone is nominally 12 times the flange thickness. This also dictates the number of elements longitudinally in

the web area, hence in the whole member. Sensitivity analyses were made to quantify the effect of aspect ratio.

1.5 Determination of nodal temperatures

In PAFEC it is necessary only to specify the temperatures at the 4 corner nodes (the default value is 0°C) of every 8 noded quadrilateral Type 36210 element; if the mid-side node temperatures are not specified, PAFEC will interpolate linearly between the adjacent corner node temperatures, and such interpolation is acceptable unless the temperature distribution is markedly curvilinear between adjacent corner nodes. In the present analyses it has been deemed unnecessary to specify mid node temperatures.

It would be convenient, for computing purposes, if thermocouples were positioned at node corners since this would avoid the need to interpolate and extrapolate from the experimental data. However this is impractical since, apart from other considerations, it presupposes that the preferred mesh is known at the outset, but this is rarely the case. It is therefore necessary to construct temperature profiles from the experimental data and read off temperatures at the corner node positions.

The specification of temperatures is made easy if, in the experiment used for the validation study, the temperatures do not vary in, say, the x direction for a particular value of y. If the member is prismatic along the x axis, such that the PAFBLOCKS mesh generation facility can be used (as it can for I-section members for example) then it is only necessary to specify one temperature and the start and finish nodes and

the TEMPERATURE module will allocate that temperature automatically to all the relevant nodes (nodes on the line of constant y).

To complete a TEMPERATURE module it is necessary, as has been said to define the temperatures at all corner nodes. This presupposes knowledge of all corner node numbers, and while this clearly provides no problems for user-defined node numbers, it can provide a problem for those nodes generated within a PAFBLOCK. One way of finding out the node numbers within a PAFBLOCK is to obtain a large scale graphic of the undeformed structure using the IN.DRAW module. The graphic has to be produced at large scale, typically A1 size, if small elements are used since the type face used to print out the node numbers is large and over printing can occur which obliterates the node numbering. In early PAFEC analyses made at Fire Research Station a suitable graphics plotter (such as a Benson plotter) was not available on site and it was necessary to have the graphic produced at Building Research Station, Garston, and then sent over by van. This was a time consuming process and two alternatives were then possible. First it was possible to get a window graphic of A4 size showing a small part of the mesh from which node numbers for the rest of the mesh could be derived. Second, it emerged from a study of large scale IN.DRAWS that PAFEC generated node numbers in a particular sequence so that where only one PAFBLOCK was used in an analysis it was possible unambiguously to derive the non-user-defined node numbers by hand.

1.6 Use of elastic analyses before plastic analysis

Before undertaking plastic analyses it was considered prudent to do some elastic analyses. This strategy would have several advantages as follows:

(i) the greater CPU time involved in iteration means that a plastic analysis is several times the cost of an elastic analysis, and this means that the data file should be free of errors if at all possible - an elastic analysis provides a good (inexpensive) way of highlighting problems in the data file.

(ii) an elastic analysis can be used to indicate where, under increasing loading, yielding is first encountered. This helps in reducing the number of iterations by indicating where the first load step should be.

(iii) an elastic analysis can, with care, be used to indicate where in the structure the highest and lowest stresses are obtained. This helps to identify the areas where elements are unlikely to go plastic and enables the CPU time of a plastic analysis to be reduced

1.7 Modelling of phase transformation in PAFEC

To take account of phase transformation a modification to the standard PAFEC package was needed. The modification was undertaken by *PAFEC Ltd*, under a small contract placed by Fire Research Station. This had to take account of (a) the fact that whenever thermal loads are applied, equivalent nodal loads are calculated internally to produce the required thermal expansion, and (b) the need to subtract thermal strains from the total strain before stresses are calculated. This was achieved by adding a new data module called the PRELOAD module in which the way in which thermal strain varies with temperature is defined in a TABLE module.

Suppose that the variation of thermal strain with temperature is as shown in Figure 1, which is an idealisation of a dilatometer determination for mild steel. The PRELOAD module would be as follows.

```
PRELOAD
CASE          TYPE        TABLE
  1            1            1
TABLE = 1
BASIS         VALUE
  0            0
 740          1.1E-2
 825          9.5E-3
1200          1.5074E-2
```

where:

CASE = load case under consideration

TYPE = 1 refers to user input of thermal strain with temperature

TABLE = the table number used to specify the variations

BASIS = values of temperature

VALUE = values of thermal strain

1.8 Validation of PAFEC phase transformation software

To check that the PAFEC PRELOAD module gave the right answers when incorporated in the PAFEC suite, it was decided to analyse the expansion of a simple (ie 4-element) steel plate with and without the PRELOAD module.

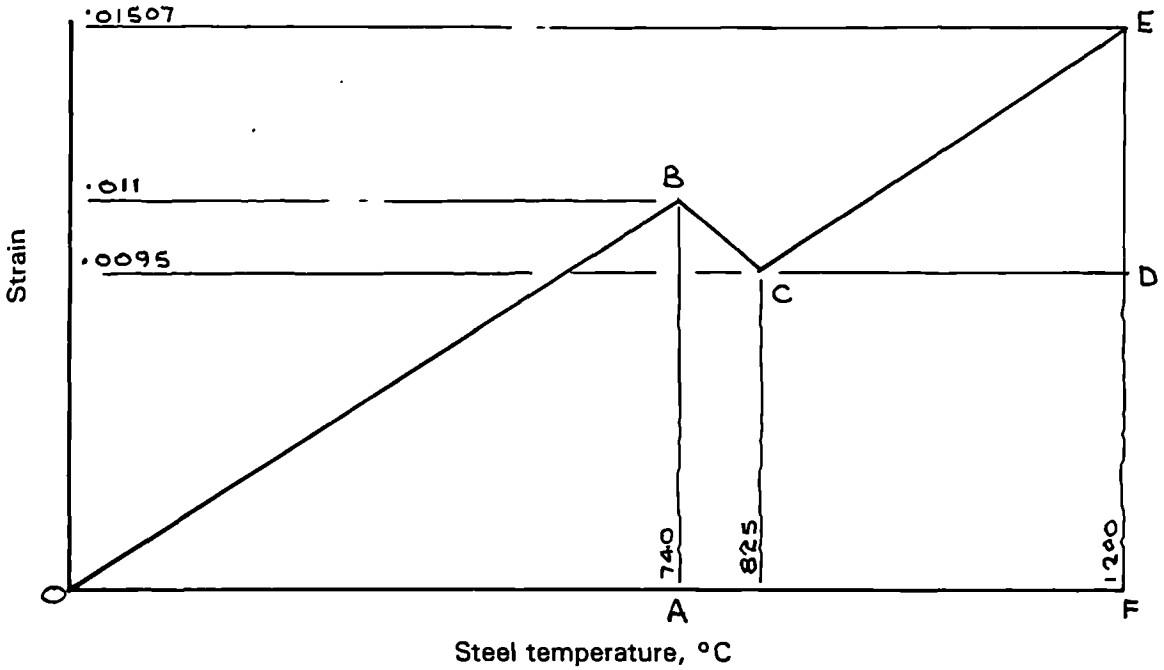

FIGURE 1. Phase transformation curve for a mild steel idealised for use in PAFEC analyses

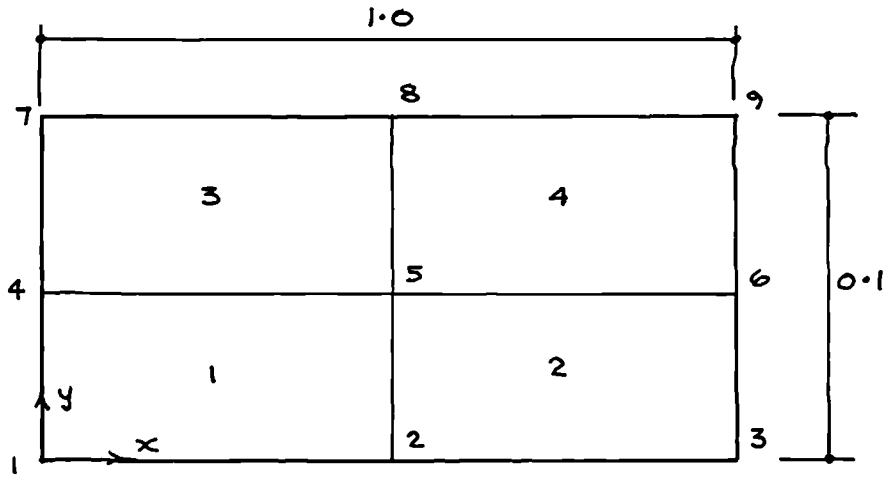

FIGURE 2. Plate configuration used to check PRELOAD module

The plate was arbitrarily chosen to be 1.0 m long by 0.1 m deep by 0.01 m thick, Figure 2. One end was fixed and the other was free to expand. Hence nodes 1, 4 and 7 were restrained in the x-direction. In the y-direction only node 1 was restrained. The displacement in the x-direction of node 3 (or 6 or 9) was of interest.

The idealised phase transformation curve is shown in Figure 1.

The value of α for the first part of the curve OB is given by $\frac{\text{expansion}}{\text{original length x temperature rise}} = \frac{0.011}{1 \times 740} = 14.8648 \times 10^{-6}/°C$. This value would be used in the analysis in which phase transformation was ignored.

To fully specify the coordinates of the idealised phase transformation curve for use in the PRELOAD module, the coordinates of point E are needed. These are obtained from the reasonable assumption that lines OA and CE are parallel and from the application of the principle of similar triangles. Hence $\frac{AB}{OA} = \frac{ED}{CD}$ therefore $ED = \frac{.011}{740} \times (1200 - 825)$ from which ED = 0.00557432 and FD = 0.015073. The TABLE in the PRELOAD module is therefore as follows:

BASIS	VALUE
0	0
740	1.1E-2
825	9.5E-3
1200	1.5074E-2

Assuming that the steel plate is heated uniformly over its whole area in temperature increments of 100°C up to 700°C and then at the phase transformation temperatures of 740 and 825°C followed by 100°C temperature increments, the output of the program in terms of the displacement of node 3 in the x-direction should exactly match the thermal strain in Figure 1 for the appropriate temperature.

The appropriate PAFEC datafiles were compiled. Table 2 is the datafile ignoring phase transformation; the data file accounting for phase transformation is identical to that shown but with the addition of the PRELOAD module, shown at the end of Table 2.

The comparison of PAFEC phase 7 outputs for displacements of node 3 are given in Table 3 and in graphical form in Figure 3. From this it is clear that the PRELOAD module, when incorporated in the PAFEC suite, works satisfactorily.

TABLE 2. PAFEC DATAFILES FOR PRELOAD VALIDATION STUDY

```
C       ASSUME ONE METRE LONG STEEL PLATE IS HEATED UNIFORMLY
C       TO DIFFERENT STEADY STATE TEMPS AND CHECK EXPANSION IN
C       LENGTH IS CORRECT.  IGNORES PHASE TRANSFORMATION BUT
C       ASSUMES SAME ALPHA (=14.8648 E-6/O CENTIGRADE)
C
CONTROL
DOUBLE
PHASE 1,7
STOP
CONTROL.END
C
NODES
NODE.NUMBER        X        Y
    1              0        0
    2              0.5      0
    3              1.0      0
    4              0        0.05
    5              0.5      0.05
    6              1.0      0.05
    7              0        0.1
    8              0.05     0.1
    9              1.0      0.1
C
ELEMENTS
ELEMENT.TYPE=36210
NUMBER        PROPERTIES        TOPOLOGY
  1                1            1  2  4  5
  2                1            2  3  5  6
  3                1            4  5  7  8
  4                1            5  6  8  9
C
PLATES.AND.SHELLS
PLATE.OR.SHELL.NUMBER     MATERIALS.NUMBER     THICKNESS
         1                       11               0.01
MATERIAL
MATERIAL.NUMBER        E          NU            ALPHA
       11           210E9        0.3        14.848E-6
C
RESTRAINTS
NODE.NUMBER          PLANE              DIRECTION
    1                  1                   12
C
TEMPERATURE
LOAD.CASE          TEMPERATURE          LIST.OF.NODES
    1                    0             1,2,3,4,5,6,7,8,9
    2                  100             1,2,3,4,5,6,7,8,9
    3                  200             1,2,3,4,5,6,7,8,9
    4                  300             1,2,3,4,5,6,7,8,9
    5                  400             1,2,3,4,5,6,7,8,9
    6                  500             1,2,3,4,5,6,7,8,9
    7                  600             1,2,3,4,5,6,7,8,9
    8                  700             1,2,3,4,5,6,7,8,9
    9                  740             1,2,3,4,5,6,7,8,9
   10                782.5             1,2,3,4,5,6,7,8,9
   11                  825             1,2,3,4,5,6,7,8,9
   12                  900             1,2,3,4,5,6,7,8,9
   13                 1000             1,2,3,4,5,6,7,8,9
   14                 1100             1,2,3,4,5,6,7,8,9
```

```
C
C /40 P.1 BEGINS, /82.5 1/2 WAY THRU P.1., 825 P.1.ENDS
END.OF.DATA
```

THE FOLLOWING PRELOAD MODULE WAS ADDED TO THE ABOVE DATAFILE TO OBTAIN THE PHASE TRANSFORMATION EFFECT

```
C
C /40 P.1 BEGINGS, /82.5 1/2 WAY THRU P.1., 825 P.1.ENDS
C
PRELOAD
TYPE=1
TABLE=1
CASE
1
2
3
4
5
6
7
8
9
10
11
12
13
14
TABLE
TABLE=1
BASIS        VALUE
  0             0
 /40         1.1E-2
 825         9.5E-3
1200         1.50/43E-2
C
END.OF.DATA
```

Load case	Temperature °C	Displacement (m) of node 3 in x-direction relative to fixed node 1	
		Without phase transformation	With phase transformation
1	0	0.000000	0.000000
2	100	0.0015146	0.0015148
3	200	0.0030292	0.0030297
4	300	0.0045442	0.0045438
5	400	0.0060585	0.0060593
6	500	0.0075743	0.0075743
7	600	0.0090883	0.0090876
8	700	0.0106030	0.0106031
9	740 +	0.0112094	0.0112085
10	782.5	0.0118518	0.0104453
11	825	0.0124973	0.0096802
12	900	0.0136329	0.0108165
13	1000	0.0151485	0.0123315
14	1100	0.0166637	0.0138464

+ Onset of phase transformation

Table 3. x-displacements of node 3 with and without phase transformation

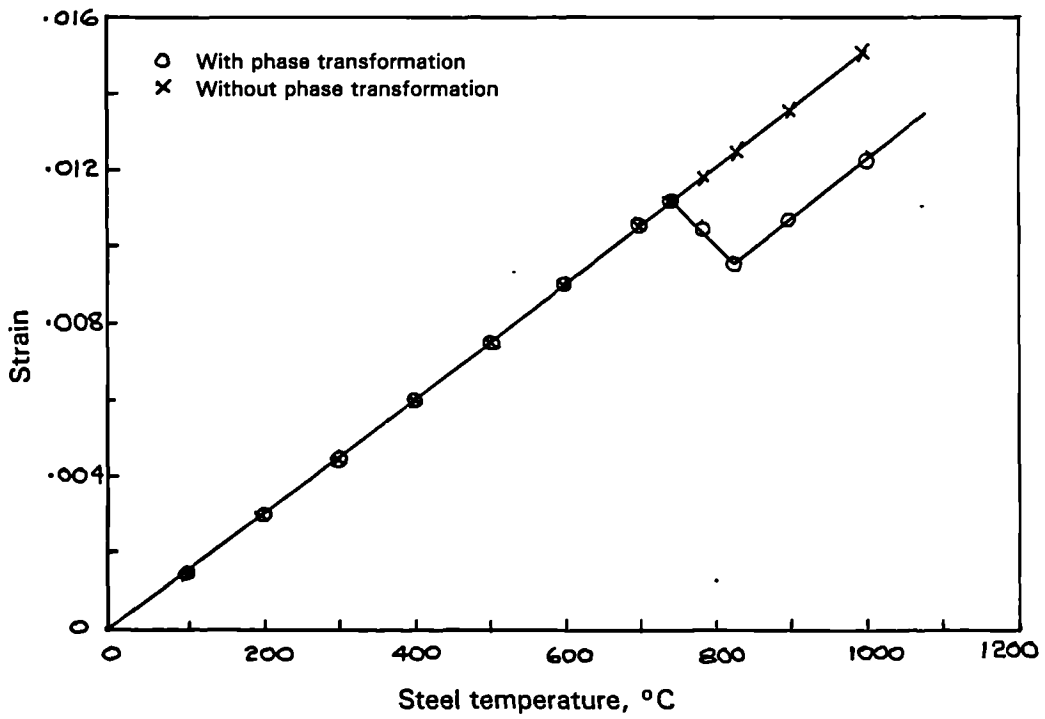

FIGURE 3. Comparison of x-displacements of node 3 with and without phase transformation

APPENDIX 2

RAW EXPERIMENTAL DATA

Thermocouple number	Thermocouple temperature (°C) at time (min) of:									
	0	2	4	6	8	10	12	14	16	18
1	14.6	14.9	15.9	18.9	25.4	35.1	47.9	63.7	80.4	96.8
2	14.5	14.9	17.0	22.5	32.5	45.8	62.6	82.2	102.1	121.6
3	14.5	15.2	20.5	31.3	49.3	71.1	96.7	124.8	152.6	178.8
4	14.6	16.5	28.3	49.9	79.8	114.9	154.6	196.3	238.5	278.8
5	14.6	19.0	39.6	73.1	115.5	164.7	219.7	276.7	333.3	388.7
6	14.5	14.8	15.5	17.7	23.9	34.3	49.3	68.8	90.9	113.3
7	14.6	14.9	16.1	20.1	29.5	43.8	63.5	87.8	114.1	140.5
8	14.5	15.0	17.5	25.6	41.5	64.6	94.5	128.7	164.5	200.0
9	14.6	15.3	20.5	35.2	61.5	98.0	143.3	194.0	247.6	299.7
10	14.7	15.8	24.6	46.8	84.1	134.8	196.4	266.7	339.9	412.6
11	13.6	13.8	14.4	16.8	22.3	33.2	48.5	68.2	91.0	114.6
12	13.6	13.9	15.1	19.3	28.8	43.2	63.4	87.8	114.7	142.2
13	13.6	14.1	16.9	25.4	41.4	64.8	94.8	129.3	165.6	201.6
14	13.6	14.4	20.2	35.6	62.1	98.9	144.2	195.0	248.8	301.4
15	13.7	15.0	24.9	48.3	86.2	137.4	199.4	269.9	343.2	416.1
16	13.4	13.7	14.4	16.8	23.0	33.6	48.7	68.1	90.6	113.7
17	13.5	13.8	15.2	19.3	29.5	44.2	64.4	88.6	115.3	142.3
18	13.6	14.1	17.2	26.4	43.2	66.9	97.2	131.4	167.3	202.6
19	13.7	14.6	21.1	37.7	65.2	102.6	147.9	198.2	251.4	303.3
20	13.7	15.3	26.6	51.9	91.4	143.7	206.1	276.4	349.2	421.7
21	13.5	13.8	14.4	16.6	22.4	32.2	46.3	64.3	85.3	106.9
22	13.5	13.9	15.1	19.3	28.3	42.1	60.9	83.7	108.7	134.1
23	13.6	14.1	16.9	25.2	40.7	63.0	91.3	123.6	157.5	190.7
24	13.7	14.5	20.3	35.6	61.4	97.1	140.3	188.3	239.0	288.6
25	13.8	15.2	25.1	47.9	85.0	134.6	193.4	260.5	330.7	400.0
26	13.4	13.8	14.4	16.0	20.2	27.3	37.7	51.1	66.9	83.7
27	13.4	13.8	14.9	17.5	23.7	33.2	46.4	62.7	81.5	101.0
28	13.6	14.0	16.1	21.4	31.3	45.6	64.4	86.8	111.3	136.8
29	13.7	14.4	18.4	27.8	43.1	64.5	91.3	122.2	155.4	189.3
30	13.8	15.2	21.8	35.5	56.7	85.2	119.7	158.4	199.9	242.9
31	13.3	13.7	14.3	16.1	20.7	28.2	38.7	52.5	68.4	86.0
32	13.2	13.6	14.7	17.9	24.5	34.2	47.5	64.2	82.8	103.1
33	13.3	13.8	16.4	22.6	33.0	47.6	66.8	89.0	113.3	139.3
34	13.4	14.5	19.8	30.6	46.6	68.4	95.1	124.8	157.1	190.6
35	13.6	15.9	24.7	39.9	61.5	89.9	123.2	158.9	198.2	239.2
36	13.2	13.6	14.1	16.5	22.6	32.7	47.4	66.0	87.1	109.3
37	13.4	13.8	15.1	19.4	29.0	43.1	62.6	86.0	111.2	137.2
38	13.3	13.7	16.7	25.6	41.8	64.7	94.2	127.6	161.7	196.2
39	13.4	14.2	20.5	36.3	63.7	100.4	145.1	194.8	246.3	297.0
40	13.5	15.0	25.7	50.3	88.7	139.9	200.9	269.8	340.9	411.8
41	13.2	13.6	14.2	16.6	23.0	33.8	49.8	69.8	92.6	116.5
42	13.3	13.7	14.9	19.4	29.3	44.4	65.4	90.3	117.2	144.9
43	13.4	14.0	17.0	26.0	43.0	67.4	99.7	133.8	170.0	206.2
44	13.5	14.3	20.8	37.3	65.4	104.1	151.2	203.8	258.5	312.0
45	13.5	15.1	26.3	51.6	92.3	146.4	211.3	284.4	359.8	434.5
46	13.2	13.6	14.2	16.8	23.1	33.9	50.0	70.0	92.8	117.1
47	13.3	13.7	15.0	19.5	29.4	44.5	65.7	90.4	117.5	145.6
48	13.4	13.9	17.0	26.3	43.3	67.7	99.0	134.1	170.5	207.3
49	13.4	14.4	20.9	37.7	65.9	104.4	151.4	203.5	257.8	311.4
50	13.5	15.0	26.4	52.0	92.6	146.2	210.6	283.1	357.7	431.6
51	14.2	14.5	15.2	17.5	23.8	34.2	49.6	68.6	89.7	113.0
52	14.1	14.5	15.9	20.4	30.2	44.9	65.3	89.1	114.7	141.9
53	14.3	14.8	18.0	27.2	44.0	67.7	98.1	131.9	167.0	202.4
54	14.4	15.3	22.0	38.9	66.8	104.7	150.8	201.7	254.5	306.7
55	14.5	16.2	27.7	53.6	94.0	147.1	210.4	281.6	354.4	426.7
56	13.8	14.1	14.8	16.7	21.8	30.1	42.7	57.7	74.4	93.9
57	13.9	14.2	15.5	19.1	27.0	38.6	55.3	73.9	94.2	116.9
58	14.0	14.5	17.3	25.2	39.3	58.8	84.2	111.3	140.6	170.3
59	14.1	15.0	21.1	35.6	59.1	90.2	128.2	169.0	211.5	254.8
60	14.3	16.0	26.6	49.0	82.8	126.0	176.6	232.9	289.8	347.3

TABLE 1. Thermocouple temperatures for unrestrained model steel beam heated along whole flange

Thermo-couple number	Thermocouple temperature (°C) at time (min) of:									
	20	22	24	26	28	30	32	34	36	38
1	108.9	117.2	129.4	142.6	161.8	177.0	187.0	196.1	203.4	209.3
2	138.6	151.8	164.7	179.6	196.7	211.6	222.6	232.0	240.0	246.7
3	204.2	226.4	245.2	264.1	282.3	298.3	311.1	321.4	332.3	341.6
4	317.1	352.6	383.7	412.9	439.2	462.6	482.1	498.4	514.9	531.4
5	442.2	492.1	537.6	578.8	615.7	648.8	676.6	700.7	726.7	757.6
6	136.8	157.6	175.8	192.7	208.0	221.3	232.3	241.2	249.0	256.6
7	166.7	189.9	210.4	228.6	244.9	257.9	269.4	279.3	287.7	296.0
8	234.7	264.5	290.9	313.5	333.4	348.4	361.9	375.1	387.2	398.4
9	350.3	396.0	436.5	471.7	500.6	521.3	543.9	568.5	591.9	610.7
10	482.9	547.9	606.1	656.9	695.4	726.3	770.4	821.4	865.0	893.6
11	138.9	160.8	180.2	197.8	213.3	226.3	236.6	245.2	253.2	260.9
12	168.7	193.0	214.4	233.0	249.3	262.2	272.9	282.3	291.5	300.1
13	235.9	266.6	293.1	315.5	335.1	349.5	362.5	375.4	388.6	399.7
14	351.8	397.6	438.0	472.8	500.9	521.3	544.4	569.6	593.7	611.8
15	485.9	550.4	607.7	657.7	693.8	726.2	771.6	823.8	866.6	895.0
16	137.6	159.2	178.5	195.8	211.1	224.2	234.3	243.3	250.7	257.8
17	168.3	192.2	213.6	232.3	248.3	261.0	271.5	281.2	289.7	297.8
18	236.5	266.2	292.9	315.3	334.2	348.3	361.1	373.8	386.1	397.1
19	352.9	397.9	437.6	471.8	499.1	519.4	541.7	565.9	589.8	607.1
20	490.5	553.9	610.5	659.9	695.6	727.6	772.2	822.2	863.8	892.7
21	129.3	150.2	168.7	185.8	201.0	214.1	224.7	233.7	241.3	248.3
22	159.0	182.1	202.6	221.0	237.3	250.5	261.1	270.6	278.8	286.7
23	223.5	252.6	278.3	300.7	320.2	335.4	347.5	359.2	370.6	381.3
24	336.1	379.6	418.0	452.0	480.7	501.9	521.0	541.1	561.6	580.4
25	466.7	528.3	583.3	631.8	673.3	701.0	733.1	771.8	813.0	850.2
26	102.3	122.1	139.8	157.1	173.0	186.7	199.1	210.1	220.0	229.9
27	122.0	143.8	162.9	181.7	198.8	213.8	227.5	239.6	250.9	261.0
28	162.7	189.1	212.9	235.5	255.9	273.9	290.5	304.7	319.0	330.9
29	224.3	258.4	289.5	317.7	343.6	367.2	389.3	408.9	427.4	444.3
30	285.7	326.7	364.5	398.1	429.0	458.0	485.2	509.7	531.8	553.4
31	105.3	124.9	144.3	161.9	178.2	192.9	205.8	217.3	226.6	237.3
32	124.9	146.4	167.1	186.1	203.8	219.6	233.9	246.3	256.4	268.0
33	165.7	191.8	216.9	239.8	260.7	279.7	297.0	312.5	325.6	339.3
34	224.7	257.5	289.2	317.6	344.4	368.9	391.6	412.0	429.9	446.4
35	278.8	317.2	354.3	387.1	419.0	448.6	475.7	499.8	520.9	538.7
36	132.4	153.9	173.1	190.6	206.7	220.0	231.3	240.9	249.1	257.0
37	162.7	186.5	207.7	226.4	243.5	256.7	268.3	278.7	287.4	296.6
38	229.9	259.8	286.5	309.0	329.5	344.6	358.3	371.4	383.7	395.4
39	346.1	390.8	430.3	464.8	493.8	514.7	536.3	559.3	582.3	602.9
40	480.4	543.7	599.1	648.4	686.8	716.5	756.9	804.1	849.4	884.9
41	141.1	163.0	182.9	200.7	216.3	228.7	239.1	248.0	255.9	263.3
42	171.7	196.0	217.7	236.5	252.5	264.8	275.9	285.9	294.8	303.3
43	240.7	271.0	297.7	320.1	338.5	352.4	365.9	379.5	391.9	403.0
44	362.9	408.4	448.5	482.7	507.5	529.2	553.2	578.8	600.7	619.5
45	505.3	570.2	627.4	676.7	708.2	747.7	796.9	847.7	886.1	919.3
46	141.5	163.1	183.3	200.7	216.3	228.7	238.5	247.4	255.2	262.1
47	172.2	196.4	218.4	237.1	253.1	265.5	275.5	285.7	294.5	302.5
48	241.8	272.2	299.3	321.9	340.5	354.5	366.8	380.7	393.6	404.2
49	361.9	407.2	447.5	481.8	507.9	529.0	551.6	577.0	600.7	620.5
50	501.9	566.3	623.0	672.6	704.8	740.7	787.5	838.3	878.7	911.7
51	135.6	156.3	175.7	192.0	207.1	219.4	229.8	238.8	246.1	251.9
52	167.0	190.2	211.4	229.0	244.9	257.2	267.7	277.9	286.1	292.7
53	235.5	265.1	291.5	312.4	331.7	345.5	357.9	371.6	382.8	392.2
54	355.6	399.8	439.4	472.6	499.6	519.3	540.7	563.7	586.3	605.4
55	495.2	558.0	613.8	662.1	697.5	727.9	769.5	916.6	859.5	891.9
56	112.1	129.6	146.8	159.1	172.4	183.2	192.9	202.4	207.1	211.4
57	137.9	157.3	175.6	189.1	203.8	215.1	226.0	236.2	240.5	245.4
58	197.7	223.5	246.5	263.9	282.2	295.7	300.8	321.4	326.5	333.4
59	294.8	331.9	365.7	392.8	418.6	440.1	459.8	477.3	488.8	501.0
60	401.6	451.9	497.8	536.9	571.8	603.3	630.6	634.4	675.1	694.7

TABLE 1. Thermocouple temperatures for unrestrained model steel beam heated along whole flange

Thermo-couple number	Thermocouple temperature (°C) at time (min) of:					
	40	42	44	46	48	50
1	215.1	220.0	225.0	227.9	232.0	236.0
2	253.0	258.5	264.1	267.2	271.7	275.9
3	350.4	357.5	365.5	370.6	375.1	381.5
4	547.2	561.5	574.6	585.5	595.1	605.7
5	788.8	817.7	842.5	863.9	883.4	902.2
6	263.9	269.1	273.6	278.2	282.5	285.9
7	303.7	309.2	313.9	319.2	323.9	327.4
8	407.7	414.9	421.4	429.2	435.5	440.2
9	626.2	639.8	652.6	665.8	678.6	689.5
10	917.4	940.1	962.1	983.5	1003.7	1022.1
11	267.9	273.2	277.5	282.2	285.4	289.1
12	307.3	313.1	317.8	322.8	325.8	330.7
13	408.7	416.4	422.7	430.1	434.5	440.8
14	627.6	642.7	656.6	670.7	682.3	694.0
15	921.9	947.7	971.8	993.9	1014.5	1033.1
16	264.3	269.7	274.0	278.9	283.3	287.1
17	304.5	310.4	315.1	320.6	324.9	329.3
18	405.5	413.6	419.9	427.6	433.4	439.2
19	622.8	638.2	651.8	666.0	678.0	689.6
20	921.2	948.3	972.7	996.0	1016.9	1035.8
21	255.5	261.1	265.8	270.1	273.3	277.0
22	294.4	300.3	305.6	310.0	312.8	317.2
23	390.9	398.0	404.7	410.4	414.9	420.3
24	596.4	609.1	620.1	630.9	640.2	650.5
25	877.1	897.3	915.7	934.4	952.3	970.1
26	239.4	246.3	252.3	257.2	261.6	266.2
27	271.7	279.3	286.1	291.2	295.9	301.2
28	343.9	353.4	362.5	369.3	375.1	382.0
29	460.9	474.8	487.7	498.5	507.5	516.5
30	572.5	590.2	606.4	620.8	633.1	645.0
31	246.6	253.6	260.5	267.5	274.0	278.8
32	278.2	286.1	293.6	301.8	308.6	312.7
33	351.9	362.3	372.0	382.4	390.9	395.6
34	463.4	478.8	493.3	506.1	517.2	526.2
35	560.1	579.7	597.6	612.3	625.5	638.0
36	264.7	270.6	275.6	280.8.	285.6	289.4
37	304.4	310.6	315.9	321.3	326.1	330.0
38	406.3	413.3	421.3	428.9	435.4	440.7
39	620.9	635.1	649.3	663.4	676.3	687.4
40	913.3	938.3	961.8	983.8	1004.1	1022.1
41	270.5	276.4	281.2	285.9	290.2	293.9
42	310.8	316.8	322.6	327.5	332.0	336.3
43	413.1	420.5	429.4	436.3	442.1	447.2
44	637.8	654.2	669.5	683.1	694.7	704.6
45	950.6	979.5	1005.2	1027.1	1043.9	1057.8
46	269.3	275.2	280.3	285.1	289.3	292.9
47	310.2	316.4	322.1	327.0	331.7	335.8
48	414.3	422.3	430.7	437.7	444.2	450.0
49	638.4	654.4	669.8	684.2	696.7	707.6
50	942.1	969.9	995.6	1018.9	1038.9	1055.4
51	258.1	264.0	269.2	274.6	279.5	283.1
52	299.4	306.3	311.9	317.4	322.4	326.1
53	401.2	410.8	417.9	425.3	432.2	436.6
54	622.3	638.3	652.3	665.4	676.9	686.9
55	919.0	941.3	958.2	972.6	983.5	992.4
56	215.6	221.2	225.2	231.0	236.4	238.9
57	250.0	256.8	260.7	267.3	272.9	274.8
58	339.2	349.1	354.23	362.3	368.0	370.9
59	512.2	525.4	535.5	546.4	555.4	562.4
60	714.0	733.4	751.9	760.6	785.5	799.3

TABLE 1. Thermocouple temperatures for unrestrained model steel beam heated along whole flange

Thermo-couple number	Thermocouple temperature (°C) at time (min) of:									
	0	2	4	6	8	10	12	14	16	18
1	19.9	19.9	19.8	19.7	19.7	19.7	19.5	19.4	19.4	19.3
2	20.1	20.0	19.9	19.8	19.8	19.8	19.7	19.6	19.5	19.4
3	20.6	20.6	20.5	20.3	20.3	20.2	20.1	20.0	19.9	19.8
4	21.5	21.4	21.3	21.1	21.0	20.8	20.7	20.5	20.3	20.2
5	22.2	22.1	21.9	21.8	21.5	21.3	21.0	20.9	20.7	20.6
6	20.7	20.6	20.5	20.3	20.3	20.3	20.2	20.1	19.9	19.8
7	21.1	21.0	20.9	20.7	20.7	20.6	20.5	20.4	20.3	20.2
8	21.6	21.5	21.4	21.2	21.2	21.0	20.9	20.8	20.7	20.6
9	22.4	22.2	22.1	21.9	21.7	21.6	21.3	21.2	21.0	20.9
10	23.0	22.8	22.6	22.4	22.2	22.0	21.7	21.5	21.3	21.2
11	21.2	21.2	21.1	20.9	20.9	20.8	20.7	20.6	20.5	20.4
12	21.5	21.5	21.3	21.1	21.1	21.0	20.8	20.7	20.5	20.4
13	22.2	22.1	22.0	21.8	21.7	21.6	21.4	21.2	21.1	20.9
14	23.0	22.9	22.7	22.5	22.3	22.1	21.9	21.8	21.5	21.4
15	23.6	23.4	23.2	23.1	22.8	22.5	22.3	22.1	21.9	21.7
16	21.4	21.4	21.2	21.1	21.1	21.0	20.9	21.0	21.0	21.1
17	21.8	21.7	21.6	21.4	21.4	21.3	21.2	21.1	21.1	21.3
18	22.5	22.3	22.2	22.0	21.9	21.7	21.5	21.5	21.4	21.6
19	23.3	23.2	22.9	22.8	22.6	22.4	22.2	22.1	22.0	22.1
20	24.0	23.9	23.6	23.5	23.2	22.8	22.6	22.6	22.5	22.5
21	21.3	21.2	21.1	21.0	21.1	21.2	21.6	22.2	23.2	24.5
22	21.6	21.6	21.4	21.3	21.4	21.5	21.9	22.5	23.5	24.8
23	22.3	22.2	22.0	21.9	22.0	22.1	22.5	23.1	24.1	25.5
24	23.2	23.0	22.8	22.8	22.7	22.7	23.1	23.8	24.8	26.4
25	24.0	23.8	23.6	23.5	23.4	23.5	23.8	24.6	25.6	27.1
26	20.6	20.6	20.7	21.0	22.2	24.2	27.5	31.8	37.0	42.6
27	21.1	21.0	21.1	21.7	23.2	25.5	29.1	33.7	39.3	45.5
28	21.9	21.9	22.2	23.1	25.0	27.9	32.0	37.4	43.8	50.9
29	22.9	22.9	23.3	24.7	27.0	30.6	35.5	41.8	49.2	57.5
30	23.5	23.5	24.2	25.8	28.6	32.6	38.1	45.1	53.3	62.3
31	21.2	21.2	21.8	24.0	28.8	36.1	46.5	59.8	74.9	90.9
32	21.5	21.6	23.0	26.7	33.3	43.3	56.7	73.0	90.8	109.4
33	22.2	22.7	25.9	32.6	43.5	58.8	78.2	100.4	124.2	148.4
34	23.0	24.7	31.0	42.3	59.6	82.7	110.4	141.4	173.3	205.4
35	23.9	27.6	37.3	53.6	77.1	107.2	142.9	181.3	221.2	260.7
36	21.1	21.1	21.6	24.3	30.9	42.1	58.3	78.6	101.1	124.5
37	21.7	21.8	23.2	28.2	38.4	54.3	75.7	100.8	127.6	154.2
38	22.4	22.6	26.2	36.1	54.1	80.0	112.0	147.8	184.0	219.1
39	23.2	24.2	31.8	49.9	80.0	121.2	170.4	224.0	278.3	330.3
40	24.0	26.2	39.1	66.7	110.5	169.4	238.2	312.6	388.7	463.0
41	21.0	21.0	21.3	23.7	30.0	41.4	58.2	79.5	103.7	128.4
42	21.3	21.3	22.4	26.9	36.6	52.5	74.2	100.3	128.6	156.6
43	21.9	22.2	25.2	34.0	50.9	76.7	108.0	144.7	181.7	218.0
44	****	****	****	****	****	****	****	****	****	****
45	23.5	25.2	35.7	59.8	100.6	156.0	219.2	292.5	366.4	443.0
46	20.5	20.5	20.9	23.3	29.9	41.4	58.7	80.7	105.4	130.8
47	20.8	20.8	22.1	26.7	36.7	52.9	75.4	102.4	131.6	159.7
48	21.3	21.6	24.8	34.1	51.4	77.7	111.0	149.0	187.5	224.1
49	22.2	23.0	29.7	46.4	75.5	116.9	167.6	223.5	280.2	332.7
50	22.9	24.7	35.7	60.9	102.7	160.8	230.5	307.1	385.0	458.6
51	19.8	19.8	20.3	23.2	30.4	42.5	59.9	81.7	105.9	130.3
52	20.0	20.1	21.6	26.8	37.7	54.6	77.5	104.2	132.8	160.3
53	20.6	20.9	24.6	34.9	53.6	80.7	114.4	151.9	189.8	226.0
54	****	****	****	****	****	****	****	****	****	****
55	21.8	23.7	35.1	60.3	101.0	156.2	223.0	297.2	373.2	444.8
56	19.0	19.0	19.7	22.9	29.7	40.7	55.8	74.5	95.1	115.4
57	19.1	19.3	21.1	26.7	36.9	51.7	70.9	93.2	116.7	140.3
58	19.7	20.4	25.0	36.0	53.5	77.1	105.4	136.6	168.0	198.8
59	20.5	22.5	32.2	51.7	80.5	116.9	159.0	204.2	250.3	295.0
60	21.2	25.4	41.6	70.8	111.3	161.0	217.6	278.6	340.7	401.5

TABLE 2. Thermocouple temperatures for unrestrained model steel beam heated along half of flange

Thermo-couple number	Thermocouple temperature (°C) at time (min) of:									
	20	22	24	26	28	30	32	34	36	38
1	19.1	18.9	18.9	18.8	18.7	18.7	18.7	18.6	18.7	18.7
2	19.31	19.1	19.1	19.0	18.9	18.9	18.9	18.9	18.8	18.9
3	19.6	19.5	19.4	19.4	19.3	19.2	19.2	19.2	19.1	19.2
4	20.2	20.0	19.9	19.8	19.7	19.6	19.6	19.6	19.5	19.5
5	20.5	20.4	20.2	20.1	20.0	19.9	19.9	19.9	19.8	19.8
6	19.7	19.6	19.5	19.5	19.5	19.5	19.6	19.6	19.6	19.8
7	20.0	19.8	19.8	19.7	19.7	19.7	19.8	19.8	19.9	20.0
8	20.4	20.2	20.2	20.1	20.1	20.0	20.1	20.1	20.2	20.2
9	20.8	20.6	20.6	20.4	20.4	20.4	20.4	20.4	20.4	20.5
10	21.1	20.9	20.8	20.7	20.7	20.6	20.6	20.6	20.6	20.7
11	20.4	20.3	20.3	20.2	20.3	20.4	20.5	20.8	21.0	21.2
12	20.4	20.3	20.3	20.2	20.3	20.5	20.5	20.8	21.0	21.3
13	20.8	20.8	20.7	20.7	20.7	20.9	20.9	21.2	21.4	21.6
14	21.3	21.2	21.2	21.1	21.2	21.2	21.3	21.5	21.7	21.9
15	21.6	21.5	21.5	21.4	21.4	21.5	21.5	21.7	21.9	22.1
16	21.3	21.6	22.1	22.5	23.1	23.9	24.6	25.4	26.3	27.2
17	21.5	21.8	22.2	22.7	23.3	24.1	24.8	25.6	26.5	27.4
18	21.7	22.1	22.5	23.0	23.6	24.3	25.1	26.0	26.8	27.7
19	22.3	22.5	22.9	23.4	24.0	24.8	25.5	26.4	27.3	28.2
20	22.7	22.9	23.4	23.8	24.5	25.2	25.9	26.8	27.7	28.6
21	26.1	28.0	30.0	32.2	34.5	37.0	39.3	41.7	44.1	46.3
22	26.5	28.4	30.5	32.7	35.1	37.5	39.9	42.3	44.7	47.0
23	27.3	29.3	31.3	33.7	36.1	38.6	41.1	43.6	46.0	48.4
24	28.2	30.3	32.5	35.0	37.7	40.2	42.9	45.6	48.1	50.7
25	29.0	31.1	33.4	35.9	38.6	41.2	43.9	46.6	49.2	51.8
26	48.5	54.7	61.1	68.0	74.8	81.1	87.0	91.9	97.1	101.3
27	51.8	58.4	65.2	72.4	79.3	85.9	91.8	97.0	102.2	106.6
28	58.4	66.0	73.7	81.5	89.0	96.1	102.7	108.5	114.2	119.3
29	66.2	75.1	83.9	92.6	101.0	109.0	116.5	123.4	129.9	135.8
30	71.8	81.4	90.9	100.2	109.2	117.7	125.8	133.3	140.1	146.5
31	106.7	122.3	137.2	150.7	162.6	173.9	183.3	191.8	199.2	205.9
32	127.6	145.2	161.4	176.3	189.5	201.7	212.1	221.5	229.6	237.2
33	171.4	193.3	213.7	232.3	248.5	263.4	276.2	287.6	297.7	307.3
34	236.4	265.2	291.7	315.6	337.3	357.0	373.9	389.3	403.4	416.7
35	298.5	333.3	365.3	394.2	420.5	444.4	465.2	484.0	501.5	518.1
36	146.9	167.4	185.9	201.8	215.5	226.5	236.5	244.6	252.1	259.3
37	178.9	201.7	221.6	238.3	252.2	263.2	273.8	282.8	290.7	298.5
38	251.5	280.3	304.9	325.1	341.0	354.4	367.5	379.9	390.1	400.5
39	378.6	421.4	458.8	488.8	511.4	533.5	556.2	578.8	597.9	615.4
40	532.4	594.1	647.9	689.9	722.2	763.4	808.0	850.6	884.9	913.5
41	152.4	174.4	193.9	210.8	224.8	235.9	245.4	253.9	261.5	268.4
42	183.2	207.7	228.6	246.5	260.5	272.1	282.5	292.1	300.4	307.8
43	252.5	283.2	308.5	330.0	345.9	359.9	373.5	386.8	397.8	407.3
44	32.4	416.4	460.9	493.5	516.5	540.8	566.6	591.1	610.9	627.4
45	515.9	581.6	638.6	682.5	717.3	763.6	814.5	859.8	896.3	926.9
46	154.6	176.1	195.6	212.0	225.8	236.5	245.3	253.4	261.2	267.8
47	186.1	209.8	230.8	248.0	261.8	272.8	282.6	291.6	300.1	307.3
48	257.6	287.5	312.9	333.6	349.1	362.8	375.8	388.4	400.0	409.3
49	382.4	426.9	465.5	496.0	518.0	541.1	564.9	588.8	609.5	627.4
50	529.5	593.9	649.7	691.2	725.3	768.8	816.5	861.0	895.1	925.3
51	153.0	174.0	192.7	209.0	222.3	232.9	241.5	249.1	256.2	262.5
52	185.5	208.7	229.0	245.8	259.1	269.9	279.2	287.6	295.5	302.3
53	258.2	287.1	311.5	331.5	346.4	359.2	371.3	382.6	393.3	402.0
54	****	425.1	466.3	495.6	516.9	537.7	559.3	580.2	598.8	99.8
55	510.7	568.8	618.1	655.2	684.4	718.7	755.0	789.6	818.6	842.9
56	135.5	153.8	170.0	184.1	196.0	205.9	213.7	220.1	225.9	230.5
57	161.8	181.7	199.5	214.4	227.0	237.1	245.4	252.4	258.4	263.5
58	227.0	252.0	273.9	292.0	307.1	319.1	329.0	338.2	345.4	352.5
59	336.1	372.3	404.2	431.4	454.4	473.0	488.4	502.4	515.2	527.3
60	458.4	508.9	553.7	592.8	626.1	653.2	676.0	697.1	718.3	739.7

TABLE 2. Thermocouple temperatures for unrestrained model steel beam heated along half of flange

Thermocouple number	Thermocouple temperature (°C) at time time (min) of:				
	40	42	44	46	48
1	18.7	18.7	18.7	16.8	19.0
2	18.9	18.9	18.9	19.0	19.1
3	19.2	19.2	19.3	19.3	19.4
4	19.5	19.6	19.6	19.6	19.7
5	19.8	19.8	19.8	19.8	19.9
6	19.9	20.0	20.1	20.3	20.5
7	20.1	20.3	20.4	20.5	20.8
8	20.3	20.5	20.6	20.7	20.9
9	20.6	20.7	20.8	20.9	21.1
10	20.8	20.9	21.0	21.1	21.3
11	21.5	21.8	22.2	22.5	22.9
12	21.5	21.8	22.2	22.5	22.9
13	21.8	22.1	22.5	22.8	23.1
14	22.2	22.4	22.8	23.1	23.4
15	22.3	22.6	22.9	23.2	23.6
16	28.0	28.9	29.7	30.6	31.4
17	28.3	29.1	30.0	30.9	31.6
18	28.6	29.5	30.4	31.2	32.1
19	29.1	30.0	30.9	31.7	32.6
20	29.6	30.4	31.3	32.2	33.1
21	48.4	50.4	52.3	54.0	55.8
22	49.0	51.1	53.0	54.8	56.6
23	50.5	52.6	54.6	56.5	58.4
24	53.0	55.2	57.4	59.4	61.6
25	54.2	56.5	58.7	60.7	62.9
26	105.6	109.1	112.6	116.2	119.6
27	111.1	114.9	118.6	122.4	126.2
28	124.4	128.7	133.0	137.4	141.9
29	141.5	146.7	151.6	157.5	163.1
30	152.5	158.1	163.5	171.3	177.9
31	212.2	218.0	223.1	227.4	231.2
32	243.8	250.3	256.1	261.4	265.8
33	315.7	324.4	332.3	340.0	345.9
34	429.0	441.3	452.5	462.7	470.9
35	534.2	549.4	563.5	574.8	584.2
36	265.2	270.1	274.9	279.1	282.6
37	304.7	309.6	314.6	318.9	322.3
38	409.0	416.2	422.0	427.1	431.3
39	630.6	643.9	654.5	663.7	670.8
40	939.7	961.3	978.1	991.4	1001.6
41	274.5	279.6	284.2	287.9	290.7
42	314.2	320.0	324.9	328.8	331.7
43	415.9	423.9	429.6	434.2	438.5
44	642.2	656.7	667.8	676.7	686.4
45	953.1	973.7	989.8	1004.5	1022.9
46	273.7	278.6	282.7	286.8	289.6
47	313.5	318.7	323.3	327.5	330.5
48	417.8	424.9	430.8	436.2	440.1
49	643.7	657.8	669.1	678.6	685.9
50	952.8	975.3	992.7	1006.4	1017.0
51	268.1	272.8	276.9	280.2	283.7
52	308.3	313.5	317.9	321.3	324.9
53	410.2	416.9	423.4	427.3	432.1
54	****	****	****	****	****
55	864.7	883.7	899.4	911.4	920.3
56	234.8	238.9	242.7	245.5	248.3
57	268.2	272.9	276.9	280.4	283.3
58	358.8	365.2	370.0	374.9	378.4
59	538.9	549.8	559.2	567.3	573.6
60	761.9	782.2	799.7	814.2	824.7

TABLE 2. Thermocouple temperatures for unrestrained model steel beam heated along half of flange

Thermo-couple number	Thermocouple temperature (°C) at time (min) of:										
	0	2	4	6	8	10	12	14	16	18	20
1	23.9	44.9	93.4	128.9	159	186.5	212	234	250	252.7	251.5
2	23.9	43.5	70.6	85.3	105.7	126	145.5	164.7	181	192	198
3	-	-	-	-	-	-	-	-	-	-	-
4	22.9	23.1	23.4	23.6	24.4	26	27.6	30	32	34.7	37.7
5	23.9	56.3	101.4	130	160.6	187.8	212.5	236	250	251	249
6	23.9	35.2	55.8	78	100	122.6	144.5	165	183	194.7	200
7	23.1	23.1	24.9	29.3	35.7	43.5	51.7	60	69	77.5	84.4
8	22.9	22.9	22.9	23	23.6	24.4	25.6	27	29.5	31.8	34.7
9	24.1	47.3	85.3	123	160	192	219	247	264	267.7	265
10	23.9	33.2	58.9	84.4	112	139.4	165	190.5	211	270.5	223.7
11	23.4	23.4	26.1	31	39	48	58	68.7	79	88.8	97
12	22.6	22.6	22.9	23	24	24.6	26	27.8	30	32.5	36
13	23.9	37.4	79.4	124	166.7	204	237	268	290	293.3	289
14	23.9	32.8	58.4	88.4	121.5	153	182	212	233	243	245
15	22.1	22.4	24.6	29.5	37.7	48	59	70.6	82.2	93	102
16	22.1	22.4	22.4	22.1	23	24	25	27	30	33	36.7
17	22.9	39.6	99.0	159.7	207	244	277	307	327	325	316
18	22.4	31.3	62.0	103	141.3	175	207.6	237	257	265	265
19	21.9	22.4	25.1	31.3	41.8	54	67.7	81	94	104.5	113
20	21.6	21.6	21.4	21.4	22.1	23.4	25	27.3	30	33.3	37.4
21	22.1	43.7	102.6	155	192.3	222	249	275	290	290	282
22	21.6	29.1	60.8	99	129.4	156.6	182	209	226	233.7	233.7
23	-	-	-	-	-	-	-	-	-	-	-
24	21.6	21.6	21.9	22	22.9	24	25.6	27.8	30.5	34	37.7

TABLE 3. Thermocouple temperatures for unrestrained full size partly built-in steel column in Cardington fire test rig, Test 1

Thermo-couple number	Thermocouple temperature (°C) at time (min) of:										
	0	2	4	6	8	10	12	14	16	18	20
1	23.1	32.8	87.4	161.2	219	264.3	305.8	348.4	392	418	425
2	23.4	33.0	70.1	104.5	134.3	166.7	199.7	230.4	261.2	290.6	309.5
3	-	-	-	-	-	-	-	-	-	-	-
4	23.1	23.1	23.4	24.1	25.1	26.6	28.3	30.8	34.2	37.9	42.3
5	22.9	39.3	100	170	219.8	266.8	309	357	403	426	429
6	22.9	28.6	54.1	91.7	126.5	162.6	201	237	274	306	325
7	22.4	22.4	23.4	28.6	36.9	48.3	60.6	74.2	88.2	103	117
8	22.6	22.6	22.6	22.6	22.9	23.9	25.6	28.1	30.8	34.5	38.6
9	22.9	35.0	93.4	161	220.3	271.3	318	367.2	415	441.7	447.6
10	22.6	27.6	57.6	102.6	147.5	192.5	236	279.8	324	357.7	373
11	22.6	22.6	24.6	30.8	42	55.5	71.5	88.2	106	124	140
12	22.4	22.4	22.4	22.6	22.6	24.1	26.1	28.3	32	36.2	41
13	23.1	29.5	82.9	156.6	224.2	282.4	336.7	389	440	471	474.7
14	22.4	27.8	57.7	106	155.4	206.6	254.4	301	350	387	401.7
15	22.1	22.1	23.4	29.5	40.6	54.6	71.5	89.3	108.3	127	145
16	21.6	21.6	21.6	21.6	22.1	23.1	25.4	28.1	31.8	36.7	42
17	22.6	29.3	86.5	165.2	234	293.3	347	398.8	453	487	487.7
18	22.1	26.8	57.0	104.7	154.4	206.6	255	302	353	393	409
19	21.9	21.9	23.9	30.8	42	57.2	75	93.8	113	134	152
20	21.4	21.4	21.4	21.4	21.9	22.9	24.9	27.6	31	35.5	40.6
21	21.6	29.8	78.4	145.5	203.4	251.7	298	345	400	436	440.7
22	21.4	24.4	47.3	87.4	131.4	173.8	215	255	300	341	359
23	-	-	-	-	-	-	-	-	-	-	-
24	21.1	21.4	21.1	21.4	21.9	22.9	24.6	27.3	30.8	35	39.8

TABLE 4. Thermocouple temperatures for unrestrained full size partly built-in steel column in Cardington fire test rig, Test 2

Thermo-couple number	Thermocouple temperature (°C) at time (min) of:									
	0	2	4	6	8	10	12	14	16	18
1	21.1	21.2	22.1	25.4	31.9	41.4	54.2	68.7	84.8	101.5
2	21.1	21.3	23.6	29.7	39.8	53.7	71.0	90.0	110.1	130.6
3	21.1	21.7	27.6	39.8	57.9	80.6	106.9	135.2	164.1	192.3
4	21.0	23.3	36.0	58.6	88.8	125.1	165.7	208.8	253.1	297.2
5	****	****	****	****	****	****	230.7	289.5	350.4	413.0
6	21.0	21.1	21.5	23.7	29.5	39.9	55.2	75.1	97.9	121.8
7	21.1	21.2	22.1	26.1	34.9	49.6	69.9	94.6	121.7	148.3
8	21.0	21.2	23.6	31.6	47.1	70.8	101.3	136.6	173.5	210.3
9	21.0	21.5	26.5	40.9	66.7	103.8	150.2	202.3	257.6	312.3
10	21.0	22.0	30.4	52.0	89.2	141.6	205.5	277.0	352.3	427.7
11	21.0	21.1	21.4	23.4	28.6	38.6	53.9	74.3	97.8	122.9
12	20.9	21.1	22.0	25.7	34.0	48.2	68.4	93.8	121.8	150.6
13	21.0	21.2	23.5	30.9	45.7	68.9	99.5	135.3	172.8	210.2
14	21.0	21.4	26.2	39.8	64.7	101.5	147.9	200.2	256.2	310.9
15	20.9	21.9	29.9	50.4	86.3	138.2	202.2	273.0	349.8	425.0
16	21.0	21.0	21.5	23.5	29.1	39.6	55.3	76.1	99.4	124.0
17	21.0	21.0	22.1	26.2	35.1	50.1	71.0	96.9	124.4	152.3
18	20.9	21.1	23.8	32.1	48.0	72.5	104.1	140.7	177.1	213.2
19	21.0	21.6	27.2	42.1	68.8	107.5	155.5	209.1	262.0	314.7
20	20.9	22.2	31.7	54.6	93.7	149.1	216.3	289.2	359.4	432.9
21	21.1	21.1	21.7	24.1	30.3	41.0	56.4	75.7	97.3	119.8
22	21.0	21.1	22.4	27.2	36.8	52.1	72.6	96.8	122.7	148.7
23	21.0	21.2	24.4	33.7	50.6	75.3	105.9	140.6	175.5	209.5
24	21.0	21.7	28.3	45.1	73.4	112.4	159.3	211.2	263.7	314.2
25	21.2	22.6	33.4	58.7	99.8	155.0	220.5	292.5	365.0	436.0
26	21.1	21.2	21.6	23.5	27.8	34.7	44.2	56.5	70.2	85.3
27	21.1	21.2	22.4	25.9	32.5	42.0	54.2	69.0	85.4	102.7
28	21.1	21.4	24.3	31.4	42.5	57.4	75.4	96.0	117.9	140.6
29	21.1	21.9	28.3	41.0	59.1	82.0	108.0	137.1	167.1	198.2
30	21.0	23.1	34.0	53.0	78.2	108.4	142.3	179.1	218.3	258.0
31	20.9	20.9	21.0	21.3	22.2	23.8	26.4	30.0	34.5	40.0
32	20.9	20.9	21.0	21.4	22.5	24.5	27.5	31.5	36.4	42.3
33	20.8	20.9	21.1	21.8	23.2	25.8	29.5	34.2	39.8	46.5
34	20.8	20.9	21.1	22.1	24.0	27.2	31.5	37.0	43.4	50.9
35	20.8	20.9	21.2	22.4	24.6	28.3	33.1	39.1	46.1	54.2
36	20.8	20.9	20.9	21.0	21.0	21.3	21.6	22.2	23.0	24.0
37	21.0	21.0	21.0	21.1	21.2	21.4	21.7	22.3	23.2	24.3
38	21.0	21.0	21.0	21.1	21.2	21.5	21.9	22.5	23.4	24.6
39	****	****	****	****	****	****	****	****	****	****
40	20.9	20.9	21.0	21.2	21.3	21.6	22.1	22.8	23.9	25.2
41	21.0	20.9	21.0	21.0	21.1	21.1	21.1	21.2	21.3	21.4
42	20.9	20.9	21.0	21.0	21.1	21.2	21.2	21.2	21.3	21.4
43	20.9	20.9	21.0	21.1	21.2	21.3	21.3	21.3	21.3	21.4
44	****	****	****	****	****	****	****	****	****	****
45	20.9	21.0	21.1	21.1	21.2	21.3	21.3	21.3	21.3	21.4
46	20.9	20.9	21.0	21.0	21.1	21.1	21.1	21.1	21.0	21.0
47	21.0	20.9	21.0	21.1	21.1	21.2	21.1	21.1	21.1	21.0
48	20.9	20.9	21.1	21.1	21.2	21.2	21.2	21.2	21.1	21.1
49	20.9	20.9	21.0	21.0	21.1	21.2	21.1	21.1	21.0	21.0
50	20.9	20.9	21.0	21.1	21.2	21.2	21.2	21.1	21.1	21.0
51	21.0	20.9	21.0	21.0	21.0	21.1	21.1	21.1	21.1	21.1
52	21.0	21.0	21.0	21.0	21.0	21.1	21.1	21.1	21.1	21.1
53	21.0	21.0	21.0	21.1	21.1	21.2	21.1	21.2	21.2	21.1
54	****	****	****	****	****	****	****	****	****	****
55	20.9	20.9	21.0	21.1	21.1	21.2	21.1	21.1	21.0	21.0
56	21.0	20.9	20.9	21.0	21.0	21.0	21.0	21.0	21.0	21.0
57	21.0	20.9	20.9	21.0	20.9	21.0	21.0	21.0	21.0	20.9
58	20.9	20.9	20.9	20.9	21.0	21.0	21.0	21.0	21.0	21.0
59	20.9	20.9	21.0	21.0	21.0	21.0	21.0	21.0	21.0	20.9
60	20.8	20.9	21.0	21.0	21.0	21.1	21.0	21.0	20.9	20.9

TABLE 5. Thermocouple temperatures for 2-span model steel beam heated along half of flange

Thermo couple number	Thermocouple temperature (°C) at time (m in) of:									
	20	22	24	26	28	30	32	34	36	38
1	116.2	130.3	145.8	15.9	170.8	177.8	187.2	196.9	197.0	205.2
2	149.9	166.0	183.2	19.8	211.1	219.6	229.4	239.5	243.4	250.2
3	219.6	243.3	265.8	265.8	302.3	313.9	325.6	337.3	346.6	355.3
4	339.3	377.3	412.1	442.7	469.0	489.2	506.9	525.1	543.0	560.6
5	472.5	527.8	578.0	622.5	660.9	690.2	716.2	748.0	783.9	820.4
6	145.3	165.8	185.4	202.4	217.6	228.7	239.1	248.3	256.3	262.4
7	175.5	198.7	220.3	238.7	254.4	265.8	277.3	287.4	296.0	303.0
8	244.5	274.9	302.3	325.3	343.9	358.0	372.7	386.2	398.9	408.8
9	362.4	409.2	451.4	487.0	513.3	536.4	562.4	588.8	611.8	630.6
10	495.9	563.3	624.0	675.9	709.7	752.0	801.9	852.3	890.8	923.3
11	147.4	170.2	190.3	208.6	223.4	235.4	245.1	254.0	262.5	269.9
12	177.8	203.0	224.8	244.3	259.3	271.5	282.1	292.7	301.7	309.9
13	245.6	277.4	304.6	328.6	346.0	361.1	375.1	389.8	402.0	413.0
14	362.8	410.5	452.7	488.8	514.0	538.7	565.6	593.0	616.3	636.4
15	496.8	564.8	625.6	676.8	710.9	756.6	811.4	863.2	901.9	936.8
16	147.7	169.2	189.0	207.0	221.5	231.8	242.3	251.6	259.9	266.3
17	178.7	202.8	224.2	243.4	258.5	269.3	280.3	290.8	300.0	306.9
18	247.8	278.3	305.1	328.4	345.9	359.7	374.0	388.7	400.9	410.6
19	365.8	411.8	453.2	488.7	513.4	537.7	564.6	591.7	613.8	632.9
20	505.4	572.5	632.5	683.2	717.2	764.7	820.3	871.0	908.5	943.2
21	141.6	160.5	179.1	195.6	209.7	221.0	230.5	238.8	247.1	254.4
22	172.9	194.4	214.8	232.6	247.3	258.8	269.0	278.4	287.5	295.5
23	241.6	269.4	295.3	316.7	334.1	348.1	361.2	374.1	386.1	396.0
24	362.2	406.1	445.7	479.3	504.5	526.9	550.6	574.9	596.0	612.4
25	503.9	568.5	626.3	676.4	709.8	750.1	797.3	845.2	880.5	906.0
26	100.6	113.3	128.2	142.2	154.7	161.7	173.3	182.6	183.4	192.4
27	120.1	135.1	151.1	166.1	180.1	189.0	200.9	210.8	215.4	223.3
28	162.7	182.9	203.1	222.2	239.8	253.0	266 9	279.0	289.1	297.5
29	229.0	257.7	285.4	311.2	335.1	355.5	374.0	390.4	405.9	419.4
30	296.7	334.0	369.5	402.6	433.1	460.2	484.0	505.3	525.6	545.0
31	45.1	49.4	56.9	64.9	72.2	77.8	84.1	90.1	95.5	98.5
32	48.2	53.4	60.7	68.7	76.2	82.3	88.8	95.0	100.6	104.2
33	53.4	60.3	68.0	76.4	84.4	91.4	98.5	105.2	111.4	116.1
34	58.8	67.1	75.6	84.5	93.2	101.4	109.0	116.4	123.5	129.5
35	62.9	71.9	81.0	90.2	99.5	108.2	116.3	124.2	131.6	138.4
36	25.5	27.3	29.1	31.1	33.3	35.8	38.0	40.4	42.6	44.7
37	25.8	27.5	29.4	31.4	33.8	36.3	38.6	41.0	43.3	45.6
38	26.1	28.0	29.9	32.0	34.5	36.9	39.4	41.8	44.2	46.6
39	****	****	****	****	****	****	****	****	****	**.*
40	26.9	29.0	31.2	33.5	36.1	38.8	41.5	44.2	47.1	49.8
41	21.7	21.7	22.0	22.4	22.9	23.5	24.1	24.8	25.5	26.3
42	21.7	21.9	22.2	22.6	23.1	23.6	24.4	25.2	25.8	26.6
43	21.6	21.9	22.2	22.6	23.2	23.8	24.4	25.3	25.9	26.8
44	****	****	****	****	****	****	****	****	****	****
45	21.7	22.0	22.3	22.8	23.4	24.0	24.8	25.6	26.3	27.4
46	21.0	21.0	21.0	21.1	21.1	21.1	21.2	21.3	21.4	21.6
47	21.1	21.1	21.0	21.1	21.1	21.1	21.2	21.3	21.4	21.7
48	21.2	21.1	21.2	21.2	21.3	21.3	21 4	21.6	21.7	22.0
49	21.0	21.0	21.0	21.0	21.2	21.3	21.4	21.5	21.7	22.0
50	21.1	21.0	21.0	21.1	21.2	21.3	21.4	21.6	21.6	22.1
51	21.1	21.0	21.0	20.9	20.8	20.8	20.8	20.8	20.8	20.8
52	21.1	21.1	21.1	20.9	20.9	20.8	20.8	20.8	20.9	20.9
53	21.2	21.2	21.2	21.1	21.0	21.0	21.0	21.0	21.0	21.1
54	****	****	****	****	****	****	****	****	****	****
55	21.0	21.0	21.0	20.9	20.9	20.9	20.8	20.9	21.0	21.1
56	21.0	21.0	20.9	20.8	20.7	20.6	20.6	20.6	20.6	20.5
57	21.0	20.9	20.9	20.8	20.7	20.7	20.6	20.6	20.6	20.6
58	21.0	21.0	20.9	20.8	20.8	20.7	20.6	20.6	20.6	20.7
59	21.0	21.0	21.0	20.9	20.8	20.7	20.7	20.7	20.7	20.8
60	21.0	21.0	21.0	20.9	20.9	20.8	20.7	20.7	20.8	20.8

TABLE 5. Thermocouple temperatures for 2-span model steel beam heated along half of flange

Thermo couple number	Thermocouple temperature (°C) at time (min) of:									
	0	2	4	6	8	10	12	14	16	18
1	21.0	21.1	21.7	23.8	28.5	35.7	45.4	57.2	70.5	83.4
2	21.1	21.2	22.6	27.0	34.7	45.7	59.7	76.0	93.3	110.7
3	21.2	21.5	25.2	34.3	48.5	67.2	89.7	114.5	140.2	165.6
4	21.3	22.2	30.5	47.5	72.0	102.5	137.8	175.4	214.3	253.3
5	****	****	****	****	****	****	****	****	****	****
6	21.4	21.5	21.7	23.0	27.1	34.7	46.6	62.6	81.9	102.5
7	21.3	21.3	21.8	24.5	30.9	41.8	57.6	78.0	101.1	125.8
8	21.3	21.4	22.7	28.3	39.5	57.4	81.6	110.7	143.1	176.0
9	****	****	24.3	34.1	52.1	80.7	117.5	160.5	206.8	121.3
10	21.4	21.8	27.0	42.1	69.1	108.4	158.9	216.9	279.4	343.5
11	21.5	21.6	21.8	22.9	26.5	33.5	45.0	61.0	80.8	102.5
12	21.5	21.6	22.1	24.4	30.2	40.6	56.0	76.4	110.2	125.7
13	21.5	21.5	22.7	27.7	38.1	55.2	79.1	108.4	141.4	175.0
14	21.5	21.6	24.4	33.6	51.3	78.7	115.0	158.4	205.9	255.1
15	21.4	21.8	26.6	40.8	66.5	104.8	155.3	214.1	277.7	343.6
16	21.4	21.5	21.6	22.8	26.3	33.4	44.8	60.8	80.5	102.1
17	21.4	21.5	22.0	24.3	30.1	40.4	56.0	76.5	100.3	125.7
18	21.5	21.6	22.8	27.8	38.3	55.5	79.7	109.1	142.0	175.3
19	21.4	21.6	24.3	33.6	51.4	79.1	115.5	158.8	206.1	254.8
20	21.4	21.8	26.7	40.9	67.2	106.4	157.9	217.3	281.2	346.5
21	21.6	21.7	21.9	23.4	27.6	35.5	47.6	63.8	82.8	102.6
22	21.6	21.7	22.3	25.1	31.9	43.4	59.8	80.2	103.0	126.7
23	21.6	21.8	23.3	29.1	41.0	59.8	84.7	113.6	144.9	176.0
24	21.7	21.9	25.2	36.0	56.1	86.0	123.7	166.2	211.2	256.8
25	21.7	22.2	28.0	44.3	73.5	115.4	167.6	225.8	286.8	348.6
26	21.7	21.8	22.1	23.8	28.2	35.9	46.5	60.0	75.6	91.7
27	21.7	21.8	22.6	26.0	32.9	43.5	57.0	73.2	91.3	109.1
28	21.7	22.0	24.2	31.1	43.0	59.6	78.6	100.1	123.7	146.7
29	21.7	22.3	27.5	40.5	60.7	85.7	112.2	141.8	173.0	204.9
30	21.8	23.3	32.9	53.6	83.1	115.4	149.0	185.6	225.2	265.0
31	21.3	21.5	22.0	23.9	28.2	35.4	45.7	58.8	74.2	91.3
32	21.3	21.6	22.6	25.9	32.2	41.8	54.7	70.4	88.3	107.4
33	21.3	21.8	24.3	30.6	40.9	55.4	73.6	94.6	117.5	141.5
34	21.4	22.4	27.9	38.7	54.9	76.2	101.5	130.0	159.7	189.8
35	21.4	23.9	32.8	48.4	70.4	97.8	129.9	164.5	200.3	236.
36	21.3	21.4	21.8	23.7	28.4	36.5	48.5	64.5	83.3	102.2
37	21.3	21.5	22.3	25.8	32.9	44.3	60.2	80.1	102.5	125.4
38	21.3	21.5	23.6	30.5	42.9	61.2	85.0	113.0	143.5	174.1
39	****	****	****	****	****	****	****	****	****	****
40	21.4	22.2	29.7	47.6	76.5	115.7	164.4	219.3	276.4	335.0
41	21.3	21.4	21.6	23.0	27.1	34.9	47.1	64.0	84.5	105.5
42	21.3	21.5	22.1	24.9	31.4	42.8	59.5	81.2	105.9	131.4
43	21.3	21.4	23.0	28.9	40.5	59.5	85.4	116.8	151.0	185.2
44	****	****	****	****	****	****	****	****	****	****
45	21.3	22.0	28.1	44.2	73.6	118.1	174.6	239.6	307.5	375.3
46	21.3	21.3	21.5	22.8	26.5	33.4	44.5	60.0	79.1	99.1
47	21.3	21.3	21.9	24.4	30.3	40.2	55.1	74.8	97.8	121.8
48	21.3	21.5	23.0	28.2	38.4	54.9	77.8	105.9	137.6	170.0
49	21.2	21.5	24.8	34.2	51.3	77.4	111.9	153.2	198.5	245.6
50	21.2	21.9	27.5	41.5	66.1	102.5	150.0	205.3	265.4	328.5
51	21.1	21.2	21.5	23.0	26.7	33.5	44.1	58.2	75.2	92.5
52	21.2	21.3	21.9	24.6	30.5	40.2	54.3	72.2	93.0	114.4
53	21.2	21.4	23.0	28.3	38.4	54.1	75.5	101.2	129.9	159.5
54	**.*	****	****	****	****	****	****	****	****	****
55	21.2	21.8	26.6	39.1	60.7	91.8	131.8	178.6	230.7	285.9
56	21.0	21.1	21.6	23.6	27.8	34.0	24.2	52.9	65.0	77.9
57	21.0	21.2	22.5	26.5	33.3	42.9	55.4	70.0	86.1	102.5
58	21.0	21.5	24.9	32.9	45.2	61.5	81.6	104.1	127.9	151.1
59	21.1	22.2	29.6	43.6	63.8	89.8	120.2	153.4	187.4	221.6
60	21.1	23.5	35.8	56.7	85.5	121.0	161.9	205.9	215.2	297.0

TABLE 6. Thermocouple temperatures for 2-span model steel beam heated along whole flange

Thermo couple number	Thermocouple temperature (°C) at time (min) of:						
	20	22	24	26	28	30	32
1	98.0	112.7	126.4	136.3	142.9	156.6	166.7
2	128.5	146.2	162.0	175.2	184.7	197.9	209.7
3	190.3	214.2	236.3	255.5	271.5	287.0	301.3
4	291.2	327.6	361.6	392.4	419.6	443.9	465.8
5	****	****	329.6	536.3	574.0	603.3	637.5
6	124.3	144.6	164.1	181.2	195.7	208.8	221.4
7	149.8	173.2	195.0	214.2	230.3	244.4	257.5
8	207.8	238.6	266.7	291.2	311.9	330.0	345.5
9	299.7	342.3	384.9	417.6	394.0	329.3	328.7
10	407.5	470.2	529.4	583.6	631.5	672.7	701.2
11	124.8	146.8	167.4	185.8	202.4	216.9	228.6
12	151.1	175.4	198.3	218.4	236.3	251.9	263.6
13	208.0	239.6	268.7	293.6	316.0	334.9	349.0
14	303.4	349.7	392.6	430.7	464.9	493.6	514.2
15	409.3	473.5	533.6	588.3	637.0	678.0	705.6
16	124.3	146.0	166.0	184.1	200.5	214.9	226.9
17	151.0	175.0	197.3	217.1	234.8	250.0	262.5
18	208.2	239.4	267.6	292.3	313.9	332.7	347.7
19	302.6	347.9	389.6	427.0	460.4	489.0	510.2
20	411.5	474.8	534.1	588.3	636.7	678.3	706.0
21	123.3	143.6	162.1	179.2	194.5	207.6	218.9
22	150.0	172.4	193.0	211.9	228.5	242.5	254.5
23	206.2	235.3	261.7	285.2	305.7	323.2	338.1
24	301.3	343.8	383.5	419.2	451.2	478.5	501.1
25	409.9	469.8	526.3	578.1	623.9	664.2	694.8
26	107.8	126.5	144.1	153.9	162.4	178.6	194.7
27	128.4	148.5	167.4	180.3	192.4	208.3	225.4
28	171.0	194.9	218.2	237.3	255.2	272.6	291.9
29	236.8	268.0	297.9	325.2	351.1	374.5	398.0
30	304.3	342.4	379.0	414.0	446.9	477.0	505.4
31	108.1	125.6	142.4	156.3	169.4	182.7	198.4
32	126.4	145.9	164.7	180.4	195.4	209.9	226.4
33	164.7	188.1	211.2	231.9	251.2	268.9	287.3
34	219.9	249.9	279.2	306.5	331.9	355.3	377.8
35	272.7	308.4	343.3	376.4	407.1	435.5	462.1
36	122.7	143.4	162.3	179.6	194.9	208.6	219.9
37	148.4	170.8	192.1	211.1	227.8	242.2	254.1
38	203.7	232.8	259.6	283.8	304.7	322.6	337.9
39	****	****	****	****	****	****	****
40	394.2	451.9	506.9	557.9	603.6	643.8	678.1
41	128.2	150.2	170.4	188.5	204.8	219.0	230.9
42	156.7	180.9	203.2	222.7	240.1	255.0	267.1
43	217.8	248.9	276.7	300.6	322.4	339.9	353.7
44	****	****	****	****	****	****	****
45	442.4	505.5	553.9	594.7	638.9	667.0	697.1
46	121.4	143.2	163.0	181.3	198.0	212.0	223.4
47	147.2	171.0	193.4	213.6	231.9	246.9	258.9
48	202.6	234.0	262.7	288.1	311.1	329.8	344.6
49	292.4	336.3	450.1	448.1	453.2	536.5	****
50	392.8	456.8	517.5	573.1	622.6	665.8	696.3
51	111.9	131.4	150.3	166.6	180.0	192.1	205.9
52	137.2	159.0	179.9	198.6	214.5	228.1	242.5
53	188.8	217.8	244.7	268.8	290.0	307.8	324.9
54	****	****	****	****	****	****	****
55	342.8	398.3	451.7	501.2	545.7	584.3	618.4
56	90.6	103.7	116.8	128.5	138.2	147.8	158.5
57	118.7	135.0	150.6	164.2	176.0	186.9	198.4
58	174.0	196.2	217.6	236.6	253.4	268.1	281.6
59	255.7	288.5	319.9	348.8	374.6	397.1	417.3
60	343.0	387.8	431.3	471.9	508.4	540.9	570.1

TABLE 6. Thermocouple temperatures for 2-span model steel beam heated along whole flange

Thermo-couple number	Thermocouple temperature (°C) at time (min) of:																		
	0	2	4	6	8	10	12	14	16	18	20	22	24	26	28	29	30	31	32
1	24.6	26.1	31.0	41.4	56.2	74.9	96.9	122.1	144.9	166.8	188.1	208.5	228.0	244.5	250.1	255.7	262.1	268.4	273.8
2	22.3	23.1	27.1	36.3	50.2	67.8	88.9	114.3	137.7	160.6	182.3	203.5	223.5	241.1	247.4	253.0	258.9	265.5	271.6
3	22.1	22.6	25.3	31.8	42.2	56.2	72.7	91.8	112.2	130.3	148.6	167.0	184.3	200.0	208.3	213.0	218.0	223.5	228.7
4	22.3	22.6	24.3	29.3	37.2	48.7	62.3	78.0	95.2	111.4	127.2	142.9	158.3	172.5	180.8	185.1	189.8	194.3	199.0
5	23.1	23.3	24.3	27.6	33.3	41.9	52.3	64.9	79.0	93.0	106.6	119.9	132.7	145.2	153.4	157.3	161.8	165.6	169.8
6	23.6	23.6	24.1	26.1	29.5	36.0	44.1	54.0	65.4	77.3	89.4	101.3	112.9	123.6	131.0	135.2	139.2	142.7	146.7
7	23.8	23.8	24.1	25.8	30.0	36.7	45.1	55.3	66.9	79.0	91.3	103.2	114.8	125.5	133.0	137.0	141.2	144.9	148.9
8	23.8	28.8	56.0	99.8	152.9	207.0	260.4	313.9	367.8	419.0	469.3	516.7	560.4	599.7	627.2	643.2	658.9	673.8	686.7
9	22.1	26.6	51.9	94.5	144.7	197.8	251.6	304.3	357.5	409.8	459.2	506.9	552.0	588.6	615.7	631.6	646.3	660.5	673.1
10	22.3	24.8	42.4	74.1	113.9	155.9	198.5	240.5	283.3	324.7	364.3	402.2	438.4	469.5	491.3	504.3	516.5	527.8	538.6
11	22.6	23.6	33.8	54.8	83.1	115.1	148.6	182.3	216.2	249.4	280.9	310.8	338.6	362.9	379.2	389.2	398.2	406.4	414.5
12	22.8	23.1	28.3	41.2	60.3	83.8	109.3	134.7	161.3	186.8	211.2	234.7	256.0	275.5	287.7	295.4	301.9	308.4	314.6
13	23.3	23.3	25.3	32.5	45.6	63.0	82.9	104.2	124.5	144.9	166.5	185.6	204.8	221.5	231.9	238.4	243.8	249.4	254.5
14	23.6	23.8	25.6	33.0	46.3	63.5	83.6	104.9	125.5	145.7	167.0	186.1	204.8	221.5	231.9	238.4	243.8	249.1	254.5
15	24.1	29.5	59.1	107.6	165.1	223.2	280.1	335.2	389.4	442.0	492.3	538.8	579.7	615.7	640.6	655.5	668.4	681.4	692.9
16	24.6	29.5	57.9	105.6	161.8	219.7	276.7	331.6	385.4	438.2	488.5	535.1	576.9	609.8	634.2	648.9	661.7	673.8	685.0
17	22.6	25.6	46.3	83.1	128.2	174.8	221.2	266.0	309.6	352.8	394.4	433.7	469.3	499.1	519.5	531.5	541.6	551.5	561.1
18	22.6	23.8	35.3	58.6	90.1	125.0	160.8	195.8	229.7	262.6	294.5	324.9	352.8	375.2	389.9	398.4	406.0	412.8	419.7
19	22.6	23.1	29.1	43.4	65.2	91.1	118.0	145.7	172.3	198.0	223.2	246.9	269.4	288.4	300.2	307.0	312.7	318.5	323.7
20	22.8	22.8	25.6	34.3	49.7	70.0	92.3	115.8	137.7	160.1	182.8	203.0	223.7	241.6	252.3	258.2	263.5	268.7	273.5
21	23.6	23.6	26.1	34.8	50.4	70.5	92.8	116.0	137.2	159.6	182.3	202.3	222.7	240.6	251.3	256.9	262.6	267.7	272.6
22	23.8	28.8	53.6	95.2	145.7	197.5	251.8	305.3	356.8	405.0	451.6	494.9	533.2	569.1	594.3	610.0	624.8	638.2	650.1
23	24.1	28.1	50.2	89.2	136.5	186.1	239.4	291.6	341.2	388.7	434.9	478.2	517.4	553.6	579.7	595.0	607.7	620.8	632.8
24	24.1	26.6	41.9	71.2	109.5	150.6	194.8	238.7	280.4	320.4	358.7	395.1	428.0	458.4	480.5	493.7	505.7	517.2	528.0
25	23.3	24.8	36.7	60.8	93.0	128.9	166.8	205.5	242.8	278.9	313.4	347.0	377.8	405.5	424.2	435.3	446.0	455.6	465.3
26	23.6	24.8	34.8	55.5	83.8	115.8	149.9	184.8	219.2	252.5	284.5	315.1	343.6	369.5	386.1	396.5	405.7	414.7	423.5
27	23.6	24.6	33.0	51.1	76.3	105.4	136.5	169.0	201.5	233.2	264.0	293.3	320.9	345.8	361.5	371.4	380.4	388.7	397.2
28	24.1	25.3	35.3	56.5	85.8	119.9	157.6	197.5	237.4	276.5	314.6	351.8	386.1	416.9	436.0	448.1	459.2	469.3	478.9

TABLE 7. Thermocouple temperatures for design-loaded model steel beam heated along whole flange

Thermo-couple number	Thermocouple temperature (°C) at time (min) of:																		
	0	2	4	6	8	10	12	14	16	18	20	22	24	26	28	29	30	31	32
29	23.8	26.8	44.8	79.7	124.1	169.5	217.7	266.5	314.9	360.5	405.7	450.0	490.4	526.1	549.2	563.5	576.7	588.9	600.2
30	24.1	26.6	44.8	78.7	124.1	167.3	214.5	264.3	311.3	358.0	403.8	444.6	489.7	525.7	547.5	561.1	574.1	586.1	597.1
31	24.3	26.3	41.0	69.8	107.3	148.8	191.8	235.7	278.4	320.4	361.5	401.7	438.4	471.6	492.3	505.2	517.4	528.5	539.5
32	24.3	25.6	37.2	61.1	92.8	128.4	166.1	204.5	242.1	278.7	314.1	348.9	381.1	410.2	428.5	440.1	450.5	460.3	470.0
33	23.1	23.6	28.1	40.0	58.2	80.7	105.1	130.6	154.4	178.0	201.3	224.7	244.5	263.5	276.0	283.5	290.2	296.6	302.9
34	23.3	23.3	25.3	31.8	43.9	60.6	79.7	100.3	120.3	139.7	159.8	179.0	197.5	214.2	225.7	231.9	238.2	244.0	249.1
35	23.3	23.6	25.3	32.0	44.4	61.1	80.2	100.8	120.9	140.4	160.1	179.0	197.5	214.0	225.5	231.7	237.9	243.5	248.6
36	23.6	29.3	59.9	108.5	166.6	222.7	279.9	336.4	392.2	446.9	496.8	544.0	587.2	625.3	648.4	662.9	676.2	687.9	698.1
37	24.1	29.3	58.2	106.1	160.6	217.2	274.0	330.6	386.6	441.0	492.1	539.8	583.9	621.1	642.5	656.5	669.3	680.7	690.7
38	24.3	27.6	48.0	84.6	127.9	172.8	218.5	263.3	307.7	350.8	392.7	432.0	468.1	498.9	517.7	529.9	540.9	547.5	555.0
39	This thermocouple was disconnected																		
40	24.3	25.1	31.3	46.5	68.3	94.0	120.6	147.9	174.3	200.0	225.0	248.9	272.1	291.6	303.8	310.3	317.5	323.3	328.3
41	23.1	23.2	25.8	34.3	49.4	69.1	90.6	113.6	135.0	156.9	178.5	198.3	219.2	236.4	247.9	253.8	259.9	265.0	269.9
42	23.3	23.6	25.8	34.1	49.7	69.1	90.4	114.6	134.5	156.6	178.7	198.0	219.2	236.2	247.7	253.3	259.4	264.5	269.6
43	23.6	27.8	51.9	91.6	141.2	193.3	249.1	305.0	361.0	417.8	474.7	530.1	579.9	621.5	649.8	666.5	681.4	694.8	707.1
44	23.8	27.1	49.0	87.7	133.7	184.3	239.2	294.0	349.4	406.2	463.4	518.4	568.4	611.0	638.0	654.8	669.6	682.9	695.0
45	24.1	26.3	41.4	70.8	107.6	147.4	190.1	233.2	277.0	321.1	366.2	410.7	452.1	486.9	508.5	521.7	533.6	545.4	555.7
46	24.3	25.3	34.0	53.3	79.5	110.0	142.4	176.0	210.3	244.2	278.4	312.7	345.1	372.1	388.0	397.9	406.7	414.7	422.8
47	24.6	24.8	29.3	41.0	58.9	80.9	105.4	131.0	157.1	183.1	209.3	235.2	261.1	283.3	296.9	304.8	312.0	318.5	324.5
48	24.6	24.6	26.6	33.3	46.0	62.5	81.7	103.2	124.0	145.2	167.3	188.1	211.5	231.4	244.0	250.8	257.4	263.3	268.4
49	23.6	23.8	26.3	34.0	47.5	64.5	84.1	105.4	126.0	145.9	168.0	188.8	211.0	229.4	241.6	248.2	254.5	259.9	264.5
50	23.61	25.3	31.5	41.9	56.2	73.7	93.3	114.1	135.5	158.6	179.7	205.3	227.7	247.2	262.1	271.6	279.9	287.5	294.0
51	23.8	24.6	31.3	41.7	56.0	73.2	92.6	113.1	134.0	156.0	177.5	203.0	225.2	244.5	259.6	268.9	277.2	284.8	291.1
52	23.8	24.6	28.8	36.7	48.5	63.0	79.7	98.1	117.3	136.7	155.6	176.2	196.3	215.0	228.9	237.7	245.5	252.8	258.9
53	24.3	24.6	27.1	32.5	41.2	52.3	65.7	80.7	96.7	112.9	129.1	145.7	162.3	178.2	190.3	197.8	204.8	211.5	217.2
54	24.3	24.6	25.8	29.5	35.8	44.4	55.0	67.4	80.7	94.5	108.8	123.6	136.7	150.4	160.8	167.5	173.5	179.7	185.1
55	24.3	24.6	25.1	27.3	31.8	38.5	47.3	57.4	69.1	81.4	94.2	106.8	119.4	131.7	140.9	146.9	152.9	158.3	163.3
56	23.6	23.8	24.3	26.6	31.0	37.5	46.0	56.0	66.9	79.0	91.3	103.5	115.8	126.9	135.7	141.4	147.2	152.4	157.3

TABLE 7. Thermocouple temperatures for design-loaded model steel beam heated along whole flange

Displacement transducer	Datalogger output (V) at time (min) of: 0	2	4	6	8	10	12	14	16	18	20	22	24	26	28	30	32
A	0	0.018	0.076	0.168	0.278	0.385	0.512	0.648	0.768	0.889	1.004	1.144	1.301	1.481	1.885	2.598	3.578
B	0	0.016	0.073	0.162	0.269	0.366	0.492	0.606	0.718	0.83	0.938	1.071	1.22	1.404	1.822	2.424	3.44

TABLE 8 Initialised transducer output voltages for design-loaded model steel beam heated along whole flange

	Designation of dimension	Dimension (mm) of specimen for test No: 1	2	3
100 mm from one end	A	40.02	50.12	60.23
	B	40.00	50.08	60.25
	C	60.12	60.2	60.48
	D	6.11	6.0	6.15
	E	6.04	6.04	6.15
	F	6.03	6.16	6.25
	G	6.13	6.14	6.25
	H	4.00	4.07	4.0
At centre	A	40.25	50.54	60.15
	B	40.23	50.54	60.15
	C	60.20	60.05	60.27
	D	6.12	5.9	6.10
	E	6.05	5.92	5.95
	F	6.05	6.18	6.05
	G	6.15	6.15	6.15
	H	4.16	4.15	4.0
100 mm from other end	A	40.22	50.15	60.30
	B	40.26	50.2	60.30
	C	60.25	60.3	60.39
	D	6.15	6.1	6.25
	E	6.03	6.12	6.05
	F	6.06	6.25	6.15
	G	6.13	6.22	6.15
	H	3.96	4.07	4.03
	J	0.00	0.24	0.15
	K	0.00	-0.25	0.20

TABLE 9. Dimensions of model steel columns after machining

Channel Number	Datalogger output at time (min) of: 0	4	8	12	16	20	24	28	32	36
0	16.9	16.6	24.1	37.4	51.0	93.8	136.9	179.8	220.8	253.2
1	*	*	*	*	*	*	*	*	*	*
2	20.1	20.1	29.1	51.2	85.3	128.2	177.7	227.2	269.9	303.9
3	20.1	20.6	34.2	63.4	105.0	156.4	212.7	263.6	307.5	342.4
4	20.1	20.6	38.4	73.2	120.5	177.7	237.4	290.9	335.5	*
5	20.1	21.1	40.1	77.2	128.2	190.5	252.0	307.5	352.9	389.1
6	19.9	20.1	26.6	49.1	90.3	147.2	215.7	285.1	348.2	398.8
7	19.9	20.1	29.1	56.5	103.6	167.0	242.0	317.5	383.9	432.9
8	19.9	20.1	34.5	70.1	125.8	200.1	282.4	367.0	434.8	482.7
9	20.1	20.9	41.3	86.5	153.4	238.4	331.7	426.5	497.3	545.9
10	20.1	21.6	47.6	101.0	176.7	270.4	372.5	477.3	548.7	599.7
11	19.9	21.9	50.0	105.2	183.4	278.3	380.5	483.9	559.1	610.3
12	19.9	19.9	24.1	47.3	89.1	148.7	221.8	295.7	362.9	416.6
13	19.9	20.1	27.3	53.6	100.7	166.5	245.2	325.5	395.3	446.6
14	20.1	20.4	30.8	65.6	121.3	197.4	283.9	372.9	444.5	495.0
15	20.1	19.1	35.2	80.8	146.0	235.2	333.8	435.7	509.6	561.2
16	18.6	20.4	40.8	93.6	166.2	265.3	373.2	483.2	558.1	610.8
17	19.9	21.1	44.5	96.0	170.3	270.6	380.5	489.1	566.6	620.9
18	19.9	19.9	26.3	48.6	90.0	149.5	221.0	296.9	367.9	421.6
19	20.1	20.1	29.1	54.6	102.2	167.5	244.7	326.2	400.2	450.6
20	19.9	20.4	34.5	68.7	123.6	200.1	284.1	376.3	449.0	499.9
21	20.1	21.6	43.3	86.0	154.1	242.0	333.8	439.1	512.4	562.4
22	19.9	22.1	49.3	98.1	175.4	271.6	371.7	485.3	558.8	610.1
23	19.9	22.4	51.0	104.5	181.3	278.8	381.5	492.6	569.5	621.4
24	19.9	19.9	25.0	44.7	82.0	135.7	198.7	268.0	334.1	381.7
25	19.9	19.9	27.6	50.5	92.4	150.4	220.1	293.3	362.7	410.0
26	19.9	20.1	31.3	59.4	110.0	176.1	251.7	332.1	406.2	452.2
27	18.6	18.9	35.9	73.7	131.6	208.6	292.8	380.8	459.6	506.3
28	19.9	20.6	42.0	84.8	152.9	235.7	327.1	421.8	501.1	548.7
29	19.9	20.9	44.0	87.7	158.1	244.2	334.5	426.3	507.2	556.3
30	19.4	19.4	23.6	44.0	83.6	137.7	204.6		335.3	387.7
31	19.6	19.6	25.6	49.5	94.34	152.9	224.9		364.4	416.8
32	19.9	20.1	29.5	60.6	112.4	179.0	257.1		407.8	456.5
33	19.9	20.4	34.7	74.2	135.2	213.0	297.1		463.6	511.2
34	19.6	20.6	39.8	87.4	155.4	240.8	331.4		507.0	554.1
35	19.4	20.4	41.0	90.1	160.4	246.6	338.1		514.1	562.9
36	19.4	19.6	25.9	53.1	101.2	162.9	234.2		371.7	422.5
37	19.4	19.4	29.3	62.0	115.7	183.4	258.7		403.6	451.6
38	19.4	19.9	36.2	78.2	141.8	219.1	299.8		452.3	497.1
39	19.4	20.4	44.7	98.4	173.8	260.7	349.8		509.4	554.6
40	19.4	21.1	51.7	115.5	202.9	295.9	392.2		556.5	602.0
41	19.6	21.6	52.9	118.8	208.3	302.9	400.0		564.5	612.2
42	19.6	19.9	24.4	46.9	91.0	151.6	225.9		372.9	424.4
43	19.6	19.9	26.1	53.1	102.6	170.3	250.5		406.6	454.2
44	19.9	20.1	30.3	64.6	121.9	201.0	287.3		451.1	497.6
45	21.4	22.1	35.9	79.8	148.9	239.6	337.4		514.3	560.7
46	22.1	22.1	41.5	94.3	172.6	270.6	377.4		561.7	608.2
47	20.9	22.4	44.2	98.8	180.5	280.6	388.4		572.1	620.0
48	20.6	20.4	24.4	45.7	85.3	141.8	212.0		346.5	394.5
49	21.4	20.6	26.6	52.9	98.16	161.4	237.9		380.1	427.0
50	20.6	20.9	31.5	65.6	119.8	194.7	277.9		430.3	475.4
51	20.1	20.9	37.7	81.0	145.8	233.7	326.9		490.7	535.8
52	19.9	21.1	43.3	94.8	170.3	266.3	367.2		537.7	582.9
53	19.6	21.1	44.5	97.2	175.6	273.0	376.3		547.5	593.3
54	19.9	19.6	20.6	28.6	46.4	72.7	105.5		173.6	201.9
55	19.6	19.9	21.4	31.5	52.2	82.2	119.1		191.8	219.8
56	19.6	19.9	23.1	36.4	61.5	97.4	138.4		217.6	245.2
57	6.703	6.700	6.701	6.761	6.939	7.129	7.377		7.809	7.980
58	9.034	9.024	8.910	8.688	8.460	8.191	7.933		7.588	7.625
59	-8.11	-8.26	-8.64	-8.58	-8.47	-9.40	-8.34		-8.90	-8.87

Channel No: 0 to 56 = °C; 57 = Volts (axial disp.); 58 = Volts (horiz. disp); 59 = m Volts (Load).
* = Faulty thermocouple; Nil entry = printer ran out of paper.

TABLE 10. Thermocouple temperatures and transducer data for model steel column, Test 1.

Channel Number	Datalogger output at time (min) of: 40	44	48	52	56	60	64	68
0	279.1	296.9	311.8	327.1	337.4	347.9	356.7	363.9
1	*	*	*	*	*	*	*	*
2	328.3	347.0	365.3	382.9	394.3	406.4	416.1	421.3
3	367.2	385.5	406.4	427.2	440.2	453.2	463.4	466.7
4	*	*	*	*	*	*	*	*
5	414.7	433.8	458.7	482.5	497.6	511.2	521.8	520.4
6	431.0	445.2	455.8	466.9	478.9	488.6	493.3	495.7
7	464.1	478.9	491.2	504.4	518.1	528.0	533.4	536.2
8	514.1	530.3	545.2	561.7	577.5	586.2	593.8	596.1
9	578.2	596.6	616.0	637.1	654.8	664.6	673.1	675.3
10	634.0	653.9	677.7	703.4	721.8	731.9	742.0	742.7
11	644.9	665.5	690.7	718.2	737.2	747.2	758.1	756.4
12	444.7	457.0	466.9	480.1	489.4	498.8	505.3	508.2
13	474.2	488.6	499.5	514.8	525.2	534.8	542.4	544.5
14	522.6	539.8	553.4	570.9	582.9	593.3	601.8	603.0
15	591.6	611.2	629.5	651.7	665.0	676.7	686.5	688.1
16	644.9	665.7	688.6	715.1	729.5	741.5	753.0	752.8
17	656.0	677.7	702.7	730.7	745.3	758.1	769.1	766.0
18	450.4	464.6	474.5	489.1	499.5	507.5	512.7	513.8
19	481.1	495.2	508.7	524.9	536.2	544.9	551.1	551.3
20	529.9	545.9	561.7	580.6	592.1	600.9	608.9	609.1
21	593.3	610.8	630.4	652.0	664.8	674.3	682.9	681.2
22	642.7	661.2	685.3	710.1	724.5	734.5	743.9	739.1
23	654.8	674.3	700.0	726.4	740.5	751.3	760.7	753.7
24	411.9	425.1	435.3	445.9	454.4	463.6	467.4	467.6
25	439.8	453.5	465.3	477.5	487.7	496.6	501.1	500.6
26	482.0	496.6	510.8	526.3	538.4	547.3	552.7	549.7
27	535.1	552.0	569.7	589.3	604.4	614.1	620.2	616.7
28	579.6	597.1	618.1	641.5	658.4	668.1	674.6	668.4
29	586.2	604.4	626.4	649.9	667.9	677.4	684.5	676.2
30	419.0	435.5	444.0	449.7	462.4	470.0	473.5	473.4
31	446.1	461.3	473.3	484.9	494.3	502.0	504.9	504.7
32	487.4	501.4	517.1	532.7	542.8	551.8	554.6	554.6
33	542.6	559.1	577.7	596.9	609.6	619.5	623.6	622.4
34	586.2	604.7	626.6	648.4	662.4	673.4	677.7	672.7
35	595.4	613.9	635.9	659.1	673.9	684.8	689.1	681.9
36	450.1	463.4	471.6	487.0	494.1	501.1	504.7	504.9
37	479.2	493.1	503.0	518.3	526.6	534.6	539.3	539.3
38	525.2	541.9	553.7	571.3	580.6	589.5	594.2	594.2
39	584.6	602.8	619.0	640.4	651.5	661.7	667.2	666.7
40	634.0	654.1	673.9	698.9	710.8	720.6	725.7	723.0
41	644.6	664.4	686.0	710.8	725.7	735.9	741.0	735.9
42	449.4	462.4	470.9	483.4	492.4	500.6	504.7	505.3
43	480.1	493.1	503.7	517.9	525.9	535.3	540.0	540.2
44	525.2	539.5	552.2	568.7	578.9	588.3	594.0	594.0
45	590.5	607.5	624.7	645.8	658.9	669.6	676.5	676.5
46	639.7	658.4	679.1	703.4	718.2	729.7	735.5	733.8
47	651.7	671.2	692.9	718.2	734.0	745.6	752.3	748.0
48	422.7	436.5	446.4	457.7	467.6	474.9	478.9	478.0
49	453.9	467.9	479.2	492.6	503.2	511.7	516.2	514.6
50	501.6	516.4	530.1	545.9	559.1	568.0	573.9	572.3
51	562.6	579.6	596.6	615.8	631.4	642.2	649.4	646.1
52	610.3	627.6	647.5	669.6	687.9	699.8	707.7	702.0
53	620.9	638.0	658.9	681.7	700.3	712.0	720.1	712.3
54	221.8	237.4	251.2	264.8	276.9	286.5	294.5	299.8
55	240.3	255.8	271.6	286.3	297.9	308.2	316.6	321.2
56	266.0	282.4	300.0	316.4	329.0	340.5	348.6	352.5
57	8.072	8.109	8.131	8.175	8.233	8.263	8.272	8.299
58	7.644	7.645	7.625	7.666	7.837	7.972	8.056	8.284
59	-8.84	-8.76	-8.71	-9.02	-8.43	-8.38	-8.040	-8.11

Channel No: 0 to 56°C; 57 = Volts (Axial disp.); 58 = Volts (Horiz. Disp); 59 = m Volts (Load); * = Faulty thermocouple

TABLE 10. Thermocouple temperatures and transducer data for model steel column, Test 1.

Channel Number	Datalogger output at time (min) of: 0	4	8	12	20	24	28	32	36	46	51	55	59	62
0	19.1	20.6	33.5	65.8	138.2	183.4	221.8	249.1	268.7	315.4	323.5	335.3	347.5	345.8
1	18.6	22.4	38.1	74.2	155.4	200.7	237.6	268.4	286.3	334.1	343.5	357.5	369.4	364.4
2	18.9	25.60	48.1	90.8	185.4	232.3	271.3	303.1	322.1	371.0	380.1	399.0	410.2	396.9
3	19.1	28.6	56.5	105.0	208.8	256.1	254.9	328.6	348.2	398.3	408.8	431.5	440.5	414.4
4	19.9	36.2	73.9	132.1	250.5	302.0	343.9	378.4	398.1	448.3	458.9	482.0	489.8	456.1
5	20.1	38.4	78.0	140.4	260.9	312.7	354.8	389.3	409.0	460.1	470.9	494.1	499.0	463.4
6	18.4	21.6	45.4	107.1	249.5	324.0	380.3	419.2	436.0	460.8	462.2	460.1	460.8	449.7
7	18.6	24.4	56.0	127.5	288.2	370.3	423.0	460.8	476.8	503.8	505.8	504.9	505.8	492.4
8	18.6	28.6	73.7	160.9	346.3	431.0	483.4	515.8	536.5	564.5	567.3	569.0	571.1	550.8
9	19.1	35.7	96.7	206.1	421.9	508.0	562.2	598.5	616.2	646.8	651.3	656.0	659.1	628.8
10	19.6	41.0	114.5	242.5	485.6	576.6	630.9	669.3	688.6	724.0	729.7	737.9	740.3	697.4
11	19.6	42.8	118.6	251.0	495.7	584.8	624.7	681.7	702.4	737.4	743.4	752.3	753.5	706.3
12	18.6	21.4	43.7	107.9	265.8	349.1	414.0	449.7	464.1	486.5	488.4	477.5	469.0	458.0
13	18.6	23.6	53.1	126.0	302.9	389.8	453.0	488.4	503.5	528.0	530.8	518.1	511.7	497.3
14	18.6	27.6	68.4	157.6	364.1	454.9	541.1	549.0	565.5	592.8	597.1	585.3	581.8	560.7
15	18.9	32.3	87.7	198.7	436.7	528.9	587.6	623.8	642.0	674.8	681.2	675.5	674.6	642.5
16	19.1	36.4	104.0	233.2	503.0	596.9	658.4	697.4	718.0	759.7	771.3	777.1	775.0	727.6
17	19.6	37.9	106.9	240.3	507.7	604.9	667.0	704.1	725.7	767.7	779.1	786.8	782.2	733.1
18	18.1	21.4	44.2	106.4	257.5	339.8	401.2	438.4	453.7					
19	18.4	23.9	54.1	125.3	295.0	382.7	442.1	478.7	494.8					
20	18.4	29.5	73.4	161.9	358.9	447.8	505.1	539.8	557.2					
21	19.1	36.9	96.0	206.9	433.8	526.3	583.9	619.8	638.5					
22	19.6	44.5	116.7	245.9	505.1	596.6	657.7	696.3	716.5					
23	20.1	47.1	121.5	252.7	507.2	602.8	664.8	703.9	725.9					
24	18.4	21.6	42.5	97.6	229.6	299.8	363.8	400.9	416.8					
25	18.4	24.4	51.2	113.8	258.0	334.8	400.2	435.3	451.6					
26	18.6	28.8	66.3	141.8	306.0	391.0	453.9	489.8	507.5					
27	19.1	34.2	84.1	175.8	361.0	455.0	517.6	555.6	573.7					
28	*	*	*	*	*	*	*	*	*					
29	20.9	44.2	125.3	220.1	424.4	532.7	587.6	624.5	644.9					
30	17.6	19.4	38.1	77.2	201.7	274.7	345.3	369.0	418.2	443.6	452.1	455.8	453.2	445.9
31	17.6	21.4	46.6	92.9	229.1	311.1	386.7	434.6	456.1	484.6	494.3	498.5	497.6	488.2
32	17.6	25.4	61.7	119.6	275.4	370.5	446.8	492.9	514.1	456.8	558.6	564.5	566.2	553.7
33	17.9	30.5	79.1	149.7	330.2	438.4	514.6	561.0	583.4	620.9	634.9	644.2	649.1	631.1
34	17.9	38.1	98.6	183.1	383.4	503.9	578.9	627.6	651.5	694.8	710.6	721.8	731.2	703.2
35	18.1	41.0	103.8	193.4	392.9	511.0	587.4	637.3	660.1	704.6	721.8	733.6	744.4	712.3
36	17.4	19.1	37.9	81.3	222.2	306.0	376.7	425.5	443.3	464.6	472.8	473.5	464.3	457.5
37	17.1	20.6	45.9	97.2	254.4	348.6	420.1	467.6	487.0	510.8	520.2	521.1	512.3	503.0
38	17.6	23.9	58.4	122.4	305.5	410.2	480.8	526.1	546.4	573.5	584.3	586.0	579.8	566.9
39	17.6	27.8	76.5	156.6	373.7	489.6	560.5	606.5	628.5	661.5	675.3	680.7	679.5	659.8
40	17.9	33.0	93.4	188.4	433.4	554.6	629.7	677.2	701.3	742.0	758.8	768.9	774.2	742.5
41	18.1	35.0	98.1	198.2	443.3	565.9	639.9	688.9	713.4	757.4	775.0	785.3	790.9	754.5
42	17.9	19.1	38.4	83.2	288.1	313.7	385.0	431.5	449.7	471.9	478.5	477.8	471.4	464.8
43	17.6	20.9	46.1	98.8	260.0	354.8	427.5	472.1	491.0	516.2	522.8	521.8	516.9	507.5
44	17.9	23.6	59.6	125.1	314.0	421.8	490.5	532.5	553.0	581.0	587.9	586.7	585.3	573.0
45	17.9	27.8	76.8	158.6	381.2	496.2	566.9	609.8	631.1	663.4	674.1	676.9	678.4	658.4
46	18.4	33.2	94.1	191.6	444.0	567.6	640.1	685.0	708.6	748.4	764.6	771.6	778.8	745.8
47	18.1	34.7	97.6	199.7	454.7	578.0	650.8	697.2	721.1	764.1	779.6	786.3	794.1	757.6
48	17.4	19.6	41.3	86.0	217.6	288.5	350.1	394.5	415.9	445.0	451.3	452.1	453.5	446.4
49	17.6	21.9	50.7	103.3	250.5	328.5	392.4	437.2	456.8	487.2	494.5	495.9	498.5	489.4
50	17.9	25.9	65.7	129.9	300.0	386.9	451.3	495.4	512.4	545.2	553.2	555.8	560.0	547.1
51	17.4	32.3	87.9	170.0	375.5	475.2	540.5	583.4	603.6	638.7	647.5	652.5	658.4	638.7
52	17.9	38.6	105.9	203.4	434.1	542.4	605.8	649.9	673.6	714.9	724.5	731.6	740.5	709.1
53	17.9	41.0	110.9	212.7	445.4	553.9	621.2	665.3	688.6	731.9	742.0	748.2	756.9	723.0
54	17.4	18.4	27.3	48.6	108.1	139.4	170.0	196.5	213.5	252.4	262.6	271.1	281.7	783.6
56	0.9986	1.015	0.9641	0.8725	0.8276	0.8239	0.8476	0.8341	0.8308	0.7260	0.6855	0.6868	1.90	1.89
57	7.049	7.047	7.080	7.183	7.527	7.790	7.988	8.152	8.219	8.372	8.434	7.240	6.877	6.836
58	3.399	3.308	3.012	2.621	1.670	1.374	1.407	1.517	1.553	2.128	2.959	8.881	9.562	9.444
59	2.59	2.66	2.72	2.79	2.80	2.59	2.85	2.83	2.81	2.59	2.49	1.43	1.12	0.36

Channel No: 0 to 54 = °C; 56 = Volts (Vert. Disp); 57 = Volts (Hor. Disp); 58 = Volts (Axial Disp); 59 = Volts (Load); * Faulty thermocouple; Nil entry = Failure of printer

TABLE 11. Thermocouple temperatures and transducer data for model steel column, Test 2.

Channel Number	Datalogger output at time (min) of: 0	4	8	12	16	20	24	28	32	36	40	44
0	20.1	21.6	34.0	60.3	94.8	134.0	177.1	216.1	244.7	266.0	282.4	305.3
1	19.9	22.6	39.8	70.1	108.3	150.4	197.6	235.7	265.0	287.0	304.8	329.7
2	20.1	25.4	49.8	87.2	130.2	177.7	227.6	265.0	295.0	317.5	337.4	365.1
3	19.9	29.8	65.8	113.1	164.4	219.3	271.3	310.1	340.3	363.9	387.4	419.0
4	20.1	38.4	91.0	151.2	213.9	275.9	333.6	374.1	404.0	428.2	452.3	484.4
5	19.9	38.9	90.8	152.7	214.9	275.9	332.4	372.7	402.6	425.6	452.3	485.8
6	20.1	21.6	40.3	85.1	145.2	220.5	297.1	357.9	397.4	419.7	430.1	434.6
7	19.9	23.6	50.7	104.7	176.1	260.9	344.8	404.5	441.9	463.6	474.0	479.2
8	19.9	26.8	68.0	138.2	225.7	326.4	417.3	474.7	509.4	531.0	541.4	548.0
9	19.9	31.8	89.1	179.2	282.7	404.5	500.6	557.4	592.4	615.8	627.6	636.8
10	20.1	37.4	111.9	225.4	347.2	491.7	591.2	649.9	687.4	713.4	727.3	740.8
11	19.9	38.1	112.6	225.9	345.8	486.5	585.0	645.8	683.6	709.9	728.9	643.4
12	20.6	21.6	37.7	80.6	143.5	229.1	316.6	381.7	419.0	439.5	444.5	439.1
13	20.1	22.9	45.9	98.6	172.5	270.6	364.4	428.2	463.2	483.9	486.7	483.4
14	20.6	25.4	60.1	128.2	219.1	336.7	437.4	496.9	528.7	550.8	553.7	553.0
15	19.9	28.8	78.7	166.7	276.9	421.8	525.2	584.1	617.2	641.3	649.6	655.3
16	20.4	33.0	96.5	206.1	332.1	500.6	607.9	668.1	705.1	730.4	751.6	764.6
17	19.9	35.5	101.0	211.5	338.1	501.8	610.5	670.7	707.7	735.0	752.5	765.8
18	19.9	21.6	39.8	83.6	144.7	226.7	303.9	367.7	409.0	434.8	443.6	442.9
19	20.1	23.4	49.5	101.9	173.8	266.5	350.1	413.3	453.2	479.2	487.2	488.4
20	19.9	27.8	69.9	138.4	230.5	341.5	431.0	489.4	527.5	553.2	561.7	568.3
21	20.1	32.5	88.8	175.1	283.9	414.5	509.4	566.6	607.3	635.2	649.9	662.7
22	20.1	38.9	112.9	220.5	351.2	505.8	602.5	661.0	707.0	735.5	767.7	788.3
23	19.9	43.5	120.5	230.3	358.2	505.1	604.4	665.5	713.9	746.3	779.1	802.1
24	20.1	21.9	40.1	81.5	132.6	185.8	237.1	289.2	347.9	408.3	456.8	501.8
25	20.1	22.9	47.8	96.9	152.7	210.8	267.7	330.9	397.9	460.1	508.0	552.0
26	20.4	26.1	62.5	124.3	186.0	248.3	318.5	397.6	474.0	539.3	584.8	626.2
27	19.9	31.5	84.8	167.0	235.4	308.7	398.6	494.5	582.5	647.5	688.6	734.8
28	20.1	37.4	105.9	204.9	276.2	360.5	466.2	576.8	673.6	739.1	785.8	834.5
29	20.1	38.4	107.1	208.1	282.0	371.5	473.5	578.9	676.0	747.5	815.0	859.8
30	19.6	21.6	41.5	82.9	131.6	180.8	226.2	275.0	331.7	393.4	446.1	493.1
31	19.6	24.1	51.9	101.9	154.6	207.6	238.3	319.2	387.2	453.2	505.6	457.1
32	20.1	28.1	69.1	130.6	188.1	243.7	304.6	382.0	462.7	533.2	580.3	612.2
33	19.9	34.2	*	167.0	*	290.9	365.4	463.4	555.3	626.2	664.4	688.9
34	19.6	44.5	118.4	209.0	271.8	341.5	434.8	543.5	643.2	713.2	748.2	771.3
35	19.6	46.4	120.3	213.5	277.9	346.0	434.1	539.3	639.7	712.3	745.1	768.9
36	19.6	21.4	42.0	86.7	147.0	222.8	295.2	358.4	403.3	430.1	444.3	452.8
37	19.6	23.6	51.7	105.7	175.9	262.1	341.5	405.2	449.2	475.7	488.9	499.9
38	19.6	27.3	68.4	135.7	219.1	320.0	405.2	467.2	508.4	535.5	549.4	561.7
39	19.6	33.0	89.8	175.6	275.0	369.9	488.4	548.3	589.0	618.8	634.7	648.7
40	19.9	41.5	115.2	223.7	336.7	478.9	572.3	632.5	675.0	708.9	726.1	747.5
41	19.9	47.1	128.7	232.5	344.6	482.5	574.2	639.2	683.4	720.1	739.1	756.6
42	19.6	22.9	42.5	87.4	149.7	230.5	313.2	377.0	417.3	436.0	445.7	452.3
43	22.4	24.9	52.2	103.3	174.6	268.0	356.3	417.5	459.8	474.9	486.7	495.0
44	22.1	29.1	68.9	136.7	226.2	338.6	440.0	493.3	531.5	548.5	560.0	569.9
45	20.9	32.0	84.8	167.0	269.9	403.3	503.5	562.2	604.7	622.1	634.2	646.3
46	20.9	37.9	109.8	215.2	335.5	493.1	595.2	657.7	699.3	723.5	737.9	758.3
47	20.9	37.9	108.5	215.9	338.4	492.2	595.0	659.6	703.2	729.7	745.6	764.1
48	20.1		49.8	96.0	154.1	224.9	291.3	347.2	389.8	409.7	419.9	428.7
49	20.1		63.5	118.4	185.5	264.1	335.0	395.3	429.6	450.4	461.0	470.9
50	19.6		91.0	161.2	242.0	333.1	410.4	467.9	502.0	521.1	532.7	543.3
51	19.6		124.6	217.6	314.4	422.3	506.8	563.8	597.3	619.8	633.0	646.1
52	19.6		144.3	250.3	360.5	482.0	569.2	627.8	663.9	689.3	706.0	719.2
53	19.6		154.9	261.2	371.5	489.4	576.6	637.3	673.6	702.4	*	*
54	19.4		31.5	53.6	84.6	118.1	151.2	184.7	209.8	228.8	245.7	262.6
56	1.549		1.384	1.314	1.279	1.246	1.222	1.221	1.251	1.256	2.04	2.01
57	6.437	6.430	6.479	6.534	6.663	6.798	7.021	7.210	7.367	7.547	7.355	7.095
58	3.388	3.272	2.856	2.316	1.824	1.256	1.034	0.9739	1.057	1.447	9.061	1.22
59	3.87	4.06	3.89	4.07	4.22	4.27	4.15	4.17	4.19	3.97	1.38	1.01

Channel No: 0 to 54 = °C; 56 = Volts (Vert. Disp); 57 = Volts (Hor. Disp); 58 = Volts (Axial Disp); 59 = Volts (Load); Nil entry = Failure of printer

TABLE 12. Thermocouple temperatures and transducer data for model steel column, Test 3.

Duration of heating (min)	Central vertical displacement transducer (v)		Central horizontal displacement transducer (v)		Axial displacement transducer (v)		Compression load transducer (mV)	(lb/in²)	% Design load
	(mm)		(mm)		(mm)				
	i	ii	iii	iv	v	vi	vii	viii	ix
0			0	0	0	0	0	0	100
4			-0.01	-0.0748	-0.003	-0.0149	0.15	78.15	102.26
8			-0.134	-1.003	-0.002	-0.0099	0.53	276.13	108.12
12			-0.346	-2.590	0.058	0.2888	0.47	244.8	107.1
16			-0.574	-4.297	0.236	1.175	0.36	187.5	105.4
20			-0.843	-6.311	0.426	2.1215	1.29	672.1	119.5
24			-1.101	-8.242	0.694	3.356	0.23	120.0	103.5
28									
32			-1.466	-10.974	1.106	5.507	0.79	411.6	112
36			-1.409	-10.547	1.279	6.369	0.69	359.5	110.4
40			-1.43	-10.70	1.369	6.817	0.73	380.3	111.0
44			-1.389	-10.398	1.409	7.022	0.65	338.6	109.8
48			-1.409	-10.547	1.428	7.111	0.60	312.6	109.1
52			-1.368	-10.241	1.472	7.33	0.91	474.1	113.8
56			-1.197	-8.960	1.53	7.619	0.32	166.7	105
60			-1.062	-7.950	1.56	7.768	0.27	140.7	104
64			-0.978	-7.321	1.569	7.813	0.29	151.1	104
68			-0.75	-5.614	1.596	7.948	0	0	100

Notes: i, iii, v, vii) Reading at stated time minus initial reading; ii) Volts x 7.525; iv) Volts x 7.486; vi) Volts x 4.980; viii) mVolts x 521 for Test 1 or mVolts x 1840 for Tests 2 and 3 = deviation from required pressure; ix) [(lb/in² + Design load pressure) ÷ Design load pressure] x 100

TABLE 13. Displacement and load transducer data for model steel column, Test 1

Duration of heating (min)	Central vertical displacement transducer (v) i	(mm) ii	Central horizontal displacement transducer (v) iii	(mm) iv	Axial displacement transducer (v) v	(mm) vi	Compression load transducer (mV) vii	(lb/in²) viii	% Design load ix
0	0	0	0	0	0	0	0	0	100
4	0.0164	0.1234	-0.091	-0.68	-0.002	-0.0099	0.07	128.5	102.9
8	-0.0345	-0.2596	-0.387	-2.897	-0.031	0.154	-0.39	-717.6	83.8
12	-0.1261	-0.9489	-0.778	-5.824	0.134	0.667	0.20	368	108.3
20	-0.171	-1.2867	-1.729	-12.94	0.478	2.380	0.21	386.4	108.6
24	-0.1747	-1.3146	-2.025	-16.506	0.741	3.690	0	0	100
28	-0.151	-1.136	-1.992	-14.912	0.939	4.676	0.26	479.4	110.7
32	-0.1645	-1.237	-1.882	-14.088	1.103	5.492	0.24	441.6	110
35	-0.1678	-1.262	-1.846	-13.819	1.17	5.826	0.22	404.8	109
40	-0.2726	-2.051	-1.271	-9.514	1.323	6.588	0	0	100
51	-0.3131	-2.356	-0.44	-3.293	1.385	6.897	-0.1	-184	95.8
55	-0.3118	-2.346	5.482	41.04	0.91	4.532	-0.16	-2134	52
59	0.9014	6.783	6.163	46.13	-0.172	-0.856	-1.47	-2705	39
62	0.8914	6.708	6.045	45.24	-0.213	-1.060	-2.23	-4103	7.8

Notes: i, iii, v, vii) Reading at stated time minus initial reading; ii) Volts x 7.525; iv) Volts x 7.486; vi) Volts x 4.980; viii) mVolts x 521 for Test 1 or mVolts x 1840 for Tests 2 and 3 = deviation from required pressure; ix) [(lb/in² + Design load pressure) ÷ Design load pressure] x 100

TABLE 14. Displacement and load transducer data for model steel column. Test 2

Duration of heating (min)	Central vertical displacement transducer (v) i	(mm) ii	Central horizontal displacement transducer (v) iii	(mm) iv	Axial displacement transducer (v) v	(mm) vi	Compression load transducer (mV) vii	(lb/in²) viii	% Design load ix
0	0	0	0	0	0	0	0	0	100
4			-0.116	-0.868	-0.007	-0.035	0.19	349	108.4
8	-0.165	-1.242	-0.532	-3.982	0.042	0.209	0.020	388	109.3
12	-0.235	-1.768	-1.072	-8.025	0.097	0.483	0.20	368	109
16	-0.270	-2.03	-1.564	-11.708	0.226	1.125	0.35	644	115.4
20	-0.303	-2.28	-2.132	-15.960	0.361	1.798	0.40	736	117.6
24	-0.327	-2.46	-2.354	-17.622	0.584	2.910	0.28	515	112.3
28	-0.328	-2.468	-2.414	-18.071	0.773	3.85	0.30	552	113.2
32	-0.298	-2.24	-2.331	-17.449	0.930	4.631	0.32	588	114.1
36	-0.293	-2.204	-1.941	-15.530	1.11	5.528	0.10	184	104.4
40					0.918	4.571			35 *
44					0.658	3.276			28 *

Notes: i, iii, v, vii) Reading at stated time minus initial reading; ii) Volts x 7.525; iv) Volts x 7.486; vi) Volts x 4.980; viii) mVolts x 521 for Test 1 or mVolts x 1840 for Tests 2 and 3 = deviation from required pressure; ix) [(lb/in² + Design load pressure) ÷ Design load pressure] x 100

TABLE 15. Displacement and load transducer data for model steel column, Test 3

APPENDIX 3 EXAMPLES OF 'PAFEC' DATAFILES

```
TITLE  DEFORMATION OF UNRESTRAINED STEEL I-SECTION
C      BEAM (ANALYSIS 130) (DFRAB) 21/06/84
C
C      ELASTIC ANALYSIS ASSUMING E VALUE=209E9 FOR ALL TEMPS.
C      TEMPS IN 7 LOAD CASES CORRESPOND TO TEMPS IN EXPERIMENT
C      AT TIME INTERVALS OF 6 MIN UP TO 48MINS OF HEATING.
C      USES PHASE TRANSFORMATION (PRELOAD) MODULE,WHICH
C      ASSUMES SLOPE OF STRAIN-TEMP LINE IS 14.E-6,
C      SO AS TO COMPARE WITH ANALYSIS 131 WHICH ASSUMES
C        SLOPE =14.8648E-6. NOTE 5.97mm FLANGE THICKNESS USED.
CONTROL
DOUBLE
PHASE=1,7
STOP
CONTROL.END
C
NODES
AXIS.NUMBER=1
NODE.NUMBER     X         Y
    1           0         0
    2          .655       0
    3           0        .00597
    4          .655      .00597
    5           0        .052
    6          .655      .052
    7           0        .098
    8          .655      .098
    9           0        .104
   10          .655      .104
C
PAFBLOCKS
ELEMENT.TYPE=36210
TYPE=1
BLOCK.NUMBER    GROUP.NUMBER    PROPERTIES    N1    N2      TOPOLOGY
     1               1              1         1     2    1   2   3   4
     2               2              2         1     2    3   4   5   6
     3               3              2         1     2    5   6   7   8
     4               4              1         1     2    7   8   9  10
C
MESH
REFERENCE    SPACING.LIST
    1              10
    2               1
C
PLATES.AND.SHELLS
PLATE.OR.SHELL.NUMBER    MATERIALS.NUMBER    THICKNESS
       1                        11               .044
       2                        11               .0042
C
MATERIAL
MATERIAL.NUMBER    E        NU       ALPHA
      11          209E9    0.3      14.E-6
C
RESTRAINTS
NODE.NUMBER    PLANE      DIRECTION
    9             1           12
```

```
C
TEMPERATURE
LOAD.CASE  TEMPERATURE      START      FINISH      STEP    LIST.OF.NODES
C  TIME=6MINS
    1          60            11         29          1       1 , 2
    1          54            41         59          1       3 , 4
    1          25.72         71         89          1       5 , 6
    1          17           101        119          1       7 , 8
    1          16.8         131        149          1       9 ,10
C  TIME=12MINS
    2         225            11         29          1       1 , 2
    2         196            41         59          1       3 , 4
    2          90            71         89          1       5 , 6
    2          38           101        119          1       7 , 8
    2          30.2         131        149          1       9 ,10
C  TIME=18MINS
    3         460            11         29          1       1 , 2
    3         396            41         59          1       3 , 4
    3         186            71         89          1       5 , 6
    3         110           101        119          1       7 , 8
    3         105.4         131        149          1       9 ,10
C  TIME=24MINS
    4         670            11         29          1       1 , 2
    4         574            41         59          1       3 , 4
    4         271            71         89          1       5 , 6
    4         170           101        119          1       7 , 8
    4         164.8         131        149          1       9 ,10
C  TIME=30MINS
    5         790            11         29          1       1 , 2
    5         692            41         59          1       3 , 4
    5         327            71         89          1       5 , 6
    5         218           101        119          1       7 , 8
    5         210.2         131        149          1       9 ,10
C  TIME=36MINS
    6         950            11         29          1       1 , 2
    6         810            41         59          1       3 , 4
    6         365            71         89          1       5 , 6
    6         244           101        119          1       7 , 8
    6         238           131        149          1       9 ,10
C  TIME=42MINS
    7        1050            11         29          1       1 , 2
    7         885            41         59          1       3 , 4
    7         394            71         89          1       5 , 6
    7         265           101        119          1       7 , 8
    7         258.3         131        149          1       9 ,10
C  TIME=42MINS
    8        1130            11         29          1       1 , 2
    8         960            41         59          1       3 , 4
    8         415            71         89          1       5 , 6
    8         280           101        119          1       7 , 8
    8         272.7         131        149          1       9 ,10
C
PRELOAD
TYPE=1
TABLE=1
CASE
 1
 2
 3
 4
 5
```

```
  6
  7
  8
 TABLE
 TABLE=1
 BASIS          VALUE
   0              0
  740           1.036E-2
  825           8.86E-3
 1200           1.411E-2
 C
 END.OF.DATA
```

```
TITLE  DEFORMATION OF UNRESTRAINED STEEL I-SECTION
C      BEAM (ANALYSIS 132) (DFR41)  11/10/84
C
C      ELASTIC ANALYSIS ASSUMING E VALUE=209E9 FOR ALL TEMPS.
C      TEMPS IN 7 LOAD CASES CORRESPOND TO TEMPS IN EXPERIMENT
C      AT TIME INTERVALS OF 6 MIN UP TO 48MINS OF HEATING.
C      USES PHASE TRANSFORMATION (PRELOAD) MODULE,WHICH
C      ASSUMES SLOPE OF STRAIN-TEMP LINE IS 14.8648E-6.
C      HALF LENGTH OF BEAM MODELLED WITH 40 ELEMENTS
C      FOR HALF LENGTH, AND TWO ELEMENTS WITHIN HOT FLANGE
C      THICKNESS, WITH A TOTAL OF 280 ELEMENTS.
CONTROL
DOUBLE
PHASE=1,7
STOP
CONTROL.END
C
NODES
AXIS.NUMBER=1
NODE.NUMBER     X         Y
    1           0         0
    2          .655       0
    3           0        .002985
    4          .655      .002985
    5           0        .00597
    6          .655      .00597
    7           0        .026
    8          .655      .026
    9           0        .039
   10          .655      .039
   11           0        .052
   12          .655      .052
   13           0        .098
   14          .655      .098
   15           0        .104
   16          .655      .104
C
PAFBLOCKS
ELEMENT.TYPE=36210
TYPE=1
BLOCK.NUMBER    GROUP.NUMBER    PROPERTIES    N1    N2      TOPOLOGY
    1               1               1         1     2    1   2   3   4
    2               2               1         1     2    3   4   5   6
    3               3               2         1     2    5   6   7   8
    4               4               2         1     2    7   8   9  10
    5               5               2         1     2    9  10  11  12
    6               6               2         1     2   11  12  13  14
    7               7               1         1     2   13  14  15  16
C
MESH
REFERENCE    SPACING.LIST
    1              40
    2               1
C
PLATES.AND.SHELLS
PLATE.OR.SHELL.NUMBER    MATERIALS.NUMBER    THICKNESS
       1                        11               .044
       2                        11               .0042
C
MATERIAL
```

```
MATERIAL.NUMBER     E        NU       ALPHA
      11          209E9    0.3      14.8648E-6
C
RESTRAINTS
NODE.NUMBER     PLANE       DIRECTION
    1             1             12
C
TEMPERATURE
LOAD.CASE  TEMPERATURE  START  FINISH  STEP    LIST.OF.NODES
C TIME=6 MINS
   1            60        18     94     2          1 , 2
   1            57       138    214     2          3 , 4
   1            54       258    334     2          5 , 6
   1            36       378    454     2          7 , 8
   1            30       498    574     2          9 ,10
   1          25.7       618    694     2         11 ,12
   1           .17       738    814     2         13 ,14
   1          16.8       858    934     2         15 ,16
C TIME=12 MINS
   2           225        18     94     2          1 , 2
   2           210       138    214     2          3 , 4
   2           196       258    334     2          5 , 6
   2           137       378    454     2          7 , 8
   2           110       498    574     2          9 ,10
   2            90       618    694     2         11 ,12
   2            38       738    814     2         13 ,14
   2          30.2       858    934     2         15 ,16
C TIME=18 MINS
   3           460        18     94     2          1 , 2
   3           425       138    214     2          3 , 4
   3           396       258    334     2          5 , 6
   3           277       378    454     2          7 , 8
   3           225       498    574     2          9 ,10
   3           186       618    694     2         11 ,12
   3           110       738    814     2         13 ,14
   3         105.4       858    934     2         15 ,16
C TIME=24 MINS
   4           670        18     94     2          1 , 2
   4           620       138    214     2          3 , 4
   4           574       258    334     2          5 , 6
   4           402       378    454     2          7 , 8
   4           325       498    574     2          9 ,10
   4           271       618    694     2         11 ,12
   4           170       738    814     2         13 ,14
   4         164.8       858    934     2         15 ,16
C TIME=30 MINS
   5           790        18     94     2          1 , 2
   5           740       138    214     2          3 , 4
   5           692       258    334     2          5 , 6
   5           483       378    454     2          7 , 8
   5           390       498    574     2          9 ,10
   5           327       618    694     2         11 ,12
   5           218       738    814     2         13 ,14
   5           210       858    934     2         15 ,16
C TIME=36 MINS
   6           950        18     94     2          1 , 2
   6           875       138    214     2          3 , 4
   6           810       258    334     2          5 , 6
   6           547       378    454     2          7 , 8
   6           435       498    574     2          9 ,10
```

```
    6          365        618     694      2          11 ,12
    6          244        738     814      2          13 ,14
    6          238        858     934      2          15 ,16
 C TIME=42 MINS
    7         1050         18      94      2           1 , 2
    7          962        138     214      2           3 , 4
    7          885        258     334      2           5 , 6
    7          596        378     454      2           7 , 8
    7          475        498     574      2           9 ,10
    7          394        618     694      2          11 ,12
    7          265        738     814      2          13 ,14
    7          258.3      858     934      2          15 ,16
 C TIME=48 MINS
    8         1130         18      94      2           1 , 2
    8         1045        138     214      2           3 , 4
    8          960        258     334      2           5 , 6
    8          633        378     454      2           7 , 8
    8          500        498     574      2           9 ,10
    8          415        618     694      2          11 ,12
    8          280        738     814      2          13 ,14
    8          272.7      858     934      2          15 ,16
C
PRELOAD
C
TYPE=1
TABLE=1
CASE
 1
 2
 3
 4
 5
 6
 7
 8
TABLE
TABLE=1
BASIS          VALUE
  0              0
 740           1.1E-2
 825           9.5E-3
1200           1.50743E-2
C
END.OF.DATA
```

```
TITLE  DEFORMATION OF UNRESTRAINED STEEL I-SECTION
C      BEAM (ANALYSIS 133) (DFR42)  11/10/84
C
C      ELASTIC ANALYSIS ASSUMING MODULUS OF ELASTICITY VARIES
C      WITH TEMPERATURE. TEMPS IN TEMP MODULE CORRESPOND WITH
C      TEMPS IN EXPERIMENT AT TIME=12MINS. USES PHASE TRANS-
C      FORMATION (PRELOAD) MODULE, WHICH ASSUMES SLOPE OF STRAIN
C      TEMP LINE IS 14.8648E-6/DEG C. HALF LENGTH OF BEAM
C      MODELLED WITH 40 ELEMENTS FOR HALF LENGTH, AND TWO
C      ELEMENTS WITHIN HOT FLANGE THICKNESS, WITH A TOTAL
C      OF 280 ELEMENTS.
CONTROL
DOUBLE
PHASE=1,7
STOP
CONTROL.END
C
NODES
AXIS.NUMBER=1
NODE.NUMBER     X         Y
    1           0         0
    2          .655       0
    3           0        .002985
    4          .655      .002985
    5           0        .00597
    6          .655      .00597
    7           0        .026
    8          .655      .026
    9           0        .039
   10          .655      .039
   11           0        .052
   12          .655      .052
   13           0        .098
   14          .655      .098
   15           0        .104
   16          .655      .104
C
PAFBLOCKS
ELEMENT.TYPE=36210
TYPE=1
BLOCK.NUMBER    GROUP.NUMBER    PROPERTIES    N1    N2      TOPOLOGY
     1               1               1        1     2    1   2   3   4
     2               2               1        1     2    3   4   5   6
     3               3               2        1     2    5   6   7   8
     4               4               2        1     2    7   8   9  10
     5               5               2        1     2    9  10  11  12
     6               6               2        1     2   11  12  13  14
     7               7               1        1     2   13  14  15  16
C
MESH
REFERENCE    SPACING.LIST
    1              40
    2               1
C
PLATES.AND.SHELLS
PLATE.OR.SHELL.NUMBER    MATERIALS.NUMBER    THICKNESS
       1                        12               .044
       2                        12               .0042
C
VARIABLE.MATERIAL.NUMBER  MATERIAL.NUMBER  TABLE.NUMBER   PROPERTY.NUMBER
```

```
        12                      11              1               2
C
MATERIAL
MATERIAL.NUMBER     NU      ALPHA
       11          0.3     14.8648E-6
C
TABLES
TABLE.NUMBER=1
BASIS.VALUE     VALUE
      0          210E9
    150          200E9
    300          191E9
    400          183E9
    500          174E9
    600          163E9
    700          153E9
    800          140E9
   1000          110E9
   1200           75E9
C
RESTRAINTS
NODE.NUMBER     PLANE     DIRECTION
    1             1          12
C
TEMPERATURE
LOAD.CASE  TEMPERATURE  START  FINISH  STEP    LIST.OF.NODES
C TIME=12 MINS
   1           225        18     94     2         1 , 2
   1           210       138    214     2         3 , 4
   1           196       258    334     2         5 , 6
   1           137       378    454     2         7 , 8
   1           110       498    574     2         9 ,10
   1            90       618.   694     2        11 ,12
   1            35       738    814     2        13 ,14
   1          30.2       858    934     2        15 ,16
C
PRELOAD
CASE    TYPE    TABLE
C
  1      1        2
TABLE
TABLE=2
BASIS    VALUE
  0        0
 740     1.1E-2
 825     9.5E-3
1200     1.5074E-2
C
END.OF.DATA
```

```
TITLE     DEFORMATION OF UNRESTRAINED STEEL I-SECTION BEAM.HALF-HEATED
C         ANALYSIS 133X  DFR17  03/07/84. .     (RE-RUN 09/10/85)
C         ELASTIC ANALYSIS ASSUMING E VALUE=210E9 FOR ALL TEMPS.TEMPS
C         IN 7 LOAD CASES CORRESPOND TO TEMPS IN EXPERIMENT AT TIME
C         INTERVALS OF 6 MIN UP TO 48 MINUTES OF HEATING.  ASSUMES
C         ALPHA=14E-6 (NO PHASE TRANSFORMATION)
C
CONTROL
DOUBLE
PHASE=1,7
STOP
CONTROL,END
C
NODES
AXIS,NUMBER=1
NODE,NUMBER     X      Y
     1          0      0
     2       .527      0
     3       .591      0
     4       .655      0
     5       .719      0
     6       .783      0
     7      1.310      0
     8          0   .00597
     9       .527   .00597
    10       .591   .00597
    11       .655   .00597
    12       .719   .00597
    13       .783   .00597
    14      1.310   .00597
    15          0    .052
    16       .527    .052
    17       .591    .052
    18       .655    .052
    19       .719    .052
    20       .783    .052
    21      1.310    .052
    22          0    .098
    23       .527    .098
    24       .591    .098
    25       .655    .098
    26       .719    .098
    27       .783    .098
    28      1.310    .098
    29          0    .104
    30       .527    .104
    31       .591    .104
    32       .655    .104
    33       .719    .104
    34       .783    .104
    35      1.310    .104
C
PAFBLOCK
ELEMENT,TYPE=36210
TYPE=1
BLOCK,NUMBER  GROUP,NUMBER  PROPERTIES  N1  N2  TOPOLOGY
     1              1            1       1   2  1, 2, 8, 9
     2              1            1       1   2  6, 7,13,14
     3              2            2       1   2  8, 9,15,16
```

```
      4              2              2        1    2 13,14,20,21
      5              3              2        1    2 15,16,22,23
      6              3              2        1    2 20,21,27,28
      7              4              1        1    2 22,23,29,30
      8              4              1        1    2 27,28,34,35
C
MESH
REFERENCE  SPACING.LIST
    1             10
    2              1
C
ELEMENTS
ELEMENT.TYPE=36210
NUMBER  GROUP.NUMBER  PROPERTIES  TOPOLOGU
   1          1             1       2  3  9 10
   2          1             1       3  4 10 11
   3          1             1       4  5 11 12
   4          1             1       5  6 12 13
   5          2             2       9 10 16 17
   6          2             2      10 11 17 18
   7          2             2      11 12 18 19
   8          2             2      12 13 19 20
   9          3             2      16 17 23 24
  10          3             2      17 18 24 25
  11          3             2      18 19 25 26
  12          3             2      19 20 26 27
  13          4             1      23 24 30 31
  14          4             1      24 25 31 32
  15          4             1      25 26 32 33
  16          4             1      26 27 33 34
C
C  GROUP 1 INCLUDES PAFBLOCKS 1 AND 2 AND INTERVENING ELEMENTS.
C  GROUP 2 INCLUDES PAFBLOCKS 3 AND 4 AND INTERVENING ELEMENTS.
C  ETC
C
PLATES.AND.SHELLS
PLATE.OR.SHELL.NUMBER  MATERIAL.NUMBER  THICKNESS
           1                   11            .044
           2                   11            .0042
C
MATERIAL
MATERIAL.NUMBER    E      NU    ALPHA
       11        210E9    0.3   14E-6
C
RESTRAINTS
NODE.NUMBER  PLANE  DIRECTION
    1          0       12
    7          0        2
C NODE 1 IS RESTRAINED IN X AND Y DIRECTION
C NODE 2 IS RESTRAINED IN Y DIRECTION
C  THE FOLLOWING TEMPS ARE SPECIFIED FOR CORNER NODES
C
TEMPERATURE
C
C  AT TIME=6 MINUTES
LOAD.CASE  TEMPERATURE  START  FINISH  STEP  LIST.OF.NODES
    1          20         76     94      1       1, 2
    1          20        105    123      1       8, 9
    1          20        182    200      1      15,16
    1          20        240    258      1      22,23
```

```
      1           20          298     316       1       29.30
      1           27                                     3
      1           26                                    10
      1           22                                    17
      1           22                                    24
      1           20                                    31
      1           42                                     4
      1           41                                    11
      1           27.5                                  18
      1           22                                    25
      1           21                                    32
      1           58                                     5
      1           56                                    12
      1           40                                    19
      1           21                                    26
      1           21                                    33
      1           75          124     142       1        6, 7
      1           68          153     171       1      13,14
      1           34          211     229       1      20,21
      1           23          269     287       1      27,28
      1           23          327     345       1      34,35
C
C   AT TIME=12 MINUTES
      2           20           76      94       1       1, 2
      2           20          105     123       1       8, 9
      2           20          182     200       1      15,16
      2           20          240     258       1      22,23
      2           20          298     316       1      29,30
      2           40                                     3
      2           38                                    10
      2           30                                    17
      2           22                                    24
      2           21                                    31
      2          100                                     4
      2           90                                    11
      2           63                                    18
      2           39                                    25
      2           38                                    32
      2          168                                     5
      2          155                                    12
      2           77                                    19
      2           48                                    26
      2           47                                    33
      2          270          124     142       1        6, 7
      2          240          153     171       1      13,14
      2          110          211     229       1      20,21
      2           60          269     287       1      27,28
      2           55          327     345       1      34,35
C
C   AT TIME=18 MINUTES
      3           20           76      94       1       1, 2
      3           20          105     123       1       8, 9
      3           20          182     200       1      15,16
      3           20          240     258       1      22,23
      3           20          298     316       1      29,30
      3           68                                     3
      3           65                                    10
      3           50                                    17
      3           42                                    24
      3           41                                    31
```

```
      3          182                                          4
      3          150                                         11
      3           98                                         18
      3           70                                         25
      3           68                                         32
      3          300                                          5
      3          276                                         12
      3          150                                         19
      3           94                                         26
      3           92                                         33
      3          530         124       142       1          6, 7
      3          470         153       171       1         13,14
      3          218         211       229       1         20,21
      3          128         269       287       1         27,28
      3          120         327       345       1         34,35
C
C   AT TIME=24 MINUTES
      4           20          76        94       1          1, 2
      4           20         105       123       1          8, 9
      4           20         182       200       1         15,16
      4           20         240       258       1         22,23
      4           20         298       316       1         29,30
      4           96                                          3
      4           94                                         10
      4           75                                         17
      4           63                                         24
      4           62                                         31
      4          255                                          4
      4          225                                         11
      4          145                                         18
      4          100                                         25
      4           95                                         32
      4          410                                          5
      4          380                                         12
      4          210                                         19
      4          138                                         26
      4          135                                         33
      4          740         124       142       1          6, 7
      4          660         153       171       1         13,14
      4          305         211       229       1         20,21
      4          193         269       287       1         27,28
      4          187         327       345       1         34,35
C
C   AT TIME=30 MINUTES
      5           20          76        94       1          1, 2
      5           20         105       123       1          8, 9
      5           20         182       200       1         15,16
      5           20         240       258       1         22,23
      5           20         298       316       1         29,30
      5          120                                          3
      5          116                                         10
      5           95                                         17
      5           83                                         24
      5           82                                         31
      5          322                                          4
      5          268                                         11
      5          180                                         18
      5          125                                         25
      5          122                                         32
      5          500                                          5
```

```
      5          462                                                  12
      5          265                                                  19
      5          178                                                  26
      5          172                                                  33
      5          925          124       142        1                 6. 7
      5          790          153       171        1                13.14
      5          350          211       229        1                20.21
      5          232          269       287        1                27.28
      5          228          327       345        1                34.35
C
C   AT TIME=36 MINUTES
      6           20           76        94        1                 1. 2
      6           20          105       123        1                 8. 9
      6           20          182       200        1                15.16
      6           20          240       258        1                22.23
      6           20          298       316        1                29.30
      6          168                                                   3
      6          163                                                  10
      6          115                                                  17
      6          100                                                  24
      6           98                                                  31
      6          355                                                   4
      6          333                                                  11
      6          210                                                  18
      6          155                                                  25
      6          153                                                  32
      6          560                                                   5
      6          520                                                  12
      6          300                                                  19
      6          204                                                  26
      6          198                                                  33
      6         1115          124       142        1                 6. 7
      6          920          153       171        1                13.14
      6          385          211       229        1                20.21
      6          256          269       287        1                27.28
      6          151          327       345        1                34.35
C
C   AT TIME=42 MINUTES
      7           20           76        94        1                 1. 2
      7           20          105       123        1                 8. 9
      7           20          182       200        1                15.16
      7           20          240       258        1                22.23
      7           20          298       316        1                29.30
      7          166                                                   3
      7          162                                                  10
      7          180                                                  17
      7          112                                                  24
      7          110                                                  31
      7          392                                                   4
      7          353                                                  11
      7          228                                                  18
      7          163                                                  25
      7          160                                                  32
      7          615                                                   5
      7          570                                                  12
      7          325                                                  19
      7          224                                                  26
      7          220                                                  33
      7         1230          124       142        1                 6. 7
      7         1000          153       171        1                13.14
```

```
     7          410          211     229       1       20.21
     7          273          269     287       1       27.28
     7          267          327     345       1       34.35
C
OUT.DRAW
PLOT.TYPE    ORIENTATION    SIZE.NUMBER
     1             1              4
C
END.OF.DATA
```

APPENDIX 4. THE RELATIONSHIP BETWEEN THE BOWING DISPLACEMENT AND AXIAL DISPLACEMENT OF A SLENDER MEMBER BOWED INTO A CIRCULAR ARC

An equation is derived below which gives the amount of shortening Δ_L between the ends of a slender member when it is caused to bow into a circular arc such that the mid-span displacement is Δ_N .

Consider an initially straight member AB of length L, Figure 1. The member is slender so that when reduced in length by Δ_L it bows without producing compressive strain within the member. Assume that the member bows into a circular arc ACB with a radius of curvature R.

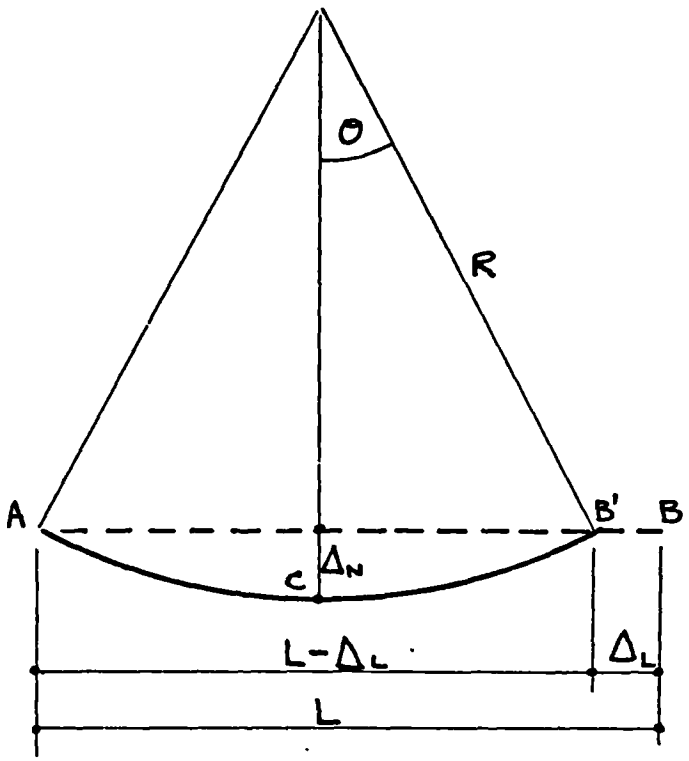

FIGURE 1. Geometry of displaced member bowed into a circular arc

From Figure 1,

$$L = 2R\theta \quad \ldots\ldots (1)$$

$$\frac{L - \Delta_L}{2} = R\sin\theta \quad \ldots\ldots (2)$$

$$R - \Delta_N = R\cos\theta \quad \ldots\ldots (3)$$

From Equations (1) and (2)

$$\Delta_L = 2R(\theta - \sin\theta) \quad \ldots\ldots (4)$$

Substituting for R from (2) in (4)

$$\Delta_L = (L - \Delta_L)\left(\frac{\theta - \sin\theta}{\sin\theta}\right) \quad \ldots\ldots (5)$$

As $\sin\theta = \theta - \theta^3/3! \ldots$, Equation (5) becomes

$$\Delta_L = (L - \Delta_L)\theta^2/6 \quad \ldots\ldots (6)$$

From Equation (3)

$\Delta_N = R\,(1 - \cos\theta)$ and substituting for R from Equation (2) gives:

$$\Delta_N = (L - \Delta_L)\,\frac{(1 - \cos\theta)}{2\sin\theta}$$

As $\cos\theta = 1 - \theta^2/2!$

$$\Delta_N = (L - \Delta_L)\theta/4 \quad \ldots\ldots (7)$$

From Equation (6)

$\theta = \sqrt{\dfrac{6\,\Delta_L}{L - \Delta_L}}$ and substituting for θ in Equation (7) gives

$$\Delta_N = \frac{(L - \Delta_L)}{4} \cdot \sqrt{\frac{6\,\Delta_L}{L - \Delta_L}} = \sqrt{\frac{6\,(L - \Delta_L)\Delta_L}{16}}$$

Ignoring 2nd order terms

$$\Delta_N = \sqrt{0.375\,L\,\Delta_L} \quad \ldots\ldots (8)$$

Transposing gives

$$\Delta_L = \frac{\Delta_N^2}{0.375\,L} \quad \ldots\ldots (9)$$